2.5.2 Vibratory Ground Motion

This section provides a detailed description of the vibratory ground motion assessment that was carried out for the VEGP ESP site resulting in the development of the VEGP ESP site Safe Shutdown Earthquake (SSE) ground motion. This assessment was performed to address seismic hazard update guidance in Regulatory Guide 1.165 Identification and Characterization of Seismic Sources and Determination of Safe Shutdown Earthquake Ground Motion, Rev. 0, March 1997 (RG 1.165), and meet the SSE requirements in paragraph (d) of 10CFR 100.23. The starting point for this site assessment is the EPRI-SOG probabilistic seismic hazard analysis (PSHA) evaluation **(EPRI NP-6395-D 1989)**.

Section 2.5.2.1 through Section 2.5.2.4 document the review and update of the available EPRI seismicity, seismic source, and ground motion models. Section 2.5.2.5 summarizes information about the seismic wave transmission characteristics of the ESP site with reference to more detailed discussion of all engineering aspects of the subsurface in Section 2.5.4.

Section 2.5.2.6 describes the development of the horizontal SSE ground motion for the VEGP ESP site. The selected SSE ground motion is based on the risk-consistent/performance-based approach from NUREG/CR-6728 **(McGuire et al. 2001)** and ASCE 43-05 **(ASCE 2005)**. Site-specific horizontal ground motion amplification factors are developed using site-specific estimates of near-surface soil and rock properties. These amplification factors are then used to scale the hard rock spectra to develop Uniform Hazard Spectra (UHS) accounting for site-specific conditions using Approach 2A of NUREG/CR-6769. Horizontal SSE spectra are developed from these soil Uniform Hazard Spectra (UHS) using the performance-based approach of ASCE 43-05. The SSE motion is defined at the free ground surface of a hypothetical outcrop of the highest competent in situ layer. This is at the top of the Blue Bluff Marl, at a depth of 86 ft. See Sections 2.5.4 and 2.5.2.5 for further discussion of the subsurface conditions.

Section 2.5.2.7 describes vertical SSE spectra, developed by scaling the horizontal SSE by a frequency-dependent vertical-to-horizontal (V/H) factor

The SSE spectra that are described in this section are considered a performance goal-based (risk-informed) site specific safe shutdown earthquake response spectra. The SSE spectra and its specific location at a free ground surface reflect the seismic hazard in terms of a PSHA and geologic characteristics of the site. The SSE spectra defined in this section would be expected to be modified as appropriate to develop ground motion for design considerations.

2.5.2.1 Seismicity

The seismic hazard analysis conducted by EPRI (NP-6395-D 1989) relied on an analysis of historical seismicity in the Central and Eastern United States (CEUS) to estimate seismicity

parameters (rates of activity and Richter b-values) for individual seismic sources. The historical earthquake catalog used in the EPRI analysis was complete through 1984. The earthquake data for the site region occurring since 1984 was reviewed and used to update the EPRI catalog.

2.5.2.1.1 Regional Seismicity Catalog Used for 1989 EPRI Seismic Hazard Analysis Study

Many seismic networks record earthquakes in the CEUS. A large effort was made during the EPRI seismic hazard analysis study to combine available data on historical earthquakes and to develop a homogeneous earthquake catalog that contained all recorded earthquakes for the region. "Homogeneous" means that estimates of body-wave magnitude, m_b, for all earthquakes are consistent, that duplicate earthquakes have been eliminated, that non-earthquakes (e.g., mine blasts and sonic booms) have been eliminated, and that significant events in the historical record have not been missed. Thus, the EPRI catalog **(EPRI NP-4726-A 1988)** forms a strong basis on which to estimate seismicity parameters.

2.5.2.1.2 Updated Seismicity Data

NRC Regulatory Guide 1.165, Identification and Characterization of Seismic Sources and Determination of Safe Shutdown Earthquake Ground Motion, Revision 0, March 1997 (RG 1.165) specifies that earthquakes of Modified Mercalli Intensity (MMI) greater than or equal to IV or magnitude greater than or equal to 3.0 should be listed for seismic sources "any part of which is within a radius of 200 mile (320 km) of the site (the site region)." In updating the EPRI catalog a latitude-longitude window of 30° to 37° N, 78° to 86° W was used. This window incorporates the 200 mi (320 km) radius "site region" and all seismic sources contributing significantly to VEGP ESP site earthquake hazard Figure 2.5.1-1 shows the VEGP ESP site and its associated site region. Figures 2.5.2-1 through 2.5.2-6 show this site region and the defined latitude-longitude window.

The updated catalog was compiled from the following sub-catalogs:

EPRI Catalog. The various data fields of the EPRI catalog are described in EPRI NP-4726-A 1988.

SEUSSN Catalog. The SEUSSN catalog is available from the Virginia Tech Seismological Observatory FTP site **(SEUSSN 2005)**. On the June 3, 2005 date of the catalog update, the SEUSSN catalog had 2,483 records dating from March 1698 to December 2003 within the site region latitude-longitude window. Of these, 1,355 records occurred in 1985 or later.

ANSS Catalog. The ANSS catalog **(ANSS 2005)** was searched on June 3, 2005, for all records within the site region latitude-longitude window, resulting in 1,710 records from 1928 to April 14, 2005. Of these, 1,375 records occurred in 1985 or later.

The Southeastern US Seismic Network (SEUSSN) and Advanced National Seismic System (ANSS) catalogs were used for the temporal update (1985 to present) of the EPRI seismicity catalog. The SEUSSN has coverage over the entire site region (defined above) and is the primary catalog used to compile the national ANSS seismicity catalog. While the SEUSSN catalog is taken as the preferred catalog, some additional events listed only in the ANSS catalog are also included in the update.

The magnitudes given in both catalogs were converted to best or expected estimate of m_b magnitude ($E[m_b]$, also called Emb), using the conversion factors given as equation 4-1 and Table 4-1 in EPRI NP-4726-A 1988:

$$Emb = 0.253 + 0.907 \cdot Md \qquad \text{(Equation 2.5.2-1)}$$

$$Emb = 0.655 + 0.812 \cdot ML \qquad \text{(Equation 2.5.2-2)}$$

where Md is duration or coda magnitude and ML is "local" magnitude.

Equation 4-2 of EPRI (NP-4726-A 1988) indicates that the equation from which mb* or Rmb is estimated from the best estimate of magnitude $E[m_b]$ or Emb and the variance of m_b, σ^2_{mb}, or Smb^2 is :

$$m_b^* = E[m_b] + (1/2) \cdot ln(10) \cdot b \cdot \sigma^2_{mb} \qquad \text{(Equation 2.5.2-3)}$$

where b = 1.0.

Values for σ^2_{mb} or Smb were estimated for the two catalogs, and m_b [Rmb] was assigned to each event added to the updated catalog.

The result of the above process was a catalog of 61 earthquakes shown in Table 2.5.2-1 as the update of the EPRI NP-4726-A seismicity catalog recommended for the site region. For the purpose of recurrence analysis, these should be considered independent events.

The 61 events in the 30° to 37° N, 78° to 86° W latitude-longitude window, incorporating the 200 mi (320 km) radius site region, from 1985 to April 2005 with Emb magnitude 3.0 or greater have been incorporated into a number of figures, including tectonic features discussed in Section 2.5.1 and EPRI Earth Science Team source maps in this section.

2.5.2.2 Geologic Structures and EPRI Seismic Source Model for the Site Region

As described in Section 2.5.1, a comprehensive review of available geological, seismological, and geophysical data has been performed for the VEGP ESP site region and adjoining areas. The following sections summarize seismic source interpretations from the 1989 EPRI probabilistic seismic hazard analysis (PSHA) study **(EPRI NP-6395-D 1989)** and from relevant post-EPRI seismic source characterization studies and the updated interpretations of new and existing sources based on more recent data.

Since publication of the EPRI seismic source model, significant new information has been developed for assessing the earthquake source that produced the 1886 Charleston earthquake. This new information shows that the Charleston seismic source should be updated according to RG 1.165. Paleoliquefaction features and other new information published since the 1986 EPRI project **(EPRI NP-4726 1986)** have significant implications regarding the geometry, M_{max}, and recurrence of M_{max} in the Charleston seismic source. Results from the 1989 EPRI study also show that the Charleston seismic source is the most significant contributor to seismic hazard at the VEGP ESP site **(EPRI NP-6395-D 1989)**. Thus, an update of the Charleston seismic source has been developed as part of the work performed for this ESP application. Details of the Updated Charleston Seismic Source (UCSS) model are presented in Section 2.5.2.2.2.4 and in a separate Engineering Study Report **(Bechtel 2006d)**.

Sensitivity studies were performed to evaluate the potential significance of the UCSS model to seismic hazard at the VEGP ESP site, as described in detail in Section 2.5.2.4. Based on this analysis, it is found that the UCSS interpretations for the Charleston area show that the Charleston seismic source still dominates the seismic hazard at the VEGP ESP site. These new interpretations of the possible locations, sizes, and recurrence intervals of large earthquakes in the Charleston area form a strong basis with which to calculate the seismic ground motion hazard for the site.

2.5.2.2.1 Summary of EPRI Seismic Sources

This section summarizes the seismic sources and parameters used in the 1986 EPRI project (**EPRI NP-4726 1986)**. The description of seismic sources is limited to those sources within 200 mi of the VEGP ESP site (i.e., the site region) and those at distances greater than 200 mi that may affect the hazard at the VEGP ESP site.

In the 1986 EPRI project, six independent Earth Science Teams (ESTs) evaluated geological, geophysical, and seismological data to develop a model of seismic sources in the CEUS. These sources were used to model the occurrence of future earthquakes and evaluate earthquake hazards at nuclear power plant sites across the CEUS.

The six ESTs involved in the 1986 EPRI project were Bechtel Group, Dames & Moore, Law Engineering, Rondout Associates, Weston Geophysical Corporation, and Woodward-Clyde Consultants. Each team produced a report (volumes 5 through 10 of EPRI NP-4726) providing detailed descriptions of how they identified and defined seismic sources. The results were implemented into a PSHA study **(EPRI NP-6395-D 1989)**. For the computation of hazard in the 1989 study, a few seismic source parameters were modified or simplified from the original parameters determined by the six ESTs. EPRI NP-6452-D (1989) summarized the parameters used in the final PSHA calculations, and this reference is the primary source for the seismicity parameters used in this current ESP application. Each EST provides more detailed descriptions

of the rationale and methodology used in evaluating tectonic features and establishing the seismic sources (refer to volumes 5 through 10 of EPRI NP-4726).

The most significant seismic sources **(EPRI NP-6395-D 1989)** developed by each EST are shown in Figures 2.5.2-1 through 2.5.2-6. For the 1989 EPRI seismic hazard calculations, a screening criterion was implemented to identify those sources whose combined hazard exceeded 99 percent of the total hazard from all sources, for two ground motions measures **(EPRI NP-6395-D 1989)**. These sources are identified in the descriptions below as "primary" seismic sources. Other sources, which together contributed less than one percent of the total hazard from all sources for the two ground motion measures, are identified in the descriptions below as "additional" seismic sources. Earthquakes with body-wave magnitude $m_b \geq 3.0$ are also shown in Figures 2.5.2-1 through 2.5.2-6 to show the spatial relationships between seismicity and seismic sources. Earthquake epicenters include both events from the EPRI earthquake catalog and for the period between 1985 and April 2005 as described in Section 2.5.2.1.2.

The maximum magnitude, interdependencies, and probability of activity for each EPRI EST's seismic sources are presented in Tables 2.5.2-2 through 2.5.2-7. These tables present the parameters assigned to each source within 200 mi of the VEGP ESP site and include primary and additional seismic sources as defined above. The tables also indicate whether new information has been identified that would lead to a revision of the source's geometry, maximum magnitude, or recurrence parameters. The seismicity recurrence parameters (a- and b-values) used in the seismic hazard studies were computed for each 1° latitude and longitude cell that intersects any portion of a seismic source.

The nomenclature used by each EST to describe the various seismic sources in the CEUS varies from team to team. In other words, a number of different names may have been used by the EPRI teams to describe the same or similar tectonic features or sources, or one team may describe seismic sources that another team does not. For example**,** the Charleston seismic source was modeled by each team but was called the Charleston Area and Charleston Faults by the Bechtel Group team; the Charleston Seismic Zone by the Dames & Moore, Law, and Weston teams; and Charleston by the Rondout and Woodward-Clyde teams. Each team's source names, data, and rationale are included in its team-specific documentation (volumes 5 through 10 of EPRI NP-4726).

The EPRI PSHA study expressed maximum magnitude (M_{max}) values in terms of body-wave magnitude (m_b), whereas most modern seismic hazard analyses describe M_{max} in terms of moment magnitude (**M**). To provide a consistent comparison between magnitude scales, this study relates body-wave magnitude to moment magnitude using the arithmetic average of three equations, or their inversions, presented in Atkinson and Boore (1995), Frankel et al (1996), and EPRI TR-102293 (1993). The conversion relations are very consistent for magnitudes 4.5 and

greater and begin to show divergence at lower magnitudes. (Table 2.5.2-23 lists m_b and **M** equivalences developed from these relations over the range of interest for this study.) Throughout this section, the largest assigned values of M_{max} distributions assigned by the ESTs to seismic sources are presented for both magnitude scales (m_b and **M**) to give perspective on the maximum earthquakes that were considered possible in each seismic source. For example, EPRI m_b values of M_{max} are followed by the equivalent **M** value.

The following sections describe the most significant EPRI sources (both primary and additional seismic sources) for each EST with respect to the VEGP ESP site. Assessment of these and other EPRI sources within the site region shows that the EPRI source parameters (M_{max}, geometry, and recurrence) are sufficient to capture the current understanding of the seismic hazard in the site region.

Except for the Charleston seismic source, no new geological, geophysical, or seismological information in the literature published since the EPRI NP-6395-D source model suggests that these sources should be modified. Each EST's characterization of the Charleston seismic source was replaced by four alternative source geometries. For each geometry, large earthquake occurrences (**M** 6.7 to 7.5) were modeled with a range of mean recurrence rates, and smaller earthquakes (m_b 5 to 6.7) were modeled with an exponential magnitude distribution, with rates and b-values determined from historical seismicity. Also, all surrounding sources for each team were redrawn so that the new Charleston source geometries were accurately represented as a "hole" in the surrounding source, and seismic activity rates and b-values were recalculated for the modified surrounding sources, based on historical seismicity. Further details and the results of sensitivity analyses performed on the modified seismic sources are presented in Section 2.5.2.4.

2.5.2.2.1.1 Sources Used for EPRI PSHA – Bechtel Group

Bechtel Group identified and characterized six primary seismic sources. All six of these primary seismic sources are located within the site region (200 mi); they are:

- Charleston Area (H)
- Charleston Faults (N3)
- Atlantic Coastal Region (BZ4)
- S Appalachians (BZ5)
- SE Appalachians (F)
- NW South Carolina (G)

Bechtel Group also characterized four additional seismic sources. These additional seismic sources are:

- Eastern Mesozoic Basins (13)

- Bristol Trends (24)
- Rosman Fault (15)
- Belair Fault (16)

Primary and additional seismic sources characterized by the Bechtel Group team within the site region are listed in Table 2.5.2-2. A map showing the locations and geometries of the Bechtel primary seismic sources is provided in Figure 2.5.2-1. Following is a brief discussion of each of the primary seismic sources characterized by the Bechtel Group team..

Charleston Area (H). The Charleston Area source (H) is located about 60 mi from the VEGP ESP site. This oblong combination source area is defined based on the historic earthquake pattern (including the Middleton Place-Summerville and Bowman seismic zones), is elongated northwest-southeast, and encompasses all of source zone N3 (described below). Sources H and N3 are interdependent; if N3 is active, it is unlikely that H is active, and vice versa. The largest M_{max} assigned by Bechtel Group to this zone is m_b 7.4 (**M** 7.9), reflecting its assumption that Charleston-type earthquakes are produced within this zone.

Charleston Faults (N3). The Charleston Faults (N3) source zone is a small area set within the Charleston Area (H) source zone and encompassing a number of identified and postulated faults in the Charleston, South Carolina, area, including the Ashley River, Charleston, and Woodstock faults. Source N3 is located approximately 85 mi from the VEGP ESP site. Sources H and N3 are interdependent; if N3 is active, it is unlikely that H is active, and vice versa. According to EPRI NP-4726, this combination was created for computational simplicity. The largest M_{max} assigned by the Bechtel Group team to this zone is m_b 7.4 (**M** 7.9), reflecting its assumption that Charleston-type earthquakes are produced within this zone.

Atlantic Coastal Region (BZ4). The VEGP ESP site is located within the Atlantic Coastal Region background source (BZ4). Source BZ4 is a large background zone that extends from offshore New England to Alabama and encompasses portions of the Coastal Plain from Georgia to southern Virginia. The largest M_{max} assigned by the Bechtel Group team to this zone is m_b 7.4 (**M** 7.9), reflecting its assumption that there is a small probability that a Charleston-type earthquake could occur within this region.

S Appalachians (BZ5). The Southern Appalachians background source (BZ5) is located about 10 mi from the VEGP ESP site. This source is a large background region that extends from New York to Alabama, including portions of the Southern Appalachians, Piedmont, and Coastal Plain. The largest M_{max} assigned by the Bechtel Group team to this zone is m_b 6.6 (**M** 6.5).

SE Appalachians (F). The VEGP ESP site is located about 10 mi from the Southeastern Appalachians source (F), a combination source zone that includes parts of Georgia and the Carolinas and flanks the southwest and northeast borders of Zone G (described below). Source

Zone F is mutually exclusive with Zone G; if F is active, G is inactive, and vice versa. The largest M_{max} assigned by the Bechtel Group team to this zone is m_b 6.6 (**M** 6.5).

NW South Carolina (G). The VEGP ESP site is located about 10 mi from the Northwestern South Carolina combination source (G). Source Zone G is mutually exclusive with Zone F; if G is active, F is inactive, and vice versa. The largest M_{max} assigned by the Bechtel Group team to this zone is m_b 6.6 (**M** 6.5).

2.5.2.2.1.2 Sources Used for EPRI PSHA – Dames & Moore

Dames & Moore identified and characterized five primary seismic sources. All five of these seismic sources are located within the site region; they are:

- Charleston Seismic Zone (54)
- Charleston Mesozoic Rift (52)
- S Appalachian Mobile Belt (Default Zone) (53)
- S Cratonic Margin (Default Zone) (41)
- S Coastal Margin (20)

Dames & Moore also identified seven additional seismic sources within the site region. These sources are:

- Appalachian Fold Belts (4)
- Kink in Fold Belt (4A)
- Jonesboro Basin (49)
- Buried Triassic Basins (50)
- Florence Basin (51)
- Dunbarton Triassic Basin (65)
- Combination Zone 4A-4B-4C-4D (C01)

Primary and additional seismic sources characterized by the Dames & Moore team within the site region are listed in Table 2.5.2-3. A map showing the locations and geometries of the Dames & Moore primary seismic sources is provided in Figure 2.5.2-2. Following is a brief discussion of these primary seismic sources.

Charleston Seismic Zone (54). The Charleston Seismic Zone (54) is a northwest-southeast oriented polygon located about 45 mi from the VEGP ESP site. This source includes the Ashley River, Woodstock, Helena Banks, and Cooke faults, as well as the Bowman and Middleton Place-Summerville seismic zones and was designed to capture the occurrence of Charleston-type earthquakes. The largest M_{max} assigned by the Dames & Moore team to this zone is m_b 7.2 (**M** 7.5).

Charleston Mesozoic Rift (52). The Charleston Mesozoic Rift source (52) is a large polygon located less than 5 mi from the VEGP ESP site. This source extends from offshore South Carolina to Gulf Shore Florida, including portions of the South Carolina and Georgia Coastal Plain. The largest M_{max} assigned by the Dames & Moore team to this zone is m_b 7.2 (**M** 7.5).

S Appalachian Mobile Belt (Default Zone) (53). The VEGP ESP site is located within the Southern Appalachian Mobile Belt (Default Zone) source (53). This default zone comprises crustal rocks that have undergone several periods of divergence and convergence. The source is bounded on the east by the East Coast magnetic anomaly and on the west by the westernmost boundary of the Appalachian gravity gradient. The largest M_{max} assigned by the Dames & Moore team to this zone is m_b 7.2 (**M** 7.5).

S Cratonic Margin (Default Zone) (41). The Southern Cratonic Margin (Default Zone) source is located about 65 mi from the VEGP ESP site. This large default zone is located between the Appalachian Fold Belt (4) and the Southern Appalachian Mobile Belt (53) and includes the region of continental margin deformed during Mesozoic rifting. Located within this default zone are many Triassic basins and border faults. The largest M_{max} assigned by the Dames & Moore team to this zone is m_b 7.2 (**M** 7.5).

S Coastal Margin (20). The Southern Coastal Margin regional source (20) is located approximately 90 mi from the VEGP ESP site. This zone is roughly parallel to the rifted continental margin from Texas to Alabama and incorporates a region of diffuse seismicity. Located within this source is a down-warped wedge of miogeosynclinal sediments of Cretaceous age and younger. The largest M_{max} assigned by the Dames & Moore team to this zone is m_b 7.2 (**M** 7.5).

2.5.2.2.1.3 Sources Used for EPRI PSHA – Law Engineering

Law Engineering identified and characterized 15 primary seismic sources all within the site region; They are:

- Charleston Seismic Zone (35)
- Eastern Basement (17)
- Reactivated E Seaboard Normal (22)
- Brunswick, NC Background (108)
- Mesozoic Basins (8 – Bridged) (C09)
- 8 – 35 (C10)
- 22 – 35 (C11)
- Eight mafic pluton sources (M33 and M36 through M42)

Law Engineering also characterized five additional seismic sources within the site region that do not contribute to 99 percent of the hazard at the VEGP ESP site. These are:

- Eastern Basement Background (217)
- Eastern Piedmont (107)
- 22 – 24 – 35 (GC13)
- 22 – 24 (GC12)
- Mesozoic Basins (8)

Primary and additional seismic sources characterized by the Law Engineering team within the site region are listed in Table 2.5.2-4. A map showing the locations and geometries of the Law Engineering primary seismic sources is provided in Figure 2.5.2-3. Following is a brief discussion of Law's primary seismic sources

Charleston Seismic Zone (35). The Charleston Seismic Zone source (35) is a northeast-southwest elongated polygon that includes the Charleston, Ashley River, and Woodstock faults, as well as parts of the offshore Helena Banks fault and most of the more recently discovered liquefaction features identified by Amick (1990). This source was designed to capture the occurrence of Charleston-type earthquakes. This source is located about 75 mi from the VEGP ESP site and overlaps with the Reactivated E Seaboard Normal (22; described below) and Buried Mesozoic Basins (8; not a 99 percent contributor) sources. The largest M_{max} assigned by the Law Engineering team to this zone is m_b 6.8 (**M** 6.8).

Eastern Basement (17). The VEGP ESP site is located 90 mi from the Eastern Basement (17) source. This source was defined as an area containing pre-Cambrian and Cambrian normal faults, developed during the opening of the proto-Atlantic Ocean, in the basement rocks beneath the Appalachian decollement. The Giles County and eastern Tennessee zones of seismicity are included in this source. The largest M_{max} assigned by the Law Engineering team to this zone is m_b 6.8 (**M** 6.8).

Reactivated E Seaboard Normal (22). The VEGP ESP site is located within the Reactivated Eastern Seaboard Normal (22) source. This source was characterized as a region along the eastern seaboard in which Mesozoic normal faults are reactivated as high-angle reverse faults. The Law Engineering team assigned a single M_{max} of m_b 6.8 (**M** 6.8) to this zone.

Brunswick, NC Background (108). The VEGP ESP site is located within the Brunswick NC Background source zone (108). The source 108 site represents a zone defined by a low-amplitude, long-wavelength magnetic anomaly pattern. The Law Engineering team interpreted this pattern as possibly indicating a zone of Mesozoic extended crust. The largest M_{max} assigned by the Law Engineering team to this zone is m_b 6.8 (**M** 6.8).

Mesozoic Basins (8 – Bridged) (C09). The VEGP ESP site is located within the Mesozoic Basins (C09) source, which comprises eight bridged basins. This source was defined based on northeast-trending sediment-filled troughs in basement rock bounded by normal faults. The largest M_{max} assigned by the Law Engineering team to this zone is m_b 6.8 (**M** 6.8).

8 – 35 (C10). The VEGP ESP site is located within the 8 – 35 combination source (C10). The largest M_{max} assigned by the Law Engineering team to this zone is m_b 6.8 (**M** 6.8).

22 – 35 (C11). The VEGP ESP site is located within the 22 – 35 combination source (C11). The largest M_{max} assigned by the Law Engineering team to this zone is m_b 6.8 (**M** 6.8).

Eight Mafic Pluton Sources (M33 and M36 through M42). The Law Engineering team identified a number of mafic pluton sources, eight of which are located within about 130 mi of the VEGP ESP site. The Law Engineering team considered pre- and post-metamorphic plutons in the Appalachians to be stress concentrators and, thus, earthquake sources. Law Engineering assigned a single M_{max} of m_b 6.8 (**M** 6.8) to all mafic pluton sources.

2.5.2.2.1.4 Sources Used for EPRI PSHA – Rondout Associates

Rondout Associates characterized two primary seismic sources both within the site region; they are:

- Charleston (24)
- South Carolina (26)

Rondout Associates also identified eight additional seismic sources within the site region. These are:

- Appalachian (49)
- Background 49 (C01)
- 49 + 32 (C09)
- Grenville (50)
- Background 50 (C02)
- 50 (02) + 12 (C07)
- Southern Appalachians (25)
- Tennessee-VA Border Zone (27)

Primary and additional seismic sources characterized by the Rondout Associates team within the site region are listed in Table 2.5.2-5. A map showing the locations and geometries of the Rondout Associates primary seismic sources is provided in Figure 2.5.2-4. Following is a brief discussion of both of these primary seismic sources.

Charleston (24). The Charleston source is a northwest-southeast-oriented area set within the larger South Carolina (26) source and located about 35 mi from the VEGP ESP site. Source 24 includes the Helena Banks, Charleston, Ashley River, and Woodstock faults, as well as the Bowman and Middleton Place-Summerville seismic zones, and was designed to capture the occurrence of Charleston-type earthquakes. The largest M_{max} assigned by the Rondout Associates team to this zone is m_b 7.0 (**M** 7.2).

South Carolina (26). The VEGP ESP site is located within the South Carolina source (26). The South Carolina source (26) is a northwest-southeast elongated area that surrounds, but does not include, Source 24 (described above). Source 26 includes most of South Carolina except the Charleston area. The largest M_{max} assigned by the Rondout Associates team to this zone is m_b 6.8 (**M** 6.8).

2.5.2.2.1.5 Sources Used for EPRI PSHA – Weston Geophysical

Weston Geophysical identified and characterized 12 primary seismic sources, all within the site region; they are:

- Charleston Seismic Zone (25)
- South Carolina (26)
- Southern Coastal Plain (104)
- 103 – 23 – 24 (C19)
- 104 – 22 (C20)
- 104 – 25 (C21)
- 104 – 22 – 26 (C23)
- 104 – 22 – 25 (C24)
- 104 – 28BCDE – 22 (C26)
- 104 – 28BCDE – 22 – 25 (C27)
- 26 – 25 (C33)
- 104 – 28BE – 25 (C35)

Weston Geophysical also characterized 13 additional seismic sources within the site region. These sources are:

- 104 – 26 (C22)
- 104 – 28BE – 26 (C34)
- 104 – 28BCDE (C25)
- 104 – 28BCDE – 22 – 26 (C28)
- Zone of Mesozoic Basin (28B)

- 28A through E (C01)
- Southern Appalachians (103)
- 103 – 23 (C17)
- 103 – 24 (C18)
- Zone of Mesozoic Basin (28D)
- Zone of Mesozoic Basin (28E)
- Appalachian Plateau (102)
- New York-Alabama-Clingman (24)

Primary and additional seismic sources characterized by the Weston Geophysical team are listed in Table 2.5.2-6. A map showing the locations and geometries of the Weston Geophysical primary seismic sources is provided in Figure 2.5.2-6. Following is a brief discussion of each of the Weston Geophysical team's primary seismic sources.

Charleston Seismic Zone (25). The Charleston Seismic Zone source is an irregularly shaped hexagon centered just northeast of Charleston, South Carolina, and located about 60 mi from the VEGP ESP site. This source includes the Helena Banks, Charleston, Ashley River, and Woodstock faults, but does not include the Bowman seismic zone. This source was designed to capture the occurrence of Charleston-type earthquakes. The largest M_{max} assigned by the Weston Geophysical team to this zone is m_b 7.2 (**M** 7.5).

South Carolina (26). The South Carolina source (26) is a large area covering most of South Carolina and the VEGP ESP site. The largest M_{max} assigned by the Weston Geophysical team to this zone is m_b 7.2 (**M** 7.5).

Southern Coastal Plain (104). The Southern Coastal Plain source (104) extends from New York to Alabama and from the Towaliga-Lowdenville-Kings Mountain fault trends on the west to the offshore East Coast magnetic anomaly on the east. Source 104 was designed to include the Central Virginia seismic zone, the Charleston seismic zone, and a number of Mesozoic basins. The largest M_{max} assigned by the Weston Geophysical team to this zone is m_b 6.6 (**M** 6.5).

Nine Combination Zones: (103 – 23 – 24 (C19); 104 – 22 (C20); 104 – 25 (C21); 104 – 22 – 26 (C23); 104 – 22 – 25 (C24); 104 – 28BCDE – 22 (C26); 104 – 28BCDE – 22 – 25 (C27); 26 – 25 (C33); and 104 – 28BE – 25 (C35)). Weston Geophysical specified a number of combination seismic source zones, nine of which are primary sources for the VEGP ESP site. The largest M_{max} assigned by the Weston Geophysical team to these combination zones is m_b 6.6 (**M** 6.5).

2.5.2.2.1.6 Sources Used for EPRI PSHA – Woodward-Clyde Consultants

Woodward-Clyde Consultants identified and characterized five primary seismic sources, all five located within the site region; they are:

- Charleston (includes "none of the above," NOTA) (30)
- S Carolina Gravity Saddle (Extended) (29)
- SC Gravity Saddle No. 2 (Combo C3) (29A)
- SC Gravity Saddle No. 3 (NW Portion) (29B)
- Vogtle Background

Woodward-Clyde Consultants also identified two additional seismic sources within the site region. These sources are:

- Blue Ridge Combo (31)
- Blue Ridge Combination – Alternate Configuration (31A)

Primary and additional seismic sources characterized by the Woodward-Clyde team within the site region are listed in Table 2.5.2-7. A map showing the locations and geometries of the Woodward-Clyde primary seismic sources is provided in Figure 2.5.2-5. Following is a brief discussion of each of the primary seismic sources identified by the Woodward-Clyde team.

Charleston (includes NOTA) (30). The Charleston seismic source (30) is a northeast-southwest-oriented rectangle that includes most of the Charleston earthquake MMI IX and X area and the Charleston Ashley River and Woodstock faults. Source 30 is located about 70 mi from the VEGP ESP site and was designed to capture the occurrence of Charleston-type earthquakes. The Charleston source (30) is mutually exclusive with Sources 29, 29A, and 29B; if 30 is active, the other three are inactive, and vice versa. The largest M_{max} assigned by the Woodward-Clyde Consultants team to this zone is m_b 7.5 (**M** 8.0).

S Carolina Gravity Saddle (Extended) (29). The South Carolina Gravity Saddle (Extended) source (29) covers most of South Carolina and parts of Georgia, including the VEGP ESP site. The South Carolina Gravity Saddle source (29) is mutually exclusive with Sources 29A, 29B, and 30; if 29 is active, the other three are inactive, and vice versa. The largest M_{max} assigned by the Woodward-Clyde Consultants team to this zone is m_b 7.4 (**M** 7.9), reflecting its assumption that Charleston-type earthquakes can occur in this zone.

SC Gravity Saddle No. 2 (Combo C3) (29A). The South Carolina Gravity Saddle No. 2 source (29A) is an irregularly shaped polygon set within the larger area of Source 29. The SC Gravity Saddle No. 2 source (29A) is mutually exclusive with Sources 29, 29B, and 30; if 29A is active, the other three are inactive, and vice versa. The largest M_{max} assigned by the Woodward-Clyde Consultants team to this zone is m_b 7.4 (**M** 7.9), reflecting its assumption that Charleston-type earthquakes can occur in this zone.

SC Gravity Saddle No. 3 (NW Portion) (29B). The South Carolina Gravity Saddle No. 3 source (29B) is an irregularly shaped polygon set within the larger area of Source 29 and includes the VEGP ESP site. The SC Gravity Saddle No. 3 source (29B) is mutually exclusive with Sources 29, 29A, and 30; if 29B is active, the other three are inactive, and vice versa. The largest M_{max} assigned by the Woodward-Clyde Consultants team to this zone is m_b 7.0 (**M** 7.2).

Vogtle Background. The VEGP ESP Background source is a large box containing the VEGP ESP site and covering most of South Carolina and Georgia as well as parts of adjoining states and extending offshore. This source is a background zone defined as a rectangular area surrounding the VEGP ESP site and is not based on any geological, geophysical, or seismological features. The largest M_{max} assigned by the Woodward-Clyde Consultants team to this zone is m_b 6.6 (**M** 6.5).

2.5.2.2.2 Post-EPRI Seismic Source Characterization Studies

Since the EPRI (NP-4726 1986, NP-6395-D 1989) seismic hazard project, three recent studies have been performed to characterize seismic sources within the VEGP ESP site region for PSHAs. These studies include the US Geological Survey's (USGS) National Seismic Hazard Mapping Project **(Frankel et al. 1996, 2002)**, the South Carolina Department of Transportation's seismic hazard mapping project **(Chapman and Talwani 2002)**, and the Nuclear Regulatory Commission's Trial Implementation Project (TIP) study **(Savy et al. 2002)**. These three studies are described below (i.e., Section 2.5.2.2.2.1 through 2.5.2.2.2.3). Based on review of recent studies it was determined that an update of the Charleston seismic source for the EPRI (NP-4726 1986, NP-6395-D 1989) seismic hazard project was required. This update is presented in Section 2.5.2.2.2.4. In addition, at the perimeter of the VEGP ESP site region is what is now identified as the Eastern Tennessee Seismic Zone (ETSZ). The significance of the ETSZ on the VEGP ESP seismic hazard is discussed in Section 2.5.2.2.2.5.

2.5.2.2.2.1 US Geological Survey Model **(Frankel et al. 2002)**

In 2002, the USGS produced updated seismic hazard maps for the conterminous United States based on new seismological, geophysical, and geological information **(Frankel et al. 2002)**. The 2002 maps reflect changes to the source model used to construct the previous version of the national seismic hazard maps **(Frankel et al. 1996)**. The most significant modifications to the CEUS portion of the source model include changes in the recurrence, M_{max}, and geometry of the Charleston and New Madrid sources.

Unlike the EPRI models that incorporate many local sources, the USGS source model in the CEUS includes only five sources: the Extended Margin background, Stable Craton background, Charleston, Eastern Tennessee, and New Madrid (Table 2.5.2-8). Except for the Charleston and New Madrid zones, where earthquake recurrence is modeled by paleoliquefaction data, the hazard for the large background or "maximum magnitude" zones is largely based on historical

seismicity and the variation of that seismicity. The USGS source model defines the M_{max} distribution for the Extended Margin background source zone as a single magnitude of **M** 7.5 with a weight of 1.0. The EPRI model, however, includes multiple source zones for each of the six ESTs for this region containing the eastern seaboard and the Appalachians. The EPRI M_{max} distributions for these sources capture a wide range of magnitudes and weights, reflecting considerable uncertainty in the assessment of M_{max} for the CEUS. An **M** 7.5 M_{max} is captured in most of the EPRI source zones, although at a lower weight than assigned by the USGS model.

As part of the 2002 update of the National Seismic Hazard Maps, the USGS developed a model of the Charleston source that incorporates available data regarding recurrence, M_{max}, and geometry of the source zone. The USGS model uses two equally weighted source geometries, one an areal source enveloping most of the tectonic features and liquefaction data in the greater Charleston area and the second a north-northeast-trending elongated areal source enveloping the southern half of the southern segment of the East Coast fault system (ECFS) (Table 2.5.2-8 and Figure 2.5.2-7). The Frankel et al. (2002) report does not specify why the entire southern segment of the ECFS is not contained in the source geometry. For M_{max}, the study defines a distribution of magnitudes and weights of **M** 6.8 [.20], 7.1 [.20], 7.3 [.45], 7.5 [.15]. For recurrence, Frankel et al. (2002) adopt a mean paleoliquefaction-based recurrence interval of 550 years and represent the uncertainty with a continuous lognormal distribution.

2.5.2.2.2.2 South Carolina Department of Transportation Model **(Chapman and Talwani 2002)**

Chapman and Talwani (2002) created probabilistic seismic hazard maps for the South Carolina Department of Transportation (SCDOT). In the SCDOT model, treatment of the 1886 Charleston, South Carolina, earthquake and similar events dominates estimates of hazard statewide.

The SCDOT model employs a combination of line and area sources to characterize Charleston-type earthquakes in three separate geometries and uses a slightly different M_{max} range (**M** 7.1 to 7.5) than the USGS 2002 model (Table 2.5.2-9 and Figure 2.5.2-8). Three equally-weighted source zones defined for this study include (1) a source capturing the intersection of the Woodstock and Ashley River faults, (2) a larger Coastal South Carolina zone that includes most of the paleoliquefaction sites, and (3) a southern ECFS source zone. The respective magnitude distributions and weights used for M_{max} are **M** 7.1 [.20], 7.3 [.60], 7.5 [.20]. The mean recurrence interval used in the SCDOT study is 550 years, based on the paleoliquefaction record.

2.5.2.2.2.3 The Trial Implementation Project Study **(Savy et al. 2002)**

The purpose of the Lawrence Livermore National Laboratory Trial Implementation Project (TIP) study is to “test and implement the guidelines developed by the Senior Seismic Hazard Analysis

Committee (SSHAC) developed under FIN L2503 (NRC 1997)" **(Savy et al. 2002, p. 1)**. To test the SSHAC PSHA methodology, the TIP study focuses on seismic zonation and earthquake recurrence models for the Watts Bar site in Tennessee and the VEGP site. The TIP study uses an expert elicitation process to characterize the Charleston seismic source, considering published data through 1996. The TIP study identifies multiple alternative zones for the Charleston source and for the South Carolina–Georgia seismic zone, as well as alternative background seismicity zones for the Charleston region. However, the TIP study focuses primarily on implementing the Senior Seismic Hazard Advisory Committee (SSHAC) PSHA methodology **(SSHAC 1997)** and was designed to be as much of a test of the methodology as a real estimate of seismic hazard. As a result, its findings are not included explicitly in this report.

2.5.2.2.2.4 Updated Charleston Seismic Source (UCSS) Model **(Bechtel 2006d)**

It has been nearly 20 years since the six EPRI ESTs evaluated hypotheses for earthquake causes and tectonic features and assessed seismic sources in the CEUS **(EPRI NP-4726 1986)**. The EPRI Charleston source zones developed by each EST are shown in Figure 2.5.2-10 and summarized in Table 2.5.2-10. Several studies that post-date the 1986 EPRI EST assessments have demonstrated that the source parameters for geometry, M_{max}, and recurrence of M_{max} in the Charleston seismic source need to be updated to capture a more current understanding for both the 1886 Charleston earthquake and the seismic source that produced this earthquake. In addition, recent PSHA studies of the South Carolina region **(Savy et al. 2002; Chapman and Talwani 2002)** and the southeastern United States (**Frankel et al. 2002)** have developed models of the Charleston seismic source that differ significantly from the earlier EPRI characterizations. Therefore, the Charleston seismic source was updated as part of this ESP application.

The UCSS model is summarized below and presented in detail in Bechtel (2006d). Methods used to update the Charleston seismic source follow guidelines provided in RG 1.165. An SSHAC Level 2 study was performed to incorporate current literature and data and the understanding of experts into an update of the Charleston seismic source model. This level of effort is outlined in the SSHAC (1997) report, which provides guidance on incorporating uncertainty and the use of experts in PSHA studies.

The UCSS model incorporates new information to re-characterize geometry, M_{max}, and recurrence for the Charleston seismic source. These components are discussed in the following sections. Paleoliquefaction data imply that the Charleston earthquake process is defined by repeated, relatively frequent, large earthquakes located in the vicinity of Charleston, indicating that the Charleston source is different from the rest of the eastern seaboard.

2.5.2.2.2.4.1 UCSS Geometry

The UCSS model includes four mutually exclusive source zone geometries (A, B, B', and C; Figure 2.5.2-9). The latitude and longitude coordinates that define these four source zones are presented in Table 2.5.2-11. Details for each source geometry are given below. The four geometries of the UCSS are defined based on current understanding of geologic and tectonic features in the 1886 Charleston earthquake epicentral region; the 1886 Charleston earthquake shaking intensity; distribution of seismicity; and geographic distribution, age, and density of liquefaction features associated with both the 1886 and prehistoric earthquakes. These features, shown in Figures 2.5.1-18 and 2.5.1-19, strongly suggest that the majority of evidence for the Charleston source is concentrated in the Charleston area and is not widely distributed throughout South Carolina. Table 2.5.2-10 provides a subset of the Charleston tectonic features differentiated by pre- and post-EPRI **(EPRI NP-4726 1986)** information. In addition, pre- and post-1986 instrumental seismicity, $m_b \geq 3$, are shown on Figures 2.5.1-18 and 2.5.1-19. Seismicity continues to be concentrated in the Charleston region in the Middleton Place–Summerville seismic zone (MPSSZ), which has been used to define the intersection of the Woodstock and Ashley River faults **(Tarr et al. 1981; Madabhushi and Talwani 1993)**. Notably, two earthquakes in 2002 (m_b 3.5 and 4.4) are located offshore of South Carolina along the Helena Banks fault zone in an area previously devoid of seismicity of $m_b > 3$. A compilation of the EPRI EST Charleston source zones is provided in Figure 2.5.2-10 as a comparison to the UCSS geometries shown in Figure 2.5.2-9.

Geometry A - Charleston

Geometry A is an approximately 100 x 50 km, northeast-oriented area centered on the 1886 Charleston meizoseismal area (Figure 2.5.2-9). Geometry A is intended to represent a localized source area that generally confines the Charleston source to the 1886 meizoseismal area (i.e., a stationary source in time and space). Geometry A completely incorporates the 1886 earthquake MMI X isoseismal **(Bollinger 1977)**, the majority of identified Charleston-area tectonic features and inferred fault intersections, and the majority of reported 1886 liquefaction features. Geometry A excludes the northern extension of the southern segment of the East Coast fault system because this system extends well north of the meizoseismal zone and is included in its own source geometry (Geometry C). Geometry A also excludes outlying liquefaction features, because liquefaction occurs as a result of strong ground shaking that may extend well beyond the areal extend of the tectonic source. Geometry A also envelopes instrumentally located earthquakes spatially associated with the MPSSZ **(Tarr et al. 1981; Tarr and Rhea 1983; Madabhushi and Talwani 1993)**.

The preponderance of evidence strongly supports the conclusion that the seismic source for the 1886 Charleston earthquake is located in a relatively restricted area defined by Geometry A. Geometry A envelopes (1) the meizoseismal area of the 1886 earthquake, (2) the area

containing the majority of local tectonic features (although many have large uncertainties associated with their existence and activity, as described earlier), (3) the area of ongoing concentrated seismicity, and (4) the area of greatest density of 1886 liquefaction and prehistoric liquefaction. These observations show that future earthquakes having magnitudes comparable to the Charleston earthquake of 1886 most likely will occur within the area defined by Geometry A. A weight of 0.70 is assigned to Geometry A (Figure 2.5.2-11). To confine the rupture dimension to within the source area and to maintain a preferred northeast fault orientation, Geometry A is represented in the model by a series of closely spaced, northeast-trending faults parallel to the long axis of the zone.

Geometries B, B', and C

While the preponderance of evidence supports the assessment that the 1886 Charleston meizoseismal area and Geometry A define the area where future events will most likely be centered, it is possible that the tectonic feature responsible for the 1886 earthquake either extends beyond or lies outside Geometry A. Therefore, the remaining three geometries (B, B', and C) are assessed to capture the uncertainty that future events may not be restricted to Geometry A. The distribution of liquefaction features along the entire coast of South Carolina and observations from the paleoliquefaction record that a few events were localized (moderate earthquakes to the northeast and southwest of Charleston), suggest that the Charleston source could extend well beyond Charleston proper. Geometries B and B' are assessed to represent a larger source zone, while Geometry C represents the southern segment of the East Coast fault system as a possible source zone. The combined geometries of B and B' are assigned a weight of 0.20, and Geometry C is assigned a weight of 0.10. Geometry B' a subset of B, formally defines the onshore coastal area as a source (similar to the SCDOT coastal source zone) that would restrict earthquakes to the onshore region. Geometry B, which includes the onshore and offshore regions, and Geometry B' are mutually exclusive and given equal weight in the UCSS model. Therefore, the resulting weights are 0.10 for Geometries B and B'.

Geometry B - Coastal and Offshore Zone

Geometry B is a coast-parallel, approximately 260 x 100 km source area that (1) incorporates all of Geometry A, (2) is elongated to the northeast and southwest to capture other, more distant liquefaction features in coastal South Carolina **(Amick 1990; Amick et al. 1990a, 1990b; Talwani and Schaeffer 2001)**, and (3) extends to the southeast to include the offshore Helena Banks fault zone (**Behrendt and Yuan 1987**; Figure 2.5.2-9). The elongation and orientation of Geometry B is roughly parallel to the regional structural grain as well as roughly parallel to the elongation of 1886 isoseismals. The northeastern and southwestern extents of Geometry B are controlled by the mapped extent of paleoliquefaction features [e.g., (**Amick 1990; Amick et al. 1990a, 1990b; Talwani and Schaeffer 2001**)].

The location and timing of paleoliquefaction features in the Georgetown and Bluffton areas to the northeast and southwest of Charleston have suggested to some researchers that the earthquake source may not be restricted to the Charleston area **(Obermeier et al. 1989; Amick et al. 1990a; Talwani and Schaeffer 2001)**. A primary reason for defining Geometry B is to account for the possibility that there may be an elongated source or multiple sources along the South Carolina coast. Paleoliquefaction features in the Georgetown and Bluffton areas may be explained by an earthquake source both northeast and southwest of Charleston, as well as possibly offshore.

Geometry B extends southeast to include an offshore area and the Helena Banks fault zone. The Helena Banks fault zone is clearly shown by multiple seismic reflection profiles and has demonstrable late Miocene offset **(Behrendt and Yuan 1987)**. Offshore earthquakes in 2002 (m_b 3.5 and 4.4) suggest a possible spatial association of seismicity with the mapped trace of the Helena Banks fault system (Figures 2.5.2-9 and 2.5.1-19). Whereas these two events in the vicinity of the Helena Banks fault system do not provide a positive correlation with seismicity or demonstrate recent fault activity, these small earthquakes are considered new data since the EPRI studies. The EPRI earthquake catalog **(EPRI NP-4726-A 1988)** was devoid of any events ($m_b \geq 3.0$) offshore from Charleston. The recent offshore seismicity also post-dates the development of the USGS and SCDOT source models that exclude any offshore Charleston source geometries.

A low weight of 0.10 is assigned to Geometry B (Figure 2.5.2-11), because the preponderance of evidence indicates that the seismic source that produced the 1886 earthquake lies onshore in the Charleston meizoseismal area and not in the offshore region. To confine the rupture dimension to within the source area and to maintain a preferred northeast fault orientation, Geometry B is represented in the model by a series of closely spaced, northeast-trending faults parallel to the long axis of the zone.

Geometry B' - Coastal Zone

Geometry B' is a coast-parallel, approximately 260 x 50 km source area that incorporates all of Geometry A, as well as the majority of reported paleoliquefaction features **(Amick 1990; Amick et al. 1990a, 1990b; Talwani and Schaeffer 2001)**. Unlike Geometry B, however, Geometry B' does not include the offshore Helena Banks fault zone (Figure 2.5.2-9).

The Helena Banks fault system is excluded from Geometry B' to recognize that the preponderance of the data and evaluations support the assessment that the fault system is not active and because most evidence strongly suggests that the 1886 Charleston earthquake occurred onshore in the 1886 meizoseismal area and not on an offshore fault. Whereas there is little uncertainty regarding the existence of the Helena Banks fault, there is a lack of evidence that this feature is still active. Isoseismal maps documenting shaking intensity in 1886 indicate an onshore meizoseismal area (the closed bull's eye centered onshore north of downtown

Charleston, Figure 2.5.1-19). An onshore source for the 1886 earthquake as well as the prehistoric events is supported by the instrumentally recorded seismicity in the MPSSZ and the corresponding high density cluster of 1886 and prehistoric liquefaction features.

Similar to Geometry B above, a weight of 0.10 is assigned to Geometry B' and reflects the assessment that Geometry B' has a much lower probability of being the source zone for Charleston-type earthquakes than Geometry A (Figure 2.5.2-11). To confine the rupture dimension to within the source area and to maintain a preferred northeast fault orientation, Geometry B' is represented in the model by a series of closely spaced, northeast-trending faults parallel to the long axis of the zone.

Geometry C - East Coast Fault System - South (ECFS-s)

Geometry C is an approximately 200 x 30 km, north-northeast-oriented source area enveloping the southern segment of the proposed East Coast fault system (ECFS-s) shown in Figure 3 of Marple and Talwani (2000) (Figures 2.5.2-9 and 2.5.2-12). The USGS hazard model **(Frankel et al. 2002)** (Figure 2.5.2-7) incorporates the ECFS-s as a distinct source geometry (also known as the zone of river anomalies [ZRA]); however, as described earlier, the USGS model truncates the northeastern extent of the proposed fault segment. The South Carolina Department of Transportation hazard model **(Chapman and Talwani 2002)** also incorporates the ECFS-s as a distinct source geometry; however, this model extends the southern segment of the proposed East Coast fault system farther to the south than originally postulated by Marple and Talwani (2000) to include, in part, the distribution of liquefaction in southeastern South Carolina **(Chapman 2005b)** (Figure 2.5.2-9).

In this ESP evaluation the area of Geometry C is restricted to envelope the original depiction of the ECFS-s by Marple and Talwani (2000). Truncation of the zone to the northeast as shown by the 2002 USGS model is not supported by available data, and the presence of liquefaction in southeastern South Carolina is best captured in Geometries B and B', rather than extending the ECFS-s farther to the south than defined by the data of Marple and Talwani (2000).

A low weight of 0.10 is assigned to Geometry C to reflect the assessment that Geometries B, B', and C all have equal, but relatively low, likelihood of producing Charleston-type earthquakes (Figure 2.5.2-11). As with the other UCSS geometries, Geometry C is represented as a series of parallel, vertical faults oriented northeast-southwest and parallel to the long axis of the narrow rectangular zone. The faults and extent of earthquake ruptures are confined within the rectangle depicting Geometry C.

UCSS Model Parameters

Based on studies by Bollinger et al. (1985, 1991) and Bollinger (1992), a 20-km-thick seismogenic crust is assumed for the UCSS. To model the occurrence of earthquakes in the characteristic part of the Charleston distribution (**M** > 6.7), the model uses a series of closely-

spaced, vertical faults parallel to the long axis of each of the four source zones (A, B, B', and C). Faults and earthquake ruptures are limited to within each respective source zone and are not allowed to extend beyond the zone boundaries, and ruptures are constrained to occur within the depth range of 0 to 20 km. Modeled fault rupture areas are assumed to have a width-to-length aspect ratio of 0.5, conditional on the assumed maximum fault width of 20 km. To obtain M_{max} earthquake rupture lengths from magnitude, the Wells and Coppersmith (1994) empirical relationship between surface rupture length and **M** for earthquakes of all slip types is used.

To maintain as much similarity as possible with the original EPRI model, the UCSS model treats earthquakes in the exponential part of the distribution (**M** < 6.7) as point sources uniformly distributed within the source area (full smoothing), with a constant depth fixed at 10 km.

2.5.2.2.2.4.2 UCSS Maximum Magnitude

The six EPRI ESTs developed a distribution of weighted M_{max} values and weights to characterize the largest earthquakes that could occur on Charleston seismic sources. On the low end, the Law Engineering team assessed a single M_{max} of m_b 6.8 to seismic sources it considered capable of producing earthquakes comparable in magnitude to the 1886 Charleston earthquake. On the high end, four teams defined M_{max} upper bounds ranging between m_b 7.2 and 7.5. For this ESP application, the m_b magnitude values have been converted to moment magnitude (**M**) as described previously. The m_b value and converted moment magnitude value for each team are shown below. The range in **M** for the six ESTs is 6.5 to 8.0.

Team	Charleston M_{max} range
Bechtel Group	m_b 6.8 to 7.4 (**M** 6.8 to 7.9)
Dames & Moore	m_b 6.6 to 7.2 (**M** 6.5 to 7.5)
Law Engineering	m_b 6.8 (**M** 6.8)
Rondout	m_b 6.6 to 7.0 (**M** 6.5 to 7.2)
Weston Geophysical	m_b 6.6 to 7.2 (**M** 6.5 to 7.5)
Woodward-Clyde Consultants	m_b 6.7 to 7.5 (**M** 6.7 to 8.0)

The **M** equivalents of EPRI m_b estimates for Charleston M_{max} earthquakes show that the upper bound values are similar to, and in two cases exceed, the largest modern estimate of **M** 7.3 ± 0.26 **(Johnston 1996)** for the 1886 earthquake. The upper bound values for five of the six ESTs also exceed the preferred estimate of **M** 6.9 by Bakun and Hopper (2004) for the Charleston event. The EPRI M_{max} estimates are more heavily weighted toward the lower magnitudes, with the upper bound magnitudes given relatively low weights by several ESTs (Tables 2.5.2-2 through 2.5.2-7). Therefore, updating the M_{max} range and weights to reflect the current range of technical interpretations is warranted for the UCSS.

Based on assessment of the currently available data and interpretations regarding the range of modern M_{max} estimates (Table 2.5.2-12), the UCSS model modifies the USGS magnitude

distribution **(Frankel et al. 2002)** to include a total of five discrete magnitude values, each separated by 0.2 **M** units (Figure 2.5.2-11). The UCSS M_{max} distribution includes a discrete value of **M** 6.9 to represent the Bakun and Hopper (2004) best estimate of the 1886 Charleston earthquake magnitude, as well as a lower value of **M** 6.7 to capture a low probability that the 1886 earthquake was smaller than the Bakun and Hopper (2004) mean estimate of **M** 6.9. Bakun and Hopper (2004) do not explicitly report a 1-sigma range in magnitude estimate of the 1886 earthquake, but do provide a 2-sigma range of **M** 6.4 to **M** 7.2.

The UCSS magnitudes and weights are as follows:

M	Weight	
6.7	0.10	
6.9	0.25	Bakun and Hopper (2004) mean
7.1	0.30	
7.3	0.25	Johnston (1996) mean
7.5	0.10	

This results in a weighted M_{max} mean magnitude of **M** 7.1 for the UCSS, which is slightly lower than the mean magnitude of **M** 7.2 in the USGS model **(Frankel et al. 2002)**.

2.5.2.2.2.4.3 UCSS Recurrence Model

In the 1989 EPRI study **(EPRI NP-6395-D 1989)**, the six EPRI ESTs used an exponential magnitude distribution to represent earthquake sizes for their Charleston sources. Parameters of the exponential magnitude distribution were estimated from historical seismicity in the respective source areas. This resulted in recurrence intervals for M_{max} earthquakes (at the upper end of the exponential distribution) of several thousand years.

The current model for earthquake recurrence is a composite model consisting of two distributions. The first is an exponential magnitude distribution used to estimate recurrence between the lower-bound magnitude used for hazard calculations and m_b 6.7. The parameters of this distribution are estimated from the earthquake catalog, as they were for the 1989 EPRI study. This is the standard procedure for smaller magnitudes and is the model used, for example, by the USGS 2002 national hazard maps **(Frankel et al. 2002)**. In the second distribution, M_{max} earthquakes (**M** ≥ 6.7) are treated according to a characteristic model, with discrete magnitudes and mean recurrence intervals estimated through analysis of geologic data, including paleoliquefaction studies. In this document, M_{max} is used to describe the range of largest earthquakes in both the characteristic portion of the UCSS recurrence model and the EPRI exponential recurrence model.

This composite model achieves consistency between the occurrence of earthquakes with **M** < 6.7 and the earthquake catalog and between the occurrence of large earthquakes (**M** ≥ 6.7) with paleoliquefaction evidence. It is a type of “characteristic earthquake” model, in which the

recurrence rate of large events is higher than what would be estimated from an exponential distribution inferred from the historical seismic record.

M_{max} Recurrence

This section describes how the UCSS model determines mean recurrence intervals for M_{max} earthquakes. The UCSS model incorporates geologic data to characterize the recurrence intervals for M_{max} earthquakes. As described earlier, identifying and dating paleoliquefaction features provides a basis for estimating the recurrence of large Charleston area earthquakes. Most of the available geologic data pertaining to the recurrence of large earthquakes in the Charleston area were published after 1990 and therefore were not available to the six EPRI ESTs. In the absence of geologic data, the six EPRI EST estimates of recurrence for large, Charleston-type earthquakes were based on a truncated exponential model using historical seismicity **(EPRI NP-4726 1986; NP-6395-D 1989)**. The truncated exponential model also provided the relative frequency of all earthquakes greater than m_b 5.0 up to M_{max} in the EPRI PSHA. The recurrence of M_{max} earthquakes in the EPRI models was on the order of several thousand years, which is significantly greater than more recently published estimates of about 500 to 600 years, based on paleoliquefaction data **(Talwani and Schaeffer 2001)**.

Paleoliquefaction Data

Strong ground shaking during the 1886 Charleston earthquake produced extensive liquefaction, and liquefaction features from the 1886 event are preserved in geologic deposits at numerous locations in the region. Documentation of older liquefaction-related features in geologic deposits provides evidence for prior strong ground motions during prehistoric large earthquakes. Estimates of the recurrence of large earthquakes in the UCSS are based on dating paleoliquefaction features. Many potential sources of ambiguity and/or error are associated with dating and interpreting paleoliquefaction features. This assessment does not reevaluate field interpretations and data; rather, it reevaluates criteria used to define individual paleoearthquakes in the published literature. In particular, the UCSS reevaluates the paleoearthquake record interpreted by Talwani and Schaeffer (2001) based on that study's compilation of sites with paleoliquefaction features.

Talwani and Schaeffer (2001) compiled radiocarbon ages from paleoliquefaction features along the coast of South Carolina. These data include ages that provide contemporary, minimum, and maximum limiting ages for liquefaction events. Radiocarbon ages were corrected for past variability in atmospheric ^{14}C using well established calibration curves and converted to "calibrated" (approximately calendric) ages. From their compilation of calibrated radiocarbon ages from various geographic locations, Talwani and Schaeffer (2001) correlated individual earthquake episodes. They identified an individual earthquake episode based on samples with a "contemporary" age constraint that had overlapping calibrated radiocarbon ages at

approximately 1-sigma confidence interval. The estimated age of each earthquake was "calculated from the weighted averages of overlapping contemporary ages" **(Talwani and Schaeffer 2001)** (p. 6,632). They defined as many as eight events (named 1886, A, B, C, D, E, F, and G in order of increasing age) from the paleoliquefaction record, and offered two scenarios to explain the distribution and timing of paleoliquefaction features (Table 2.5.2-13).

The two scenario paleoearthquake records proposed by Talwani and Schaeffer (2001) have different interpretations for the size and location of prehistoric events (Table 2.5.2-13). In their Scenario 1, the four prehistoric events that produced widespread liquefaction features similar to the large 1886 Charleston earthquake (A, B, E, and G) are interpreted to be large, Charleston-type events. Three events, C, D, and F, are defined by paleoliquefaction features that are more limited in geographic extent than other events and are interpreted to be smaller, moderate-magnitude events (approximately **M** 6). Events C and F are defined by features found north of Charleston in the Georgetown region, and Event D is defined by sites south of Charleston in the Bluffton area. In their Scenario 2, all events are interpreted as large, Charleston-type events. Furthermore, Events C and D are combined into a large Event C'. Talwani and Schaeffer (2001) justify the grouping of the two events based on the observation that the calibrated radiocarbon ages that constrain the timing of Events C and D are indistinguishable at the 95 percent (2-sigma) confidence interval.

The length and completeness of the paleoearthquake record based on paleoliquefaction features is a source of epistemic uncertainty in the UCSS. The paleoliquefaction record along the South Carolina coast extends from 1886 to the mid-Holocene **(Talwani and Schaeffer 2001)**. The consensus of the scientists who have evaluated these data **(Talwani and Schaeffer 2001; Talwani 2005; Obermeier 2005)** is that the paleoliquefaction record of earthquakes is complete only for the most recent about 2,000 years and that it is possible that liquefaction events are missing from the older portions of the record. The suggested incompleteness of the paleoseismic record is based on the argument that past fluctuations in sea level have produced time intervals of low water table conditions (and thus low liquefaction susceptibility), during which large earthquake events may not have been recorded in the paleoliquefaction record **(Talwani and Schaeffer 2001)**. While this assertion may be true, it cannot be ruled out that the paleoliquefaction record may be complete back to the mid-Holocene.

2-Sigma Analysis of Event Ages

Analysis of the coastal South Carolina paleoliquefaction record performed for the VEGP ESP application is based on the Talwani and Schaeffer (2001) data compilation. As described above, Talwani and Schaeffer (2001) use calibrated radiocarbon ages with 1-sigma error bands to define the timing of past liquefaction episodes in coastal South Carolina. The standard in paleoseismology, however, is to use calibrated ages with 2-sigma (95.4 percent confidence

interval) error bands [e.g., **(Sieh et al. 1989; Grant and Sieh 1994)**]. Likewise, in paleoliquefaction studies, to more accurately reflect the uncertainties in radiocarbon dating, the use of calibrated radiocarbon dates with 2-sigma error bands (as opposed to narrower 1-sigma error bands) is advisable **(Tuttle 2001)**. The Talwani and Schaeffer (2001) use of 1-sigma error bands may lead to over-interpretation of the paleoliquefaction record such that more episodes are interpreted than actually occurred. In recognition of this possibility, the conventional radiocarbon ages presented in Talwani and Schaeffer (2001) have been recalibrated and reported with 2-sigma error bands. The recalibration of individual radiocarbon samples and estimation of age ranges for paleoliquefaction events show broader age ranges with 2-sigma error bands which are used to obtain broader age ranges for paleoliquefaction events in the Charleston area.

Event ages based on overlapping 2-sigma ages of paleoliquefaction features are presented in Table 2.5.2-13. Paleoearthquakes have been distinguished based on grouping paleoliquefaction features that have contemporary radiocarbon samples with overlapping calibrated ages. Event ages have then been defined by selecting the age range common to each of the samples. For example, an event defined by overlapping 2-sigma sample ages of 100 to 200 cal yr BP and 50 to 150 cal yr BP would have an event age of 100 to 150 cal yr BP. The UCSS study considers the "trimmed" ages to represent the approximately 95 percent confidence interval, with a "best estimate" event age as the midpoint of the approximately 95 percent age range.

The 2-sigma analysis identified six distinct paleoearthquakes in the data presented by Talwani and Schaeffer (2001). As noted by that study, Events C and D are indistinguishable at the 95 percent confidence interval, and in the UCSS, those samples define Event C' (Table 2.5.2-13). Additionally, the UCSS 2-sigma analysis suggests that Talwani and Schaeffer (2001) Events F and G may have been a single, large event, defined in the UCSS as F'. One important difference between the UCSS result and that of Talwani and Schaeffer (2001) is that the three Events C, D, and F in their Scenario 1, which are inferred to be smaller, moderate-magnitude events, are grouped into more regionally extensive Events C' and F' (Table 2.5.2-13). Therefore, in the UCSS, all earthquakes in the 2-sigma analysis have been interpreted to represent large, Charleston-type events. The incorporation of large Events C' and F' into the UCSS model is, in effect, a conservative approach. In the effort to estimate the recurrence of M_{max} events (**M** 6.7 to 7.5), moderate-magnitude (about **M** 6) earthquakes C and D would be eliminated from the record of large (M_{max}) earthquakes in the UCSS model, thereby increasing the calculated M_{max} recurrence interval and lowering the hazard without sufficient justification. For these reasons the UCSS model uses a single, large Event C' (instead of separate, smaller Events C and D) and a single, large Event F' (instead of separate, smaller Events F and G). Analysis suggests that there have been four large earthquakes in the most-recent, about 2,000-year portion of the record (1886 and Events A, B, and C'). In the entire about 5,000-year

paleoliquefaction record, there is evidence for six large, Charleston-type earthquakes (1886, A, B, C', E, F'; Table 2.5.2-13). Figure 2.5.2-12a shows the geographic distribution of liquefaction features associated with each event in the UCSS model. The distributions of paleoliquefaction sites for Events A, B, C', E, and F' are all very similar to the coastal extent of the liquefaction features from the 1886 earthquake.

Recurrence intervals developed from the earthquakes recorded by paleoliquefaction features assume that these features were produced by large M_{max} events and that both the about 2,000-year and about 5,000-year records are complete. However, the UCSS mentions at least two concerns regarding the use of the paleoliquefaction record to characterize the recurrence of past M_{max} events. First, it is possible that the paleoliquefaction features associated with one or more of these pre-1886 events were produced by multiple moderate-sized events closely spaced in time. If this were the case, then the calculated recurrence interval would yield artificially short recurrence for M_{max}, since it was calculated using repeat times of both large (M_{max}) events and smaller earthquakes. Limitations of radiocarbon dating and limitations in the stratigraphic record often preclude identifying individual events in the paleoseismologic record that are closely spaced in time (i.e., separated by only a few years to a few decades). Several seismic sources have demonstrated tightly clustered earthquake activity in space and time that are indistinguishable in the radiocarbon and paleoseismic record:

- New Madrid (1811, 1811, 1812)
- North Anatolian Fault (1999 and 1999)
- San Andreas Fault (1812 and 1857)

Therefore the UCSS acknowledges the distinct possibility that M_{max} occurs less frequently than what is calculated from the paleoliquefaction record.

A second concern is that the recurrence behavior of the M_{max} event may be highly variable through time. For example, the UCSS considers it unlikely that **M** 6.7 to **M** 7.5 events have occurred on a Charleston source at an average repeat time of about 500 to 600 years **(Talwani and Schaeffer 2001)** throughout the Holocene Epoch. Such a moment release rate would likely produce tectonic landforms with clear geomorphic expression, such as are present in regions of the world with comparably high rates of moderate to large earthquakes (for example, faults in the Eastern California shear zone with sub-millimeter per year slip rates and recurrence intervals on the order of about 5,000 years have clear geomorphic expression **(Rockwell et al. 2000)**). Perhaps it is more likely that the Charleston source has a recurrence behavior that is highly variable through time, such that a sequence of events spaced about 500 years apart is followed by quiescent intervals of thousands of years or longer. This sort of variability in inter-event time may be represented by the entire mid-Holocene record, in which both short inter-event times (e.g., about 400 years between Events A and B) are included in a record with long inter-event times (e.g., about 1,900 years between Events C' and E).

Recurrence Rates

The UCSS model calculates two average recurrence intervals covering two different time intervals, which are used as two recurrence branches on the logic tree (Figure 2.5.2-11). The first average recurrence interval is based on the four events that occurred within the past about 2,000 years. This time period is considered to represent a complete portion of the paleoseismic record based on published literature [e.g., (**Talwani and Schaeffer 2001**)] and feedback from those researchers questioned **(Talwani 2005; Obermeier 2005)**. These events include 1886, A, B, and C' (Table 2.5.2-13). The average recurrence interval calculated for the most recent portion of the paleoliquefaction record (four events over the past about 2,000 years) is given 0.80 weight on the logic tree (Figure 2.5.2-11).

The second average recurrence interval is based on events that occurred within the past about 5,000 years. This time period represents the entire paleoseismic record based on paleoliquefaction data **(Talwani and Schaeffer 2001)**. These events include 1886, A, B, C', E, and F' as listed in Table 2.5.2-13. As mentioned previously, published papers and researchers questioned suggest that the older part of the record (older than about 2,000 years ago) may be incomplete. Whereas this assertion may be true, it is also possible that the older record, which exhibits longer inter-event times, is complete. The average recurrence interval calculated for the 5,000-year record (six events) is given 0.20 weight on the logic tree (Figure 2.5.2-11). The 0.80 and 0.20 weighting of the 2,000-year and 5,000-year paleoliquefaction records, respectively, reflect incomplete knowledge of both the current short-term recurrence behavior and the long-term recurrence behavior of the Charleston source.

The mean recurrence intervals for the most-recent 2,000-year and past 5,000-year records represent the average time interval between earthquakes attributed to the Charleston seismic source. The mean recurrence intervals and their parametric uncertainties were calculated according to the methods outlined by Savage (1991) and Cramer (2001). The methods provide a description of mean recurrence interval, with a best estimate mean T_{ave} and an uncertainty described as a lognormal distribution with median $T_{0.5}$ and parametric lognormal shape factor $\sigma_{0.5}$.

The lognormal distribution is one of several distributions, including the Weibull, Double Exponential, and Gaussian, among others, used to characterize earthquake recurrence **(Ellsworth et al. 1999a)**. Ellsworth et al. (1999a) and Matthews et al. (2002) propose a Brownian-passage time model to represent earthquake recurrence, arguing that it more closely simulates the physical process of strain build-up and release. This Brownian-passage time model is currently used to calculate earthquake probabilities in the greater San Francisco Bay region **(WGCEP 2003)**. Analyses show that the lognormal distribution is very similar to the Brownian-passage time model of earthquake recurrence for cases where the time elapsed since the most recent earthquake is less than the mean recurrence interval **(Cornell and Winterstein**

1988; Ellsworth et al. 1999a). This is the case for Charleston, where 120 years have elapsed since the 1886 earthquake and the mean recurrence interval determined over the past 2,000 years is about 548 years. The UCSS study has chosen to calculate average recurrence interval using a lognormal distribution because its statistics are well known **(NIST/SEMATECH 2006)** and it has been used in numerous studies [e.g.,**(Savage 1991; WGCEP 1995; Cramer 2001)**].

The average interval between earthquakes is expressed as two continuous lognormal distributions. The average recurrence interval for the 2,000-year record, based on the three most recent inter-event times (1886-A, A-B, B-C'), has a best estimate mean value of 548 years and an uncertainty distribution described by a median value of 531 years and a lognormal shape factor of 0.25. The average recurrence interval for the 5,000-year record, based on five inter-event times (1886-A, A-B, B-C', C'-E, E-F'), has a best estimate mean value of 958 years and an uncertainty distribution described by a median value of 841 years and a lognormal shape factor of 0.51. At one standard deviation, the average recurrence interval for the 2,000-year record is between 409 and 690 years; for the 5,000-year record, it is between 452 and 1,564 years. Combining these mean values of 548 and 958 years with their respective logic tree weights of 0.8 and 0.2 results in a weighted mean of 630 years for Charleston M_{max} recurrence.

The mean recurrence interval values used in the UCSS model are similar to those determined by earlier studies. Talwani and Schaeffer (2001**)** consider two possible scenarios to explain the distribution in time and space of paleoliquefaction features. In their Scenario 1, large earthquakes have occurred with an average recurrence of 454 $\pm$21 years over about the past 2,000 years; in their Scenario 2, large earthquakes have occurred with an average recurrence of 523 $\pm$100 years over the past 2,000 years. Talwani and Schaeffer (2001) state that, "In anticipation of additional data we suggest a recurrence rate between 500 and 600 years for **M** 7+ earthquakes at Charleston". For the 2,000-year record, the 1-standard-deviation range of 409 to 690 years completely encompasses the range of average recurrence interval reported by Talwani and Schaeffer (2001). The best-estimate mean recurrence interval value of 548 years is comarable to the midpoint of the Talwani and Schaeffer (2001) best-estimate range of 500 to 600 years. The best estimate mean recurrence interval value from the 5,000-year paleoseismic record of 958 years is outside the age ranges reported by Talwani and Schaeffer (2001), although they did not determine an average recurrence interval based on the longer record.

In the updated seismic hazard maps for the conterminous United States, Frankel et al. (2002) use a mean recurrence value of 550 years for characteristic earthquakes in the Charleston region. This value is based on the above-quoted 500 to 600 year estimate from Talwani and Schaeffer (2001). Frankel et al. (2002) do not incorporate uncertainty in mean recurrence interval in their calculations.

For computation of seismic hazard, discrete values of activity rate (inverse of recurrence interval) are required as input to the PSHA code (Cornell 1968). To evaluate PSHA based on mean hazard, the mean recurrence interval and its uncertainty distribution should be converted to mean activity rate with associated uncertainty. The final discretized activity rates used to model the UCSS in the PSHA reflect a mean recurrence of 548 years and 958 years for the 2,000-year and 5,000-year branches of the logic tree, respectively. Lognormal uncertainty distributions in activity rate are obtained by the following steps: (1) invert the mean recurrence intervals to get mean activity rates; (2) calculate median activity rates using the mean rates and lognormal shape factors of 0.25 and 0.51 established for the 2,000-year and 5,000-year records, respectively; and (3) determine the lognormal distributions based on the calculated median rate and shape factors. The lognormal distributions of activity rate can then be discretized to obtain individual activity rates with corresponding weights.

2.5.2.2.2.5 Eastern Tennessee Seismic Zone

The Eastern Tennessee Seismic Zone (ETSZ) is one of the most active seismic zones in Eastern North America. This region of seismicity in the southern Appalachians is described in Section 2.5.1.1.4.6. Despite its high rate of activity, the largest known earthquake was magnitude 4.6 **(Chapman et al 2002)**. No evidence for larger prehistoric earthquakes, such as paleoliquefaction features, has been discovered **(Chapman et al 2002; Wheeler 2005)**. While the lack of large earthquakes in the relatively short historical record cannot preclude the future occurrence of large events, there is a much higher degree of uncertainty associated with the assignment of Mmax for the ETSZ than other CEUS seismic source zones, such as New Madrid and Charleston, where large historical earthquakes are known to have occurred.

The EPRI source model **(EPRI NP-4726 1986)** includes various source geometries and parameters to represent the seismicity of the ETSZ. All but one of the EPRI Earth Science Teams (ESTs) modeled local source zones to capture this area of seismicity and some ESTs included more than one zone. The Law team did not include a specific, local source for the ETSZ, however the ETSZ and Giles County seismic zones were included in a larger seismic source zone called the Eastern Basement (17). A wide range of Mmax values and associated probabilities were assigned to these sources to reflect the uncertainty of multiple experts from each EST. The moment magnitude (**M**) equivalents of body-wave magnitude (m_b) Mmax values assigned by the ESTs range from **M** 4.8 to 7.5. The Dames & Moore sources for the ETSZ included the largest upper-bound Mmax value of **M** 7.5. Sources from the Woodward-Clyde and Rondout teams were also assigned large upper-bound Mmax values of **M** 7.2.

Subsequent hazard studies have used Mmax values within the range of maximum magnitudes used by the six EPRI models. Collectively, upper-bound maximum values of Mmax used by the EPRI teams ranged from **M** 6.3 to 7.5. Using three different methods specific to the Eastern Tennessee seismic source, Bollinger (1992) estimated an M_{max} of **M** 6.3. The Bollinger (1992)

model also included the possibility that the ETSZ was capable of generating a larger magnitude event and included an **M** 7.8 (m_b 7.37) with a low probability of 5% in the M_{max} distribution. The 5% weighted **M** 7.8 by Bollinger (1992) slightly exceeds the ERPI range, but the **M** 6.3 value was given nearly the entire weight (95%) in his characterization of the ETSZ. This smaller magnitude is much closer to the mean magnitude (about **M** 6.2) of the EPRI study. The Trial Implementation Project (TIP) **(Savy et al. 2002)** also provided a broad M_{max} distribution for the ETSZ. This study developed magnitude distributions for all ETSZ source zone representations that ranged from as low as **M** 4.5 to as high as **M** 7.5, with a mode of about **M** 6.5 for almost each distribution **(Savy et al. 2002**, pages F-12 to F-19 of Appendix F**)**. The broad distribution of the TIP study magnitude distribution for the ETSZ source zones is very similar to the EPRI distribution of **M** 4.8 to **M** 7.5. The USGS source model assigns a single M_{max} value of **M** 7.5 for the ETSZ **(Frankel et al 2002)**. The most recent characterizations of the ETSZ M_{max} by the USGS and TIP study consider **M** 7.5 as the largest magntitude in the distribution, and this magnitude is captured by the range of M_{max} values used in EPRI (NP-4726 1986). Therefore, it is concluded that no new information has been developed since 1986 that would require a significant revision to the EPRI seismic source model.

For the VEGP ESP site, the contribution to hazard from the ETSZ sources in the EPRI study was minimal. With the exception of the Law source 17 (Eastern Basement), none of the ETSZ sources contributed more than one percent of the site hazard, and thus were excluded from the final hazard calculations **(EPRI NP-6452-D 1989)**. The ground motion hazard at the VEGP ESP site is dominated by the Charleston seismic source, and the inclusion of new recurrence values for Charleston based on paleoliquefaction serves to increase the relative contribution of Charleston with respect to any distant source, such as the ETSZ. No modifications to the EPRI parameters for ETSZ source zones were made as part of this ESP study.

2.5.2.3 Correlation of Seismicity with Geologic Structures and EPRI Sources

The final part of the review and update of the 1989 EPRI seismic source model was a correlation of updated seismicity with the 1989 model source. The EPRI seismicity catalog covers earthquakes in the CEUS through 1984, as described in Section 2.5.2.1. Figures 2.5.2-1 through 2.5.2-6 shows the distribution of earthquake epicenters from both the EPRI (pre-1985) and updated (post-1984 through April 2005) earthquake catalogs in comparison to the seismic sources identified by each of the EPRI ESTs.

Comparison of the additional events of the updated earthquake catalog to the EPRI earthquake catalog shows:

- There are no new earthquakes within the site region that can be associated with a known geologic structure.

- There are no unique clusters of seismicity that would suggest a new seismic source not captured by the EPRI seismic source model.
- The updated catalog does not show a pattern of seismicity that would require significant revision to the geometry of any of the EPRI seismic sources.
- The updated catalog neither shows nor suggests any increase in M_{max} for any of the EPRI seismic sources.
- The updated catalog does not imply a significant change in seismicity parameters (rate of activity, b-value) for any of the EPRI seismic sources (see also Section 2.5.2.4.2).

2.5.2.4 Probabilistic Seismic Hazard Analysis and Controlling Earthquakes

PSHA is an accepted method for determining seismic design levels (RG 1.165). The PSHA developed here relies on seismic source inputs from the EPRI-SOG study **(EPRI NP-6395-D 1989a)**, which is accepted by the NRC (RG 1.165), on updates to those sources as described in Section 2.5.2.2, and on ground motion models **(EPRI 1009684 2004)** that have been accepted under other ESP applications.

The final SSE ground motion for the VEGP ESP site is developed using a performance-based approach, which has as its foundation a well-justified PSHA for the VEGP ESP site. Ground motion levels corresponding to mean annual frequencies of exceedance (MAFEs) of 10^{-4} to 10^{-6} are developed, because this range encompasses the range of motions necessary to establish the SSE ground motion under several criteria.

The seismic hazard at the VEGP ESP was first calculated using the assumptions of the EPRI (NP-6395-D 1989) study. This was to confirm that the 1989 results could be replicated. Then the seismic sources were updated with the UCSS models, including sources surrounding the Charleston source for each team, as described in Section 2.5.2.2.2. Also, the EPRI (1009684 2004) ground motion model was adopted for calculations of seismic hazard at seven structural frequencies. Sensitivity studies were conducted to determine the effects of these changes.

The seismic hazard was calculated for hard rock conditions for a range of ground motions corresponding to a range of annual frequencies of exceedance. This hard rock hazard formed the basis with which to integrate the effects of surficial materials on ground motion, to calculate the seismic hazard at a horizon appropriate for seismic design. The ASCE 43-05 2005 procedure was used to recommend an appropriate SSE seismic spectrum. This procedure requires ground motion amplitudes and slopes of seismic hazard curves in the range of 10^{-4} to 10^{-5} annual frequency of exceedance. To obtain a full design spectrum from structural frequencies of 0.1 to 100 Hz, a smooth site-specific spectral shape was fit to the seven structural frequencies for which specific seismic hazard calculations were made.

2.5.2.4.1 1989 EPRI Probabilistic Seismic Hazard Analysis, Deaggregation, and 1 Hz, 2.5 Hz, 5 Hz, and 10 Hz Spectral Velocities

PSHA calculations were initially made using the original 1989 EPRI-SOG seismic sources and ground motion assumptions **(EPRI NP-6395-D 1989)**. The purpose of this calculation was to validate Risk Engineering Inc.'s (REI) proprietary FRISK88 seismic hazard code, the EPRI-SOG seismic sources, the EPRI-SOG source combinations, and the EPRI-SOG attenuation equations, as modeled by the FRISK88 code. The results used in this replication were the peak ground acceleration (PGA) results available for VEGP site (see Appendix E, Table 3-103 of **(EPRI NP-6395-D 1989)**).

Seismic sources used to represent the seismic hazard for each of the six teams in the EPRI-SOG study are shown in Table 2.5.2-14. These are the primary sources used for the VEGP site in the original EPRI-SOG study, as documented in the EQHAZARD input files transmitted by EPRI.

The ground motion attenuation relations and their relative weights used in this analysis are those specified in the EPRI-SOG study (see Table 4-1 of **(EPRI NP-6395-D 1989)**). Following Table 4-1 of EPRI NP-6395-D, a standard deviation of (log) amplitude of 0.5 was assumed for each ground motion equation. These equations were used to calculate hard rock hazard.

The VEGP site is classified in EPRI NP-6395-D 1989 as a "Soil V" site (see Table 2-2 of **(EPRI NP-6395-D 1989)**). The site amplification factor versus PGA for this site class is shown in Figure 2-6 of EPRI NP-6395-D. To avoid having to apply site amplification factors to the rock curves, the results calculated here were compared to original EPRI-SOG hard rock results received from EPRI.

Results of this seismic hazard calculation are compared to the EPRI-SOG results in Table 2.5.2-15.

Agreement is excellent, generally within 5.1 percent in hazard for amplitudes up to 1g. For the 85 percent, replication is slightly less accurate, with a difference of -11.5 percent and -11.7 percent at 0.05g and 0.1g, respectively. This slight difference is of less concern, because the mean hazard curve is used to develop the SSE ground motions. Comparison plots of the mean, median, and 85 percent PGA hazard curves are shown in Figures 2.5.2-13 through 2.5.2-15.

This comparison validates the FRISK88 code, the EPRI-SOG seismic sources, the EPRI-SOG source combinations, and the EPRI-SOG attenuation equations.

2.5.2.4.2 Effects of New Regional Earthquake Catalog

The effects of the new regional earthquake catalog were examined by comparing seismicity rates in two regions critical to seismic hazard at the VEGP ESP site: the Charleston, South

Carolina, region and the local region in South Carolina and into Georgia around the VEGP ESP site. The importance of these regions to seismic hazard is addressed in Section 2.5.2.4.6. The effects of two seismicity catalogs were compared: (1) the EPRI-SOG **(EPRI NP-4726-A 1988)** earthquake catalog (through 1984) and (2) the EPRI-SOG catalog updated to include more recent seismicity (Section 2.5.2.1). The fundamental question to be addressed is whether or not the seismicity recorded since 1984 indicates that the seismic activity rates used in the EPRI-SOG study **(EPRI NP-6395-D 1989)** are inadequate or insufficiently conservative for assessment of the seismic hazard at the VEGP ESP site.

Seismicity rates were assessed for two sources in the site region, as follows: (1) a small rectangular source around the Charleston seismicity and (2) a triangular-shaped source representing seismicity in South Carolina and a strip of Georgia incorporating the VEGP ESP site. Figure 2.5.2-16 shows a map of these two sources, along with the earthquakes from the EPRI-SOG catalog and from the updated catalog.

The seismicity in these two sources was investigated by running program EQPARAM (from the EPRI EQHAZARD package), first for the original EPRI catalog and then using the updated EPRI catalog (through April 2005). Full smoothing of a- and b-values was selected for the comparison because this was a common choice of many of the ESTs in the EPRI-SOG study. Further, if comparisons were made on an individual degree-cell basis, the rates in some cells might increase and in others might decrease; furthermore, for a source such as the triangular South Carolina source, a composite rate would have to be used to compare seismic rates using the earthquake catalog through 1984 to those using the earthquake catalog through April 2005. The choice of full smoothing achieves this composite rate directly and automatically, since it is a composite rate for the entire source.

From the a- and b-values calculated with EQPARAM, recurrence rates were calculated for different magnitudes. Figures 2.5.2-17 and 2.5.2-18 compare the annual recurrence rates for the Charleston source and for the triangular South Carolina source, respectively. For the rectangular Charleston source, the updated catalog indicates that seismicity rates are about the same. For the triangular South Carolina source, the updated catalog indicates that seismicity rates have decreased when the seismicity from 1985 to April 2005 is added.

The conclusion is that the seismicity recorded since 1984 does not indicate that seismic activity rates have increased in those sources contributing most to the hazard at the VEGP ESP site under the assumptions of the EPRI-SOG study. Therefore, for original sources of the EPRI-SOG teams and the original seismicity rates from the EPRI-SOG **(EPRI NP-4726-A 1988)** earthquake catalog (through 1984) were used here for calculations of seismic hazard. These rates give an accurate estimate of seismicity for Charleston sources, and are slightly conservative for local sources, when compared to rates from the updated (through April 2005) catalog. Where the geometries of EPRI-SOG sources were modified to account for new

information on the Charleston earthquake source (see Section 2.5.2.4.4 below), new seismicity rates were calculated using the updated earthquake catalog (through April 2005) in order to use the most recent information available.

2.5.2.4.3 New Maximum Magnitude Information

Geological and seismological data published since the 1986 EPRI seismic source model are presented in Section 2.5.1. Based on a review of these data, there are no significant changes in the EPRI M_{max} parameters, with the exception of the Charleston seismic source. A summary of M_{max} values for each EPRI EST is provided in Tables 2.5.2-2 through 2.5.2-7.

Changes to M_{max} for the Charleston seismic source are discussed in Section 2.5.2.2.2 and in a separate Engineering Study Report **(Bechtel 2006d)**.

2.5.2.4.4 New Seismic Source Characterizations

The effect of new geoscience information is to modify the interpretations for the Charleston seismic source. The EPRI-SOG teams used an exponential model to represent earthquakes for sources in the Charleston area, and some teams adopted interpretations that included (with a low weight) the possibility that a specific Charleston source did not exist (i.e., that large earthquakes could occur in a large region in the eastern US). The new interpretation of the Charleston source (see Section 2.5.2.2.2) indicates that a unique source of large earthquakes exists with weight 1.0 and that large magnitudes occur with a rate of occurrence unrelated to the rate of smaller magnitudes. Typical recurrence intervals for large Charleston earthquakes for the EPRI-SOG teams were on the order of 2,000 years, whereas the new information indicates recurrence intervals of 500 to 1,000 years.

In addition, the geometry of the Charleston sources has changed. Some EPRI-SOG teams drew relatively broad zones within which a Charleston-size earthquake could occur or specified (under some interpretations) that Charleston-size earthquakes were not restricted to southeast South Carolina but could occur over broad areas. The new geologic and tectonic information presented in Section 2.5.2.2.2 describes a relatively restricted zone within which Charleston-size earthquakes are modeled.

These changes in rate of occurrence and location of Charleston sources generally have the effect of increasing seismic hazard at the VEGP ESP site, compared to the EPRI-SOG study. It is not possible to determine the specific effect of one change, because (for example) changing the geometry of the Charleston source affects the geometries and seismicity rates of local sources and background sources for each EPRI-SOG team. The total effect of the new geoscience information is taken into account in the revised PSHA results presented in Section 2.5.2.4.6.

Figure 2.5.2-19 (reproducing Figure 2.5.2-9 content relevant to this discussion) shows the geometry of the four sources used to characterize the Charleston seismic source (Section 2.5.2.2.2).

To update the EPRI-SOG model, these four geometries of the Charleston source were overlaid onto each of the six EPRI-SOG team sources, and new geometries were created for all EPRI-SOG team sources surrounding the Charleston source. Figure 2.5.2-20a shows an example of the original geometry, and Figures 2.5.2-20b through 2.5.2-20e show the new geometries created for the Rondout team, source 26. The purpose in creating the new geometries was to ensure that, in incorporating the new Charleston sources, no area was left without seismicity. Seismicity parameters for the new EPRI-SOG team source geometries were calculated using the same methodology and same smoothing assumptions as in the EPRI-SOG project and using the updated seismicity catalog (through April 2005). This procedure ensured that the principles underlying the seismicity representations for each EPRI-SOG team source surrounding Charleston were maintained.

The four geometries used to represent the Charleston source were modeled, for seismic hazard calculations, with parallel faults striking northeast-southwest and spaced at 10 km intervals. This spacing was narrow enough not to affect the calculated hazard (i.e., a spacing of 5 km would not have produced significantly different results). Activity rates for the faults were equally divided among the faults, and they were represented as vertical faults from the surface to a depth of 20 km. A rupture length equation (given magnitude) was used to represent a finite rupture length, and an aspect ratio (width-to-length) of 0.5 was assumed. The specific equation selected was for surface rupture length for all rupture types from Wells and Coppersmith (1994).

A characteristic earthquake was modeled for the new Charleston source geometries, with the following magnitudes and weights (Figure 2.5.2-11):

M	Weight
6.7	0.1
6.9	0.25
7.1	0.3
7.3	0.25
7.5	0.1

The magnitudes and weights were discussed in Section 2.5.2.2.2.4.2 The rate of occurrence of the characteristic earthquake was modeled with two 5-point discrete distributions representing (respectively) the 2,000-year and 5,000-year paleoliquefaction intervals described in Section 2.5.2.2.2.4.3. These distributions are as follows:

2,000-Year Interval		5,000-Year Interval	
Activity Rate	Weight	Activity Rate	Weight
1.22×10^{-3}	0.101	3.65×10^{-4}	0.101
1.45×10^{-3}	0.244	6.12×10^{-4}	0.244
1.77×10^{-3}	0.310	9.20×10^{-4}	0.310
2.16×10^{-3}	0.244	1.38×10^{-3}	0.244
2.78×10^{-3}	0.101	2.32×10^{-3}	0.101

These distributions give mean activity rates of 1.823×10^{-3} and 1.044×10^{-3}, respectively, which correspond to recurrence intervals of 548 years and 958 years, and have logarithmic shape factors of 0.25 and 0.51, as described in Section 2.5.2.2.2.4.3.

In addition to the characteristic earthquake, smaller earthquakes were modeled for each of the four source geometries for magnitudes between the lower-bound magnitude ($m_b = 5.0$) and M_{max} value of $m_b = 6.7$, with an exponential magnitude distribution. The activity rate and b-value for this distribution were determined using the EPRI-SOG catalog, EQPARAM software, and full smoothing of seismicity parameters across the source. For this exponential model, the rectangular geometries of the Charleston sources were assumed (see Figure 2.5.2-19), with earthquakes uniformly distributed within the source.

The source combinations of the EPRI-SOG teams were reviewed and modified to accurately incorporate the four new Charleston seismic sources into each team's model. This generally resulted in four times as many source combinations, because a single Charleston source was being replaced by four alternative Charleston sources. As an example, the Rondout team originally had one source combination applicable to the VEGP ESP site:

Source Combination	Weight	Sources
1	1.0	26, 24

The revised model for the Rondout team had four source combinations applicable to the VEGP ESP site:

Source Combination	Weight	Sources
1	0.7	Charleston-A, 26-A
2	0.1	Charleston-B, 26-B
3	0.1	Charleston-B´, 26-B´
4	0.1	Charleston-C, 26-C

where, for example, "26-A" indicates Rondout source 26 with new Charleston source geometry A removed. See Figures 2.5.2-20b through 2.5.2-20e for maps of these source geometries.

Incorporating this new geoscience information into the PSHA for the VEGP ESP site ensures that the PSHA results reflect the most recent information and interpretations of seismicity in the southeastern US. This provides a strong basis for the SSE ground motions.

2.5.2.4.5 New Ground Motion Models

The ground motion models developed by the 2004 EPRI-sponsored study **(EPRI 1009684 2004)** were used to examine the effects on seismic hazard of current estimates of seismic shaking as a function of earthquake magnitude and distance. For general area sources, nine estimates of median ground motion are combined with four estimates of aleatory uncertainty, giving 36 combinations. For fault sources in rifted regions, which applies to the ECFS fault segments, 12 estimates of median ground motion are combined with four estimates of aleatory uncertainty, giving 48 combinations. When both area sources and faults are active, a specific correlation of area source models and fault source models is used to represent ground motion models that might apply together. These families of models (36 for area sources, 48 for fault sources) represent the epistemic uncertainty in ground motion, and contribute to the epistemic uncertainty in seismic hazard.

Conclusions regarding a comparison of the EPRI NP-6395-D (1989) ground motion models with the EPRI 1009684 (2004) ground motion models depend on the specific magnitude, distance, and structural frequency being compared. Some comparison plots are shown in EPRI 1009684. In general, median ground motion amplitudes are similar at high frequencies. At low frequencies, the EPRI 1009684 models show lower median ground motions, because these models incorporate the possibility of a two-corner seismic source. Seismic hazard is affected by the median ground motion and also by the standard deviation. The EPRI 1009684 standard deviations are universally higher than those of EPRI NP-6395-D, which leads to higher seismic hazards.

2.5.2.4.6 Updated EPRI Probabilistic Seismic Hazard Analysis, Deaggregation, and 1 Hz, 2.5 Hz, 5 Hz, and 10 Hz Spectral Accelerations Incorporating Significant Increases Based on the Above Sensitivity Studies

Sensitivity studies were conducted to determine which magnitudes and distances contribute most to the seismic hazard at the VEGP ESP site. This was done following the guidelines of RG 1.165, modified for use in calculating SSE spectra using a performance-based procedure. Specifically, the seismic hazard was deaggregated at mean annual frequencies of exceedance (MAFEs) of 10^{-4}, 10^{-5}, and 10^{-6}. Deaggregations were conducted for two sets of spectral frequencies: a “high-frequency” set consisting of 10 Hz and 5 Hz and a “low-frequency” set consisting of 2.5 Hz and 1 Hz. Figure 2.5.2-21 shows a mean uniform hazard spectrum (UHS) for hard rock conditions at the VEGP ESP site for several MAFEs from 10^{-4} to 10^{-6}, and Table

2.5.2-16 lists the values of the mean UHS for hard rock conditions for these MAFEs for frequencies of 100 Hz (PGA), 25 Hz, 10 Hz, 5 Hz, 2.5 Hz, 1 Hz, and 0.5 Hz.

Figures 2.5.2-22 through 2.5.2-27 show the magnitude-distance deaggregations for three MAFEs and for the high- and low-frequency sets. For the low frequencies, earthquakes from the Charleston sources dominate the hazard at all MAFEs considered. For the high frequencies, local earthquakes contribute substantially to the hazard at 10^{-5} and dominate the contribution to hazard at the 10^{-6} MAFE level.

Figure 2.5.2-28 and 2.5.2-29 show marginal magnitude distributions from the deaggregations for high- and low-frequencies, respectively, for the three MAFEs. For the low frequencies, the large earthquakes from the Charleston dominate the hazard at all three MAFEs. For the high frequencies, large earthquakes dominate 10^{-4} but the smaller earthquakes dominate 10^{-6}.

Figures 2.5.2-30 and 2.5.2-31 show marginal distance distributions from the deaggregations for high- and low-frequencies, respectively, for the three MAFEs. These deaggregations are consistent with those for magnitude, in terms of the contribution of large earthquakes from the Charleston sources.

The contribution of the Charleston sources to hazard can be understood by plotting and comparing hazard curves from individual sources. Figure 2.5.2-32 shows such a comparison, using as an example the sources from the Rondout team (which is the simplest interpretation). Figure 2.5.2-32, for 10 Hz spectral acceleration, shows that the main Charleston source (geometry A, marked “C-A” in Figure 2.5.2-32, with a weight of 0.7) dominates for MAFEs of 10^{-3} to 10^{-4} but that the local source “RND-26-A” dominates for lower MAFEs (below about 3×10^{-5}). At the 10^{-6} MAFE, most of the contribution to total hazard is from the local source. Figure 2.5.2-33, showing hazard curves for the Rondout team for 1 Hz spectral acceleration, indicates that the Charleston sources dominate the total hazard at all MAFEs (at least above 10^{-7}). Note that in both Figures 2.5.2-32 and 2.5.2-33, the mean hazard curve for each source includes the probability that that source is active. Thus, the hazard curves for Charleston sources B, B´, and C (labeled C-B, C-B´, and C-C) are lower than the hazard curve for Charleston source A (labeled C-A), primarily because the former three have much lower probabilities of activity than does source A.

These results indicate that seismic sources representing earthquakes in the Charleston region have a large contribution to seismic hazard for hard rock conditions at the VEGP ESP site. The local seismic source representing seismicity in South Carolina also can have an important contribution to hazard for high frequency ground motion, particularly for MAFEs around 10^{-5} and lower.

2.5.2.5 Seismic Wave Transmission Characteristics of the Site

The uniform hazard spectra described in the preceding section are defined on hard rock (shear-wave velocity of 9,200 ft/sec), which is located more than 1,000 ft below the current ground surface at the VEGP ESP site. The subsurface materials at the VEGP ESP site are described in detail in Section 2.5.4. The material characterization is summarized in the following groups:

I Upper Sand Stratum (Barnwell Group) – predominantly sands, silty sands, and clayey sands, with occasional clay seams. A Shelly Limestone (Utley Limestone) layer was encountered at the base of the Upper Sand Stratum or the top of the Blue Bluff Marl. The limestone contains solution channels, cracks, and discontinuities, and was the cause of severe fluid loss observed during drilling for the VEGP ESP site subsurface investigation.

II Marl Bearing Stratum (Blue Bluff Marl or Lisbon Formation) – slightly sandy, cemented, calcareous clay.

III Lower Sand Stratum (comprises several formations from the Still Branch just beneath the Blue Bluff Marl to the Cape Fear just above the Dunbarton Triassic Basin rock) – fine to coarse sand with interbedded silty clay and clayey silt.

IV Dunbarton Triassic Basin Rock – red sandstone, breccia, and mudstone, weathered along the upper 120 ft.

V Paleozoic Crystalline Rock – a competent rock with high shear-wave velocity that underlies the Triassic Basin rock. The non-capable Pen Branch fault, forms the boundary between the Triassic Basin and Paleozoic basement rocks (see Section 2.5.1.2.4 for a detailed discussion of the Pen Branch fault).

The Upper Sand Stratum (Barnwell Group) will be removed because it is not considered competent material. It is susceptible to liquefaction (Section 2.5.4.8) and dissolution-related ground deformation (Section 2.5.3.8.2); also the shear-wave velocity of the Upper Sand Stratum is generally below 1000 ft/sec, see Table 2.5.4-6.

Therefore the highest in situ competent material for the VEGP ESP site is the Blue Bluff marl at 86 ft depth. Its shear-wave velocity is greater than 1000 ft/sec with the average value of 2,354 ft/sec (Section 2.5.4.4.2.1). For soil characteristics like those found at the VEGP ESP site, the "free ground surface" of a hypothetical outcrop is judged compatible with the words "free ground surface" in 100.23 (d) (1) of 10 CFR Part 100 and the guidance provided in NUREG-0800 Section 3.7.1 on defining the "free ground surface." Therefore the VEGP ESP SSE is defined in the free field on the free ground surface of a hypothetical outcrop of the Blue Bluff Marl.

All safety-related structures will be founded on structural backfill that will be placed on top of the Blue Bluff Marl after complete removal of the Upper Sand Stratum. The structural fill will be a

sandy or silty sand material following the guidelines used during construction of VEGP Units 1 and 2.

To determine the SSE at the 86-ft depth of the top of the Blue Bluff Marl it is necessary to adjust the uniform hazard hard rock spectra (presented in Section 2.5.2.4) for amplification or deamplification as vibratory ground motion is propagated through the subsurface materials above the 9,200 ft/s shear-wave velocity horizon. This section describes the analyses performed to develop site amplification functions associated with the different hard rock ground motions presented in Section 2.5.2.4. These site amplification functions are used in Section 2.5.2.6 along with the hard rock ground motions to develop site-specific SSE ground motion.

2.5.2.5.1 Development of Site Amplification Functions

2.5.2.5.1.1 Methodology

The method adopted here to account for the effects of surficial soils on seismic hazard follows the procedure in NUREG/CR-6728 and NUREG/CR-6769 (**McGuire et al. 2001, 2002**), described as "Approach 2A." This procedure requires 6 steps:

1. The seismic hazard is calculated for hard rock conditions for the seven structural frequencies, over a range of ground motion amplitudes, resulting in a range of annual frequencies of exceedance.
2. For ground motion amplitudes corresponding to annual frequencies of 10^{-4}, 10^{-5}, and 10^{-6}, the seismic hazard is deaggregated for high frequencies (HF) and low frequencies (LF), as described in Section 2.5.2.4.6, to determine the dominant magnitudes and distances for those amplitudes and frequencies.
3. HF hard rock spectra are developed to represent earthquakes dominating the 5-10 HZ ground motions, and LF hard rock spectra are developed to represent earthquakes dominating the 1-2.5 Hz ground motions. These hard rock spectra represent the mean magnitude and distance of earthquakes that dominate the seismic hazard for those structural frequencies.
4. The rock and soil column is modeled, and soil amplitudes are calculated at the control point elevation for input hard rock motions corresponding to frequencies of exceedance of 10^{-4}, 10^{-5}, and 10^{-6}. These calculations are made separately for ground motions dominating the HF hard rock motion and the LF hard rock motion, and the input motions have a spectrum determined by the HF or LF hard rock spectral shape, as appropriate. Multiple hard rock motions are used, and multiple soil column properties are used, so that the mean soil amplitudes can be determined accurately.
5. The soil amplification factors (AFs) are developed at 300 frequencies using analyses described in this section based on the HF and LF hard rock spectral shapes. The AFs

represent the mean spectral acceleration (SA) at the control point, divided by input SA at hard rock, at each frequency. At each frequency, the envelope motion is determined. This is the motion (HF or LF) that gives the higher mean soil motion, for that structural frequency and MAFE. At frequencies above 8 Hz, this is always the HF motion. At frequencies below 2 Hz, this is always the LF motion. At intermediate frequencies, the envelope motion depends on the frequency and the MAFE.

6. The uniform hazard response spectra at MAFEs of 10^{-4} and 10^{-5} at the control point location are calculated as follows. Starting from the 10^{-4} and 10^{-5} SA hard rock values (from the hazard calculations described in 2.5.2.4) at the seven structural frequencies, interpolation is performed between those SA values to obtain 10^{-4} and 10^{-5} SA values at the 300 structural frequencies using the HF and LF spectral shapes for hard rock. The choice of HF or LF is based on the envelope motion determined in the previous step. The UHS for 10^{-4} at the control point location is calculated by multiplying the hard rock 10^{-4} SA values at the 300 frequencies by the mean AFs for 10^{-4} from step 5, again using the HF or LF mean AF corresponding to the envelope motion. (At some intermediate frequencies between 2 and 8 Hz, the HF and LF AFs are weighted in order to achieve a smooth transition between HF and LF spectra.) The UHS for 10^{-5} is calculated in a similar way, using the 10^{-5} rock SA values and the 10^{-5} AFs.

This gives an accurate calculation of the soil hazard at the desired control point elevation. In step 3, it is sufficiently accurate to use the mean magnitude to generate spectral shapes for the HF and LF spectra (Approach 2A of NUREG/CR-6728 and NUREG/CR-6769 **(McGuire et al. 2001, 2002)**). Using multiple magnitudes (Approach 2B of NUREG/CR-6728 and NUREG/CR-6769) does not materially affect the calculated soil spectra, as documented in NUREG/CR-6769 **(McGuire et al. 2002)**.

From the 10^{4} and 10^{-5} SA values at the control point elevation, design spectra are calculated using the procedure recommended by ASCE 43-05 2005. This procedure is used to establish the SSE spectral amplitudes at the 300 structural frequencies. To obtain a final horizontal SSE, spectrum smoothing of the raw spectral shape is performed as described in 2.5.2.6.3.

2.5.2.5.1.2 Base Case Soil/Rock Column and Uncertainties

Development of a base case soil/rock column, is described in Section 2.5.4. Summaries of the low strain shear wave velocity, material damping, and strain-dependency properties of the base case materials, as these parameters are used in the site response analyses, are provided below in Section 2.5.2.5.1.2.1. Section 2.5.2.5.1.2.2 describes the methodology and results of randomization to address the uncertainties in soil/rock column parameters.

2.5.2.5.1.2.1 Base Case Soil/Rock Column

2.5.2.5.1.2.1.1 Soil Column

The base case shear-wave velocity model for the soil column is provided in Figure 2.5.4-7, and the corresponding values are listed in Table 2.5.4-11. The base case assumes that the uppermost 86 feet of native material will be excavated and replaced with structural fill. Shear-wave velocity was not measured for the compacted backfill during the ESP subsurface investigation (APPENDIX 2.5A). Interpolated values based on measurements made on fill for existing Units 1 and 2 **(Bechtel 1984)** are used instead. The backfill shear-wave velocity values are summarized in Table 2.5.4-10 (these values are also included in Table 2.5.4-11).

The variation with strain of shear modulus and damping of the soil were developed for two sets of degradation relationships:

- Based on relationships developed for EPRI **(EPRI TR-102293 1993)** and
- Based on relationships developed for SRS **(Lee 1996)**.

The EPRI relationships are widely used and accepted in the industry and, while the SRS curves were developed for the adjacent SRS site, the Blue Bluff Marl soil unit at the ESP site has higher velocities than the corresponding soil unit at the SRS site. Analyses are performed for both sets of degradation curves and equally weighted in developing the final spectral amplification factors. Details of the derivation and extension of the degradation curves are presented in Section 2.5.4.7.2.

The base case degradation curves for shear modulus and damping for the EPRI-based assumption are presented in Figures 2.5.4-9 and 2.5.4-11, respectively. The base case degradation curves for shear modulus and damping for the SRS-based assumption are presented in Figures 2.5.4-10 and 2.5.4-12, respectively. The corresponding tables of values are presented in Table 2.5.4-12 and 2.5.4-13, for the EPRI-based and SRS-based relationships, respectively.

Unit weights, derived from the ESP laboratory testing program (APPENDIX 2.5A) for the shallow soils and calculation **(WSRC 1998)** for the deep sands are provided in Table 2.5.4-4.

2.5.2.5.1.2.1.2 Rock Column

Due to the geometry of the Pen Branch fault, the shear-wave velocity character of the Triassic Basin and Paleozoic crystalline rocks below the Coastal Plain sediments, and the possible presence of a low velocity zone between the Triassic Basin and the Paleozoic crystalline rocks, a set of six (6) rock column models were used in combination with the base case soil column, described above, to adequately model uncertainty in the rock/soil column for site response analysis.

As discussed in Section 2.5.4.2.5, a rock density of 2.75 gm/cc (172 pcf) is used for the crystalline rock, and 2.53 gm/cc (158 pcf) for the Triassic rock. Based on inspection of Figures 2.5.4-11 and 2.5.4-12, the low strain damping of soils is on the order of 0.5 percent, which generally increases to 0.6 percent to 2 percent for strain compatible conditions. Rock, which would be expected to have lower damping than soil, was therefore assumed to behave as a linearly elastic material with one percent damping for all rock types.

The above-described shear-wave velocity profile, degradation relationships, and material densities were then used to develop randomized soil/rock profiles described in the following section.

2.5.2.5.1.2.2 Randomization of Site Profiles

To account for variations in shear-wave velocity across the site, sixty artificial profiles were generated using the stochastic model described in EPRI **(EPRI TR-102293 1993)** and extended in Toro (1996), with some modifications to account for the conditions at the VEGP ESP site. These artificial profiles represent the soil/rock column from the top of the Paleozoic crystalline rock (with a shear-wave velocity of 9,200 feet/s) to the ground surface. This model uses as inputs the following quantities: (1) the median shear-wave velocity profile, which is equal to the base-case soil and rock profiles defined in Sections 2.5.2.5.1.2.1.1 and 2.5.2.5.1.2.1.2; (2) the logarithmic standard deviation of shear-wave velocity as a function of depth, which is set to 10 percent for the structural backfill, is set to values obtained from soil-randomization studies performed at the SRS site **(Toro 1997; Toro 2005)** for the soil strata, and is set to values consistent with the six rock-column models described in Section 2.5.2.5.1.2.1.2; (3) the correlation coefficient between velocities in adjacent layers, which is taken from the second SRS soil-randomization study referenced above; (4) the probabilistic characterization of layer thickness as a function of depth, which is taken from the second SRS soil-randomization study referenced above, modified to allow for sharp changes in the base-case velocity profile; and (5) the depth to bedrock, which is randomized to account for the range of depths associated with the Pen Branch fault described in Section 2.5.2.5.1.2.1.2.

Figure 2.5.2-34 depicts the summary statistics for the 60 shear-wave velocity profiles. It is worth noting that the depth to the Blue Bluff Marl and to the Triassic Basin rock vary little between the profiles, and that the logarithmic standard deviation in shear-wave velocity is lower than typical values (e.g., **(Toro 1996)**). These features are a consequence of the availability of shear-wave velocity data from the VEGP ESP site and from the nearby SRS, and of the uniformity exhibited by these data. As a consequence of this uniformity, the average amplification factors computed from site-response calculations using these profiles may not be as smooth as those obtained using artificial profiles with more variability.

The degradation curves for shear modulus and damping were also randomized to account for the epistemic and aleatory uncertainty in these properties. These randomizations used as input

the following quantities: (1) the median degradation curves, which are equal to the base-case degradation curves in Sections 2.5.2.5.1.2.1.1 and 2.5.2.5.1.2.1.2; (2) the uncertainties in the degradation properties of soil, which are taken from Costantino (1996), except for the engineered backfill, for which they are reduced by 1/3; and (3) the uncertainty in the damping ratio for the Triassic Basin rock, which is represented by a 5-95 percentile range of 0.7-1.5, which corresponds to a logarithmic standard deviation of 0.41. For each randomized velocity profile, one set of randomized degradation curves was generated for the EPRI curves and another set was generated for the SRS curves.

2.5.2.5.1.3 Development of Low-Frequency and High-Frequency Target Spectra

Spectrum-compatible target spectra were developed for the two different frequency ranges: HF (5-10 Hz) and LF (1-2.5 Hz), as defined in Reg. Guide 1.165, at each of three annual probability levels (10^{-4}, 10^{-5}, and 10^{-6}). The target spectra are based on the computed mean magnitude (Mbar) and distance (Dbar) values from the deaggregation of the hazard curves. For the HF cases (5-10 Hz), only those sources less than 105 km were used to compute the Mbar and Dbar values. For the LF cases (1-2.5 Hz), only those sources at distances greater than 105 km were used to compute the Mbar and Dbar values. This distinction was made based on the noted dominance of the Charleston source for low frequencies and long return periods. The computed Mbar and Dbar results were based on the average of the 5 – 10 Hz values for the HF cases and the average of the 1 – 2.5 Hz for the LF cases. These computed values are given in Table 2.5.2-17. Based on the similar Mbar and Dbar values for each of the three probability levels for the HF and LF cases, a single recommended Mbar and Dbar pair was selected to represent the computed values for each of the HF and LF cases. For the LF case, the recommended distance was set at 130 km to model the Charleston source. For the HF case, the recommended distance is approximately equal to the log-average of the three computed values rounded to the nearest km. The recommended magnitude value is approximately equal to the linear average of the three computed magnitude values. The recommended magnitude values for both the high- and low-frequency cases are equal to the linear average of the three magnitude values rounded to the nearest tenth of a magnitude unit.

Given the Mbar and Dbar values, the Central and Eastern United States spectral shape (log-average of the single and double corner source models) from NUREG/CR-6728 **(McGuire et al. 2001)** were computed for both the HF and LF cases. These spectral shapes were scaled to the corresponding uniform hazard spectral (UHS) values (see Table 2.5.2-16) at 7.5 Hz and 1.75 Hz for the HF and LF cases, respectively. An additional requirement that the envelop spectrum of the scaled target spectra for a given annual probability level be no less than 90 percent of the UHS was applied. In any case for which this requirement was not met, either the scaled HF or LF target spectrum was increased to meet this requirement at the seven frequencies at which the hard rock UHS is computed. For the HF case, this requirement caused an increase of the

25 Hz spectral acceleration value at the 10^{-6} probability level. For the LF case at all three probability levels, the scaled LF spectra fall below the 90 percent UHS limit at 1 and 0.5 Hz. Thus, the scaled LF spectra were increased to 90 percent of the UHS value for the 1 and 0.5 Hz values, and for frequencies less than 0.5 Hz, the spectral shape of the LF spectrum scaled to the 90 percent of the 0.5 Hz UHS value was used.

The scaled spectra were interpolated (log-log) to the recommended sampling rate of 100 equally log spaced values per frequency decade. The HF and LF target spectra for the three annual probability levels used to develop the spectrum-compatible time histories are shown in Figures 2.5.2-35a and b.

2.5.2.5.1.4 Selection of Seed Time Histories

The selection of the seed input time histories used in the spectral matching procedure was guided by the deaggregation results described in the previous section. For the HF case, the recommended Mbar and Dbar values are 5.6 and 12 km. For the low frequency case, the recommended Mbar and Dbar values are 7.2 and 130 km. These values were considered appropriate for all three MAFEs. Based on these recommended magnitude and distance values, a total of 30 seed time histories were selected for both the HF and LF cases.

Based on the limited number of strong ground motion acceleration time histories from stations located in the Eastern North America, 58 of the 60 selected seed input time histories were recorded at stations located in other regions than the Eastern North America. The additional two seed time histories that are used for the HF case were recorded in Eastern Canada. Time histories were selected based on the database of recorded strong ground motion records, recommended magnitude and distance values, and shear-wave velocities in the top 30 meters at recording sites of greater than 600 m/sec (about 1,970 ft/sec). The selected seed time histories are listed in Table 2.5.2-18A and Table 2.5.2-18B, for the HF and LF cases, respectively.

The spectral matching was performed based on a given horizontal target spectra with a spectral damping of 5 percent. The spectral matching procedure is a time domain spectral matching procedure and emphasis was placed on maintaining the phasing characteristics of the initial time history in the final modified spectrum-compatible time history. In addition, emphasis was placed on maintaining the characteristic of the normalized Arias intensities (the integral of the square of the acceleration-time history, a ground motion parameter that captures the potential destructiveness of an earthquake) of the initial and final modified spectrum-compatible time histories. The spectral matching criteria given in NUREG/CR-6728 **(McGuire et al. 2001)** that are applicable with the use of multiple time histories were used to check the average spectrum from the 30 time histories for a given frequency range (high- or low-frequency) and annual probability level. This is the recommended procedure in NUREG/CR-6728 **(McGuire et al. 2001)** when multiple time histories are being generated and used.

The selected 60 seed time histories were first matched to their respective 10^{-6} high and low frequency target spectra. As an example, the acceleration, velocity, and displacement time histories for one of the thirty 10^{-6} HF target spectrum seed time histories are shown in Figure 2.5.2-45a. The final modified spectrum-compatible acceleration, velocity, and displacement time histories (matched to the 10^{-6} HF target spectrum) are plotted in Figure 2.5.2-45b. Figure 2.5.2-46 shows the 10^{-6} HF target spectrum (thick grey line), the response spectrum from the initial acceleration time history scaled to the target PGA value (thin blue line), and the response spectrum from the final modified spectrum-compatible time history (thin red line). The initial and final modified spectrum-compatible normalized Arias intensities for this example are plotted in Figure 2.5.2-47. These results are representative of the goodness of fit for all spectrum-compatible time histories. For the 10^{-5} probability level, the final modified spectrum-compatible time histories from the 10^{-6} probability level were used as the input time histories for the spectral matching. In a similar fashion, the final modified spectrum-compatible time histories for the 10^{-5} probability level were used as the input time histories for the spectral matching at the 10^{-4} probability level. The results of the spectral matching for the high and low frequency cases at each of the three annual probability levels are shown in Figures 2.5.2-36a through f. These spectrum-compatible time histories were used in the site response analysis presented in the next section.

2.5.2.5.1.5 Site Response Analyses

The site response analyses were conducted using randomized shear-wave velocity profiles and soil modulus and damping relationships discussed in Section 2.5.2.5.1.2.1.3 to account for variation in the dynamic soil properties across the VEGP ESP Site. Two separate sets of degradation relationships for shear modulus and damping were applied in the site response analyses: EPRI-based curves and SRS-based curves (see Section 2.5.2.5.1.2). The depth to hard rock (V_s > 9200 fps) was also randomized to reflect its uncertainty. All site response analyses assumed that the sedimentary rock below 1049 ft (depth to bottom of Coastal Plain sediments) remains linear during earthquake shaking with one percent damping for all rock types. This randomization process resulted in 60 randomized soil/rock profiles (that included combinations of depths to hard rock and degradation relationships) for each family of degradation curves (i.e., EPRI or SRS). Additional details about the generation of profiles for the site response analyses are included in Section 2.5.2.5.1.2.

Each of the 60 randomized soil profiles were paired with 30 seed time histories (each time history was applied to two of the randomized soil profiles) for each of the hard rock input motions (i.e., 30 time histories for the HF spectra and 30 time histories for the low frequency spectra). Three different mean annual frequency of exceedance events (10^{-4}, 10^{-5}, and 10^{-6}, see Section 2.5.2.5.1.3) were analyzed for each profile - seed time history pairing in order to

calculate the amplification at the top of Blue Bluff Marl (86-ft depth) resulting from input motion at the 9,200 ft/s shear-wave velocity horizon.

The computer program SHAKE **(Bechtel 2000)** was used to perform these analyses. Amplification between the top of Blue Bluff Marl (86-ft depth) and the input motion, in terms of five percent damped acceleration spectral ratios, was extracted from each analysis resulting in 720 spectral amplifications (see Table 2.5.2-19).

The mean of the site amplification functions based on the suite of multiple input spectrum-compatible time histories for each group of 60 randomized soil profiles was used to develop site amplification factors for the VEGP ESP Site, as described in NUREG/ CR-6728 **(McGuire et al. 2001)**.

Figure 2.5.2-37 depicts the mean spectral amplification results of a typical analysis for HF content of a 10^{-4} MAFE seismic event using EPRI degradation curves. The average curve shown was determined by averaging the logarithms of amplification values for each frequency. As described in Section 2.5.2.5.1.2.1.1, analyses are performed for both sets of degradation curves and equally weighted in the subsequent development of the final spectral amplification factors.

In order to implement site response analysis Approach 2A, as discussed in Section 2.5.2.5.1.1, the amplification factors are prepared as a function of hard rock input motion. Tables 2.5.2-20a and 2.5.2-20b present the amplification factors at the top of the Blue Bluff Marl {depth 86 feet} for input rock motions corresponding to 10^{-4}, 10^{-5}, and 10^{-6} HF and LF MAFE spectra respectively (see Figures 2.5.2-35a and b). These results are presented for 30 structural frequencies, including the seven structural frequencies at which seismic hazards were calculated.

2.5.2.6 Safe Shutdown Earthquake Ground Motion

2.5.2.6.1 Criterion for SSE

The criterion used to calculate the recommended design spectrum comes from ASCE 43-05 **(ASCE 2005).** This criterion is based on the mean seismic hazard curves for multiple structural frequencies at the prescribed elevation, taking into account the effect of rock and soil above the hard rock horizon. The spectral amplitudes at this elevation corresponding to a mean annual frequency of exceedance (MAFE) of 10^{-4} are scaled so that structures and components designed to the scaled spectral amplitudes will achieve a target performance goal corresponding to a mean annual frequency of onset of significant inelastic deformation (FOSID) of 10^{-5} per year. The soil hazard curves that form the basis for this calculation were developed following Approach 2A as described in Section 2.5.2.5.1.1.

2.5.2.6.2 Discrete Frequency SSE Response Spectrum Amplitudes

Table 2.5.2-21 shows ground motion amplitudes corresponding to MAFEs of 10^{-4}, 10^{-5}, and (for information purposes only) 10^{-6} for hard rock conditions (thirty structural frequencies are tabulated including, the seven frequencies developed in Section 2.5.2.4 and an additional twenty three frequencies from the 300 frequency values per step 6 of 2.5.2.5.1.1). Table 2.5.2-21 also shows ground motion amplitudes for the free ground surface of a hypothetical outcrop point of the highest competent in situ layer (top of Blue Bluff Marl); these were calculated from the hard rock motions and the amplification factors of Section 2.5.2.5.

The SSE (the design response spectrum (DRS) in the nomenclature of the ASCE 43-05 **(ASCE 2005)**) is derived from the amplitudes for MAFEs of 10^{-4} and 10^{-5} in Table 2.5.2-21. That is, the Amplitude Ratio, A_R, of 10^{-5} to 10^{-4} amplitudes is determined for spectral accelerations (SA) at each structural frequency:

$$A_R = SA(10^{-5})/SA(10^{-4}) \qquad \text{(Equation 2.5.2-4)}$$

and the SSE is calculated as:

$$SSE = SA(10^{-4}) \times \max(1.0, 0.6\, A_R^{0.8}) \qquad \text{(Equation 2.5.2-5)}$$

Table 2.5.2-22 shows thirty of the SSE values calculated from Equation 2.5.2-5, at the free ground surface of a hypothetical outcrop of the top of Blue Bluff Marl. In Table 2.5.2-22, the last term in Equation 2.5.2-5, $0.6\, A_R^{0.8}$, is indicated as "DF2" in the table.

2.5.2.6.3 Full SSE Spectrum

The SSE values at the 300 structural frequencies, thirty of which are provided in Table 2.5.2-22, are used to define the raw SSE ground motion response spectrum. This spectrum is then smoothed by a running average filter for the 100-points-per-decade spectral amplitudes above 1 Hz, but is constrained to go through the seven structural frequencies at which hazard calculations were made. (An exception was made for 5 Hz, where the site amplification analysis indicated a trough, so the 5 Hz SSE value was smoothed based on amplitudes at adjacent frequencies, which raised the 5 Hz SSE value slightly and improved the shape of the spectrum.) This step smooths out the spectral peaks and troughs above 1 Hz that are not statistically significant, but maintains the low-frequency peaks and troughs representing lower-mode soil column response for this site.

Figure 2.5.2-38 shows the raw spectrum and the smoothed SSE Spectrum. The smoothed spectrum is the VEGP ESP horizontal SSE and is specified at the free ground surface of a hypothetical outcrop of the top of the Blue Bluff marl. Figure 2.5.2-44 also shows the VEGP ESP horizontal SSE.

2.5.2.7 Vertical SSE Spectrum.

The method to develop the vertical SSE is to develop a vertical-to-horizontal scaling factor [V/H], which is then applied to the horizontal SSE, presented above.

2.5.2.7.1 Development of V/H

Reg. Guide 1.60 presents acceptable standard response spectral shapes as a function of frequency that may be considered for the seismic design of nuclear power plants. These shapes are given for both horizontal and vertical ground motions as a function of damping. The shapes are independent of peak ground acceleration (PGA), which is used as a scaling factor. The ratio of the vertical to horizontal spectral shapes results in a V/H scaling function that is a value of 2/3 for frequencies less than 0.25 Hz, 1.0 for frequencies higher than 3.5 Hz, and varies between 2/3 and 1 for frequencies between 0.25 and 3.5 Hz.

A significant increase in the number of strong ground motion observations and advances in earthquake ground motion modeling since the publication of Reg. Guide 1.60 suggest that the V/H ratios implied in Reg. Guide 1.60 may not be appropriate for a given site **(EPRI TR-102293 1993; McGuire et al. 2001)**. The horizontal and vertical ground motions and the V/H ratios are observed to depend on magnitude, distance, site conditions, and regional tectonic setting (e.g. western US [WUS] vs. central and eastern US [CEUS]), which presents distinctive characteristics of earthquake source, attenuation along regional path, and shallow crust).

NUREG/CR-6728 **(McGuire et al. 2001)** presents V/H ratios for soft rock WUS sites and hard rock CEUS sites as a function of horizontal peak acceleration, as a proxy for the combined dependence on magnitude and distance. While the WUS rock V/H ratios are based on the significant empirical database of WUS strong ground motion, there are too few CEUS recordings to develop empirically-based CEUS V/H relations. NUREG/CR-6728 follows up on a technique presented in EPRI TR-102293 of using earthquake ground motion modeling to develop CEUS rock V/H. Due to assumptions and the estimation of various required parameters, the explicit results of the CEUS modeling are not considered robust, but can be used as guidelines for the difference between V/H ratios for WUS and CEUS rock sites. For the rock CEUS V/H ratios NUREG/CR-6728 uses the WUS ratios and modifies them based on the difference in trends obtained between WUS and CEUS rock sites from their modeling studies. For example, a peak in the V/H ratio is expected to occur at higher frequencies for CEUS than for WUS sites because site kappa values in the CEUS are typically lower than in the WUS.

The VEGP ESP site, however, is a deep soil site, not a hard rock site. V/H relations for soil sites are not given in NUREG/CR-6728 **(McGuire et al. 2001)**, and, again, an insufficient number of ground motion observations have been made to develop empirical CEUS relationships for soil sites. Appendix J of NUREG/CR-6728, however, does discuss the use of modeling by which V/H ratios can be developed for CEUS soil sites. The method mirrors that

used in NUREG/CR-6728 in developing the CEUS rock V/H relations, and can be represented by the following formula:

$$V/H_{CEUS,Soil} = V/H_{WUS,Soil,Empirical} * [V/H_{CEUS,Soil,Model} / V/H_{WUS,Soil,Model}] \quad \text{(Equation 2.5.2-6)}$$

The first term of Equation 2.5.2-6 can be a readily available WUS relationship, such as Abrahamson and Silva (1997), which presents both vertical and horizontal ground motion attenuation relations for deep soil sites. Magnitude and distance is specified, which allows hazard contribution-appropriate specification for a given location.

The second term is a WUS-to-CEUS "transfer function" to modify the WUS ratios from the first term to give the required $V/H_{CEUS,Soil}$. The development of this second term entails ground motion modeling of both CEUS [numerator] and WUS [denominator] ground motions appropriate for the given site (e.g., the major contributing or controlling earthquake by magnitude and distance) and considers the site-specific conditions. The model for developing $V/H_{WUS,Soil,Model}$ considers generic site soil conditions, as implicitly considered in the $V/H_{WUS,Soil,Empirical}$ term. The model for developing $V/H_{CEUS,Soil,Model}$ model can consider as site-specific soil conditions as possible.

Upon developing $V/H_{CEUS,Soil}$ from Eq. 2,5,2-6, the vertical SSE response spectrum is then defined by

$$Sa_{SSE,Vertical} = Sa_{SSE,Horizontal} * V/H_{CEUS,Soil} \quad \text{(Equation 2.5.2-7)}$$

As discussed above, the first term on the right-hand side of Equation 2.5.2-6 can be implemented using the ground motion attenuation relationship of Abrahamson and Silva (1997). The development of the WUS-to-CEUS transfer function (the second right-had side term of Equation 2.5.2-6) needs significant analytical effort, contains potentially significant uncertainties, and requires a number of assumptions. Two studies guide the development of a best estimate of $V/H_{CEUS,Soil}$ and, through Equation 2.5.2-7, the definition of the vertical SSE response spectrum.

2.5.2.7.1.1 Estimate of V/H from NUREG/CR-6728

Appendix J of NUREG/CR-6728 **(McGuire et al. 2001)** discusses various characteristics of vertical strong motions and, building upon the work presented in EPRI TR-102293, presents the methodology to estimate V/H for CEUS rock and soil sites. This method is that represented by Equation 2.5.2-6, above. A generic CEUS soil column is considered in their presentation of the method. In the appendix, plots of the numerator and denominator of the WUS-to-CEUS transfer function are shown, Figures J-32 and J-31, respectively, for **M**6.5 and a suite of distances [1, 5,

10, 20, and 40km]. An estimate of the WUS-to-CEUS transfer function can be made for **M**6.5 at the given distances using these results shown in these figures.

As discussed above, the SSE response spectrum is based on slopes of the 10^{-4} and 10^{-5} ground motion hazard curves and the scaling of the 10^{-4} ground motions. For a hypothetical outcrop point at the 86-foot depth top of the Blue Bluff Marl, the resulting horizontal SSE ground motions at the seven spectral control points are generally only slightly higher than the 10^{-4} ground motion levels. That is, the horizontal SSE is dominated by the 10^{-4} ground motion.

In reviewing the high-frequency distance deaggregation at the 10^{-4} hazard level (Figure 2.5.2-30), about one-quarter of the hazard is coming from "near" events, or about distances less than 20 km, while about three-quarters of the hazard is coming from "far" events, or distances centered at about 130 km. In reviewing the corresponding distance deaggregation at the 10^{-5} hazard level in the same figure, the bimodal nature of the deaggregation is yet apparent, but the relative contribution of the near and far events is about the same.

In reviewing the low-frequency magnitude-distance deaggregations at both the 10^{-4} and 10^{-5} hazard levels (Figure 2.5.2-31), hazard contribution is clearly dominated by the distant event centered on about 130 km.

The magnitudes and distances that can be attributed to the near and far events are taken as those used in the development of the high-frequency and low-frequency target spectra for the site response analysis: **M**5.6 at a distance of 12 km and **M**7.2 at a distance of 130 km, respectively.

Figure 2.5.2-39 is a plot of the first term of Equation 2.5.2-6 for both near and far events using the attenuation relationship of Abrahamson and Silva (1997).

Figure 2.5.2-40 is a plot of estimates of the second term of Equation 2.5.2-6 (ratio of V/H ratios) developed as the quotient of the curves in NUREG/CR-6728 **(McGuire et al. 2001)** Figure J-32 and J-31 for highest available distances of 10, 20, and 40 km. The Appendix J figures are given only for **M**6.5. Therefore, an estimate of an equivalent ground motion proxy magnitude and distance must be made to estimate the second term of Equation 2.5.2-6. The **M**6.5, 20 km curve may be considered a reasonable proxy for the "near" event of **M**5.6 at 12 km. The greatest distance given in the two figures of Appendix J is 40 km, so this has to be used as the proxy, along with the associated **M**6.5, for the "far" event of **M**7.2 at 130 km. Given the trend of the V/H values (decreasing with distance for a given magnitude), it is expected that the "far" event proxy may be conservative (high in value), as compared to the value expect if equivalent ratio of ratio curves had been explicitly available for **M**7.2 at 130 km. Figure 2.5.2-40 shows the recommended "near" and "far" versions of the second term of Equation 2.5.2-6. Some smoothing has been applied that may be reflecting certain aspects (peaks, valleys) of the response reflecting the generic soil models used.

Figure 2.5.2-41 is a plot of $V/H_{CEUS,Soil}$ of Equation 2.5.2-6 considering both "near" and "far" events. Given the observations made earlier with regard to the relative contributions of the deaggregation "near" and "far" events to the 10^{-4} and 10^{-5} hazards, and the relative contribution of these two hazard levels to the horizontal SSE design response spectrum, the "near" and "far" estimates of $V/H_{CEUS,Soil}$ are weighted approximately 1:3, resulting in the final $V/H_{CEUS,Soil}$ shown in Figure 2.5.2-41, as derived from the available results in NUREG/CR-6728.

2.5.2.7.1.2 Estimate of V/H from Lee (2001)

As a second estimate of the required V/H ratio, the results of the study for the MOX Fuel Fabrication Facility [MFFF] at the Savannah River Site are considered **(Lee 2001)**. The methodology used in that study followed the same approach as presented in NUREG/CR-6728 and EPRI TR-102293, and used in the section above, with the primary exception that the function $V/H_{CEUS,Soil,Model}$ of Equation 2.5.2-6 is developed using a site-specific model of the soil conditions. Lee (2001) notes that the following vertical and horizontal modeling assumptions are made based on validations:

Vertical motions are modeled as a combination of pure SV-waves and SV-P converted waves arriving at the base of the soil/alluvium materials at inclined angles of incidence computed using ray tracing methods;

Horizontal component spectra are computed assuming pure S-waves arriving at vertical incidence;

Linear elastic analysis is assumed for computing the vertical motions;

Low strain behavior (i.e., no wave induced dynamic strain degradation) compressional and shear-wave site velocity profiles are used in computing vertical spectra;

Damping for computing vertical spectra is the low strain level damping used to compute horizontal spectra;

For computing horizontal motions, wave induced dynamic strain degradation of the shear-wave velocity and increased damping of the profile is permitted (in an equivalent linear analysis).

The consequence of these assumptions is that the model-derived V/H ratios (particularly for the MFFF site) may be conservatively high over some range of spectral frequencies and at high loading levels.

Lee (2001) directly presents final V/H ratios (i.e., the resulting $V/H_{CEUS,Soil}$ of Equation 2.5.2-6) for several magnitudes and distances. V/H ratios for **M**5.5 at 10 and 20 km and **M**6.0 at 10 and 20 km were interpolated to estimate the "near" V/H ratio for **M**5.6 at 12 km. V/H ratios for **M**7.0 at 100 km and **M**7.5 at 100 km were interpolated to estimate a "far" V/H ratio for **M**7.2 at 100 km. The distance of 100 km was the greatest considered in Lee (2001), but is considered adequate, if not slightly conservative, for a proxy of the 130 km desired for the "far" event.

Figure 2.5.2-42 is a plot of $V/H_{CEUS,Soil}$ of Equation 2.5.2-6 considering both "near" and "far" events. As before, given the observations made earlier with regard to the relative contributions of the deaggregation "near" and "far" events to the 10^{-4} and 10^{-5} hazards, and the relative contribution of these two hazard levels to the horizontal SSE design response spectrum, the "near" and "far" estimates of $V/H_{CEUS,Soil}$ are weighted approximately 1:3, resulting in the final $V/H_{CEUS,Soil}$ shown in Figure 2.5.2-42, as derived from the available results in Lee (2001).

2.5.2.7.1.3 Recommended V/H

The results of two studies have been used to guide in the development of best estimates of $V/H_{CEUS,Soil}$, as discussed above and summarized in Figure 2.5.2-43. The $V/H_{CEUS,Soil}$ developed from Lee (2001) gives a higher value V/H ratio than that developed from the available NUREG/CR-6728 results for frequencies greater than about 0.7 Hz. Both results give minimum V/H values, particularly in the lower frequencies, which appear lower than engineering judgment may suggest acceptable in the current state-of- -knowledge.

Given the site specific nature of the Lee (2001) estimate, which would argue against considering an average of the two results, an approximate envelope of the results is recommended, wherein some smoothing is considered and a minimum V/H value of 0.5 is considered. The recommended final V/H ratio is shown in Figure 2.5.2-43. This V/H ratio is described as follows:

Frequencies	**V/H ratio**
≤ 1 Hz	0.5
1 to 15 Hz	log-log interpolate between 0.5 and 0.9
≥ 15 Hz	0.9

In Figure 2.5.2-43 the V/H ratio from RG 1.60 is shown for comparison. The recommended V/H ratio is marginally less than the Reg. Guide ratio at all frequencies.

2.5.2.7.2 Recommended Vertical SSE Spectrum

To develop the vertical SSE spectrum, the horizontal SSE spectrum is scaled by the recommended V/H ratios provided in 2.5.2.7.1.3. Figure 2.5.2-44 shows the resulting vertical and horizontal SSE spectra.

2.5.2.8 Operating Basis Earthquake Ground Motion

The Operating Basis Earthquake (OBE) ground motion spectra was not determined as part of the Vogtle ESP submittal. Requirements related to the OBE are provided in paragraph IV (a) (2) of Appendix S to 10 CFR Part 50, "Earthquake Engineering Criteria for Nuclear Power Plants." Under General Information in this appendix, the following statement is made: "This appendix applies to applications for the design certification or combined license pursuant to part 52 of this chapter or a construction permit…" Since OBE requirements are related to the design

and performance of safety related systems, the OBE ground motion spectra will be determined during the COL stage as required under Appendix S.

Table 2.5.2-1 Earthquakes 1985–2005, Update to the EPRI (NP-4726-A 1988) Seismicity Catalog with $Em_b \geq 3.0$, Within a 30° to 37° N, 78° to 86° W Latitude-Longitude Window, Incorporating the 200 mi (320 km) Radius Site Region

Year	Mo	Dy	Hr	Mn	Sec	Lat	Lon	Z(km)	Int	Emb	Smb	Rmb
1985	12	22	0	56	5.0	35.701	-83.720	13.4		3.25	0.30	3.35
1986	1	7	1	26	43.3	35.610	-84.761	23.1		3.06	0.30	3.17
1986	2	13	11	35	45.6	34.755	-82.943	5.0		3.50	0.10	3.51
1986	3	13	2	29	31.4	33.229	-83.226	5.0	4	3.30	0.25	3.37
1986	7	11	14	26	14.8	34.937	-84.987	13.0	6	3.80	0.10	3.81
1986	9	17	9	33	49.5	32.931	-80.159	6.7	4	3.30	0.25	3.37
1987	3	16	13	9	26.8	34.560	-80.948	3.0		3.06	0.30	3.17
1987	3	27	7	29	30.5	35.565	-84.230	18.5	6	4.20	0.10	4.21
1987	7	11	0	4	29.5	36.105	-83.816	25.1	5	3.79	0.10	3.80
1987	7	11	2	48	5.9	36.103	-83.819	23.8	4	3.43	0.10	3.44
1987	9	1	23	2	49.4	35.515	-84.396	21.1		3.06	0.30	3.17
1987	9	22	17	23	50.1	35.623	-84.312	19.4	5	3.50	0.10	3.51
1987	11	27	18	58	29.3	36.852	-83.110	26.8	5	3.50	0.10	3.51
1987	12	12	3	53	28.8	34.244	-82.628	5.0		3.00	0.10	3.01
1988	1	9	1	7	40.6	35.279	-84.199	12.2	4	3.30	0.25	3.37
1988	1	23	1	57	16.4	32.935	-80.157	7.4	5	3.50	0.25	3.57
1988	2	16	15	26	54.8	36.595	-82.274	4.0	4	3.30	0.10	3.31
1988	2	18	0	37	45.4	35.346	-83.837	2.4	4	3.50	0.10	3.51
1989	6	2	5	4	34.0	32.934	-80.166	5.8	4	3.30	0.25	3.37
1990	8	17	21	1	15.9	36.934	-83.384	0.6	5	4.00	0.10	4.01
1990	11	13	15	22	13.0	32.947	-80.136	3.4	5	3.50	0.10	3.51
1991	6	2	6	5	34.9	32.980	-80.214	5.0	5	3.50	0.25	3.57
1991	9	24	7	21	7.0	35.701	-84.117	13.3	4	3.30	0.10	3.31
1991	10	30	14	54	12.6	34.904	-84.713	8.1		3.06	0.30	3.17
1992	1	3	4	21	23.9	33.981	-82.421	3.3	5	3.50	0.25	3.57
1992	8	21	16	31	56.1	32.985	-80.163	6.5	6	4.10	0.10	4.11
1993	1	15	2	2	50.9	35.039	-85.025	8.1	4	3.30	0.10	3.31
1993	7	12	4	48	20.8	36.035	-79.823	5.0	4	3.30	0.10	3.31
1993	8	8	9	24	32.4	33.597	-81.591	8.5	5	3.50	0.10	3.51
1994	2	12	2	40	24.5	36.800	-82.000	5.0		3.42	0.41	3.61
1994	4	5	22	22	0.4	34.969	-85.491	24.3	5	3.50	0.10	3.51
1994	4	16	20	10	12.2	35.752	-83.968	1.8	5	3.50	0.25	3.57
1995	3	11	8	15	52.3	36.959	-83.133	1.0		3.80	0.10	3.81
1995	3	11	9	50	4.4	36.990	-83.180	1.0		3.30	0.10	3.31
1995	3	18	22	6	20.8	35.422	-84.941	26.0		3.25	0.30	3.35
1995	4	17	13	46	0.0	32.997	-80.171	8.4	6	3.90	0.10	3.91
1995	6	26	0	36	17.1	36.752	-81.481	1.8	5	3.40	0.10	3.41
1995	7	5	14	16	44.7	35.334	-84.163	10.0	4	3.70	0.10	3.71
1995	7	7	21	1	3.0	36.493	-81.833	10.0	4	3.06	0.10	3.08
1996	4	19	8	50	14.0	36.981	-83.018	0.0		3.90	0.10	3.91
1997	5	19	19	45	35.8	34.622	-85.353	2.7	4	3.06	0.10	3.08
1997	7	19	17	6	34.4	34.953	-84.811	2.8	4	3.61	0.10	3.62
1997	7	30	12	29	25.3	36.512	-83.547	23.0	5	3.80	0.10	3.81
1998	4	13	9	56	15.6	34.471	-80.603	6.6	5	3.90	0.10	3.91
1998	6	5	2	31	3.9	35.554	-80.785	9.4		3.34	0.10	3.35

Table 2.5.2-1 (cont). Earthquakes 1985–2005, Update to the EPRI (NP-4726-A 1988) Seismicity Catalog with $Em_b \geq 3.0$, Within a 30° to 37° N, 78° to 86° W Latitude-Longitude Window, Incorporating the 200 mi (320 km) Radius Site Region

Year	Mo	Dy	Hr	Mn	Sec	Lat	Lon	Z(km)	Int	Emb	Smb	Rmb
1998	6	17	8	0	23.9	35.944	-84.392	11.3	5	3.60	0.10	3.61
1999	1	17	18	38	5.1	36.893	-83.799	1.0	3	3.06	0.27	3.15
2000	1	18	22	19	32.2	32.920	-83.465	19.2	5	3.50	0.10	3.51
2001	3	7	17	12	23.8	35.552	-84.850	6.8	3	3.20	0.10	3.21
2001	3	21	23	35	34.9	34.847	-85.438	0.0	3	3.16	0.27	3.24
2001	6	11	18	27	54.3	30.226	-79.885	10.0		3.33	0.41	3.53
2001	7	26	5	26	46.0	35.971	-83.552	14.3	3	3.25	0.10	3.26
2002	11	8	13	29	3.2	32.422	-79.950	3.9		3.50	0.41	3.69
2002	11	11	23	39	29.7	32.404	-79.936	2.4		4.23	0.41	4.42
2003	3	18	6	4	24.2	33.689	-82.888	5.0		3.50	0.41	3.69
2003	4	29	8	59	38.1	34.445	-85.620	9.1	6	4.70	0.10	4.71
2003	5	2	10	48	43.5	34.512	-85.604	10.0		3.01	0.41	3.20
2003	5	5	10	53	49.9	33.055	-80.190	11.4		3.06	0.30	3.17
2003	7	13	20	15	17.0	32.335	-82.144	5.0		3.58	0.41	3.77
2004	7	20	9	13	14.4	32.972	-80.248	10.3		3.17	0.41	3.37
2004	9	17	15	21	43.6	36.932	-84.006	1.2		3.66	0.41	3.85

Table 2.5.2-2 Summary of Bechtel Seismic Sources

Source	Description	Pa[1]	Mmax (m_b) and Wts.[2]	Smoothing Options and Wts.[3]	Inter-dependencies[4]	New Information to Suggest Change in Source: Geometry?[5]	Mmax?[6]	RI?[7]
Sources within 200 mi (320 km) that contribute to 99% of hazard								
H	**Charleston Area**	0.50	6.8 [0.20] 7.1 [0.40] 7.4 [0.40]	1 [0.33] 2 [0.34] 4 [0.33]	P(H|N3)=0.15	**Yes[8]**	**Yes[8]**	**Yes[8]**
N3	**Charleston Faults**	0.53	6.8 [0.20] 7.1 [0.40] 7.4 [0.40]	1 [0.33] 2 [0.34] 4 [0.33]	P(N3|H)=0.16	**Yes[8]**	**Yes[8]**	**Yes[8]**
BZ4	Atlantic Coastal Region	1.00	6.6 [0.10] 6.8 [0.40] 7.1 [0.40] 7.4 [0.10]	1 [0.33] 2 [0.34] 3 [0.33]	Background; P_B=1.00	No	No	No
BZ5	S. Appalachians	1.00	5.7 [0.10] 6.0 [0.40] 6.3 [0.40] 6.6 [0.10]	1 [0.33] 2 [0.34] 3 [0.33]	Background; P_B=1.00	No	No	No
F	S.E. Appalachians	0.35	5.4 [0.10] 5.7 [0.40] 6.0 [0.40] 6.6 [0.10]	1 [0.33] 2 [0.34] 4 [0.33]	ME with G; ME with 13, 15, 16, 17	No	No	No
G	NW South Carolina	0.35	5.4 [0.10] 5.7 [0.40] 6.0 [0.40] 6.6 [0.10]	1 [0.33] 2 [0.34] 4 [0.33]	ME with F; ME with 13, 15, 16, 17	No	No	No
Other Sources within 200 mi (320 km) that do not contribute to 99% of hazard								
13	Eastern Mesozoic Basins	0.10	5.4 [0.10] 5.7 [0.40] 6.0 [0.40] 6.6 [0.10]	1 [0.33] 2 [0.34] 4 [0.33]	no overlap with H or N3; ME with all sources in BZ5	No	No	No
24	Bristol Trends	0.25	5.7 [0.10] 6.0 [0.40] 6.3 [0.40] 6.6 [0.10]	1 [0.33] 2 [0.34] 4 [0.33]	ME with 19, 25, 25A	No	No	No
15	Rosman Fault	0.05	5.4 [0.10] 5.7 [0.40] 6.0 [0.40] 6.6 [0.10]	1 [0.33] 2 [0.34] 4 [0.33]	ME with all other sources	No	No	No
16	Belair Fault	0.05	5.4 [0.10] 5.7 [0.40] 6.0 [0.40] 6.6 [0.10]	1 [0.33] 2 [0.34] 4 [0.33]	ME with all other sources	No	No	No

Table 2.5.2-2 (cont.) Summary of Bechtel Seismic Sources

1 Pa = probability of activity; (from EPRI NP-6452-D 1989)
2 Maximum Magnitude (Mmax) and weights (wts.); (from EPRI NP-6452-D 1989)
3 Smoothing options are defined as follows (from EPRI NP-6452-D 1989):
1 = constant a, constant b (no prior b);
2 = low smoothing on a, high smoothing on b (no prior b);
3 = low smoothing on a, low smoothing on b (no prior b);
4 = low smoothing on a, low smoothing on b (weak prior of 1.05).
Weights on magnitude intervals are [1.0, 1.0, 1.0, 1.0, 1.0, 1.0, 1.0].
4 ME = mutually exclusive; PD = perfectly dependent
5 No, unless (1) new geometry proposed in literature or (2) new seismicity pattern
6 No, unless (1) new data suggests Mmax exceeds or differs significantly from the EPRI Mmax distribution or (2) exceeded by historical seismicity.
7 RI = recurrence interval; assumed no change if no new paleoseismic data or rate of seismicity has not significantly changed
8 Replace this source with the Updated Charleston Seismic Source (UCSS) Model

Table 2.5.2-3 Summary of Dames & Moore Seismic Sources

Source	Description	Pa[1]	Mmax (m_b) and Wts.[2]	Smoothing Options and Wts.[3]	Inter-dependencies[4]	New Information to Suggest Change in Source: Geometry?[5]	Mmax?[6]	RI?[7]
Sources within 200 mi (320 km) that contribute to 99% of hazard								
54	**Charleston Seismic Zone**	1.00	6.6 [0.75] 7.2 [0.25]	1 [0.22] 2 [0.08] 3 [0.52] 4 [0.18]	none	**Yes[8]**	**Yes[8]**	**Yes[8]**
52	Charleston Mesozoic Rift	0.46	4.7 [0.75] 7.2 [0.25]	3 [0.75] 4 [0.25]	ME with 47 thru 50, 65; ME with 52	No	No	No
53	S. Appalachian Mobile Belt (Default Zone)	0.26	5.6 [0.80] 7.2 [0.20]	1 [0.75] 2 [0.25]	Default for 47 thru 52, 65	No	No	No
41	S. Cratonic Margin (Default Zone)	0.12	6.1 [0.80] 7.2 [0.20]	1 [0.75] 2 [0.25]	Default for 42, 43, and 46	No	No	No
20	S. Coastal Margin	1.00	5.3 [0.80] 7.2 [0.20]	1 [0.75] 2 [0.25]	none	No	No	No
Other Sources within 200 mi (320 km) that do not contribute to 99% of hazard								
4	Appalachian Fold Belts	0.35	6.0 [0.80] 7.2 [0.20]	1 [0.75] 2 [0.25]	ME with 4A, 4B, 4C, 4D	No	No	No
4A	Kink in Fold Belt	0.65	5.0 [0.75] 7.2 [0.25]	3 [0.75] 4 [0.25]	ME with 4	No	No	No
49	Jonesboro Basin	0.28	6.0 [0.75] 7.2 [0.25]	3 [0.75] 4 [0.25]	PD with 47, 48, 50, 51, 65; ME with 52	No	No	No
50	Buried Triassic Basins	0.28	6.0 [0.75] 7.2 [0.25]	3 [0.75] 4 [0.25]	PD with 47, 48, 49, 51, 65; ME with 52	No	No	No
51	Florence Basin	0.28	6.0 [0.75] 7.2 [0.25]	3 [0.75] 4 [0.25]	PD with 47 thru 50, 65; ME with 52	No	No	No
65	Dunbarton Triassic Basin	0.28	5.9 [0.75] 7.2 [0.25]	3 [0.75] 4 [0.25]	PD with 47 thru 51; ME with 52	No	No	No
C01	Combination zone 4-4A-4B-4C-4D	NA	6.0 [0.80] 7.2 [0.20]	1 [0.75] 2 [0.25]	NA	No	No	No

Table 2.5.2-3 (cont.) Summary of Dames & Moore Seismic Sources

1 Pa = probability of activity; (from EPRI NP-6452-D 1989)
2 Maximum Magnitude (Mmax) and weights (wts.); (from EPRI NP-6452-D 1989)
3 Smoothing options are defined as follows (from EPRI NP-6452-D 1989)
1 = No smoothing on a, no smoothing on b (strong prior of 1.04);
2 = No smoothing on a, no smoothing on b (weak prior of 1.04);
3 = Constant a, constant b (strong prior of 1.04);
4 = Constant a, constant b (weak prior of 1.04).
Weights on magnitude intervals are [0.1, 0.2, 0.4, 1.0, 1.0, 1.0, 1.0]
4 ME = mutually exclusive; PD = perfectly dependent
5 No, unless (1) new geometry proposed in literature or (2) new seismicity pattern
6 No, unless (1) new data suggests Mmax exceeds or differs significantly from the EPRI Mmax distribution or (2) exceeded by historical seismicity.
7 RI = recurrence interval; assumed no change if no new paleoseismic data or rate of seismicity has not significantly changed
8 Replace this source with the Updated Charleston Seismic Source (UCSS) Model

Table 2.5.2-4 Summary Law Engineering Seismic Sources

Source	Description	Pa[1]	Mmax (m_b) and Wts.[2]	Smoothing Options and Wts.[3]	Inter-dependencies[4]	New Information to Suggest Change in Source: Geometry?[5]	Mmax?[6]	RI?[7]
Sources within 200 mi (320 km) that contribute to 99% of hazard								
35	**Charleston Seismic Zone**	0.45	6.8 [1.00]	2a [1.00]	Overlaps 8 and 22	**Yes[8]**	**Yes[8]**	**Yes[8]**
17	Eastern Basement	0.62	5.7 [0.20] 6.8 [0.80]	1b [1.00]	none	No	No	No
22	Reactivated E. Seaboard Normal	0.27	6.8 [1.00]	2a [1.00]	ME with 8 and 21; overlaps 24, 35, and 39	No	No	No
108	Brunswick, NC Background	1.00	4.9 [0.50] 5.5 [0.30] 6.8 [0.20]	2a [1.00]	Background; P_B=0.42	No	No	No
C09	Mesozoic Basins (8 - Bridged)	NA	6.8 [1.00]	2a [1.00]	NA	No	No	No
C10	8-35	NA	6.8 [1.00]	2a [1.00]	NA	No	No	No
C11	22 - 35	NA	6.8 [1.00]	2a [1.00]	NA	No	No	No
M33	Mafic Pluton	0.43	6.8 [1.00]	5 [1.00]	none	No	No	No
M36	Mafic Pluton	0.43	6.8 [1.00]	5 [1.00]	none	No	No	No
M37	Mafic Pluton	0.43	6.8 [1.00]	5 [1.00]	none	No	No	No
M38	Mafic Pluton	0.43	6.8 [1.00]	5 [1.00]	none	No	No	No
M39	Mafic Pluton	0.43	6.8 [1.00]	5 [1.00]	none	No	No	No
M40	Mafic Pluton	0.43	6.8 [1.00]	5 [1.00]	none	No	No	No
M41	Mafic Pluton	0.43	6.8 [1.00]	5 [1.00]	none	No	No	No
M42	Mafic Pluton	0.43	6.8 [1.00]	5 [1.00]	none	No	No	No

Table 2.5.2-4 (cont.) Summary Law Engineering Seismic Sources

Source	Description	Pa[1]	Mmax (m_b) and Wts.[2]	Smoothing Options and Wts.[3]	Inter-dependencies[4]	New Information to Suggest Change in Source: Geometry?[5]	Mmax?[6]	RI?[7]
Other Sources within 200 mi (320 km) that do not contribute to 99% of hazard								
217	Eastern Basement Background	1.00	4.9 [0.50] 5.7 [0.50]	1b [1.00]	Background; P_B=0.29; same geometry as 17	No	No	No
107	Eastern Piedmont	1.00	4.9 [0.30] 5.5 [0.40] 5.7 [0.30]	1a [1.00]	Background; P_B=0.42	No	No	No
GC13	22 - 24 - 35	NA	6.8 [1.00]	2a [1.00]	NA	No	No	No
GC12	22 - 24	NA	6.8 [1.00]	2a [1.00]	NA	No	No	No
8	Mesozoic Basins	0.27	6.8 [1.00]	a and b values calculated for C09	ME with 22; overlaps with 35	No	No	No

1 Pa = probability of activity; (from EPRI NP-6452-D 1989)
2 Maximum Magnitude (Mmax) and weights (wts.); (from EPRI NP-6452-D 1989)
3 Smoothing options are defined as follows: (from EPRI NP-6452-D 1989)
1a = High smoothing on a, constant b (strong prior of 1.05);
1b = High smoothing on b, constant b (strong prior of 1.00);
1c = High smoothing on a, constant b (strong prior of 0.95);
1d = High smoothing on a, constant b (strong prior of 0.90);
1e = High smoothing on a, constant b (strong prior of 0.70);
2a = Constant a, constant b (strong prior of 1.05);
2c = Constant a, constant b (strong prior of 0.95);
2d = Constant a, constant b (strong prior of 0.90).
Weights on magnitude intervals are all 1.0 for above options.
3a = High smoothing on a, constant b (strong prior of 1.05).
Weights on magnitude intervals are [0.0, 1.0, 1.0, 1.0, 1.0, 1.0, 1.0] for option 3a.
4 ME = mutually exclusive; PD = perfectly dependent
5 No, unless (1) new geometry proposed in literature or (2) new seismicity pattern
6 No, unless (1) new data suggests Mmax exceeds or differs significantly from the EPRI Mmax distribution or (2) exceeded by historical seismicity.
7 RI = recurrence interval; assumed no change if no new paleoseismic data or rate of seismicity has not significantly changed
8 Replace this source with the Updated Charleston Seismic Source (UCSS) Model

Table 2.5.2-5 Summary of Roundout Seismic Sources

Source	Description	Pa[1]	Mmax (m_b) and Wts.[2]	Smoothing Options and Wts.[3]	Inter-dependencies[4]	New Information to Suggest Change in Source: Geometry?[5]	Mmax?[6]	RI?[7]
Sources within 200 mi (320 km) that contribute to 99% of hazard								
24	**Charleston**	1.00	6.6 [0.20] 6.8 [0.60] 7.0 [0.20]	1 [1.00] (a=-0.710, b=1.020)	none	**Yes[8]**	**Yes[8]**	**Yes[8]**
26	South Carolina	1.00	5.8 [0.15] 6.5 [0.60] 6.8 [0.25]	1 [1.00] (a=-1.390, b=0.970)	none	No	No	No
Other Sources within 200 mi (320 km) that do not contribute to 99% of hazard								
49	Appalachian	1.00	4.8 [0.20] 5.5 [0.60] 5.8 [0.20]	2 [1.00]	Background; P_B=1.00	No	No	No
C01	Background 49	NA	4.8 [0.20] 5.5 [0.60] 5.8 [0.20]	3 [1.00]	none	No	No	No
C09	49+32	NA	4.8 [0.20] 5.5 [0.60] 5.8 [0.20]	3 [1.00]	none	No	No	No
50	Grenville	1.00	4.8 [0.20] 5.5 [0.60] 5.8 [0.20]	2 [1.00]	Background; P_B=1.00	No	No	No
C02	Background 50	NA	4.8 [0.20] 5.5 [0.60] 5.8 [0.20]	3 [1.00]	does not contain 12 or 13	No	No	No
C07	50 (02) + 12	NA	4.8 [0.20] 5.5 [0.60] 5.8 [0.20]	3 [1.00]	none	No	No	No
25	Southern Appalachians	0.99	6.6 [0.30] 6.8 [0.60] 7.0 [0.10]	1 [1.00] (a=-0.630, b=1.150)	none	No	No	No
27	Tennessee-VA Border Zone	0.99	5.2 [0.30] 6.3 [0.55] 6.5 [0.15]	1 [1.00] (a=-1.120, b=0.930)	none	No	No	No

1 Pa = probability of activity; (from EPRI NP-6452-D 1989)
2 Maximum Magnitude (Mmax) and weights (wts.); (from EPRI NP-6452-D 1989)
3 Smoothing options are defined as follows: (from EPRI NP-6452-D 1989)
1, 6, 7, 8 = a, b values as listed above, wth weights shown;
3 = Low smoothing on a, constant b (strong prior of 1.0);
5 = a, b values as listed above, with weights shown.
4 ME = mutually exclusive; PD = perfectly dependent
5 No, unless (1) new geometry proposed in literature or (2) new seismicity pattern
6 No, unless (1) new data suggests Mmax exceeds or differs significantly from the EPRI Mmax distribution or (2) exceeded by historical seismicity.
7 RI = recurrence interval; assumed no change if no new paleoseismic data or rate of seismicity has not significantly changed
8 Replace this source with the Updated Charleston Seismic Source (UCSS) Model

Table 2.5.2-6 Summary of Weston Seismic Sources

Source	Description	Pa[1]	Mmax (m_b) and Wts.[2]	Smoothing Options and Wts.[3]	Inter-dependencies[4]	New Information to Suggest Change in Source: Geometry?[5]	Mmax?[6]	RI?[7]
Sources within 200 mi (320 km) that contribute to 99% of hazard								
25	**Charleston Seismic Zone**	0.99	6.6 [0.90] 7.2 [0.10]	1b [1.00]	none	**Yes[8]**	**Yes[8]**	**Yes[8]**
26	South Carolina	0.86	6.0 [0.67] 6.6 [0.27] 7.2 [0.06]	1b [1.00]	none	No	No	No
104	Southern Coastal Plain	1.00	5.4 [0.24] 6.0 [0.61] 6.6 [0.15]	1a [0.20] 2a [0.80]	Background; P_B=1.00	No	No	No
C19	103-23-24	NA	5.4 [0.26] 6.0 [0.58] 6.6 [0.16]	1a [1.00]	NA	No	No	No
C20	104-22	NA	6.0 [0.85] 6.6 [0.15]	1a [0.30] 2a [0.70]	NA	No	No	No
C21	104-25	NA	5.4 [0.24] 6.0 [0.61] 6.6 [0.15]	1a [0.30] 2a [0.70]	NA	No	No	No
C23	104-22-26	NA	5.4 [0.80] 6.0 [0.14] 6.6 [0.06]	1a [0.50] 2a [0.50]	NA	No	No	No
C24	104-22-25	NA	5.4 [0.80] 6.0 [0.14] 6.6 [0.06]	1a [0.50] 2a [0.50]	NA	No	No	No
C26	104-28BCDE-22	NA	5.4 [0.24] 6.0 [0.61] 6.6 [0.15]	1a [0.30] 2a [0.70]	NA	No	No	No
C27	104-28BCDE-22-25	NA	5.4 [0.30] 6.0 [0.70]	1a [0.70] 2a [0.30]	NA	No	No	No
C33	26-25		6.6 [0.90] 7.2 [0.10]	1b [1.00]	NA	No	No	No
C35	104-28BE-25	NA	5.4 [0.24] 6.0 [0.61] 6.6 [0.15]	1a [0.20] 1b [0.80]	NA	No	No	No
Other Sources within 200 mi (320 km) that do not contribute to 99% of hazard								
C22	104-26	NA	5.4 [0.24] 6.0 [0.61] 6.6 [0.15]	1a [0.30] 1b [0.70]	NA	No	No	No
C34	104-28BE-26	NA	5.4 [0.24] 6.0 [0.61] 6.6 [0.15]	1a [0.20] 1b [0.80]	NA	No	No	No

Table 2.5.2-6 (cont.) Summary of Weston Seismic Sources

Source	Description	Pa[1]	Mmax (m_b) and Wts.[2]	Smoothing Options and Wts.[3]	Inter-dependencies[4]	New Information to Suggest Change in Source: Geometry?[5]	Mmax?[6]	RI?[7]
C25	104-28BCDE	NA	5.4 [0.24] 6.6 [0.61] 6.6 [0.15]	1a [0.30] 2a [0.70]	NA	No	No	No
C28	104-28BCDE-22-26	NA	5.4 [0.30] 6.0 [0.70]	1a [0.70] 2a [0.30]	NA	No	No	No
28B	Zone of Mesozoic Basin	0.26	5.4 [0.65] 6.0 [0.25] 6.6 [0.10]	1b [1.00]	PD with 28C, 28D, and 28E	No	No	No
C01	28A thru E	NA	5.4 [0.65] 6.0 [0.25] 6.6 [0.10]	1b [1.00]	NA	No	No	No
103	Southern Appalachians	1.00	5.4 [0.26] 6.0 [0.58] 6.6 [0.16]	1a [0.20] 2a [0.80]	Background; P_B=1.00	No	No	No
C17	103-23	NA	5.4 [0.26] 6.0 [0.58] 6.6 [0.16]	1a [0.70] 2a [0.30]	NA	No	No	No
C18	103-24	NA	5.4 [0.26] 6.0 [0.58] 6.6 [0.16]	1a [0.70] 1b [0.30]	NA	No	No	No
28D	Zone of Mesozoic Basin	0.26	5.4 [0.65] 6.0 [0.25] 6.6 [0.10]	1b [1.00]	PD with 28B, 28C, and 28E	No	No	No
28E	Zone of Mesozoic Basin	0.26	5.4 [0.65] 6.0 [0.25] 6.6 [0.10]	1b [1.00]	PD with 28B, 28C, and 28D	No	No	No
102	Appalachian Plateau	1.00	5.4 [0.62] 6.0 [0.29] 6.6 [0.09]	1a [0.20] 2a [0.80]	Background; P_B=1.00	No	No	No
24	New York-Alabama-Clingman	0.90	5.4 [0.26] 6.0 [0.58] 6.6 [0.16]	1b [1.00]	Contained in 103	No	No	No

1 Pa = probability of activity; (from EPRI NP-6452-D 1989)
2 Maximum Magnitude (Mmax) and weights (wts.); (from EPRI NP-6452-D 1989)
3 Smoothing options are defined as follows: (from EPRI NP-6452-D 1989)
1a = Constant a, constant b (medium prior of 1.0);
1b = Constant a, constant b (medium prior of 0.9);
1c = Constant a, constant b (medium prior of 0.7);
2a = Medium smoothing on a, medium smoothing on b (medium prior of 1.0);
2b = Medium smoothing on a, medium smoothing on b (medium prior of 0.9);
2c = Medium smoothing on a, medium smoothing on b (medium prior of 0.7).
4 ME = mutually exclusive; PD = perfectly dependent
5 No, unless (1) new geometry proposed in literature or (2) new seismicity pattern
6 No, unless (1) new data suggests Mmax exceeds or differs significantly from the EPRI Mmax distribution or (2) exceeded by historical seismicity.

Table 2.5.2-6 (cont.) Summary of Weston Seismic Sources

Source	Description	Pa[1]	Mmax (m_b) and Wts.[2]	Smoothing Options and Wts.[3]	Inter-dependencies[4]	New Information to Suggest Change in Source:		
						Geometry?[5]	Mmax?[6]	RI?[7]

7 RI = recurrence interval; assumed no change if no new paleoseismic data or rate of seismicity has not significantly changed

8 Replace this source with the Updated Charleston Seismic Source (UCSS) Model

Table 2.5.2-7 Summary of Woodward-Clyde Seismic Sources

Source	Description	Pa[1]	Mmax (m_b) and Wts.[2]	Smoothing Options and Wts.[3]	Inter-dependencies[4]	New Information to Suggest Change in Source: Geometry?[5]	Mmax?[6]	RI?[7]
Sources within 200 mi (320 km) that contribute to 99% of hazard								
30	**Charleston (includes NOTA)**	0.573	6.8 [0.33] 7.3 [0.34] 7.5 [0.33]	2 [0.10] 3 [0.10] 4 [0.10] 5 [0.10] 9 [0.60] (a = -1.005, b = 0.852)	ME with 29, 29A	**Yes[8]**	**Yes[8]**	**Yes[8]**
29	**S. Carolina Gravity Saddle (Extended)**	0.122	6.7 [0.33] 7.0 [0.34] 7.4 [0.33]	2 [0.25] 3 [0.25] 4 [0.25] 5 [0.25]	ME with 29A, 29B, and 30	**Yes[8]**	**Yes[8]**	**Yes[8]**
29A	**SC Gravity Saddle No. 2 (Combo C3)**	0.305	6.7 [0.33] 7.0 [0.34] 7.4 [0.33]	2 [0.25] 3 [0.25] 4 [0.25] 5 [0.25]	ME with 29, 29B, and 30	**Yes[8]**	**Yes[8]**	**Yes[8]**
29B	SC Gravity Saddle No. 3 (NW Portion)	0.183	5.4 [0.33] 6.0 [0.34] 7.0 [0.33]	2 [0.25] 3 [0.25] 4 [0.25] 5 [0.25]	ME with 29, 29A	No	No	No
	Vogtle Background		5.8 [0.33] 6.0 [0.34] 6.6 [0.33]		None	No	No	No
Other Sources within 200 mi (320 km) that do not contribute to 99% of hazard								
31	Blue Ridge Combo	0.024	5.9 [0.33] 6.3 [0.34] 7.0 [0.33]	2 [0.25] 3 [0.25] 4 [0.25] 5 [0.25]	ME with 31A	No	No	No
31A	Blue Ridge Combination - Alternate Configuration	0.211	5.9 [0.33] 6.3 [0.34] 7.0 [0.33]	2 [0.25] 3 [0.25] 4 [0.25] 5 [0.25]	ME with 31	No	No	No

1 Pa = probability of activity; (from EPRI NP-6452-D 1989)
2 Maximum Magnitude (Mmax) and weights (wts.); (from EPRI NP-6452-D 1989)
3 Smoothing options are defined as follows: (from EPRI NP-6452-D 1989)
1 = Low smoothing on a, high smoothing on b (no prior);
2 = High smoothing on a, high smoothing on b (no prior);
3 = High smoothing on a, high smoothing on b (moderate prior of 1.0);
4 = High smoothing on a, high smoothing on b (moderate prior of 0.9);
5 = High smoothing on a, high smoothing on b (moderate prior of 0.8);
6 = Low smoothing on a, high smoothing on b (moderate prior of 1.0);

Table 2.5.2-7 (cont.) Summary of Woodward-Clyde Seismic Sources

7 = Low smoothing on a, high smoothing on b (moderate prior of 0.9);
8 = Low smoothing on a, high smoothing on b (moderate prior of0.8).
Weights on magnitude intervals are all 1.0.
9 = a and b values as listed.

4 ME = mutually exclusive; PD = perfectly dependent

5 No, unless (1) new geometry proposed in literature or (2) new seismicity pattern

6 No, unless (1) new data suggests Mmax exceeds or differs significantly from the EPRI Mmax distribution or (2) exceeded by historical seismicity.

7 RI = recurrence interval; assumed no change if no new paleoseismic data or rate of seismicity has not significantly changed

8 Replace this source with the Updated Charleston Seismic Source (UCSS) Model

Table 2.5.2-8 Summary of USGS Seismic Sources (Frankel et al. 2002)

Source	Mmax (Mw) and Wts.	Largest Mmax Value Considered by USGS	
		Mw	mb[1]
Sources within 200 mi (320 km)			
Extended Margin Background	7.5 [1.00]	7.5	7.2
Charleston	**6.8 [0.20]** **7.1 [0.20]** **7.3 [0.45]** **7.5 [0.15]**	**7.5**	**7.2**
Eastern Tennessee	7.5 [1.00]	7.5	7.2
Selected Sources Beyond 200 mi (320km)			
New Madrid	7.3 [0.15] 7.5 [0.20] 7.7 [0.50] 8.0 [0.15]	8.0	7.5
Stable Craton Background	7.0 [1.00]	7.0	6.9

1 m_b converted from Mw using average of Atkinson and Boore (1995), Frankel et al (1996), and EPRI (TR-102293 1993) relations

Table 2.5.2-9 Chapman and Talwani (2002) Seismic Source Zone Parameters

Charleston Characteristic Sources	Mean Recurrence	Mmax[2] m_{blg}	Mmax[2] M
Charleston Area Source	550 years	nr	7.1 [.2] 7.3 [.6] 7.5 [.2]
ZRA Fault Source (Zone of River Anomalies)	550 years	nr	7.1 [.2] 7.3 [.6] 7.5 [.2]
Ashley River-Woodstock Fault Source (modeled as 3 parallel faults)	550 years	nr	7.1 [.2] 7.3 [.6] 7.5 [.2]

Non-Characteristic Background Sources		a[1]	b[1]	m_{blg}	M
1.	Zone1	0.242	0.84	6.84	7.00
2.	Zone2	-0.270	0.84	6.84	7.00
3.	Central Virginia	1.184	0.64	6.84	7.00
4.	Zone4	0.319	0.84	6.84	7.00
5.	Zone5	0.596	0.84	6.84	7.00
6.	Piedmont and Coastal Plain	1.537	0.84	6.84	7.00
6a.	Pied&CP NE	0.604	0.84	6.84	7.00
6b.	Pied&CP SW	1.312	0.84	6.84	7.00
7.	South Carolina Piedmont	2.220	0.84	6.84	7.00
8.	Middleton Place	1.690	0.77	6.84	7.00
9.	Florida and continental margin	1.371	0.84	6.84	7.00
10.	Alabama	1.800	0.84	6.84	7.00
11.	Eastern Tennessee	2.720	0.90	6.84	7.00
12.	Southern Appalachian	2.420	0.84	6.84	7.00
12a.	Southern Appalachian North	2.185	0.84	6.84	7.00
13.	Giles County, VA	1.070	0.84	6.84	7.00
14.	Central Appalachians	1.630	0.84	6.84	7.00
15.	Western Tennessee	2.431	1.00	6.84	7.00
16.	Central Tennessee	2.273	1.00	6.84	7.00
17.	Ohio-Kentucky	2.726	1.00	6.84	7.00
18.	West VA-Pennsylvania	2.491	1.00	6.84	7.00
19.	USGS (1996) gridded seismicity rates and b value	nr[3]	0.95	6.84	7.00

1 a and b values in terms of m_{blg} magnitude, reported in Chapman and Talwani (2002).

2 Mmax range for characteristic events was designed to "represent the range of magnitude estimates of the 1886 Charleston shock proposed by Johnston (1996)" (Chapman and Talwani, 2002, p. 12). Square brackets indicate weights assigned to characteristic magnitudes. For non-characteristic background events, a truncated form of the exponential probability density function was used (Chapman and Talwani, 2002, p. 6-7).

3 nr = not reported

Table 2.5.2-10 Local Charleston-Area Tectonic Features

Name of Feature	Evidence	Key References
Adams Run fault	**subsurface stratigraphy**	**Weems and Lewis (2002)**
Ashley River fault	microseismicity	Talwani (1982, 2000) Weems and Lewis (2002)
Appalachian detachment (decollement)	gravity & magnetic data seismic reflection & refraction	Cook *et al.* (1979, 1981) Behrendt *et al.* (1981, 1983) Seeber and Armbruster (1981)
Blake Spur fracture zone	oceanic transform postulated to extend westward to Charleston area	Fletcher *et al.* (1978) Sykes (1978) Seeber and Armbruster (1981)
Bowman seismic zone	microseismicity	Smith and Talwani (1985)
Charleston fault	subsurface stratigraphy	Colquhoun *et al*. (1983) Lennon (1986) Talwani (2000) Weems and Lewis (2002)
Cooke fault	seismic reflection	Behrendt *et al.* (1981, 1983) Hamilton *et al.* (1983) Wentworth and Mergner-Keefer (1983) Behrendt and Yuan (1987)
Drayton fault	seismic reflection	Hamilton *et al.* (1983) Behrendt *et al*. (1983) Behrendt and Yuan (1987)
East Coast fault system/ Zone of river anomalies (ZRA)	**geomorphology** **seismic reflection** **microseismicity**	**Marple and Talwani (1993)** **Marple and Talwani (2000, 2004)**
Gants fault	seismic reflection	Hamilton *et al*. (1983) Behrendt and Yuan (1987)
Garner-Edisto fault	subsurface stratigraphy	Colquhoun *et al.* (1983)
Helena Banks fault zone	seismic reflection	Behrendt *et al.* (1981, 1983) Behrendt and Yuan (1987)
Middleton Place-Summerville seismic zone	microseismicity	Tarr et al. (1981) Madabhushi and Talwani (1993)
Sawmill Branch fault	**microseimicity**	**Talwani and Katuna (2004)**
Summerville fault	**microseimicity**	**Weems *et al.* (1997)**
Woodstock fault	geomorphology microseismicity	Talwani (1982, 1999, 2000) Marple and Talwani (1990, 2000)

Notes: Those tectonic features identified following publication of the EPRI teams' reports (post-1986) are highlighted by **bold-face** type.

Table 2.5.2-11 Geographic Coordinates (Latitude and Longitude) of Corner Points of Updated Charleston Seismic Source (UCSS) Geometries

Source Geometry	Longitude (decimal degrees)	Latitude (decimal degrees)
A	-80.707	32.811
A	-79.840	33.354
A	-79.527	32.997
A	-80.392	32.455
B	-81.216	32.485
B	-78.965	33.891
B	-78.3432	33.168
B	-80.587	31.775
B'	-78.965	33.891
B'	-78.654	33.531
B'	-80.900	32.131
B'	-81.216	32.485
C	-80.397	32.687
C	-79.776	34.425
C	-79.483	34.351
C	-80.109	32.614

Table 2.5.2-12 Comparison of Post-EPRI NP-6395-D 1989 Magnitude Estimates for the 1886 Charleston Earthquake

Study	Magnitude Estimation Method	Reported Magnitude Estimate	Assigned Weights	Mean Magnitude (**M**)
Johnston *et al.* (1994)	worldwide survey of passive-margin, extended-crust earthquakes	**M**7.56 ± 0.35 [a]	--	7.56
Martin and Clough (1994)	geotechnical assessment of 1886 liquefaction data	**M**7 - 7.5	--	7.25
Johnston (1996)	isoseismal area regression, accounting for eastern North America anelastic attenuation	**M**7.3 ± 0.26	--	7.3
Chapman and Talwani (2002) (South Carolina Department of Transportation)	consideration of available magnitude estimates	**M**7.1 **M**7.3 **M**7.5	0.2 0.6 0.2	7.3
Frankel *et al.* (2002) (USGS National seismic hazard mapping project)	consideration of available magnitude estimates	**M**6.8 **M**7.1 **M**7.3 **M**7.5	0.20 0.20 0.45 0.15	7.2
Bakun and Hopper (2004)	isoseismal area regression, including empirical site corrections	M_I 6.4 - 7.2 [b]	--	6.9 [c]

Notes:

[a] Estimate from Johnston *et al.* (1994) Chapter 3.

[b] 95% confidence interval estimate; M_I (intensity magnitude) is considered equivalent to **M** (Bakun and Hopper, 2004).

[c] Bakun and Hopper's (2004) *preferred* estimate.

Table 2.5.2-13 Comparison of Talwani and Schaeffer (2001) and UCSS Age Constraints on Charleston-Area Paleoliquefaction Events

Liquefaction Event	Event Age (YBP) [b]	Talwani and Schaeffer (2001) [a] *scenario 1*		Talwani and Schaeffer (2001) [a] *scenario 2*		(this study)
		Source	**M**	**Source**	**M**	**Event Age** (YBP) [b, c, d]
1886 A.D.	64	Charleston	7.3	Charleston	7.3	64
A	546 ± 17	Charleston	7+	Charleston	7+	600 ± 70
B	1,021 ± 30	Charleston	7+	Charleston	7+	1,025 ± 25
C	1,648 ± 74	*Northern*	6+	--	--	--
C'	1,683 ± 70	--		Charleston	7+	1,695 ± 175
D	1,966 ± 212	*Southern*	6+	--	--	--
E	3,548 ± 66	Charleston	7+	Charleston	7+	3,585 ± 115
F	5,038 ± 166	*Northern*	6+	Charleston	7+	--
F'	--	--	--	--	--	5,075 ± 215
G	5,800 ± 500	Charleston	7+	Charleston	7+	--

Notes:

[a] Modified after Talwani and Schaeffer's (2001) Table 2.

[b] Years before present, relative to 1950 A.D.

[c] Event ages based upon our recalibration of radiocarbon (to 2-sigma using OxCal 3.8 (Bronk Ramsey, 1995; 2001) data presented in Talwani and Schaeffer's (2001) Table 2.

[d] See Table B-1 for recalibrated 2-sigma sample ages and Table B-2 for 2-sigma age constraints on paleoliquefaction events.

Table 2.5.2-14 Seismic Sources Used for Each 1986 EPRI Team

Earth Science Team	Sources used
Bechtel	F, G, H, ,N3,BZ4, BZ5
Dames & Moore	20, 41, 52, 53, 54
Law Engineering	17, 22, 35, 108, C09, C10, C11, M33, M36, M37, M38, M39, M40, M41, M42
Rondout Associates	24, 26
Woodward-Clyde Cons.	29, 29A, 29B, 30, 32
Weston Geophysical Corp.	25, 26, 104, C19, C20, C21, C23, C24, C26, C27, C33, C35

Table 2.5.2-15 Comparison of Seismic Hazard at VEGP ESP

Mean Hazard Comparison

PGA cm/s^2	EPRI-SOG hazard	REI 2005 hazard	% diff
50	8.15E-04	8.23E-04	0.97%
100	2.23E-04	2.26E-04	1.48%
250	2.84E-05	2.91E-05	2.29%
500	4.04E-06	4.21E-06	4.11%
700	1.36E-06	1.42E-06	4.71%
1000	3.82E-07	4.02E-07	5.10%

Median Hazard Comparison

PGA cm/s^2	EPRI-SOG hazard	REI 2005 hazard	% diff
50	5.65E-04	5.75E-04	1.84%
100	1.43E-04	1.45E-04	1.05%
250	1.99E-05	2.16E-05	8.69%
500	2.53E-06	2.63E-06	3.95%
700	7.86E-07	8.13E-07	3.41%
1000	2.05E-07	2.19E-07	6.73%

85% Hazard Comparison

PGA cm/s^2	EPRI-SOG hazard	REI 2005 hazard	% diff
50	1.49E-03	1.32E-03	-11.54%
100	4.16E-04	3.67E-04	-11.71%
250	4.96E-05	4.79E-05	-3.51%
500	7.01E-06	7.16E-06	2.15%
700	2.44E-06	2.46E-06	0.61%
1000	6.98E-07	7.08E-07	1.42%

Table 2.5.2-16 Hard Rock Mean UHS Results (in g) for VEGP ESP

Mean annual frequency of exceedance	Spectral frequency						
	PGA	25 Hz	10 Hz	5 Hz	2.5 Hz	1 Hz	0.5 Hz
10^{-4}	0.214	0.551	0.399	0.317	0.223	0.101	0.0653
$5x10^{-5}$	0.288	0.762	0.532	0.412	0.294	0.134	0.0924
10^{-5}	0.559	1.54	0.983	0.728	0.512	0.235	0.185
$5x10^{-6}$	0.747	2.06	1.28	0.914	0.635	0.294	0.241
10^{-6}	1.48	4.09	2.33	1.54	1.02	0.465	0.423

Table 2.5.2-17 Computed and Recommended Mbar and Dbar Values Used for Development of High and Low Frequency Target Spectra

High Frequency (5-10 Hz)				
	10^{-4}	**10^{-5}**	**10^{-6}**	**Recommended Values**
Mbar (Mw)	5.5	5.6	5.6	5.6
Dbar (km)	17.7	11.5	9.1	12
Low Frequency (1-2.5 Hz)				
	10^{-4}	**10^{-5}**	**10^{-6}**	**Recommended Values**
Mbar (Mw)	7.2	7.2	7.2	7.2
Dbar (km)	136.5	134.3	132.9	130

Table 2.5.2-18a Candidate High-Frequency (M5.6, R = 12km) Time Histories for Spectral Matching

Earthquake	Date	Mw	Station	Distance (km)	Vs30m (m/s)
Saguenay	11/25/88	5.9	GSC Site 16	51.9	"???"
San Francisco	03/22/57	5.28	Golden Gate Park	11.13	874.0
Coyote Lake	08/06/79	5.74	Gilroy Array #1	10.67	1428.0
Mammoth Lakes-09	06/11/80	4.85	USC McGee Creek	7.49	684.9
Coalinga-04	07/09/83	5.18	Sulphur Baths (temp)	14.47	617.4
Coalinga-05	07/22/83	5.77	Sulphur Baths (temp)	13.40	617.4
Morgan Hill	04/24/84	6.19	Gilroy - Gavilan Coll.	14.84	729.7
Morgan Hill	04/24/84	6.19	Gilroy Array #1	14.91	1428.0
N. Palm Springs	07/08/86	6.06	Silent Valley - Poppet Flat	17.03	684.9
Whittier Narrows-01	10/01/87	5.99	Mt Wilson - CIT Seis Sta	22.73	821.7
Whittier Narrows-02	10/04/87	5.27	Mt Wilson - CIT Seis Sta	18.74	821.7
Anza-02	10/31/01	4.92	Anza - Pinyon Flat	12.37	724.9
Anza-02	10/31/01	4.92	Anza - Tripp Flats Training	24.73	684.9
Anza-02	10/31/01	4.92	Idyllwild - Keenwild Fire Sta.	29.07	845.4
Gilroy	05/14/02	4.90	Gilroy - Gavilan Coll.	2.82	729.7

Table 2.5.2-18b Candidate Low-Frequency (M7.2, R = 130 km) Time Histories for Spectral Matching

Earthquake	Date	Mw	Station	Distance (km)	Vs30m (m/s)
San Fernando	02/09/1971	6.61	Isabella Dam (Aux Abut)	130.98	684.9
Loma Prieta	10/18/1989	6.93	SF-Rincon Hill	74.14	873.1
Loma Prieta	10/18/1989	6.93	So. San Francisco, Sierra Pt.	63.15	1020.6
Loma Prieta	10/18/1989	6.93	Yerba Buena Island	75.17	659.8
Northridge	01/17/1994	6.69	Rancho Cucamonga-Deer Canyon	79.99	821.7
Northridge	01/17/1994	6.69	Wrightwood-Jackson Flat	64.66	821.7
Kobe	01/16/1995	6.90	OKA	86.94	609.0
Kocaeli	08/17/1999	7.51	Bursa Sivil	65.53	659.6
Chi-Chi	09/20/1999	7.62	ILA031	83.31	649.3
Kobe	01/16/1995	6.90	MZH	70.26	609.0
Hector Mine	10/16/1999	7.13	Anza-Pinyon Flat	89.98	724.9
Hector Mine	10/16/1999	7.13	Anza-Tripp Flats Training	102.40	684.9
Hector Mine	10/16/1999	7.13	Banning-Twin Pines Road	83.43	684.9
Hector Mine	10/16/1999	7.13	Heart Bar State Park	61.21	684.9
Hector Mine	10/16/1999	7.13	Seven Oaks Dam Project Office	87.20	659.6

Table 2.5.2-19 Site Response Analyses Performed

Probability (per year) ->	10^{-4}		10^{-5}		10^{-6}				Total No. Analyses
Time Histories Analyzed ->	30 High Freq.	30 Low Freq.	30 High Freq.	30 Low Freq.	30 High Freq.	30 Low Freq.			
Randomized Soil Columns (EPRI) ->	60	60	60	60	60	60			360
Randomized Soil Columns (SRS) ->	60	60	60	60	60	60			360
									720

Table 2.5.2-20a Amplification Factors as a Function of Input Hard Rock Motion at Top of Blue Bluff Marl (depth 86 feet), as Developed from Site Response Analysis using SRS and EPRI Soil Degradation Models, for High-frequency Rock Motions

	10^{-4}			10^{-5}			10^{-6}		
Freq, Hz	Hard rock input motion	mean amp. factors		Hard rock input motion	mean amp. factors		Hard rock input motion	mean amp. factors	
		EPRI	SRS		EPRI	SRS		EPRI	SRS
100	0.294	1.18	1.20	0.703	0.979	0.920	1.60	0.766	0.620
76	0.400	0.903	0.930	0.957	0.740	0.695	2.17	0.571	0.462
60	0.499	0.769	0.799	1.19	0.606	0.573	2.71	0.456	0.369
50	0.595	0.697	0.722	1.42	0.531	0.500	3.23	0.386	0.313
40	0.631	0.775	0.819	1.51	0.553	0.523	3.43	0.379	0.306
30	0.655	0.961	1.02	1.57	0.664	0.626	3.63	0.398	0.319
25	0.647	1.14	1.21	1.55	0.812	0.768	3.71	0.446	0.354
20	0.615	1.33	1.39	1.47	0.991	0.937	3.34	0.579	0.453
16.5	0.575	1.47	1.52	1.38	1.133	1.07	3.13	0.705	0.560
13.4	0.521	1.67	1.69	1.25	1.312	1.23	2.83	0.875	0.685
12.2	0.494	1.78	1.81	1.18	1.417	1.33	2.69	0.953	0.754
10	0.438	1.81	1.82	1.05	1.600	1.50	2.38	1.15	0.928
8.1	0.377	2.19	2.18	0.902	1.747	1.65	2.05	1.34	1.09
7	0.339	2.30	2.26	0.811	1.984	1.87	1.84	1.47	1.21
6	0.298	2.05	2.03	0.713	2.096	1.93	1.62	1.68	1.38
5	0.257	2.11	2.08	0.615	2.022	1.88	1.40	1.90	1.56
4	0.212	2.56	2.54	0.507	2.300	2.16	1.15	2.09	1.70
3.3	0.175	2.88	2.81	0.419	2.687	2.51	0.952	2.42	2.00
2.5	0.131	3.16	3.05	0.314	3.089	2.83	0.713	2.78	2.33
2	0.101	2.49	2.38	0.242	2.651	2.38	0.549	2.96	2.39
1.5	0.064	3.22	3.12	0.154	3.193	2.86	0.350	3.28	2.48
1	0.035	2.34	2.30	0.0828	2.542	2.41	0.188	3.00	2.55
0.8	0.024	2.63	2.59	0.0563	2.695	2.55	0.128	2.95	2.54
0.7	0.0187	3.15	3.10	0.0447	3.141	2.97	0.101	3.31	2.86
0.61	0.0148	3.80	3.78	0.0354	3.842	3.69	0.0804	4.02	3.52
0.5	0.0109	3.40	3.43	0.0260	3.597	3.59	0.0590	4.00	3.81
0.33	0.00525	2.19	2.19	0.0126	2.269	2.25	0.0286	2.52	2.40
0.25	0.00314	1.98	1.97	0.00751	2.059	2.00	0.0171	2.24	2.07
0.15	0.00106	2.06	2.04	0.00254	2.149	2.05	0.00577	2.37	2.06
0.1	0.000370	2.27	2.23	0.000890	2.341	2.18	0.00201	2.43	2.06

Table 2.5.2-20b Amplification Factors as a Function of Input Hard Rock Motion at Top of Blue Bluff Marl (depth 86 feet), as Developed from Site Response Analysis using SRS and EPRI Soil Degradation Models, for Low-frequency Rock Motions

	10^{-4}			10^{-5}			10^{-6}		
Freq, Hz	Hard rock input motion	mean amp. factors EPRI	mean amp. factors SRS	Hard rock input motion	mean amp. factors EPRI	mean amp. factors SRS	Hard rock input motion	mean amp. factors EPRI	mean amp. factors SRS
100	0.224	1.31	1.25	0.517	1.111	0.896	1.03	0.931	0.591
76	0.305	0.987	0.942	0.704	0.828	0.667	1.40	0.692	0.439
60	0.380	0.802	0.765	0.878	0.660	0.532	1.74	0.550	0.349
50	0.453	0.695	0.662	1.047	0.557	0.449	2.08	0.462	0.293
40	0.483	0.677	0.644	1.115	0.532	0.428	2.22	0.437	0.277
30	0.506	0.764	0.73	1.168	0.529	0.417	2.32	0.417	0.264
25	0.505	0.90	0.86	1.167	0.570	0.440	2.32	0.422	0.266
20	0.493	1.07	1.02	1.139	0.653	0.492	2.26	0.445	0.276
16.5	0.476	1.21	1.16	1.101	0.762	0.57	2.19	0.481	0.293
13.4	0.453	1.41	1.34	1.046	0.877	0.66	2.08	0.536	0.316
12.2	0.440	1.49	1.42	1.017	0.943	0.71	2.02	0.571	0.335
10	0.413	1.61	1.54	0.954	1.151	0.87	1.90	0.68	0.389
8.1	0.381	1.91	1.82	0.880	1.343	1.05	1.75	0.83	0.46
7	0.359	2.09	1.96	0.830	1.534	1.23	1.65	0.97	0.55
6	0.334	1.99	1.88	0.771	1.734	1.35	1.53	1.12	0.66
5	0.307	1.97	1.89	0.709	1.804	1.38	1.41	1.36	0.78
4	0.275	2.46	2.37	0.635	1.967	1.62	1.26	1.57	0.93
3.3	0.246	2.90	2.78	0.569	2.443	2.05	1.13	1.94	1.21
2.5	0.209	3.29	3.05	0.483	2.813	2.29	0.960	2.43	1.61
2	0.181	2.34	2.16	0.418	2.817	2.24	0.831	2.82	1.82
1.5	0.137	3.30	3.07	0.318	3.124	2.29	0.632	3.19	1.70
1	0.0917	2.27	2.21	0.214	2.697	2.42	0.423	3.70	2.32
0.8	0.0768	2.67	2.56	0.193	2.754	2.41	0.405	3.26	2.42
0.7	0.0703	3.25	3.10	0.184	3.233	2.80	0.397	3.50	2.48
0.61	0.0652	4.00	3.90	0.177	3.933	3.43	0.390	3.94	2.71
0.5	0.0590	3.66	3.72	0.167	4.107	4.01	0.382	4.75	3.46
0.33	0.0317	1.97	2.00	0.0901	2.219	2.30	0.206	2.85	2.96
0.25	0.0209	1.64	1.65	0.0592	1.726	1.75	0.136	2.05	2.06
0.15	0.0095	1.36	1.36	0.0270	1.395	1.39	0.0617	1.55	1.54
0.1	0.0047	1.30	1.29	0.0134	1.321	1.31	0.0307	1.45	1.40

Table 2.5.2-21 Spectral Accelerations (SA, in g) for Hard Rock Conditions and for Hypothetical Outcrop of Highest Competent In Situ Layer (Top of Blue Bluff Marl)

	Hard Rock spectral accel, g			Soil spectral accel, g		
Freq	10^{-4}	10^{-5}	10^{-6}	10^{-4}	10^{-5}	10^{-6}
100	0.214	0.559	1.480	0.255	0.531	1.025
76	0.293	0.777	2.059	0.268	0.558	1.063
60	0.394	1.057	2.802	0.311	0.629	1.167
50	0.464	1.257	3.334	0.333	0.656	1.180
40	0.517	1.416	3.758	0.423	0.778	1.310
30	0.545	1.511	4.011	0.545	0.984	1.452
25	0.551	1.540	4.090	0.646	1.217	1.636
20	0.522	1.419	3.685	0.723	1.390	1.925
16.5	0.493	1.309	3.330	0.758	1.474	2.139
13.4	0.456	1.176	2.914	0.784	1.523	2.299
12.2	0.438	1.115	2.727	0.800	1.553	2.349
10	0.399	0.983	2.330	0.722	1.522	2.405
8.1	0.375	0.904	2.071	0.831	1.551	2.517
7	0.359	0.852	1.909	0.801	1.658	2.574
6	0.339	0.792	1.728	0.671	1.601	2.650
5	0.317	0.728	1.540	0.612	1.306	2.665
4	0.287	0.659	1.369	0.694	1.190	2.419
3.3	0.259	0.595	1.213	0.735	1.335	2.350
2.5	0.223	0.512	1.020	0.706	1.300	2.184
2	0.193	0.445	0.886	0.440	1.153	2.036
1.5	0.152	0.352	0.698	0.484	0.952	1.705
1	0.101	0.235	0.465	0.226	0.597	1.396
0.8	0.091	0.230	0.489	0.237	0.595	1.388
0.7	0.083	0.220	0.481	0.264	0.664	1.436
0.61	0.076	0.207	0.462	0.299	0.761	1.535
0.5	0.065	0.185	0.423	0.238	0.745	1.741
0.33	0.038	0.107	0.245	0.075	0.242	0.712
0.25	0.026	0.072	0.166	0.042	0.126	0.341
0.15	0.012	0.033	0.075	0.016	0.046	0.116
0.1	0.006	0.016	0.036	0.007	0.021	0.051

Table 2.5.2-22 SSE Amplitudes (g) for the Hypothetical Outcrop of Highest Competent In Situ Layer (Top of Blue Bluff Marl)

	Soil amplitudes				raw	smoothed
Freq	10^{-4}	10^{-5}	AR	DF2	SSE	SSE
100	0.255	0.531	2.08	1.08	0.275	0.275
76	0.268	0.558	2.08	1.08	0.289	0.295
60	0.311	0.629	2.02	1.05	0.328	0.326
50	0.333	0.656	1.97	1.03	0.344	0.366
40	0.423	0.778	1.84	0.978	0.423	0.435
30	0.545	0.984	1.80	0.962	0.545	0.551
25	0.646	1.217	1.88	0.995	0.646	0.646
20	0.723	1.390	1.92	1.01	0.732	0.725
16.5	0.758	1.474	1.95	1.02	0.774	0.764
13.4	0.784	1.523	1.94	1.02	0.800	0.795
12.2	0.800	1.553	1.94	1.02	0.816	0.803
10	0.722	1.522	2.11	1.09	0.787	0.787
8.1	0.831	1.551	1.87	0.989	0.831	0.789
7	0.801	1.658	2.07	1.07	0.860	0.773
6	0.671	1.601	2.39	1.20	0.807	0.758
5	0.612	1.306	2.13	1.10	0.673	0.748
4	0.694	1.190	1.71	0.924	0.694	0.724
3.3	0.735	1.335	1.82	0.967	0.735	0.710
2.5	0.706	1.300	1.84	0.977	0.706	0.706
2	0.440	1.153	2.62	1.30	0.571	0.580
1.5	0.484	0.952	1.96	1.03	0.499	0.480
1	0.226	0.597	2.65	1.31	0.295	0.295
0.8	0.237	0.595	2.51	1.25	0.297	0.297
0.7	0.264	0.664	2.51	1.25	0.332	0.332
0.61	0.299	0.761	2.55	1.27	0.379	0.379
0.5	0.238	0.745	3.13	1.50	0.356	0.356
0.33	0.0750	0.242	3.23	1.53	0.115	0.115
0.25	0.0420	0.126	3.00	1.44	0.0606	0.0606
0.15	0.0158	0.0458	2.90	1.41	0.0222	0.0222
0.1	0.00718	0.0207	2.88	1.40	0.0100	0.0100

Table 2.5.2-23 Conversion between body-wave (m_b) and moment (M) magnitudes.

Convert	To	Convert	To
m_b	M	M	m_b
4.00	3.77	4.00	4.28
4.10	3.84	4.10	4.41
4.20	3.92	4.20	4.54
4.30	4.00	4.30	4.66
4.40	4.08	4.40	4.78
4.50	4.16	4.50	4.90
4.60	4.24	4.60	5.01
4.70	4.33	4.70	5.12
4.80	4.42	4.80	5.23
4.90	4.50	4.90	5.33
5.00	4.59	5.00	5.43
5.10	4.69	5.10	5.52
5.20	4.78	5.20	5.61
5.30	4.88	5.30	5.70
5.40	4.97	5.40	5.78
5.50	5.08	5.50	5.87
5.60	5.19	5.60	5.95
5.70	5.31	5.70	6.03
5.80	5.42	5.80	6.11
5.90	5.54	5.90	6.18
6.00	5.66	6.00	6.26
6.10	5.79	6.10	6.33
6.20	5.92	6.20	6.40
6.30	6.06	6.30	6.47
6.40	6.20	6.40	6.53
6.50	6.34	6.50	6.60
6.60	6.49	6.60	6.66
6.70	6.65	6.70	6.73
6.80	6.82	6.80	6.79
6.90	6.98	6.90	6.85
7.00	7.16	7.00	6.91
7.10	7.33	7.10	6.97
7.20	7.51	7.20	7.03
7.30	7.69	7.30	7.09
7.40	7.87	7.40	7.15
7.50	8.04	7.50	7.20
		7.60	7.26
		7.70	7.32
		7.80	7.37
		7.90	7.43
		8.00	7.49

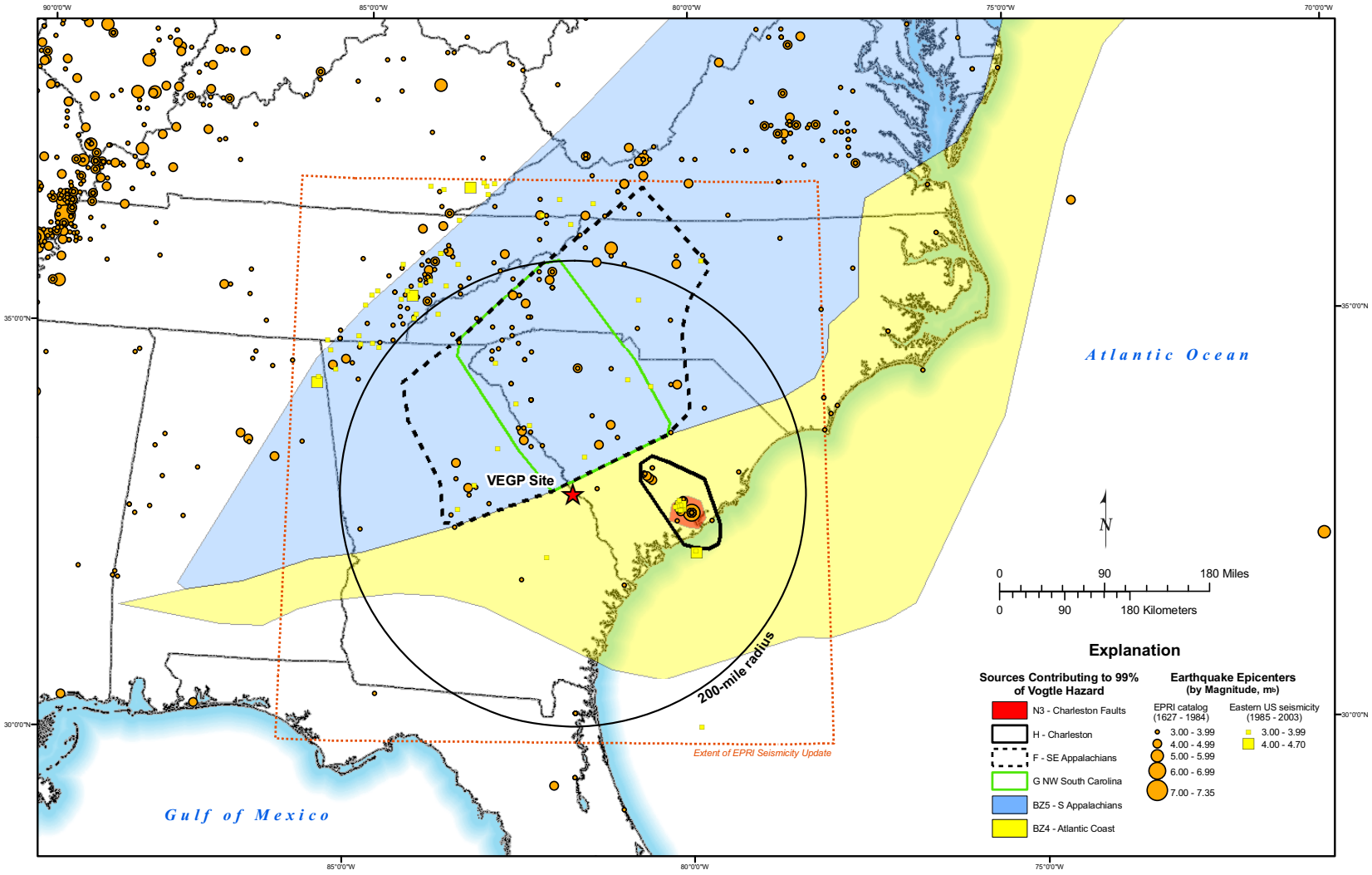

Figure 2.5.2-1 Bechtel EPRI Zones

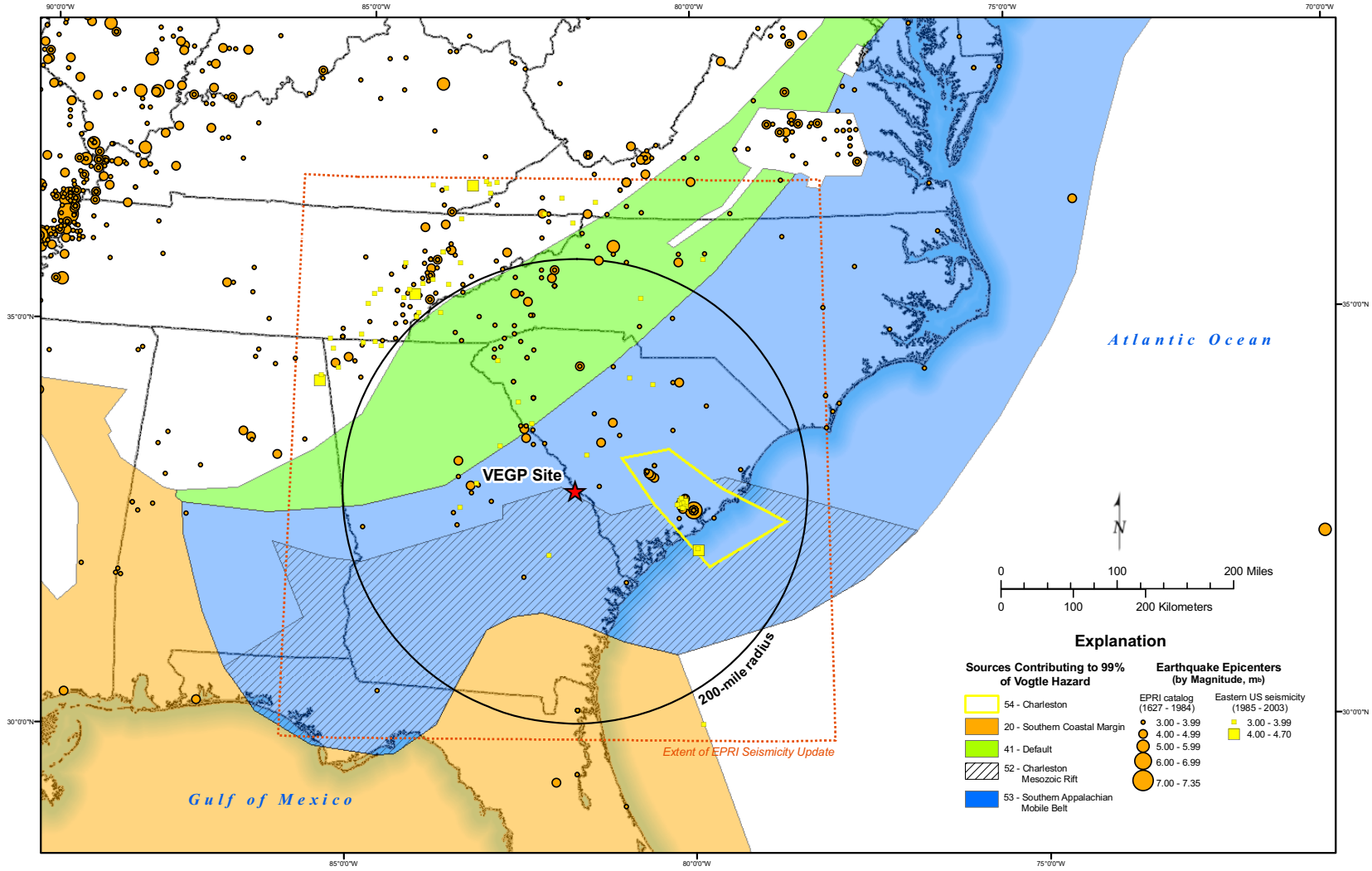

Figure 2.5.2-2 Dames and Moore EPRI Zones

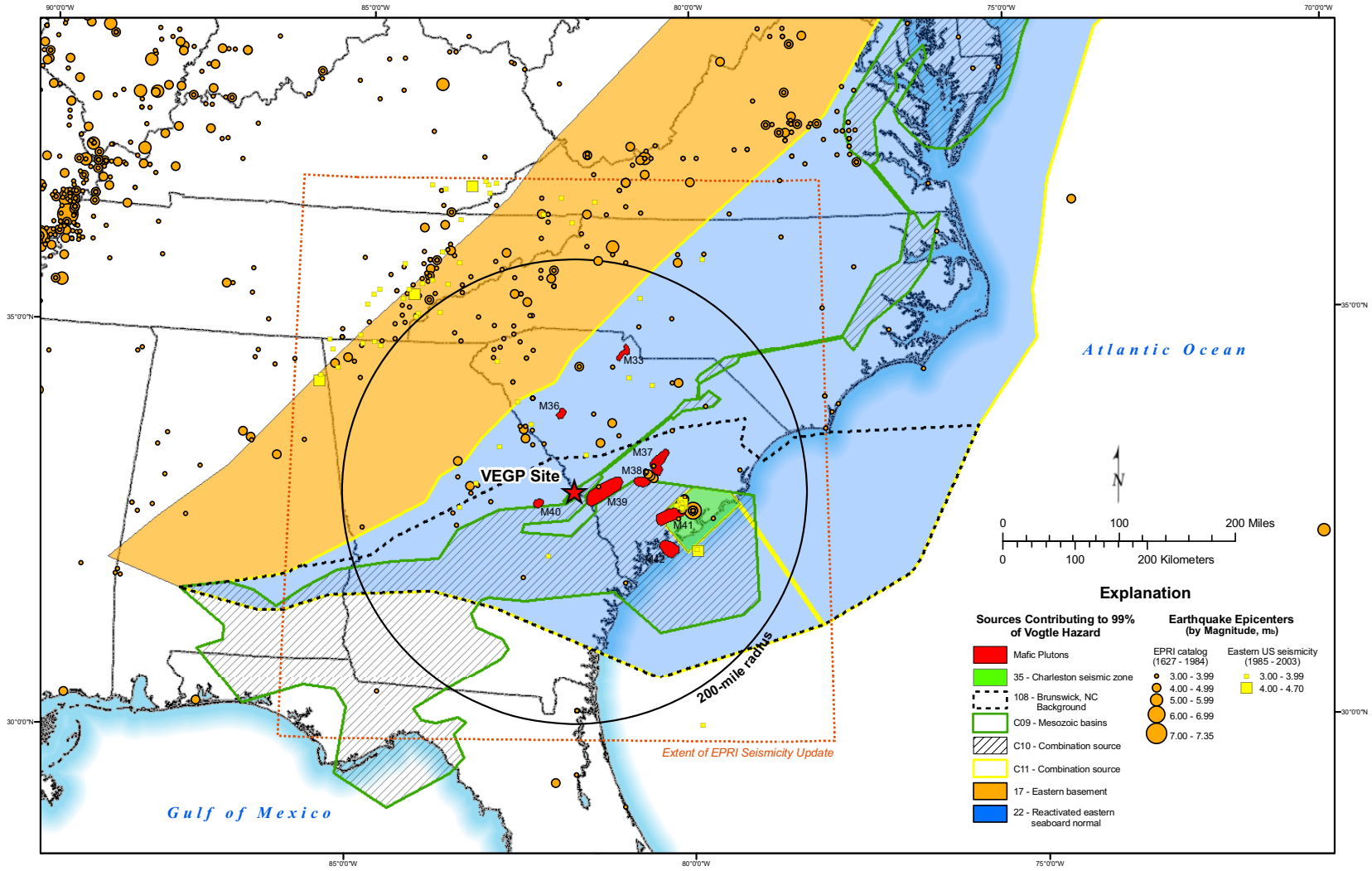

Figure 2.5.2-3 LAW EPRI Zones

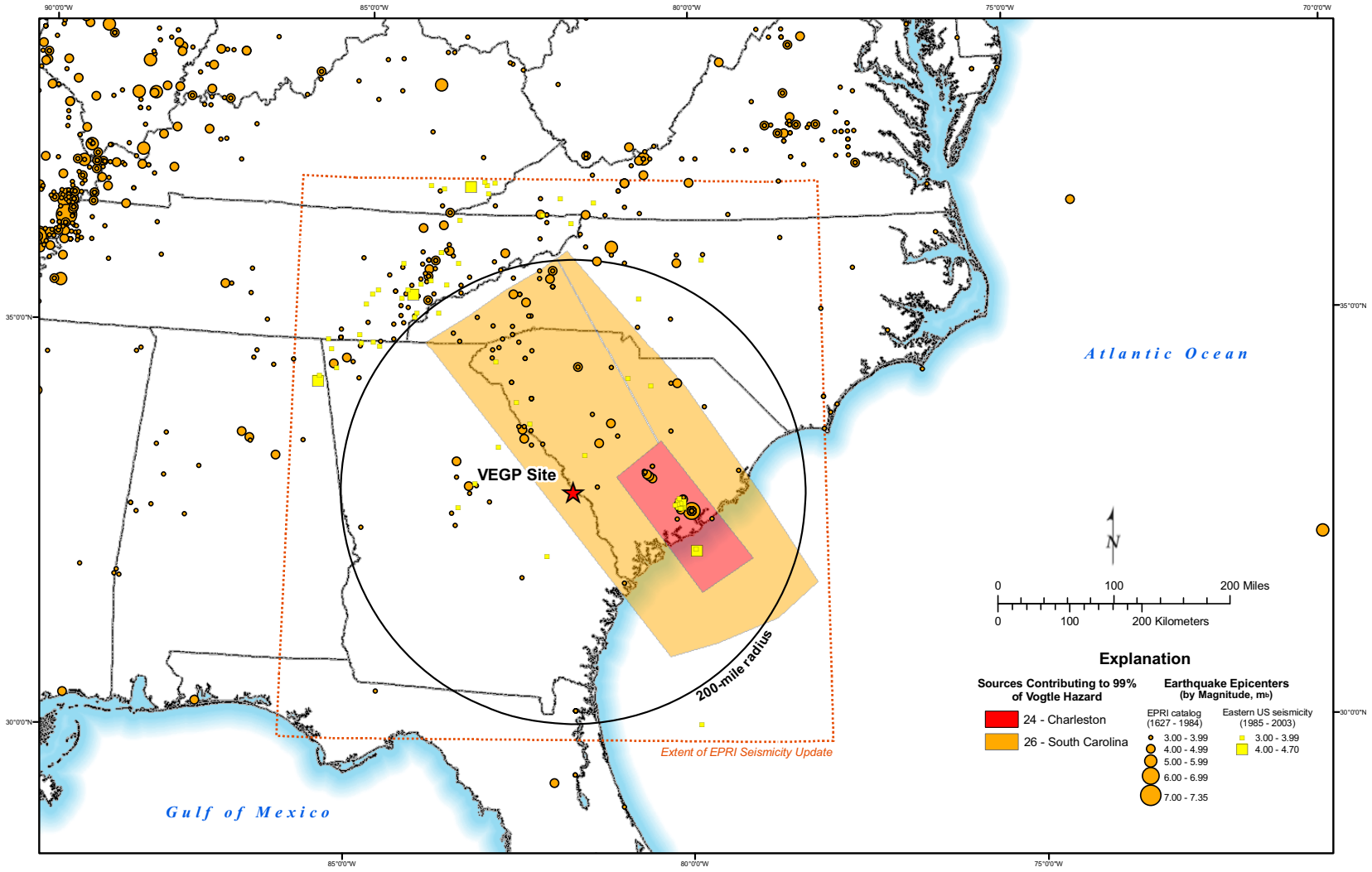

Figure 2.5.2-4 Rondout EPRI Zones

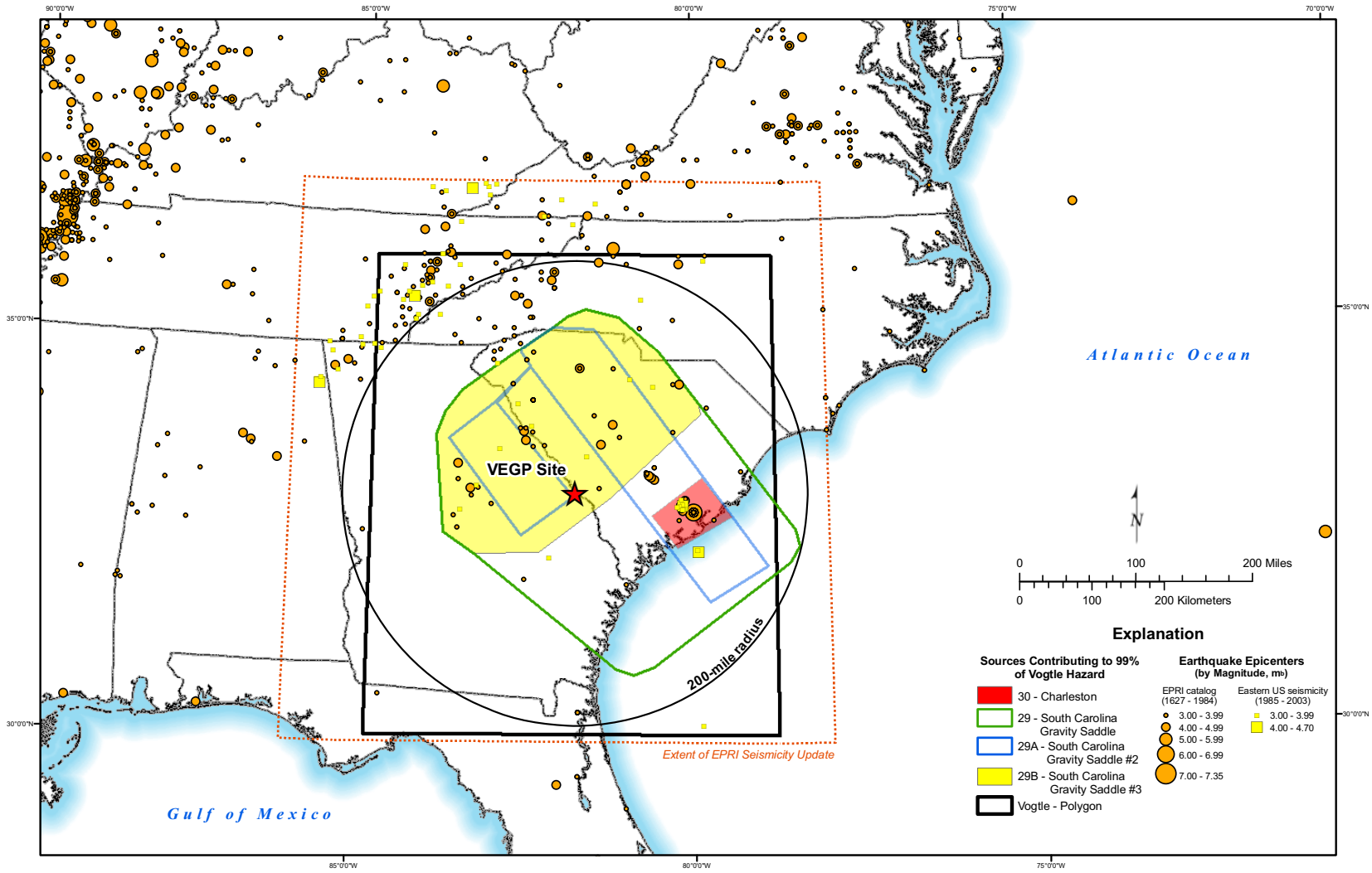

Figure 2.5.2-5 Woodward-Clyde EPRI Zones

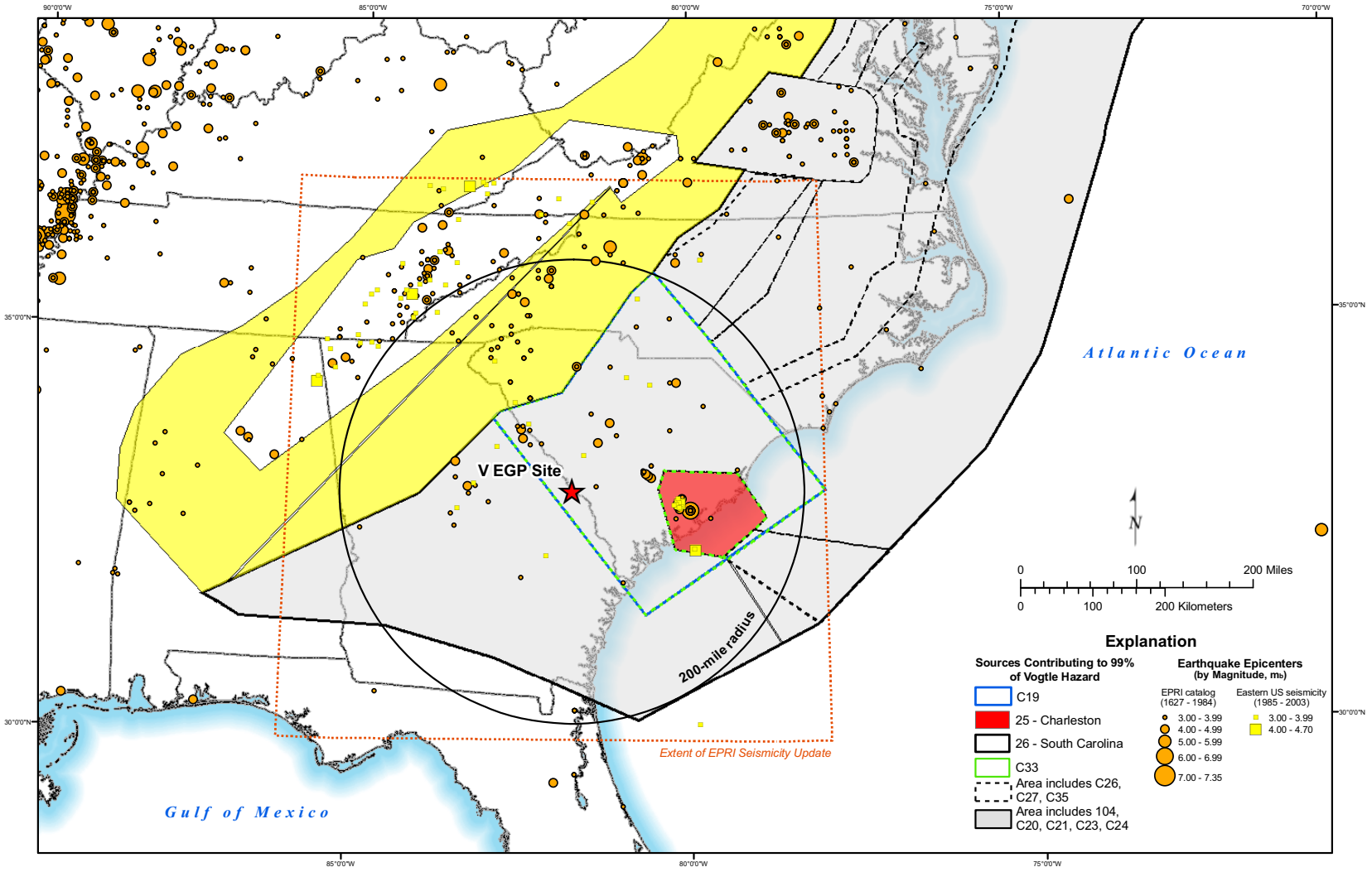

Figure 2.5.2-6 Weston EPRI Zones

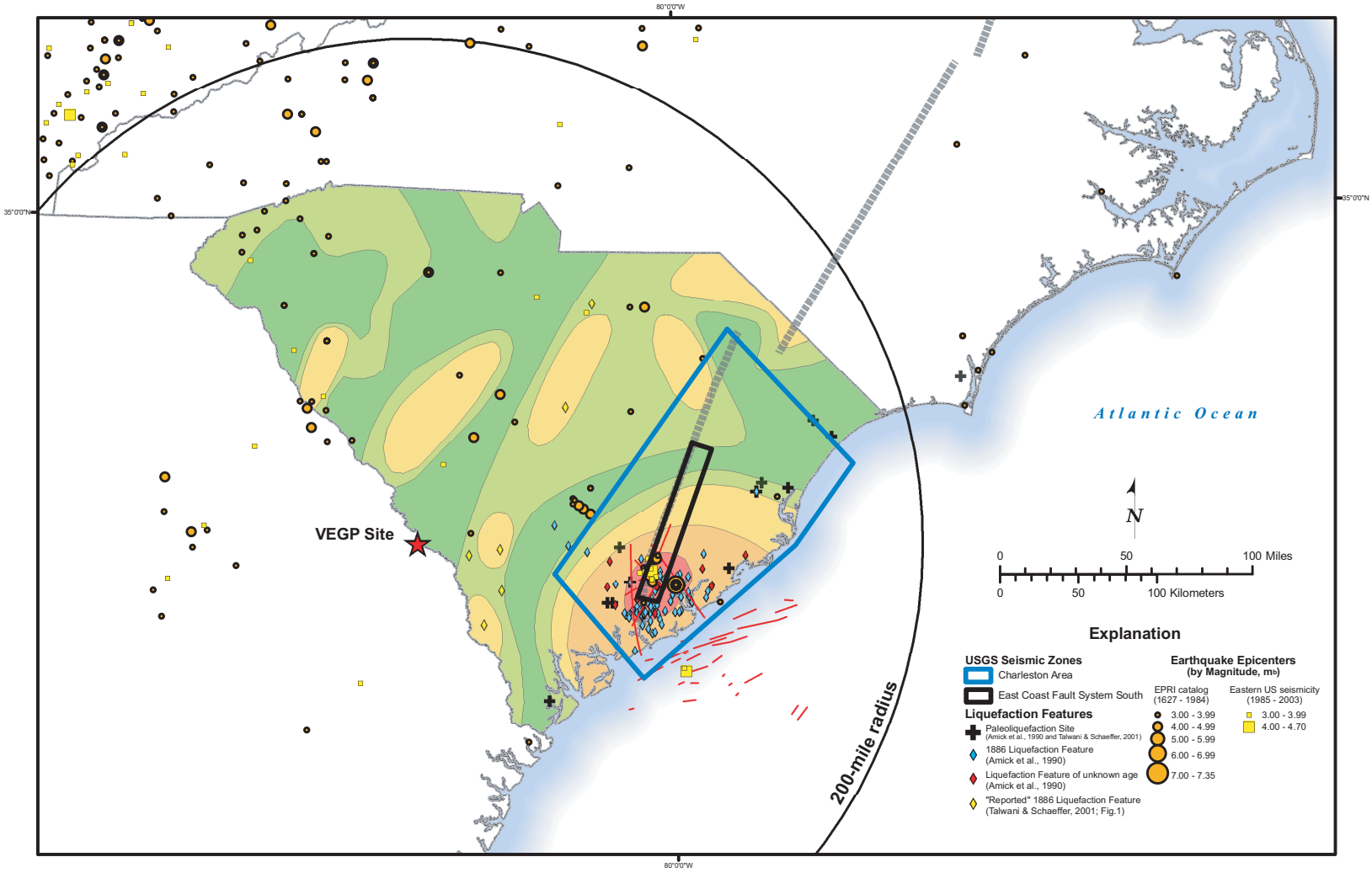

Figure 2.5.2-7 USGS Model

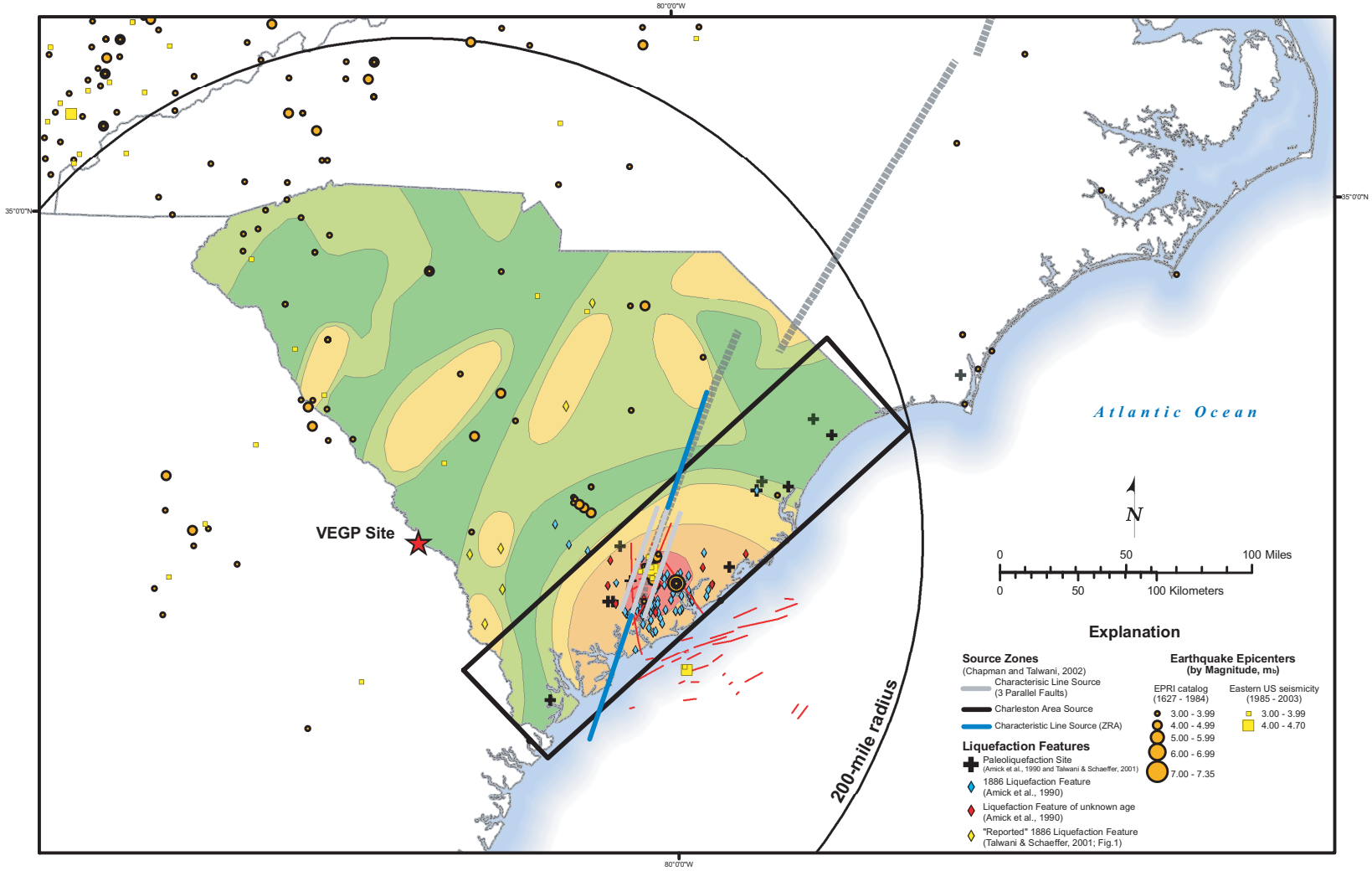

Figure 2.5.2-8 SCDOT Model

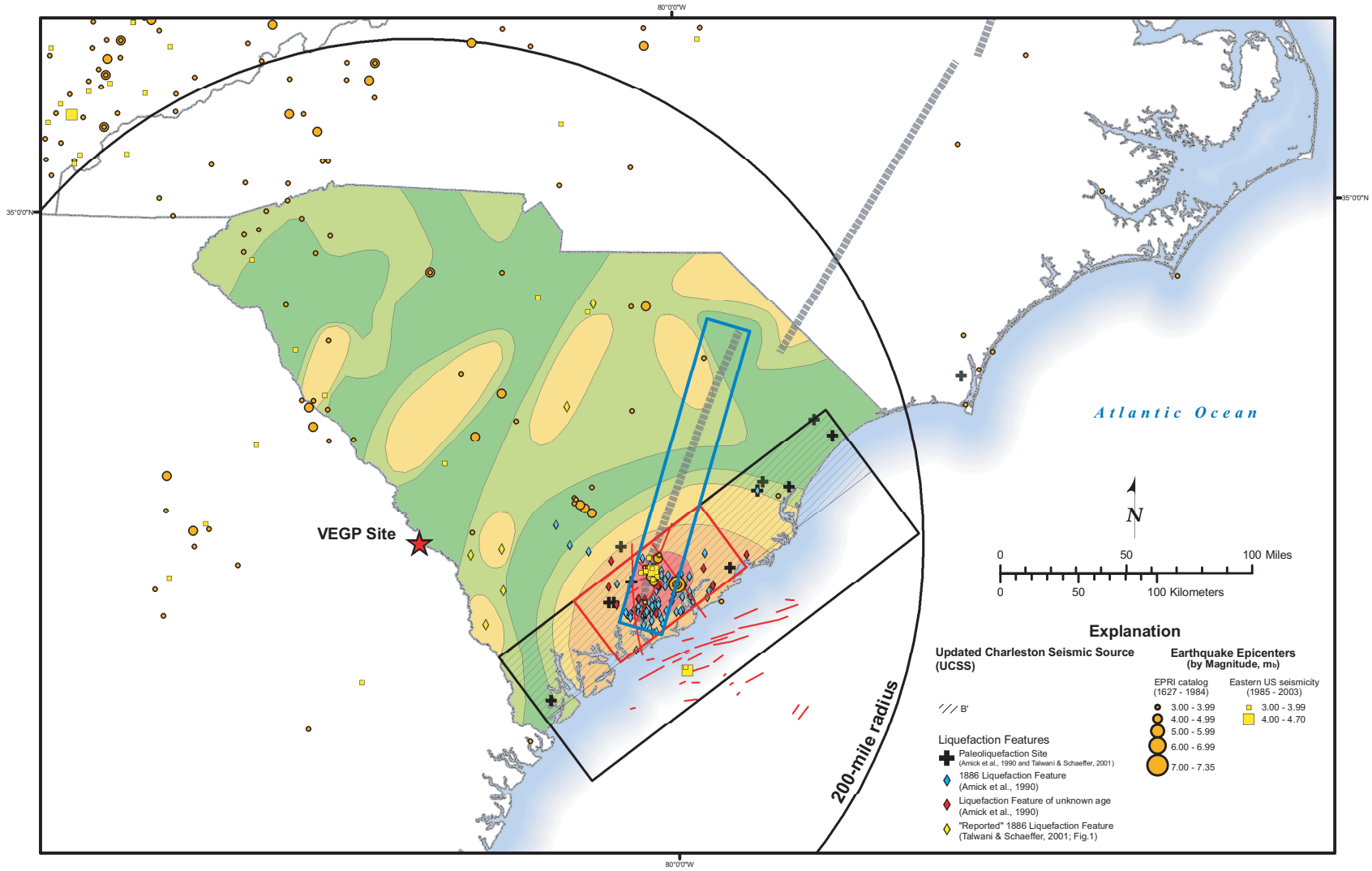

Figure 2.5.2-9 UCSS Map.

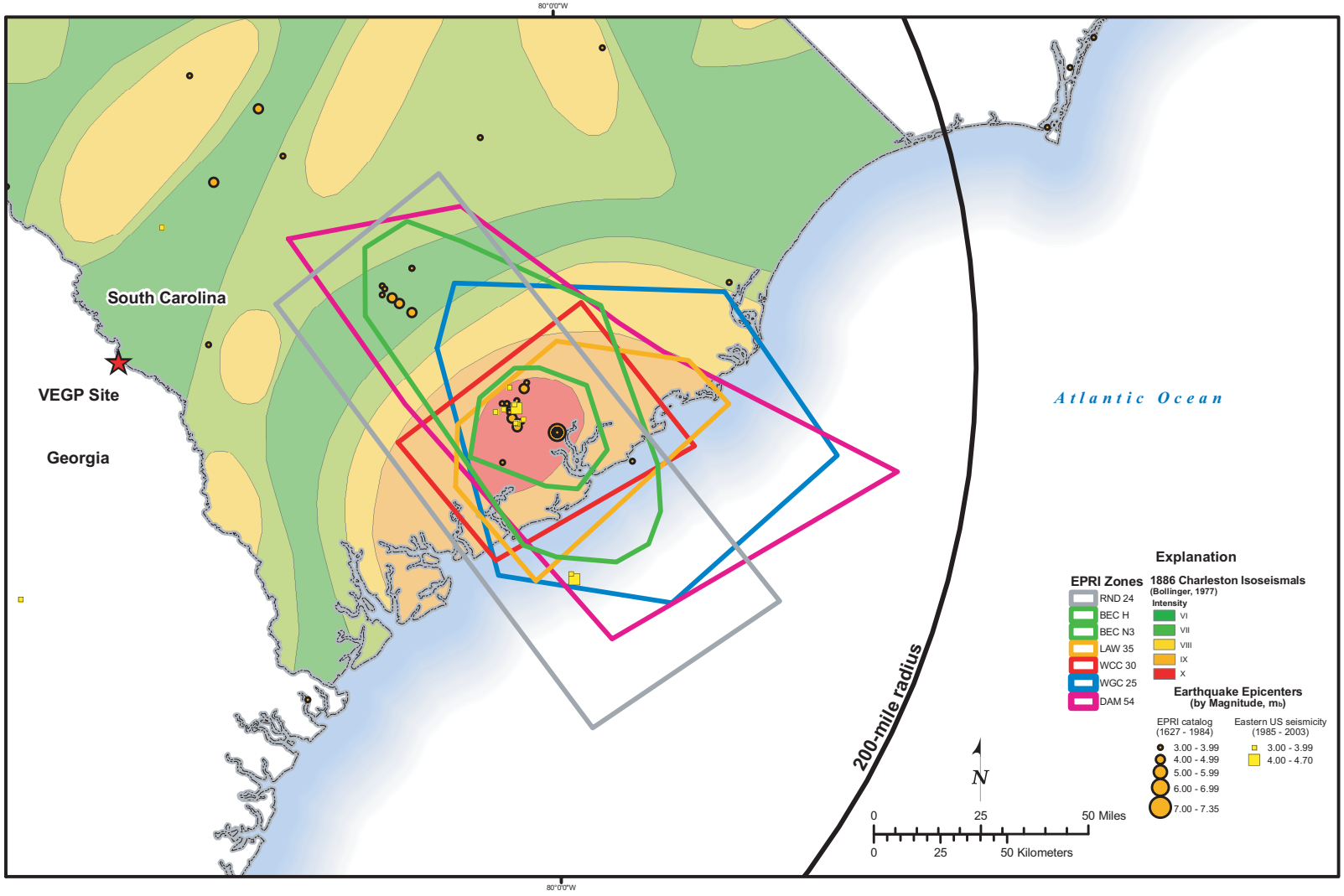

Figure 2.5.2-10 EPRI All Charleston Map

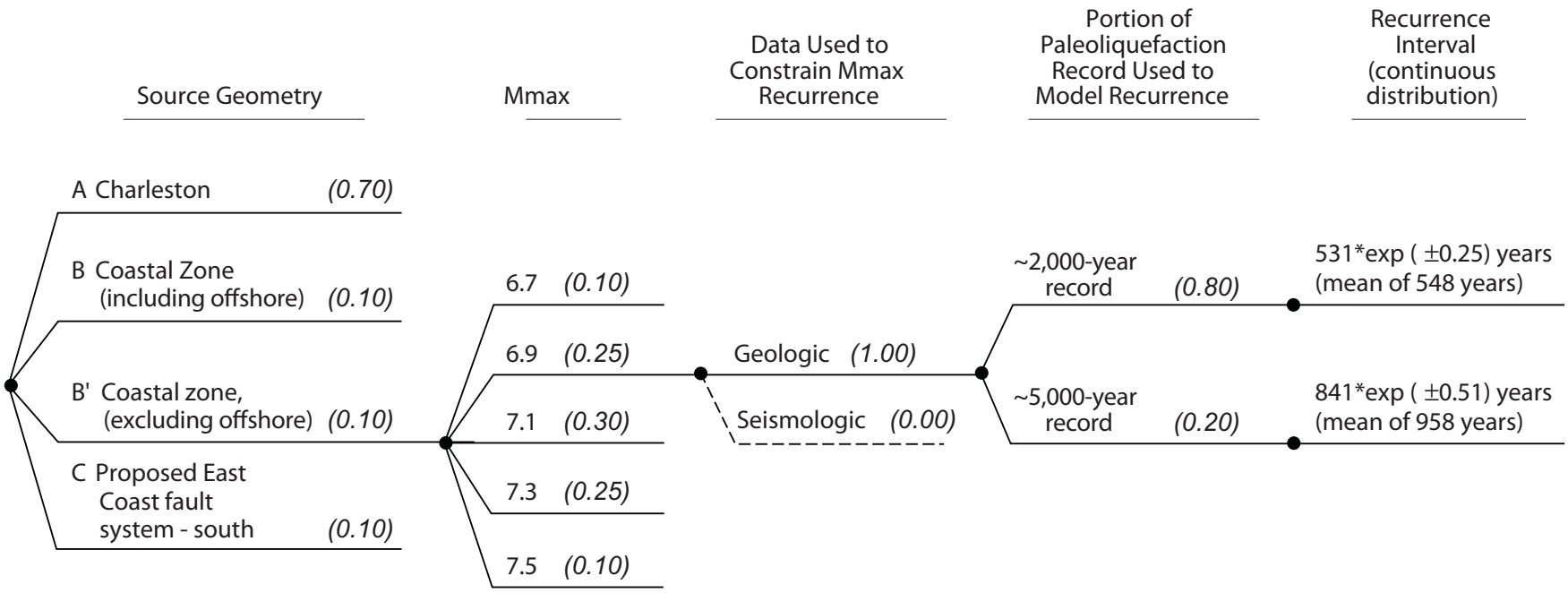

Figure 2.5.2-11 Updated Charleston Seismic Source (USGS) Logic Tree with Weights for each Branch Shown in Italics

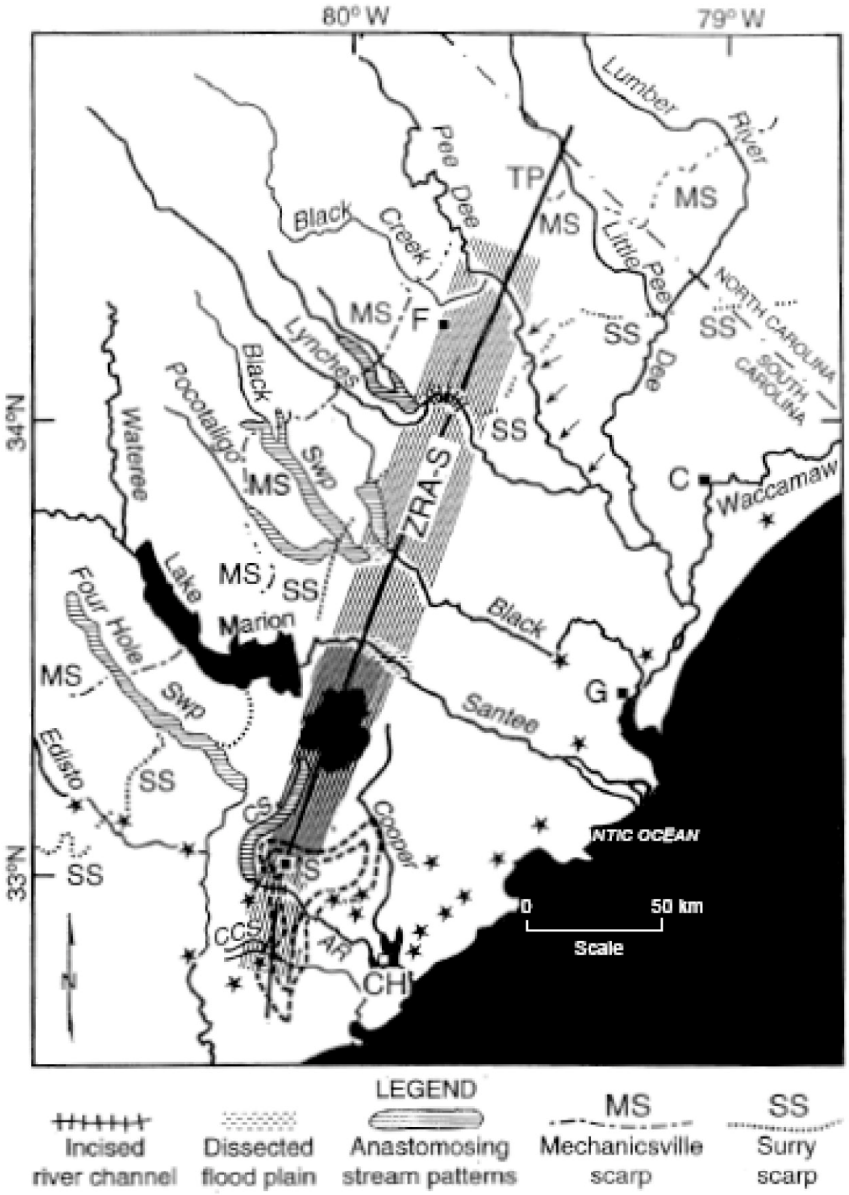

Map of ZRA-S from Marple and Talwani (2000). Figure shows southern zone of river anomalies (ZRA-S; striped area), anastomosing stream patterns, pre 1886 sandblow sites (stars), and topographic profile (TP, bold line) approximately along the ZRA-S axis. Arrows along Pee Dee River denote reach flowing against southwest valley wall. Closed dashed contours near Summerville are highest-intensity isoseismals of the 1886 Charleston, South Carolina, earthquake (from Dutton, 1889). Abbreviations are as follows: AR - Ashley River; C - Conway; CCS - Caw Caw Swamp; CH - Charleston; CS - Cypress Swamp; F - Florence; G - Georgetown; LM - Lake Moultrie; MS - Mechanicsville littoral scarp; S - Summerville; SS - Surry littoral scarp.

Figure 2.5.2-12 Map of ZRA-S from Marple and Talwani (2000)

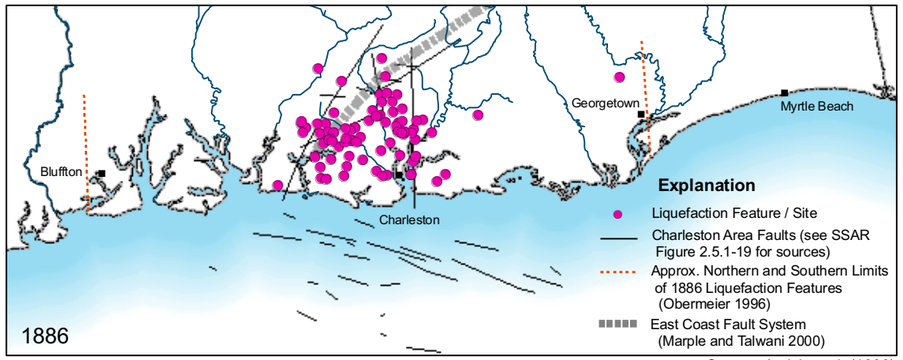

Source: Amick et al. (1990)

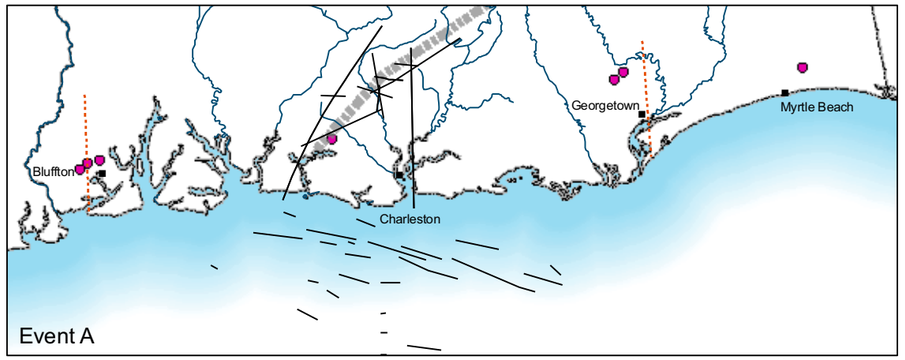

Source: Talwani and Schaeffer (2001)

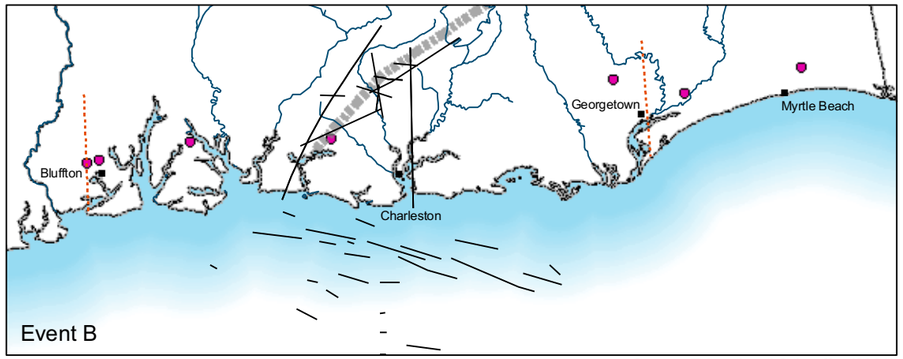

Source: Talwani and Schaeffer (2001)

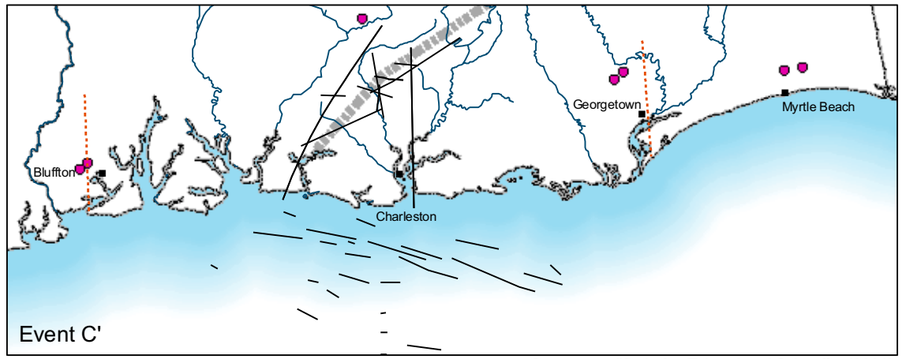

Source: modified after Talwani and Schaeffer (2001)

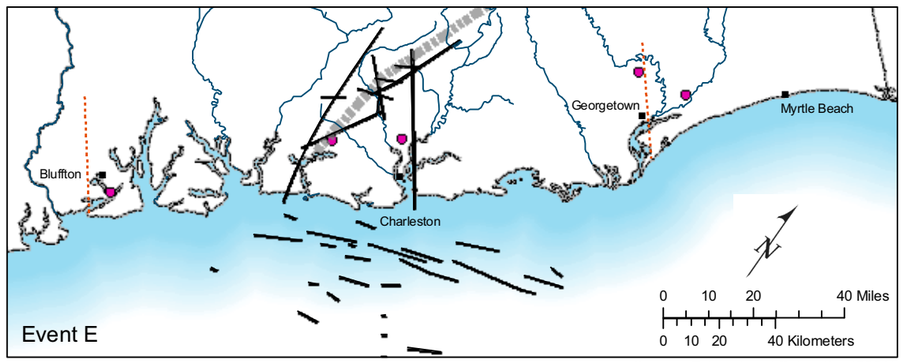

Source: Talwani and Schaeffer (2001)

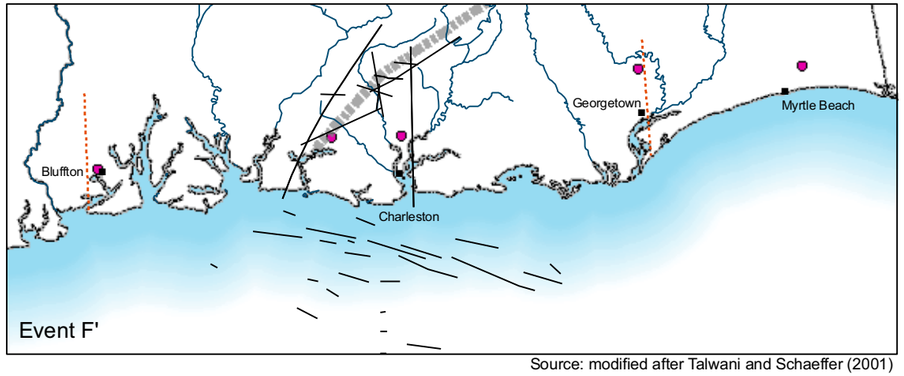

Source: modified after Talwani and Schaeffer (2001)

Figure 2.5.2-12a Geographic Distribution of Liquefaction Features Associated with Charleston Earthquakes

This page is intentionally blank.

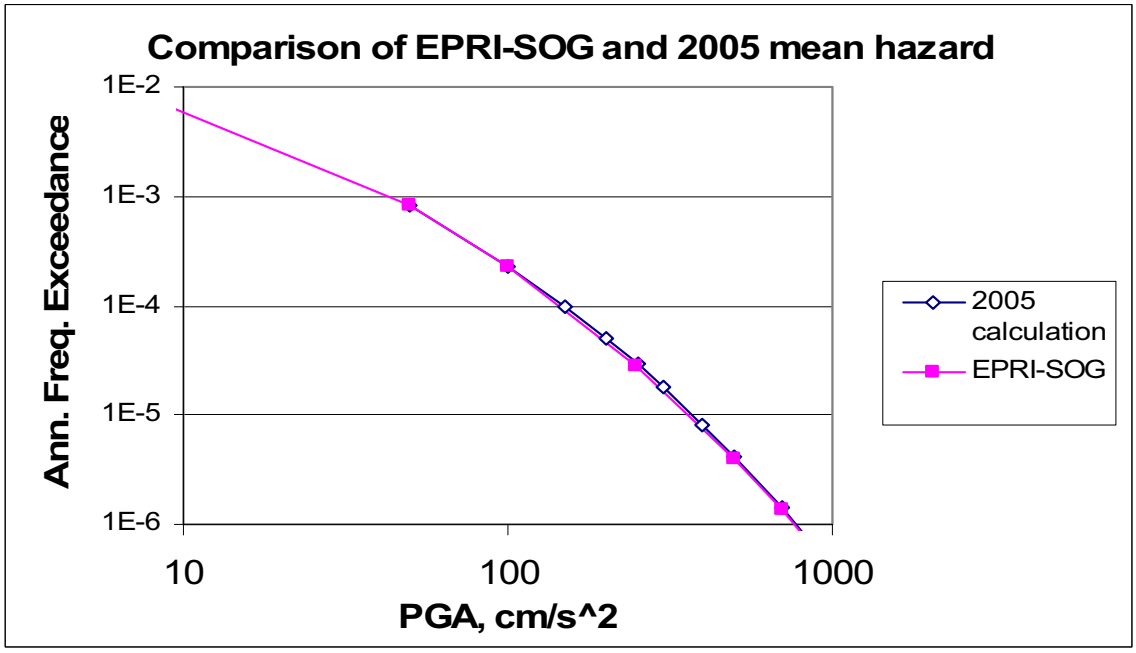

Figure 2.5.2-13 PGA Mean Seismic Hazard Curves for Current (2005) Calculation and for EPRI-SOG

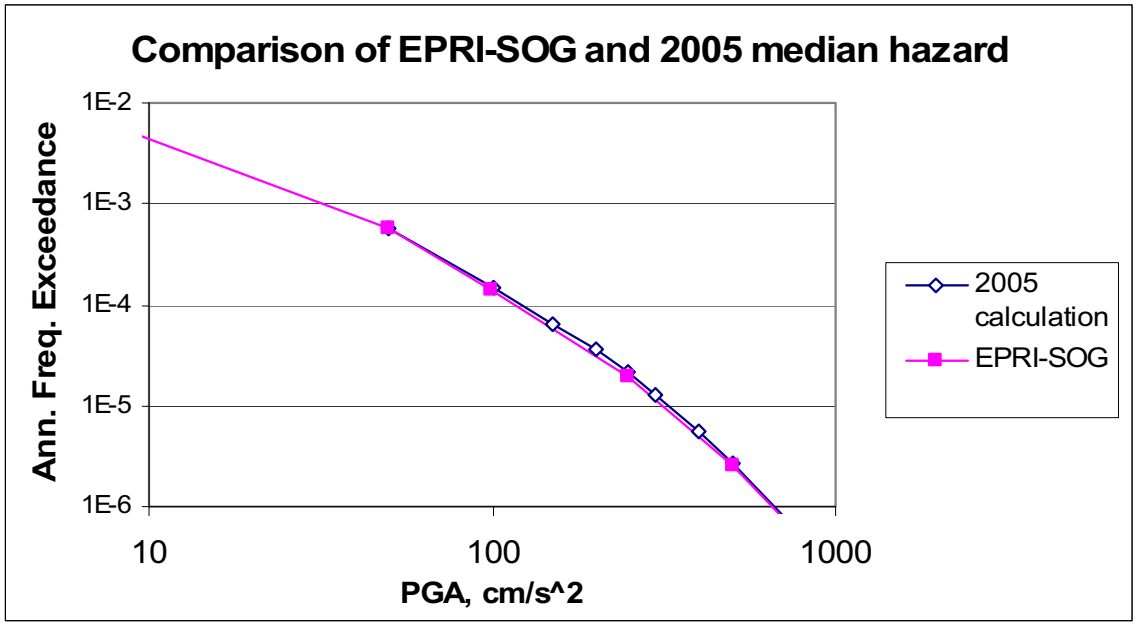

Figure 2.5.2-14 PGA Median Seismic Hazard Curves for Current (2005) Calculation and for EPRI-SOG

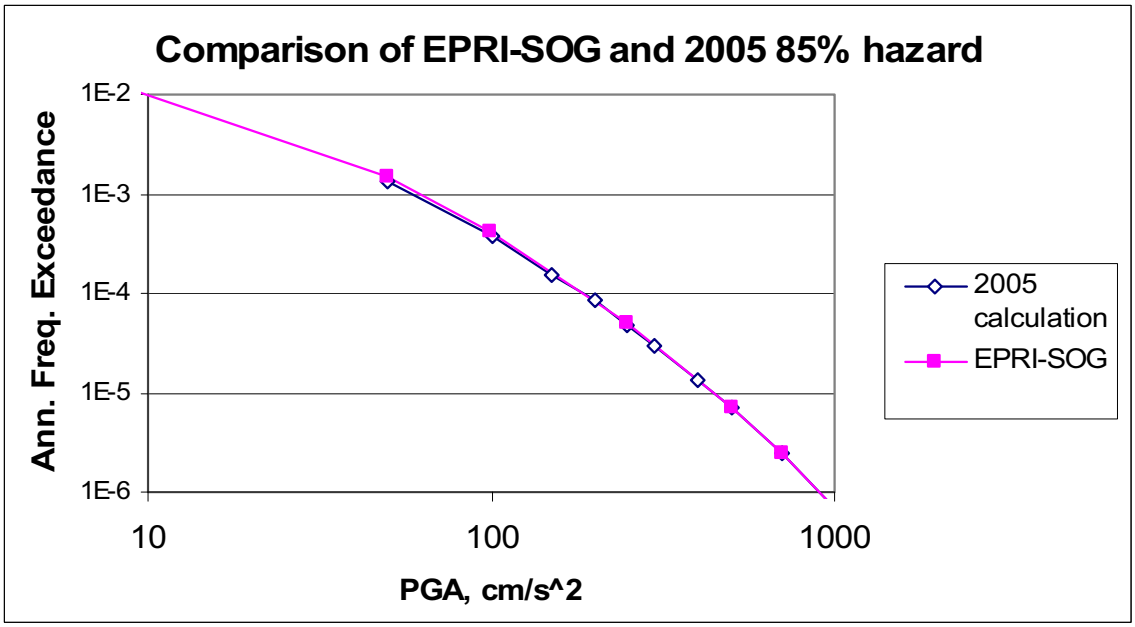

Figure 2.5.2-15 PGA 85 Percent Seismic Hazard Curves for Current (2005) Calculation and for EPRI-SOG

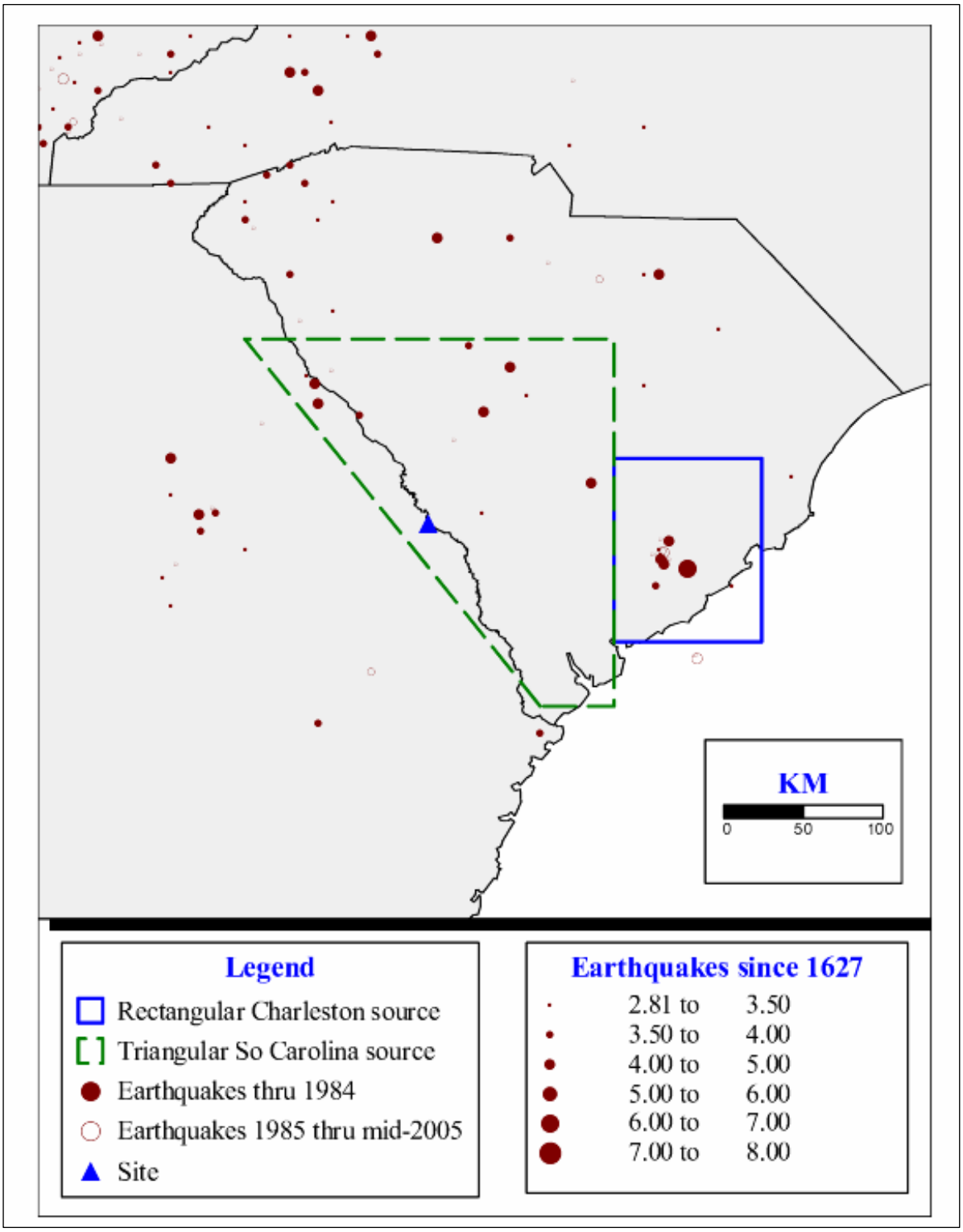

Figure 2.5.2-16 Map Showing Two Areas Used To Examine Effect of New Seismicity Information

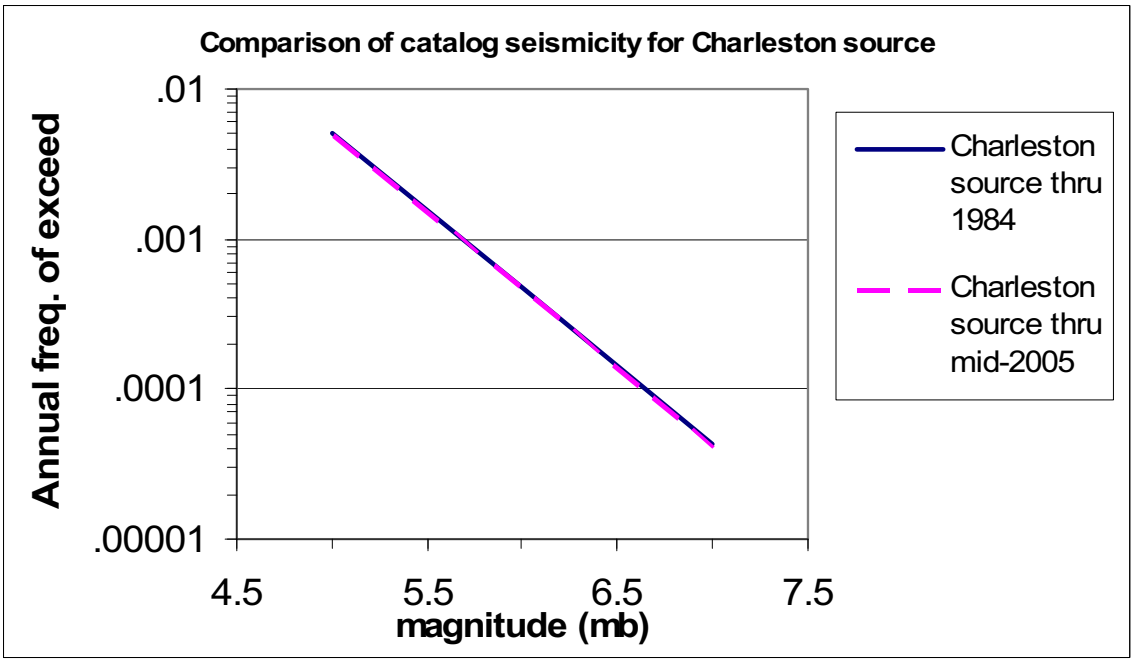

Figure 2.5.2-17 Comparison of Recurrence Rates for Rectangular Charleston Source

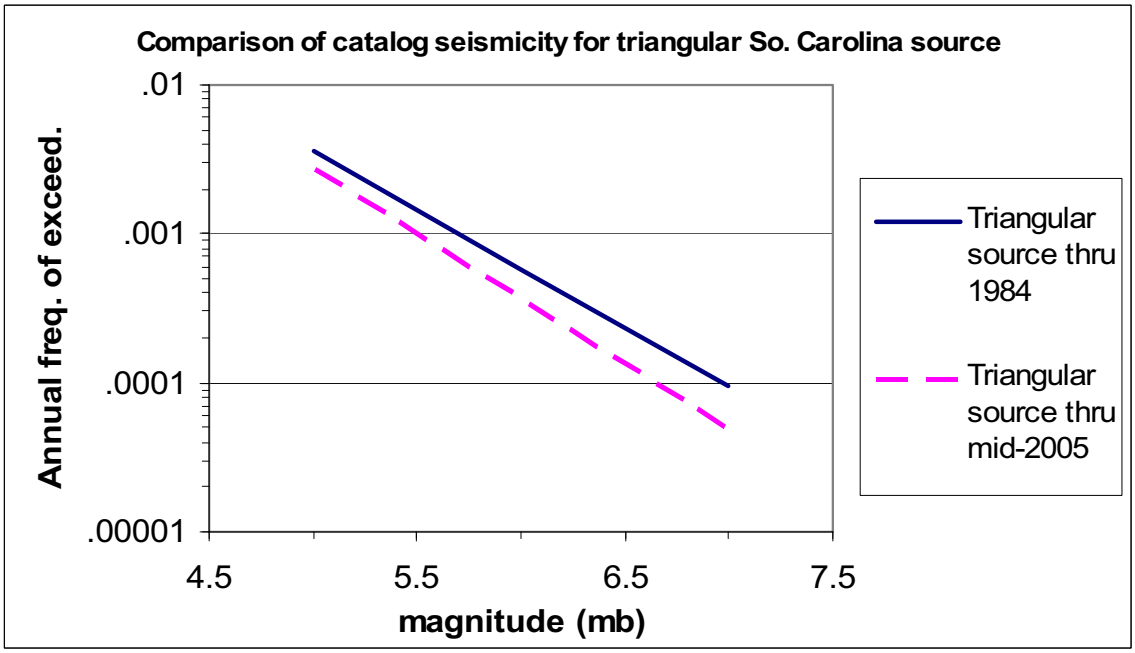

Figure 2.5.2-18 Comparison of Recurrence Rates for Triangular South Carolina Source

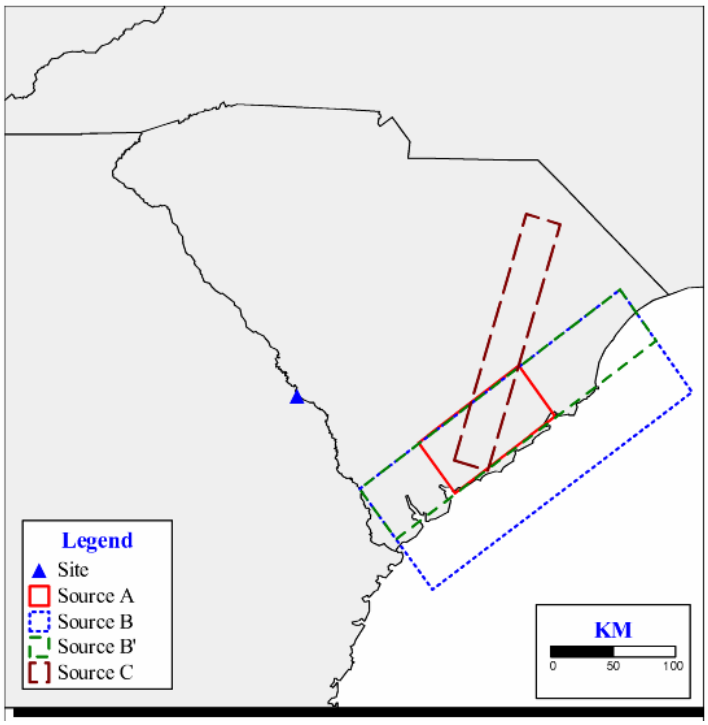

Figure 2.5.2-19 Geometry of Four New Charleston Sources

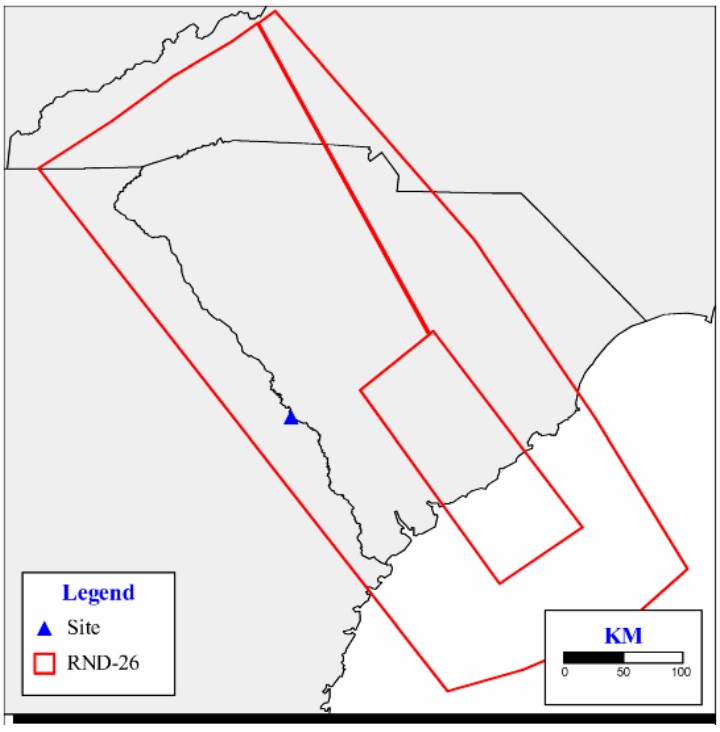

Figure 2.5.2-20a Original Rondout Source 26

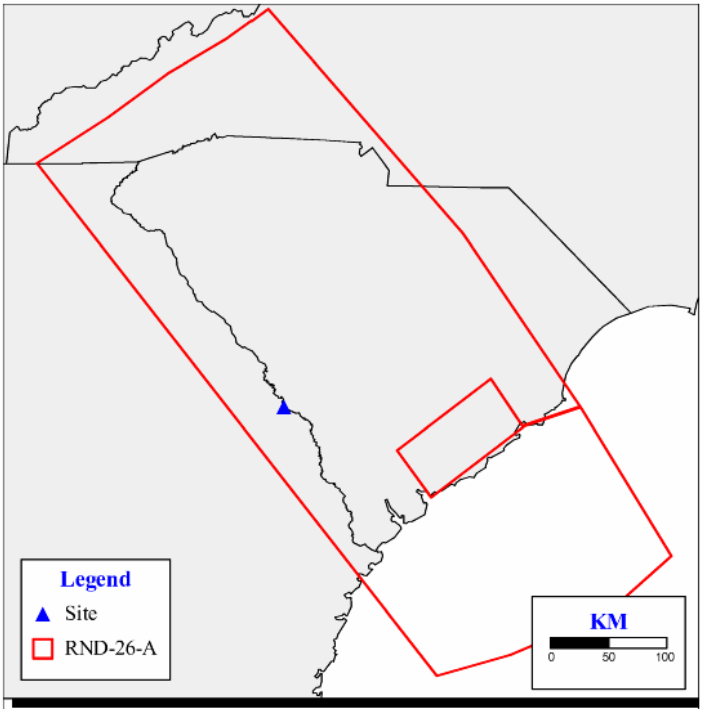

Figure 2.5.2-20b New Rondout Source 26-A that Surrounds Charleston Source A

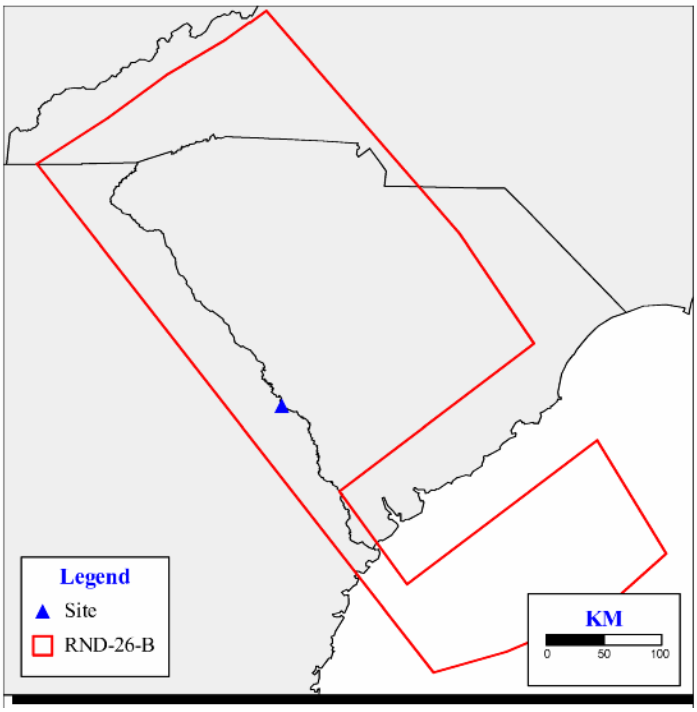

Figure 2.5.2-20c New Rondout Source 26-B that Surrounds Charleston Source B

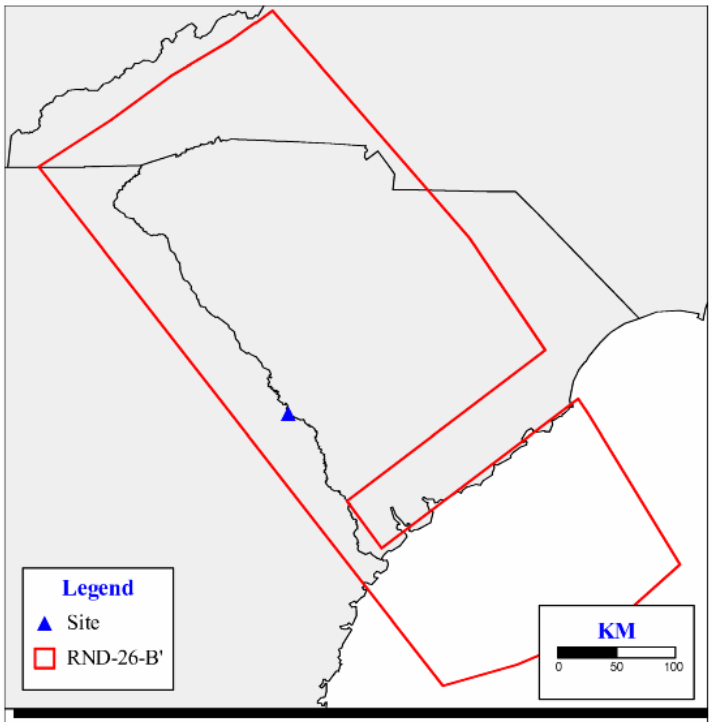

Figure 2.5.2-20d New Rondout Source 26-B´ that Surrounds Charleston Source B

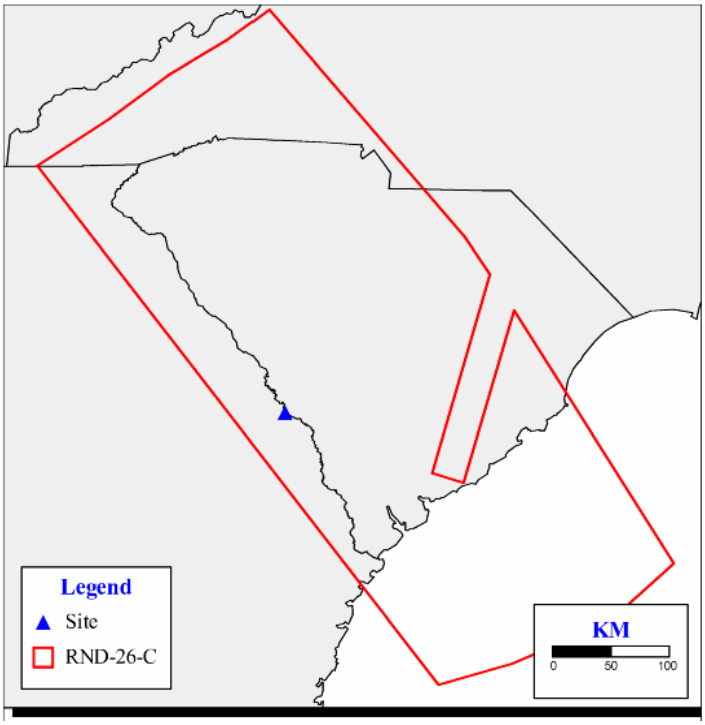

Figure 2.5.2-20e New Rondout Source 26-C that Surrounds Charleston Source C

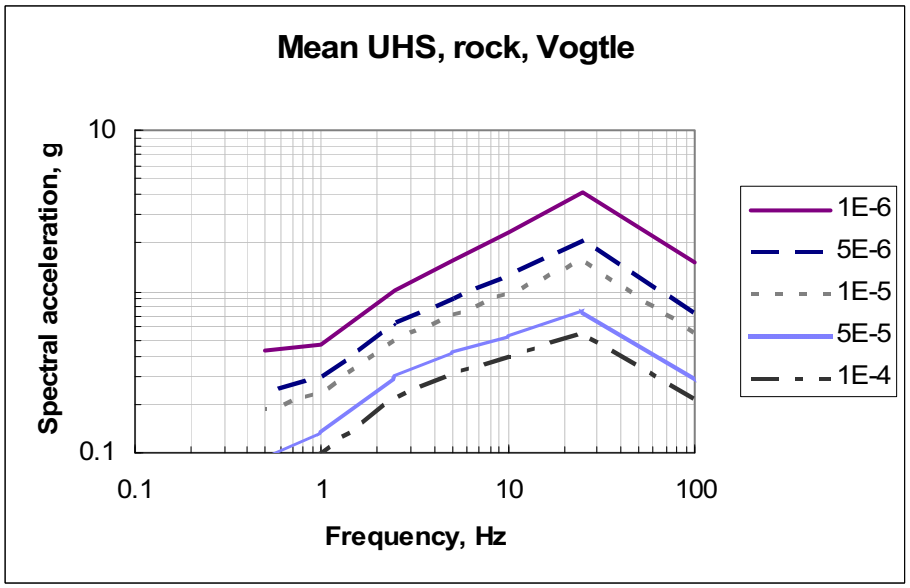

Figure 2.5.2-21 Mean Uniform Hazard Spectra, Hard Rock Conditions, for VEGP ESP

High Frequency, 1.0e-4

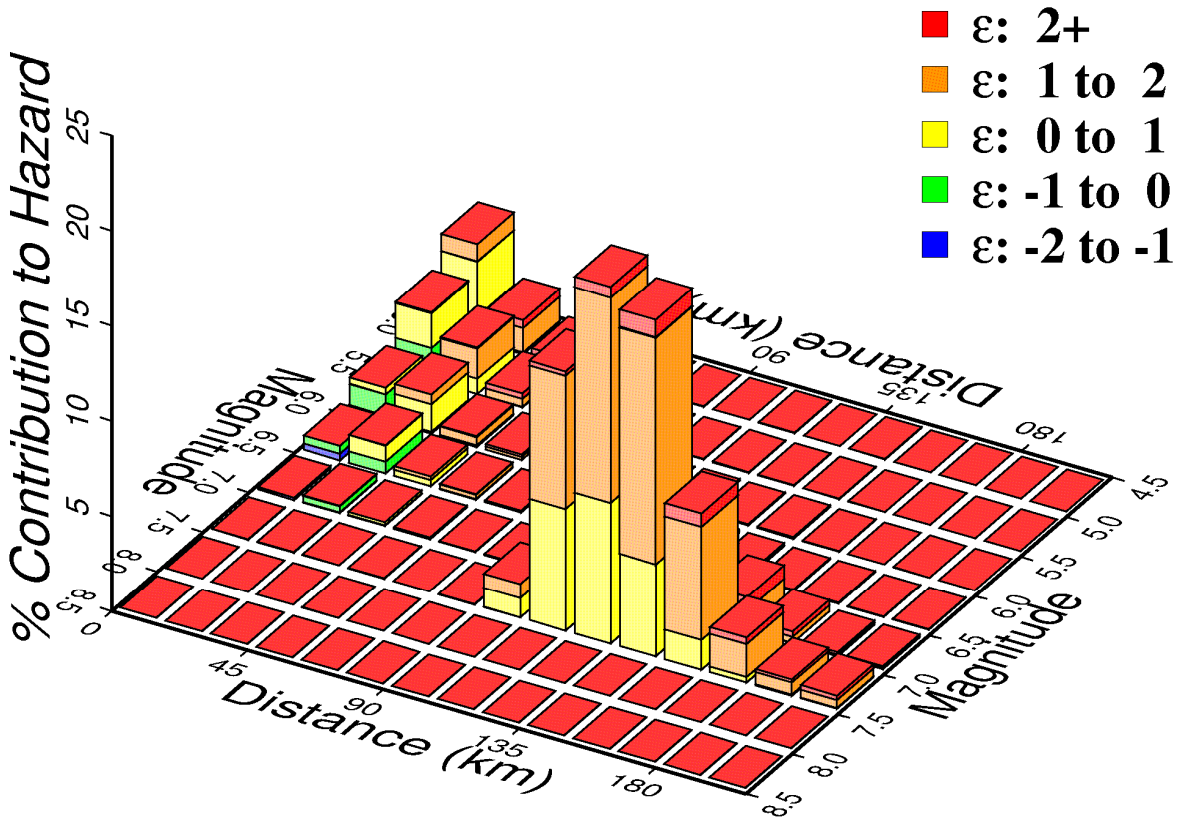

Figure 2.5.2-22 Magnitude-Distance Deaggregation for High Frequencies, 10^{-4} Mean Annual Frequency of Exceedance

Low Frequency, 1.0e-4

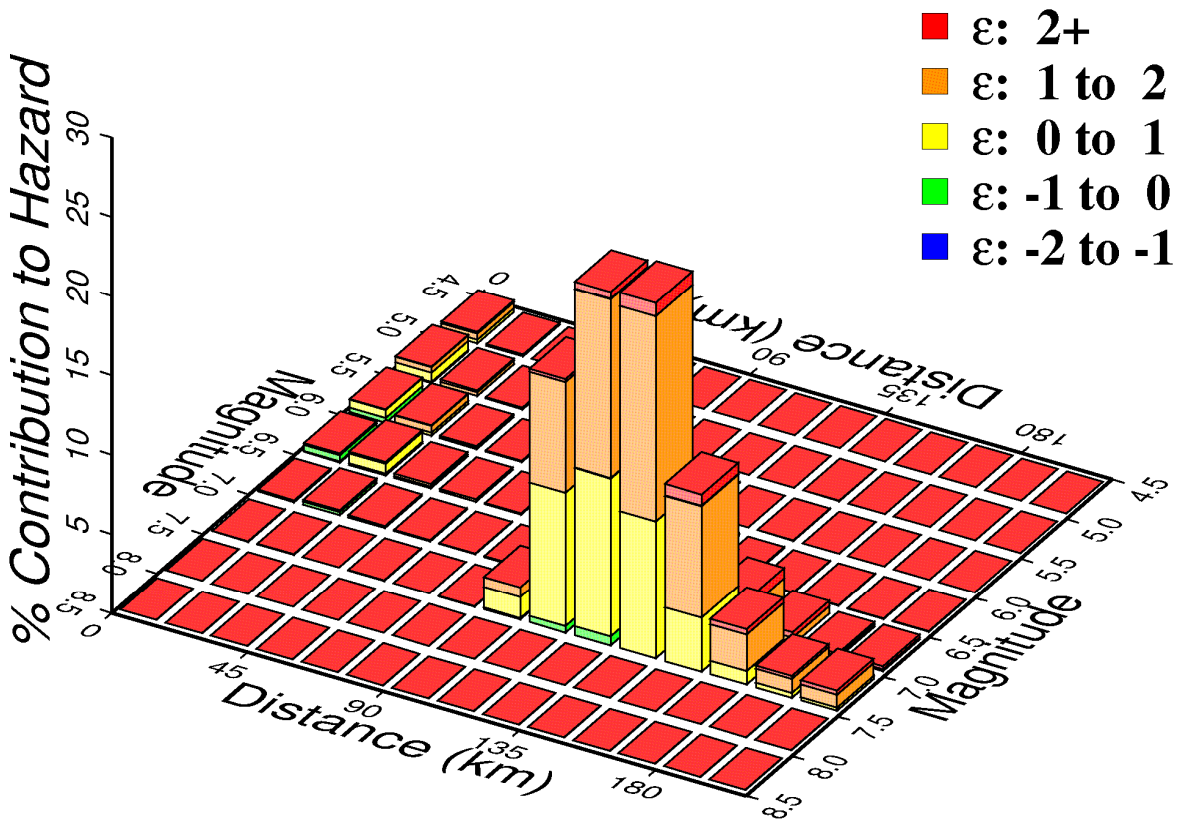

Figure 2.5.2-23 Magnitude-Distance Deaggregation for Low Frequencies, 10^{-4} Mean Annual Frequency of Exceedance

High Frequency, 1.0e-5

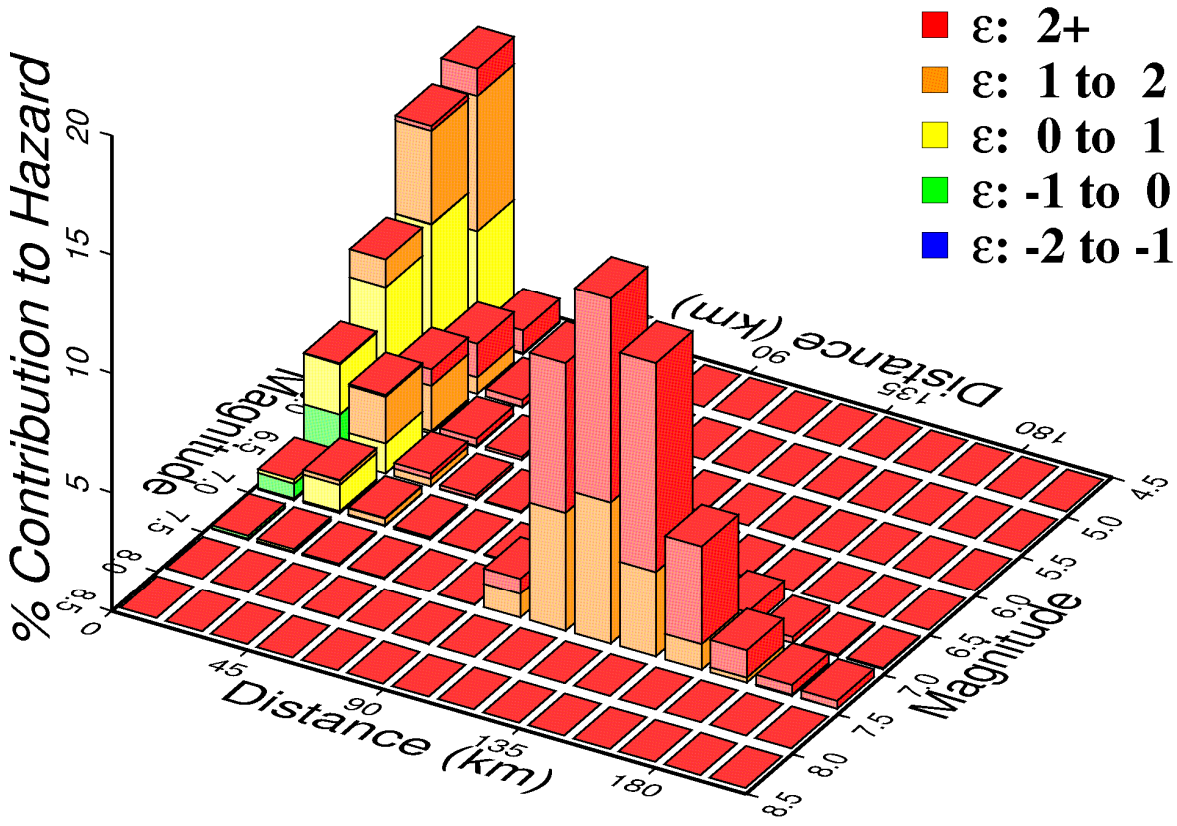

Figure 2.5.2-24 Magnitude-Distance Deaggregation for High Frequencies, 10^{-5} Mean Annual Frequency of Exceedance

Low Frequency, 1.0e-5

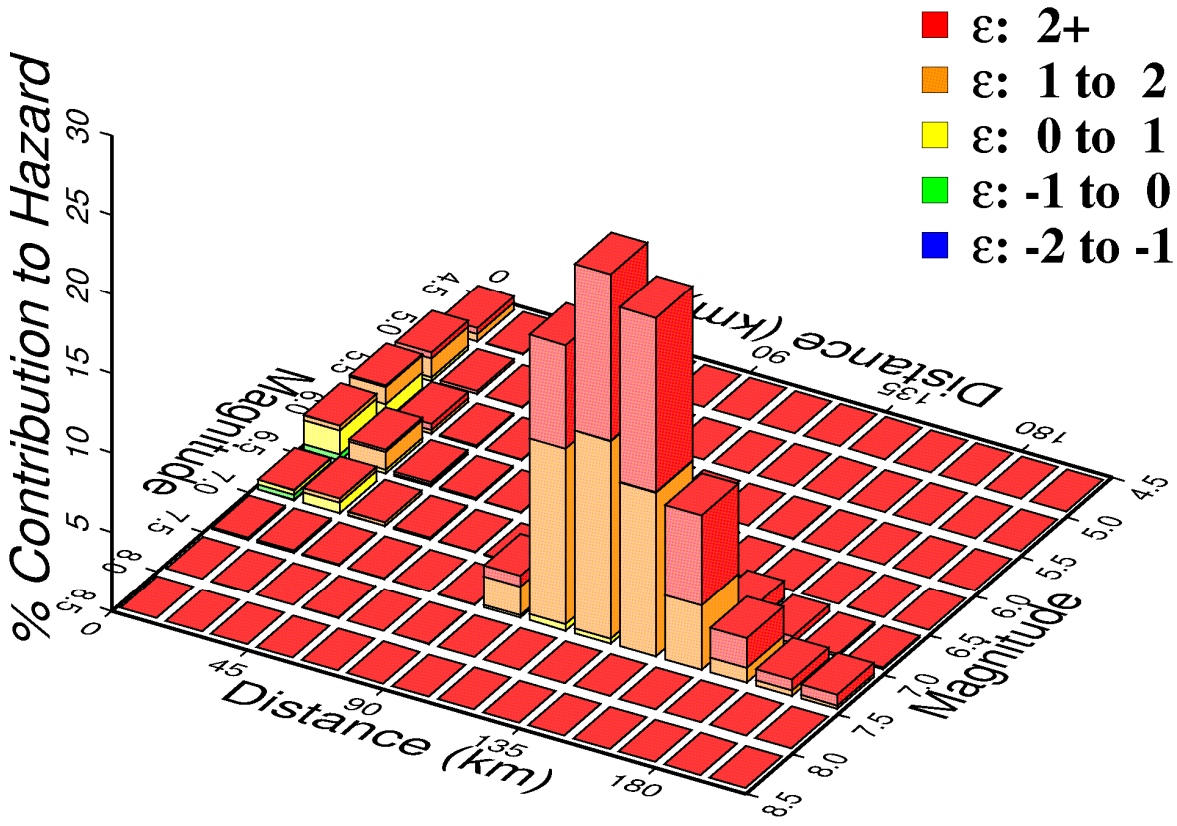

Figure 2.5.2-25 Magnitude-Distance Deaggregation For Low Frequencies, 10^{-5} Mean Annual Frequency of Exceedance

High Frequency, 1.0e-6

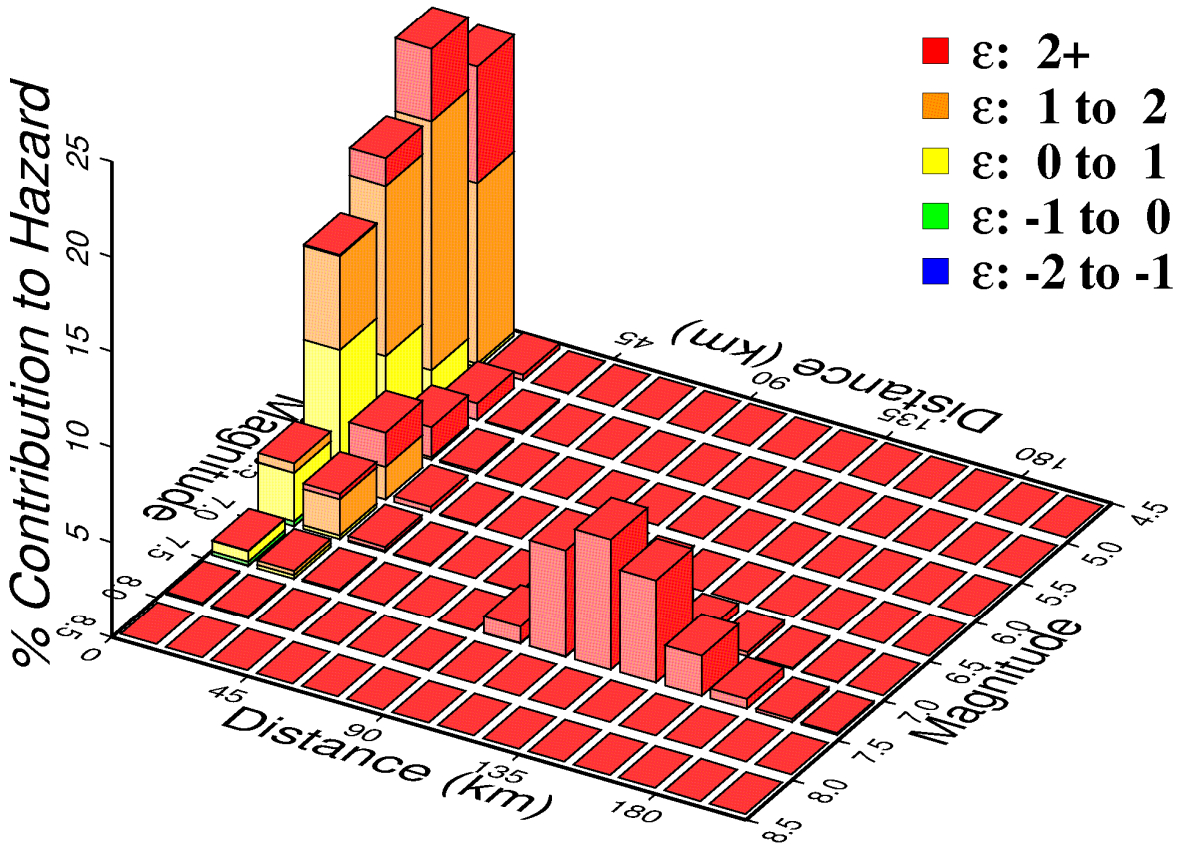

Figure 2.5.2-26 Magnitude-Distance Deaggregation for High Frequencies, 10^{-6} Mean Annual Frequency of Exceedance

Low Frequency, 1.0e-6

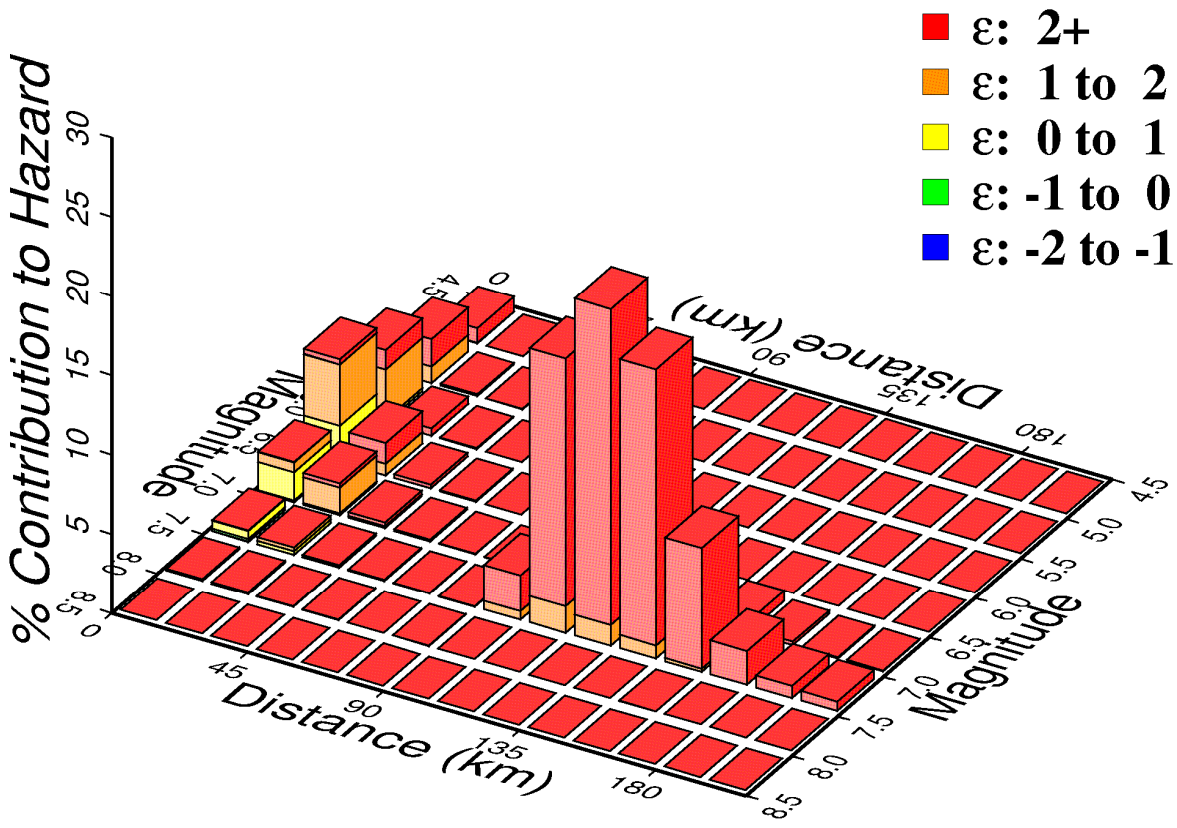

Figure 2.5.2-27 Magnitude-Distance Deaggregation for Low Frequencies, 10^{-6} Mean Annual Frequency of Exceedance

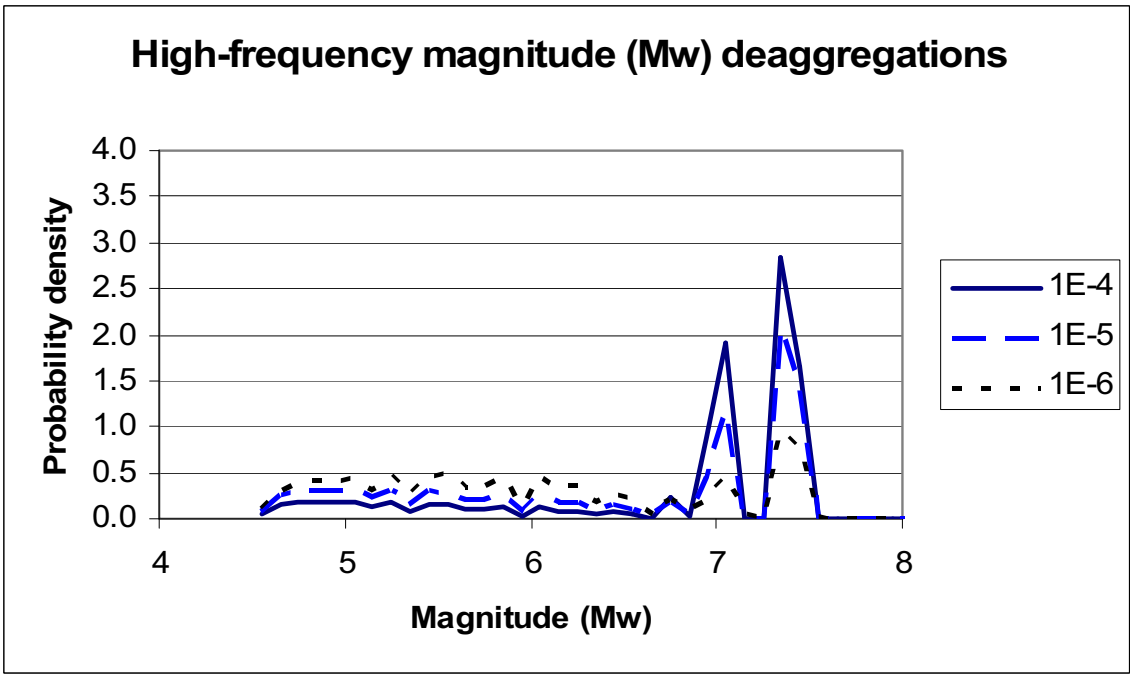

Figure 2.5.2-28 Magnitude Deaggregation for High Frequencies for Three Mean Annual Frequencies of Exceedance

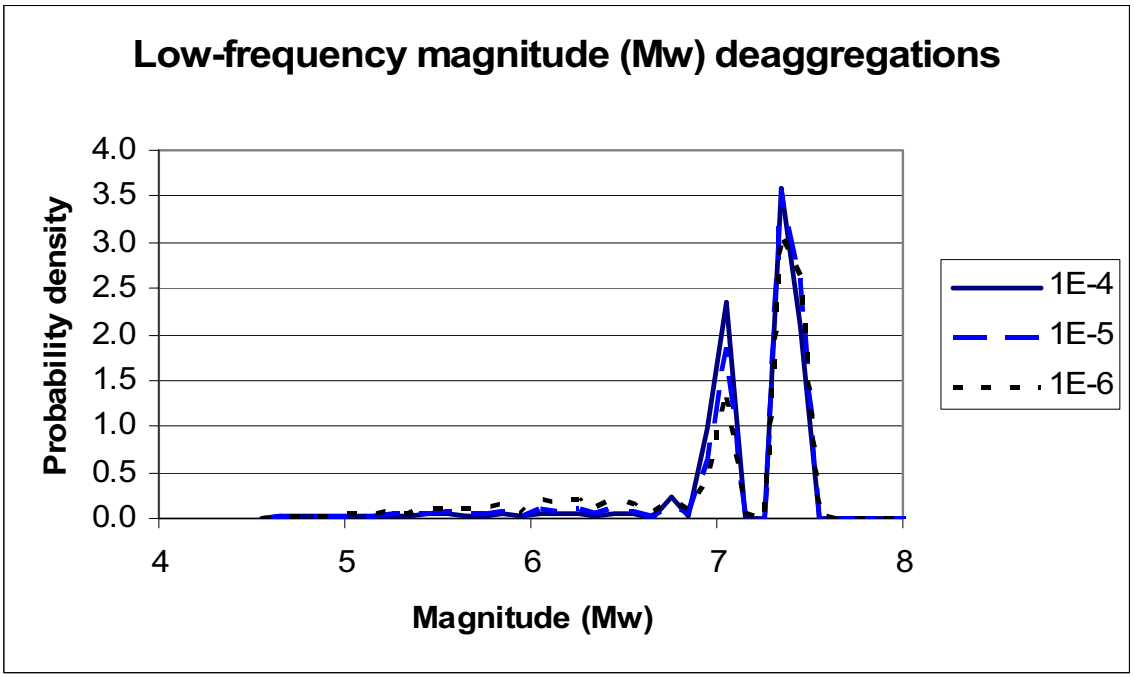

Figure 2.5.2-29 Magnitude Deaggregation for Low Frequencies for Three Mean Annual Frequencies of Exceedance

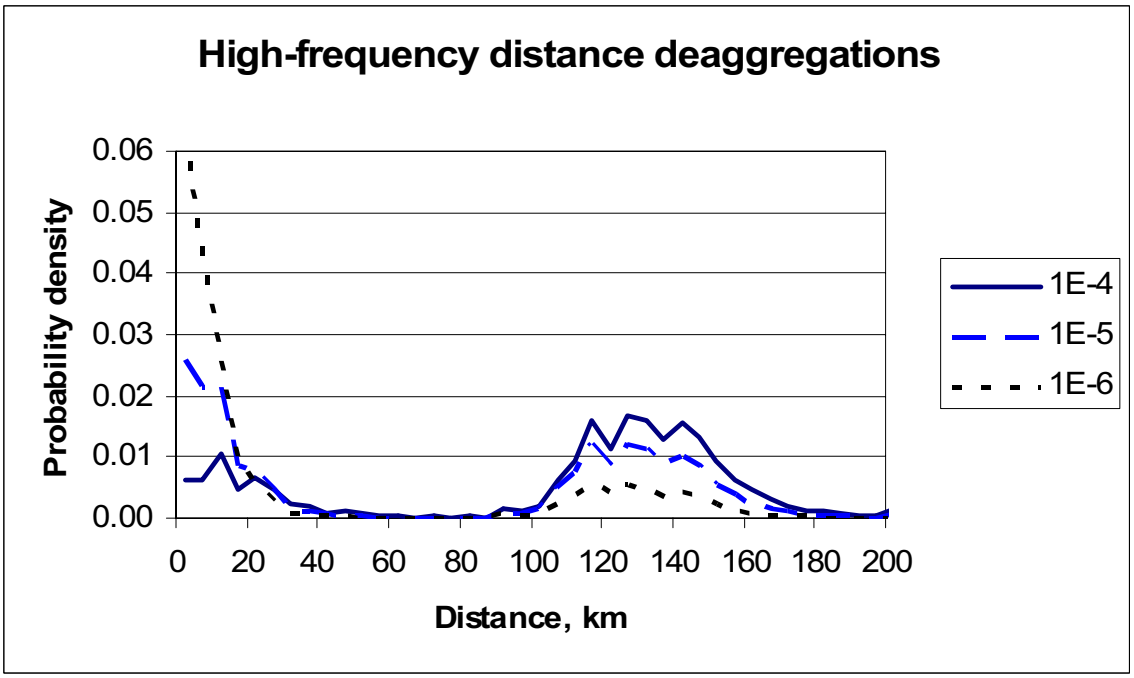

Figure 2.5.2-30 Distance Deaggregation for High Frequencies for Three Mean Annual Frequencies of Exceedance

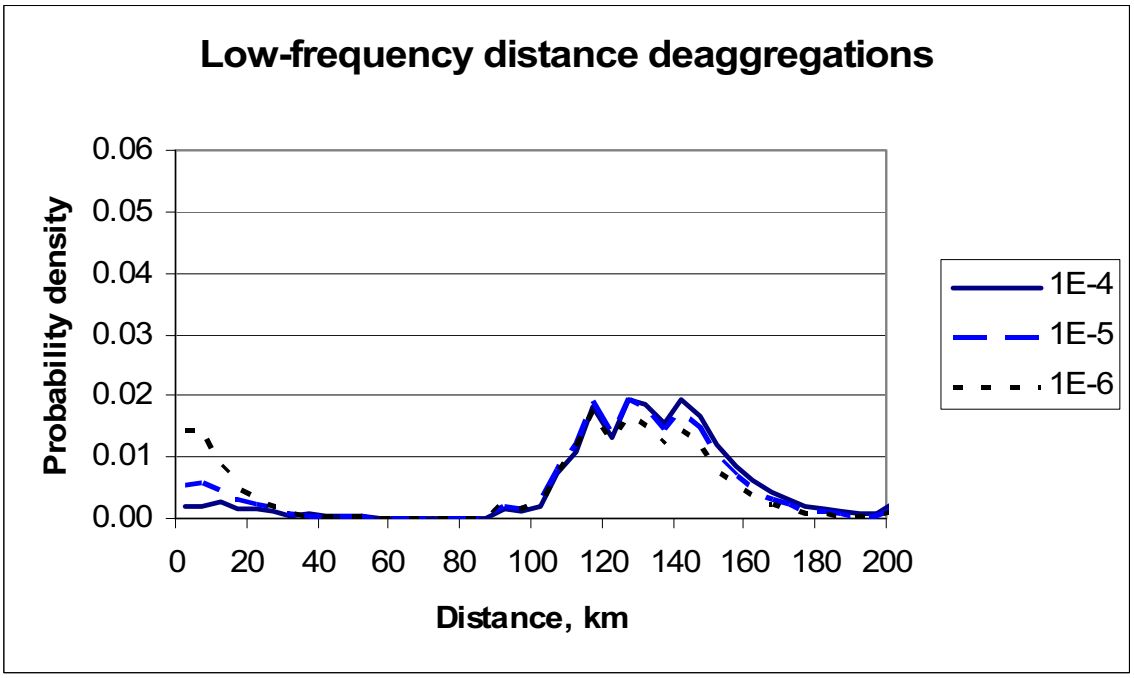

Figure 2.5.2-31 Magnitude Deaggregation for Low Frequencies for Three Mean Annual Frequencies of Exceedance

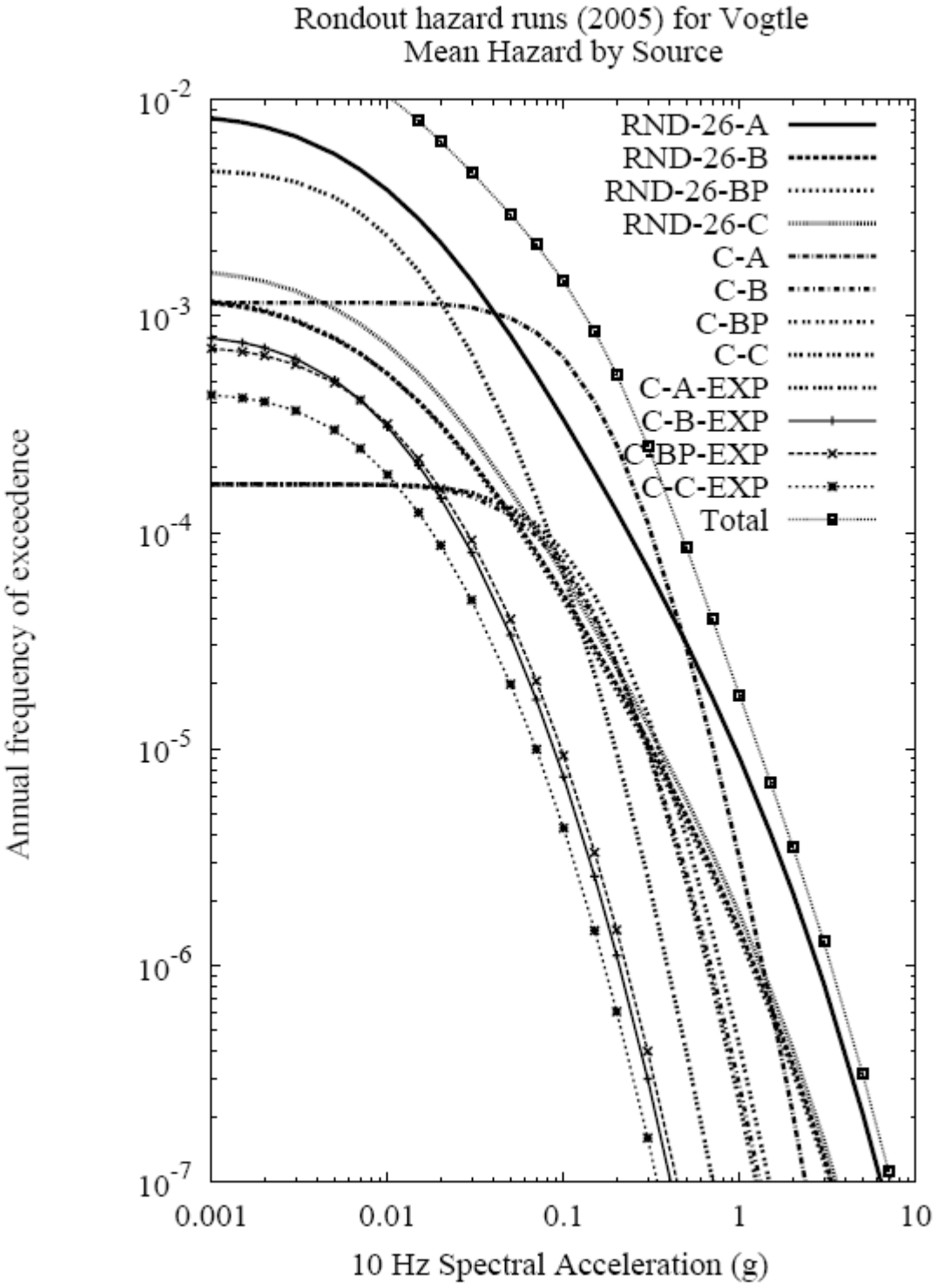

Figure 2.5.2-32 10 Hz Seismic Hazard Curves by Seismic Source for Rondout Team

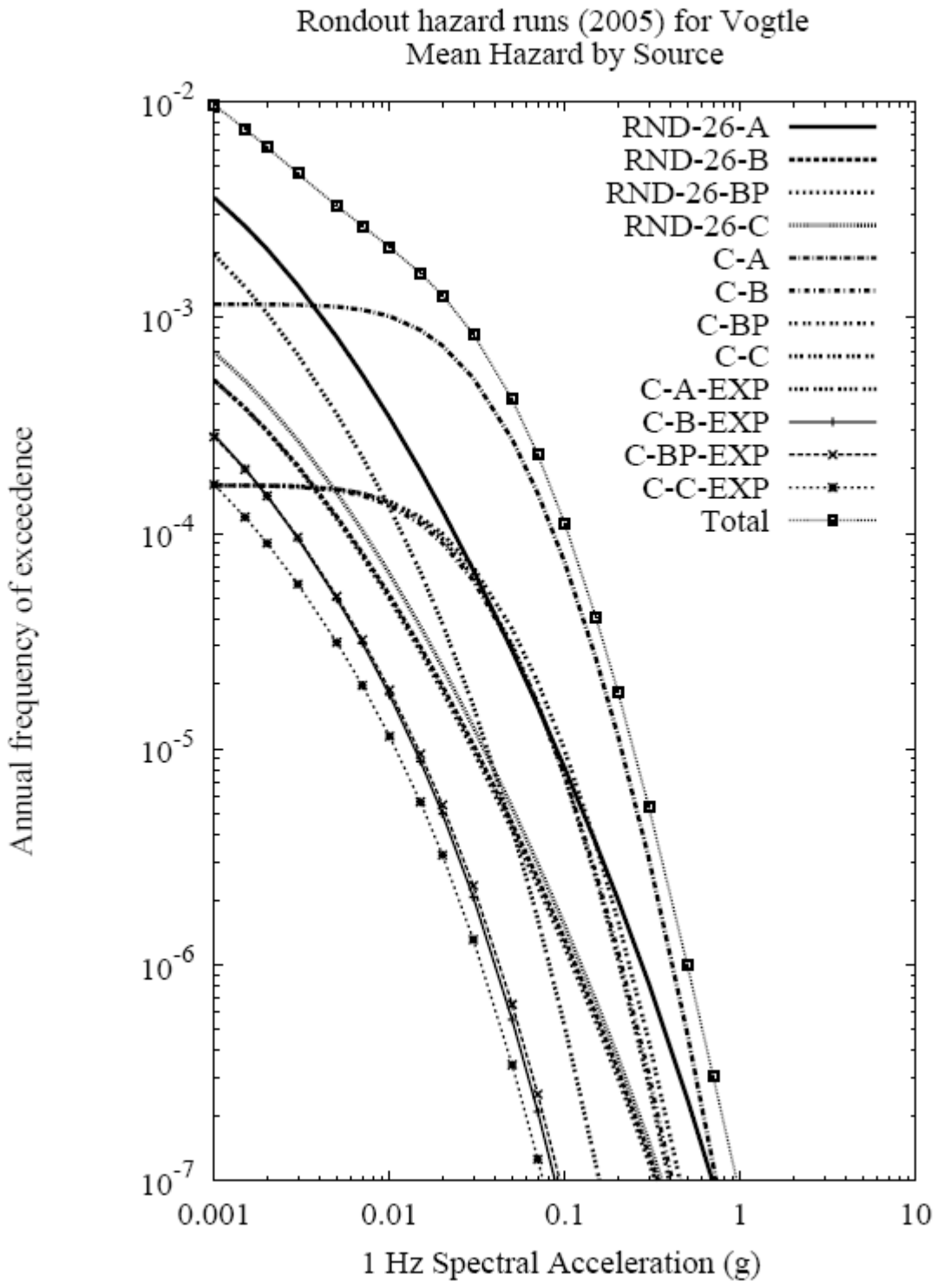

Figure 2.5.2-33 1 Hz Seismic Hazard Curves by Seismic Source for Rondout Team

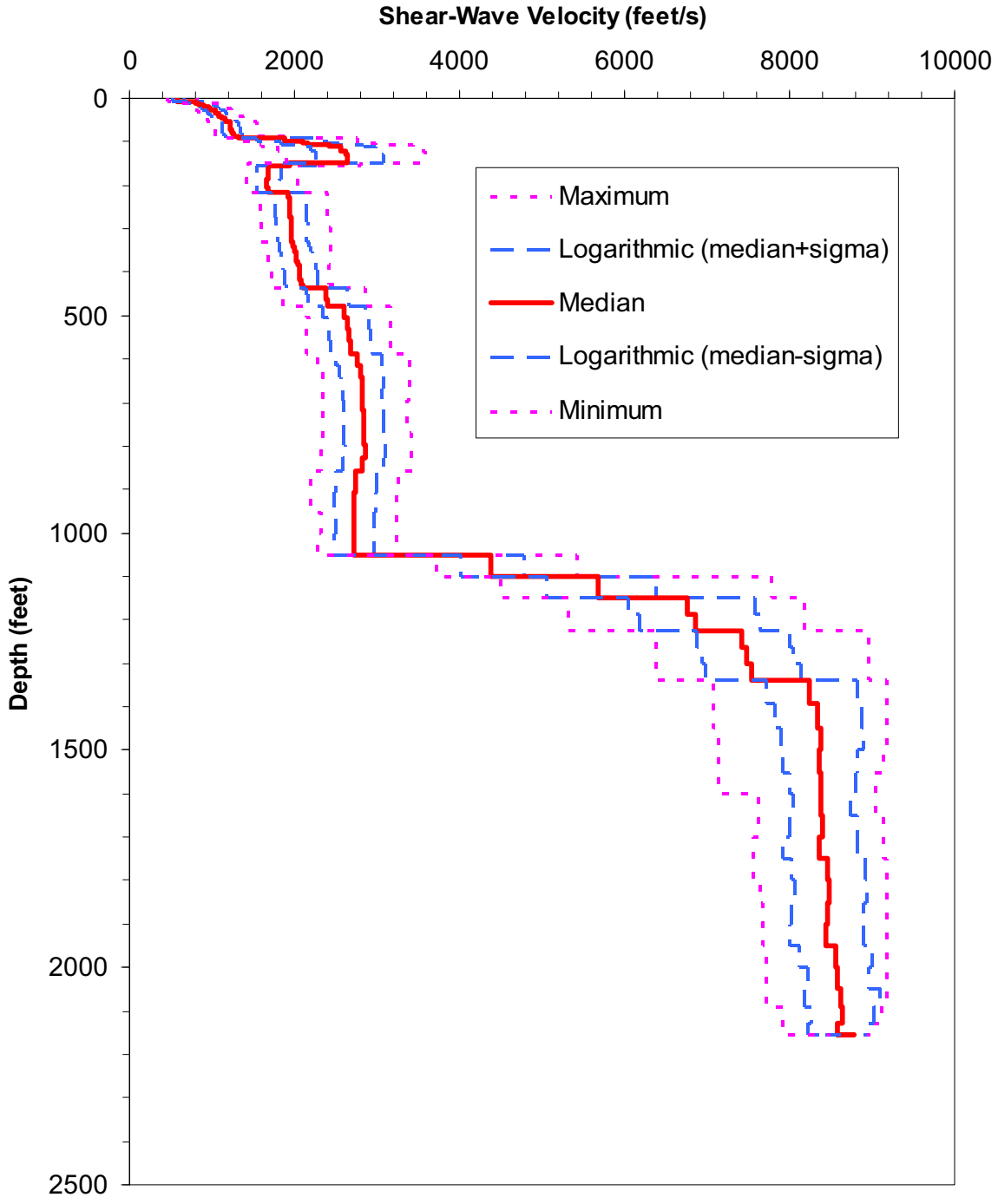

Note: Statistics do not include the velocities on the crystalline bedrock.

Figure 2.5.2-34 Summary Statistics Calculated from the 60 Shear-Wave Velocity Profiles

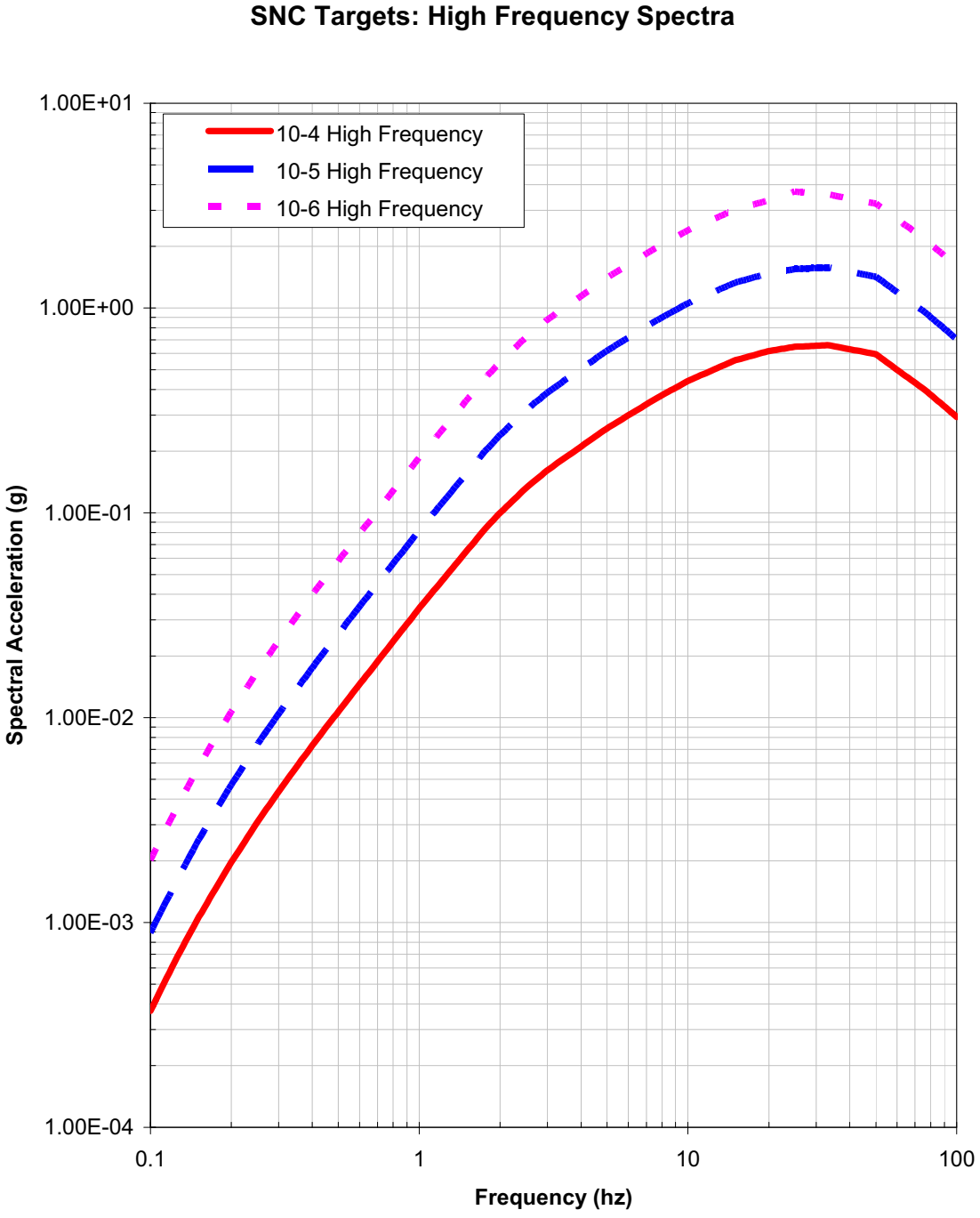

Figure 2.5.2-35a High Frequency Target Spectra for the Three Annual Probability Levels of 10^{-4}, 10^{-5}, and 10^{-6}

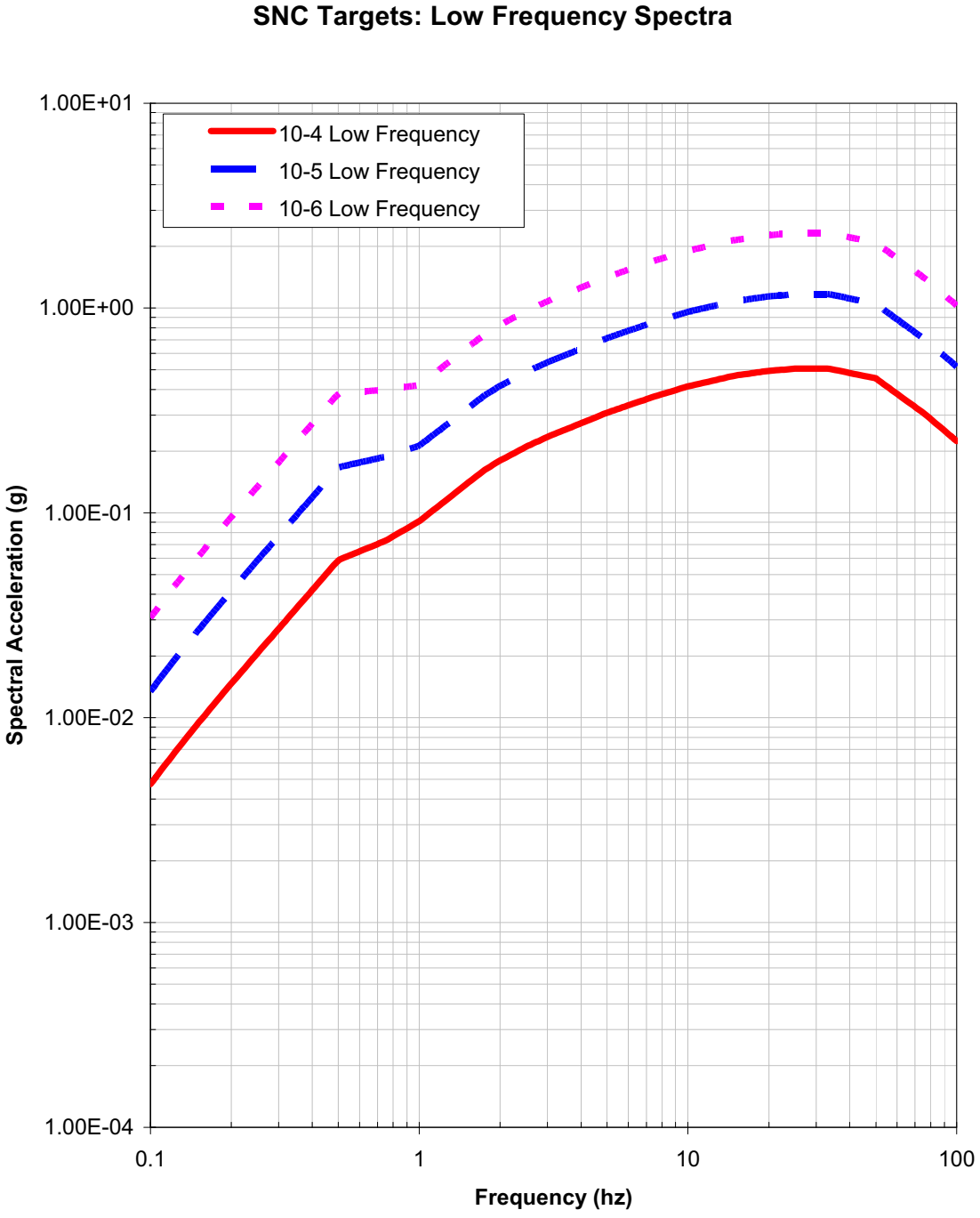

Figure 2.5.2-35b Low Frequency Target Spectra for the Three Annual Probability Levels of 10^{-4}, 10^{-5}, and 10^{-6}

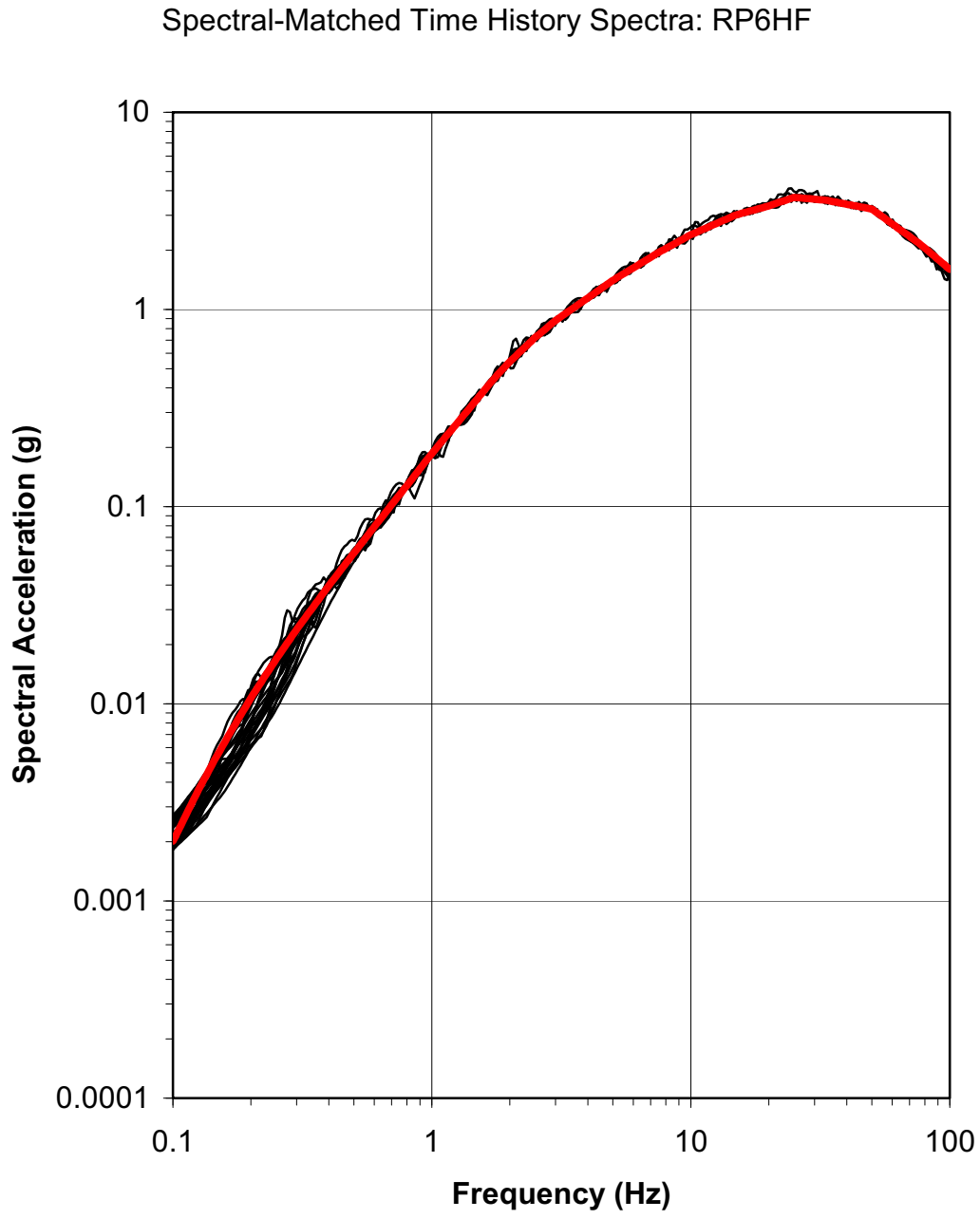

Note: Heavy red line is the target spectrum and thin black lines are the individual matches.

Figure 2.5.2-36a High Frequency (10^{-6}) Match for the 30 Time Histories

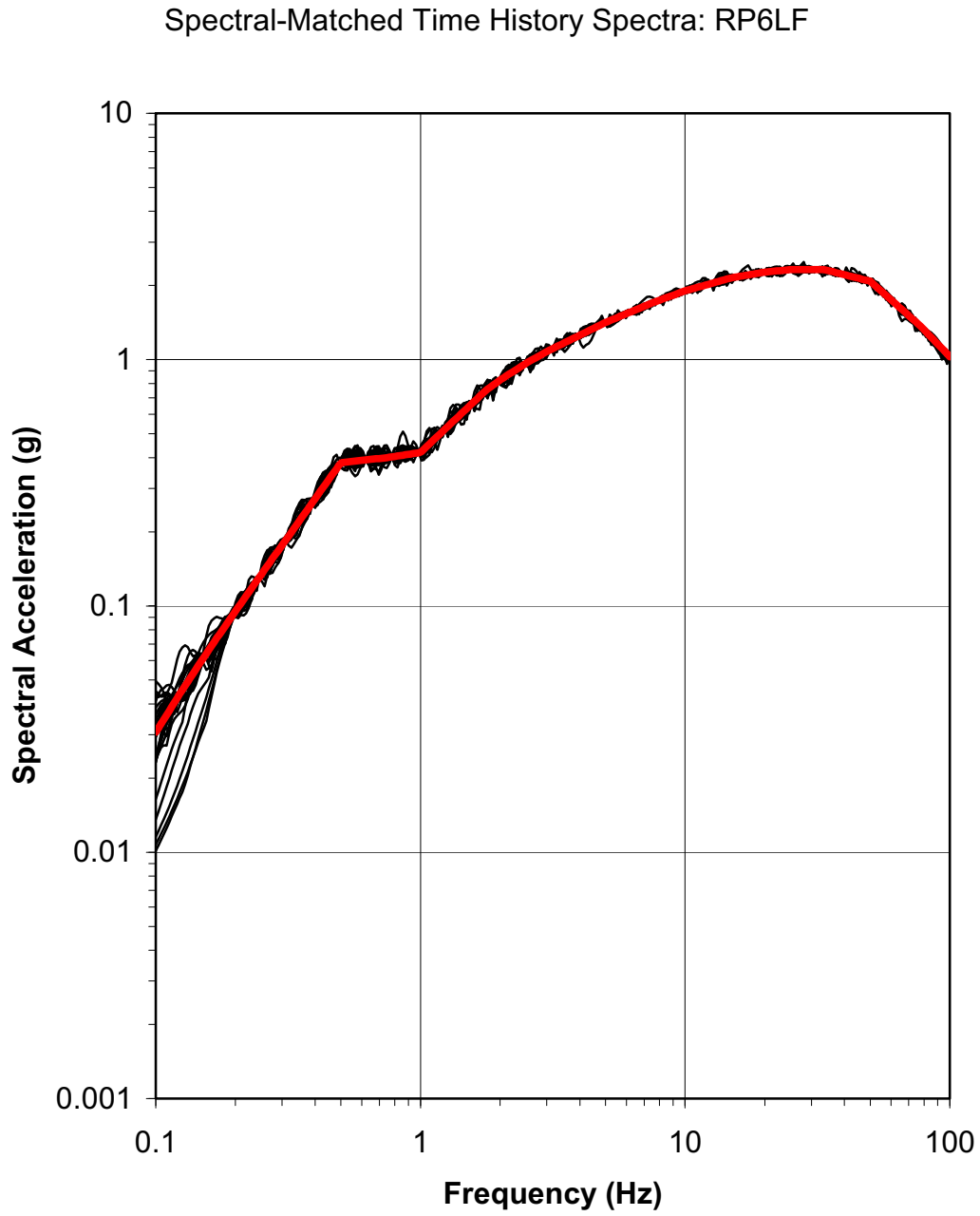

Note: Heavy red line is the target spectrum and thin black lines are the individual matches.

Figure 2.5.2-36b Low Frequency (10^{-6}) Match for the 30 Time Histories

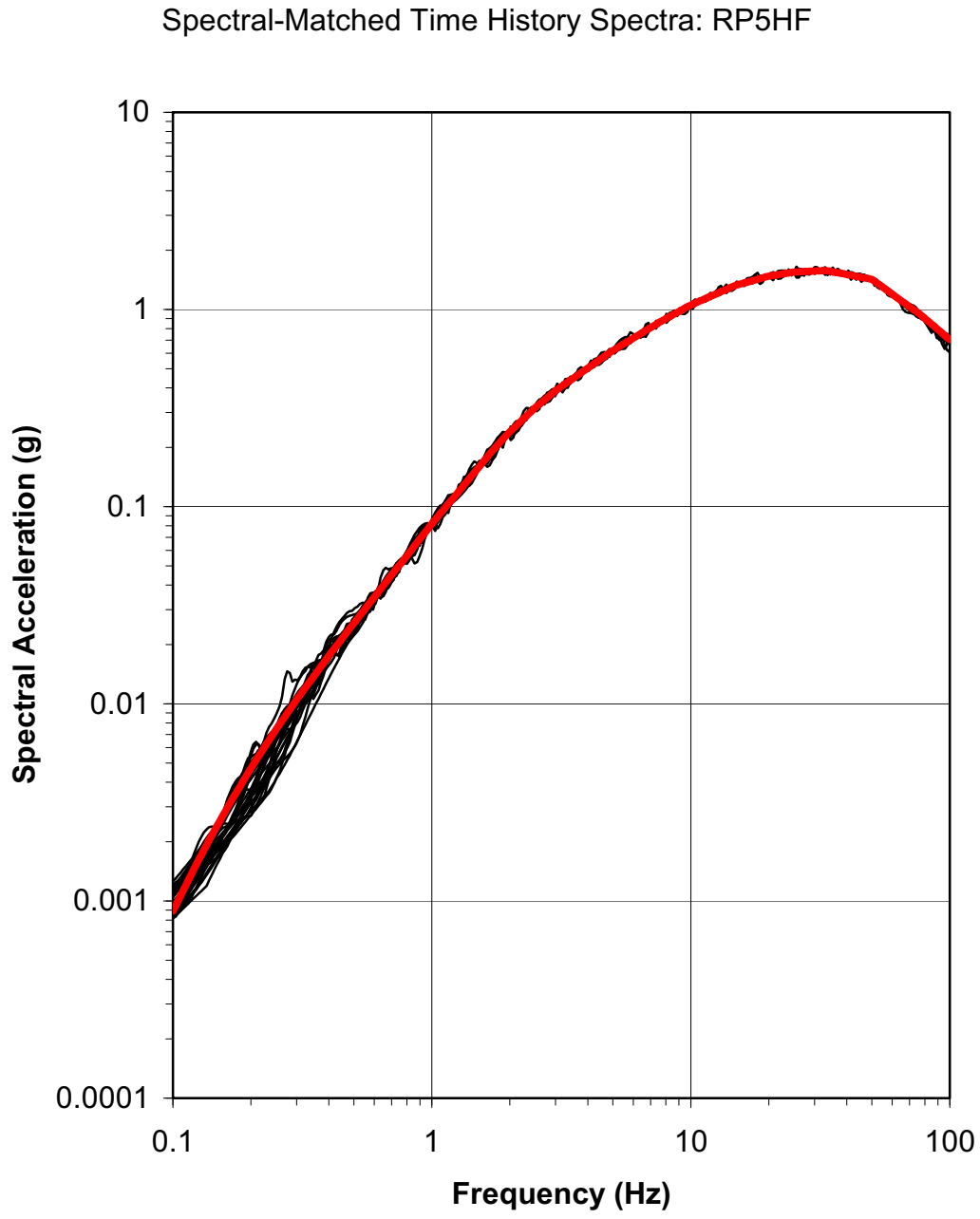

Note: Heavy red line is the target spectrum and thin black lines are the individual matches.

Figure 2.5.2-36c High Frequency (10^{-5}) Match for the 30 Time Histories

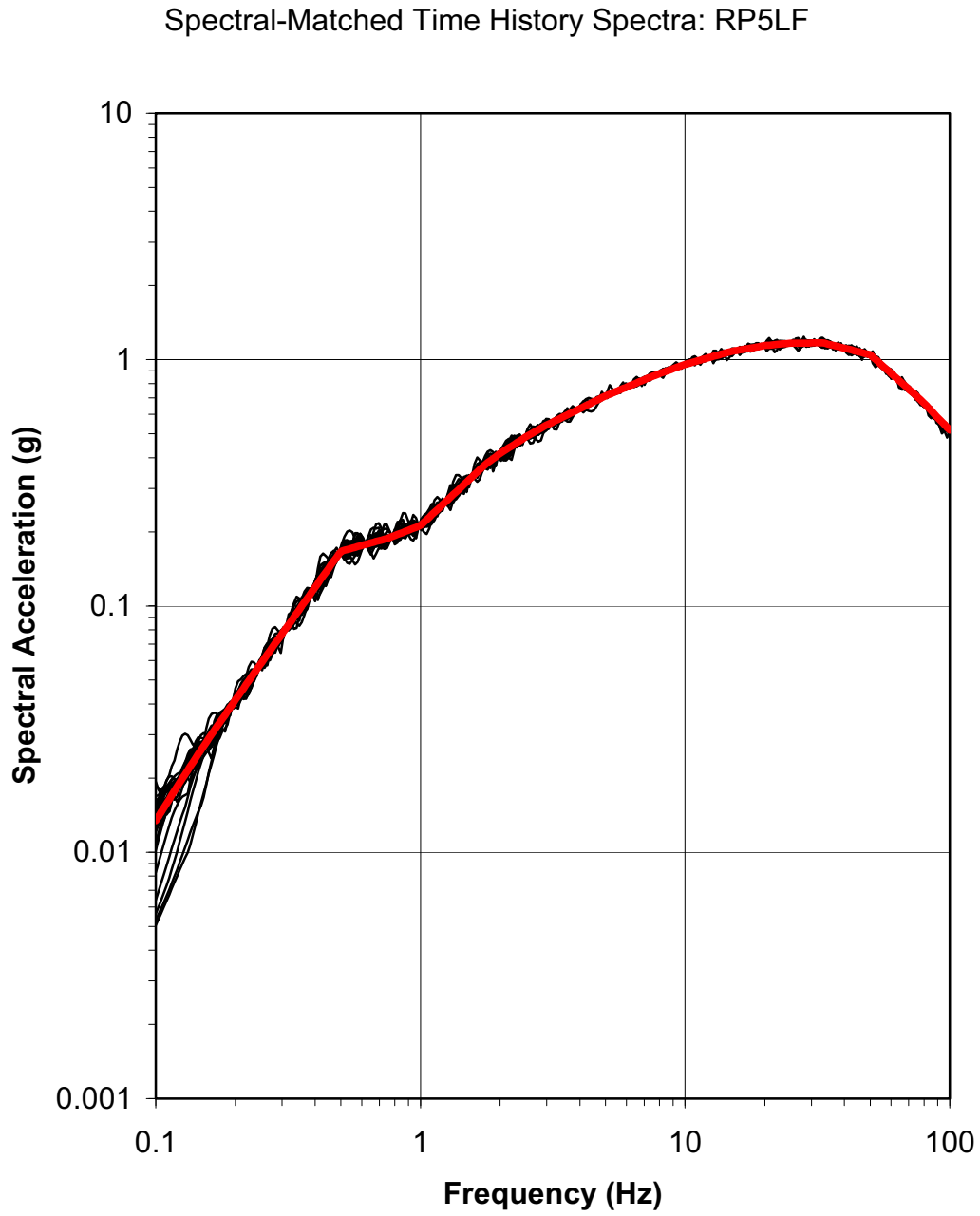

Note: Heavy red line is the target spectrum and thin black lines are the individual matches.

Figure 2.5.2-36d Low Frequency (10^{-5}) Match for the 30 Time Histories

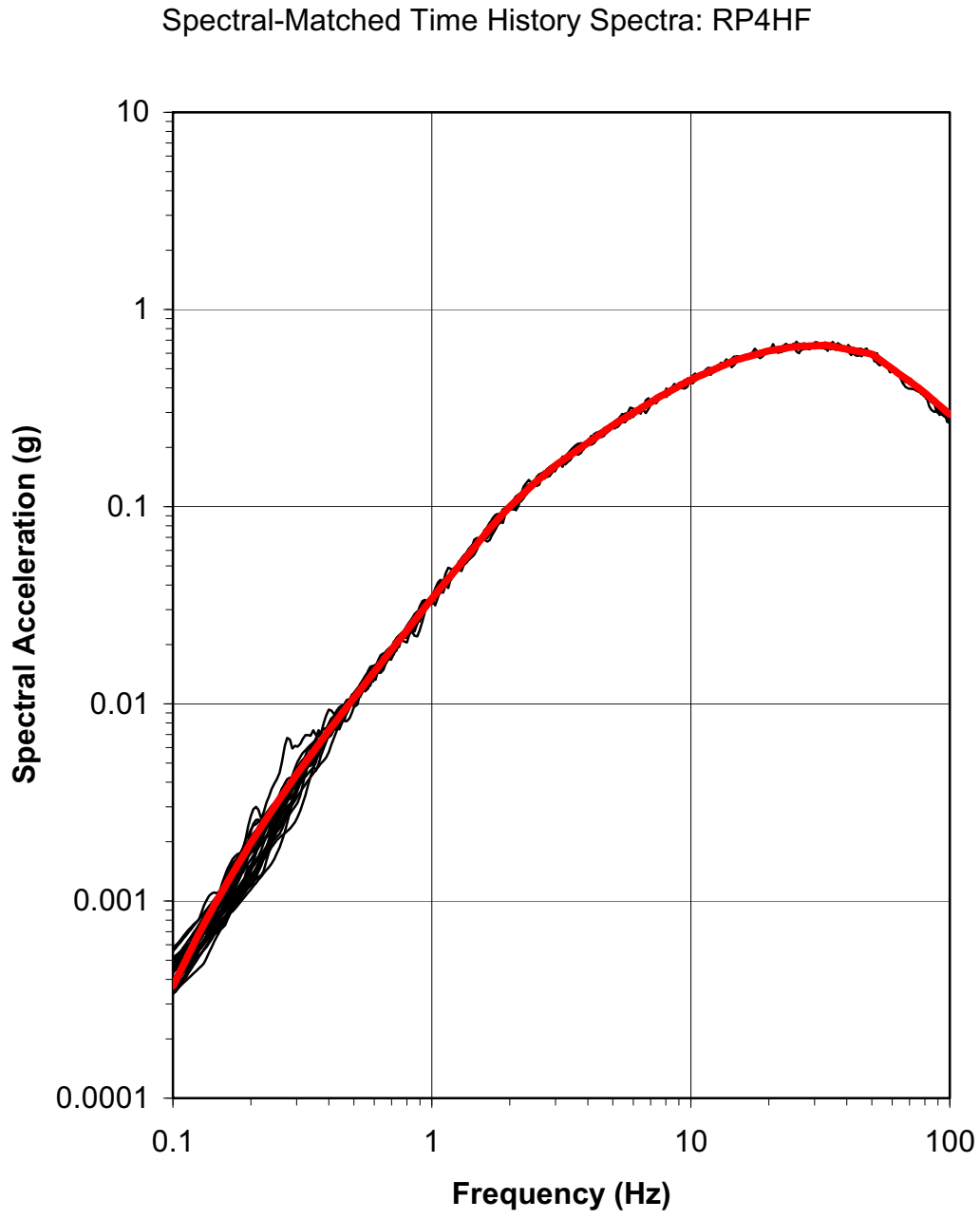

Note: Heavy red line is the target spectrum and thin black lines are the individual matches.

Figure 2.5.2-36e High Frequency (10^{-4}) Match for the 30 Time Histories

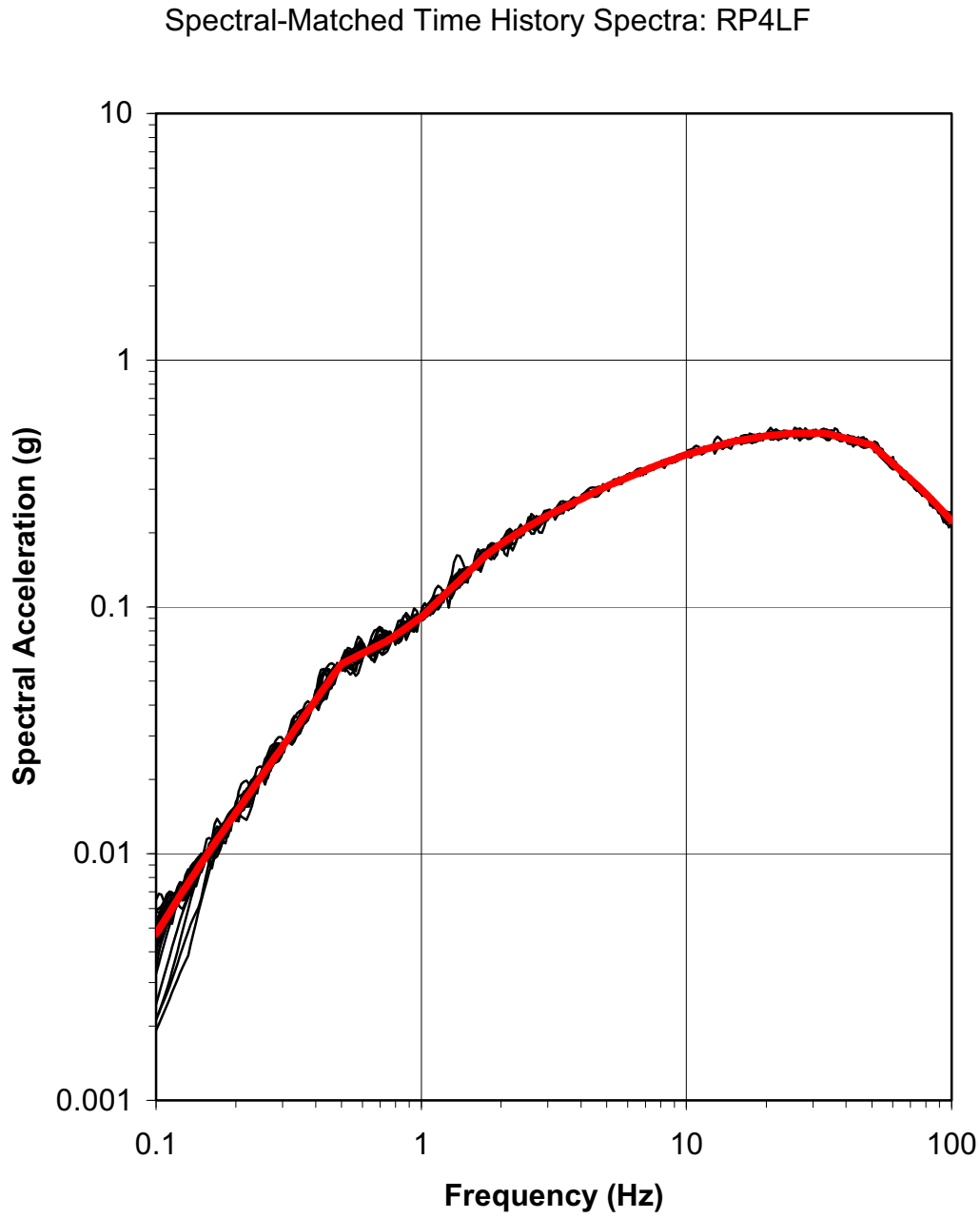

Note: Heavy red line is the target spectrum and thin black lines are the individual matches.

Figure 2.5.2-36f Low Frequency (10^{-4}) Match for the 30 Time Histories

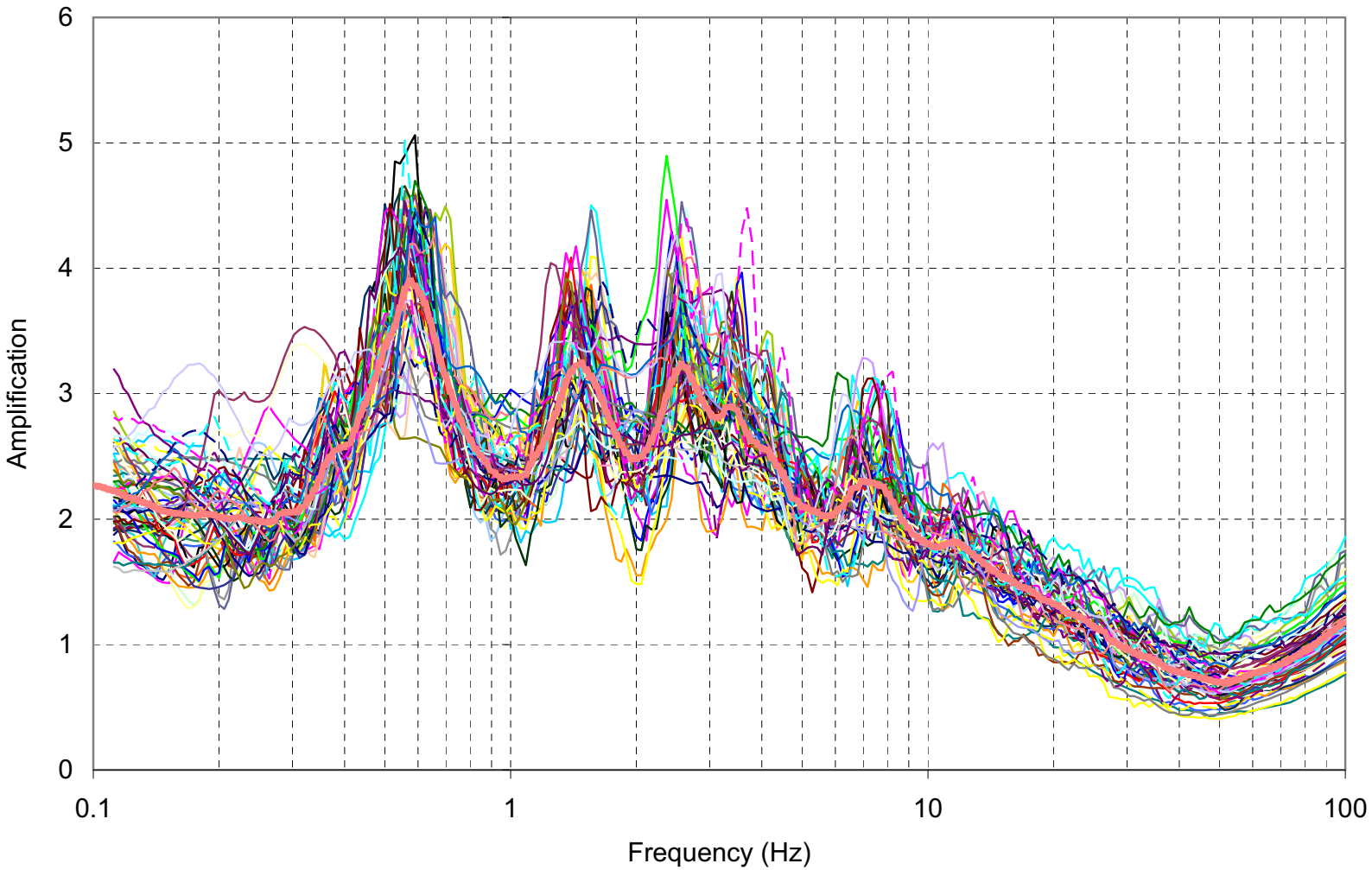

Figure 2.5.2-37 Typical Results of Spectral Amplification at 86-ft Depth (Top of Blue Bluff Marl) Using EPRI Degradation Curves for High Frequency Time Histories of 10^{-4} MAFE Input Motion Level

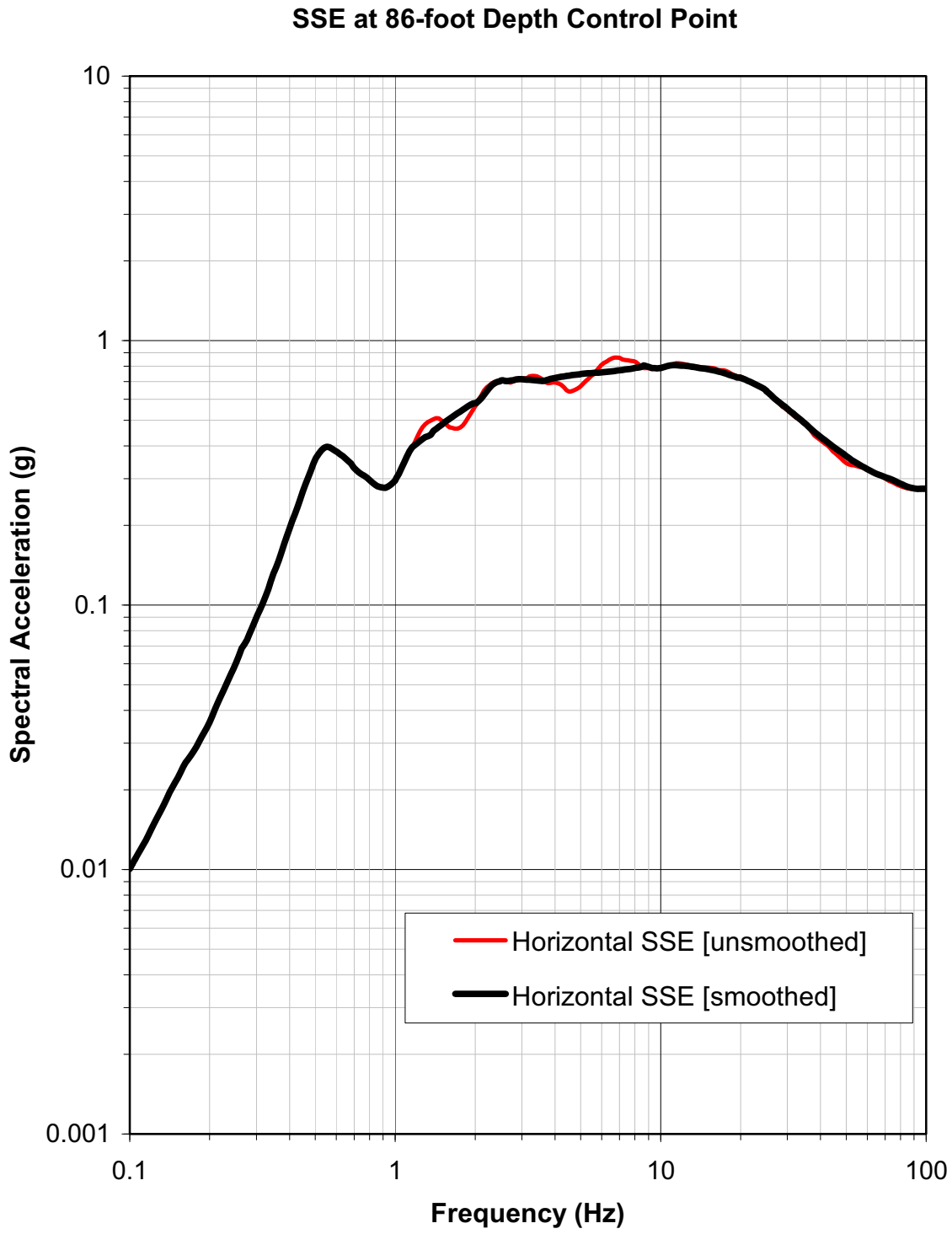

Figure 2.5.2-38 Horizontal Raw and Smoothed SSE, Top of Blue Bluff Marl

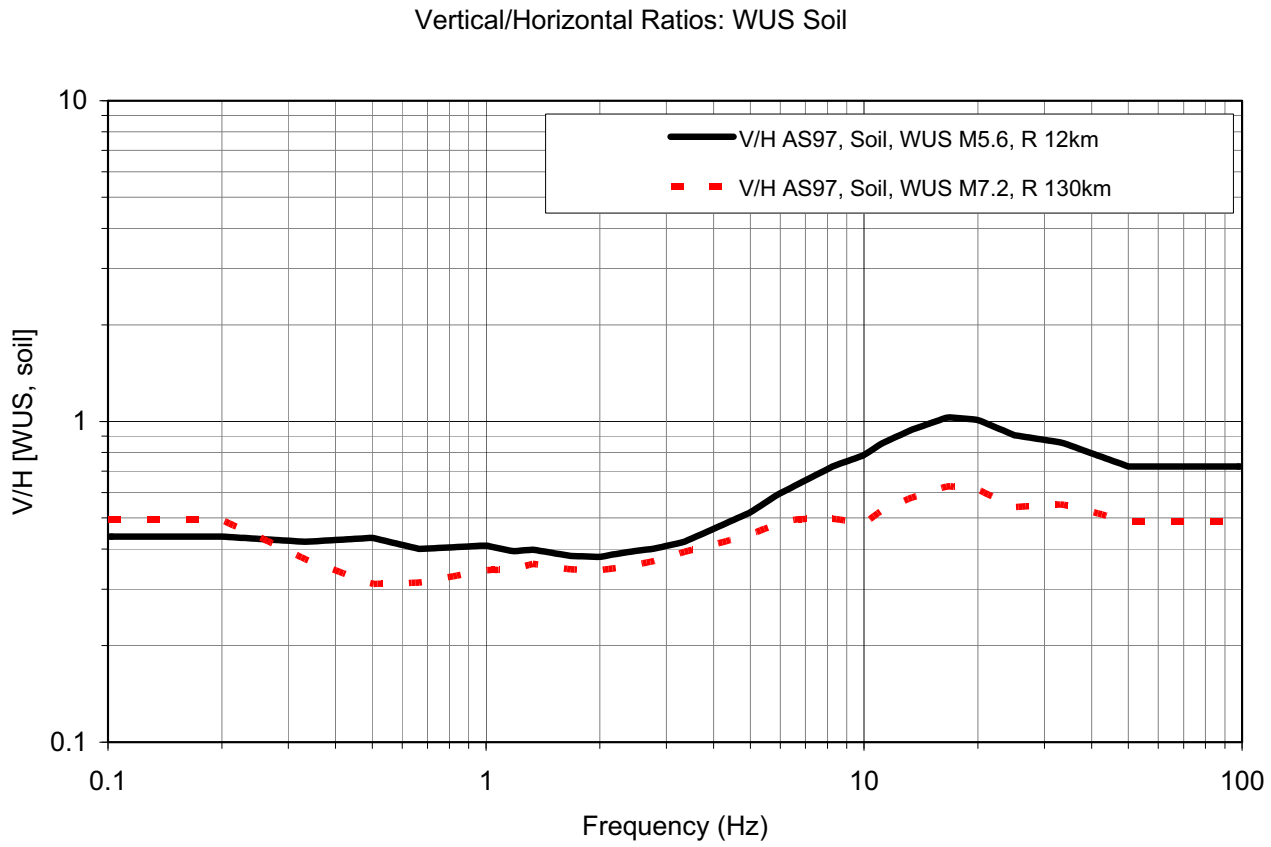

Figure 2.5.2-39 Plots of $V/H_{WUS,Soil,Empirical}$ Term of Equation 2.5.2-6 for "Near" [M5.6 at a Distance of 12 km] and "Far" [M7.2 at a Distance of 130 km] Events Using the Attenuation Relation of Abrahamson and Silva (1997)

NUREG/CR-6728, Figure J-31 and J-32

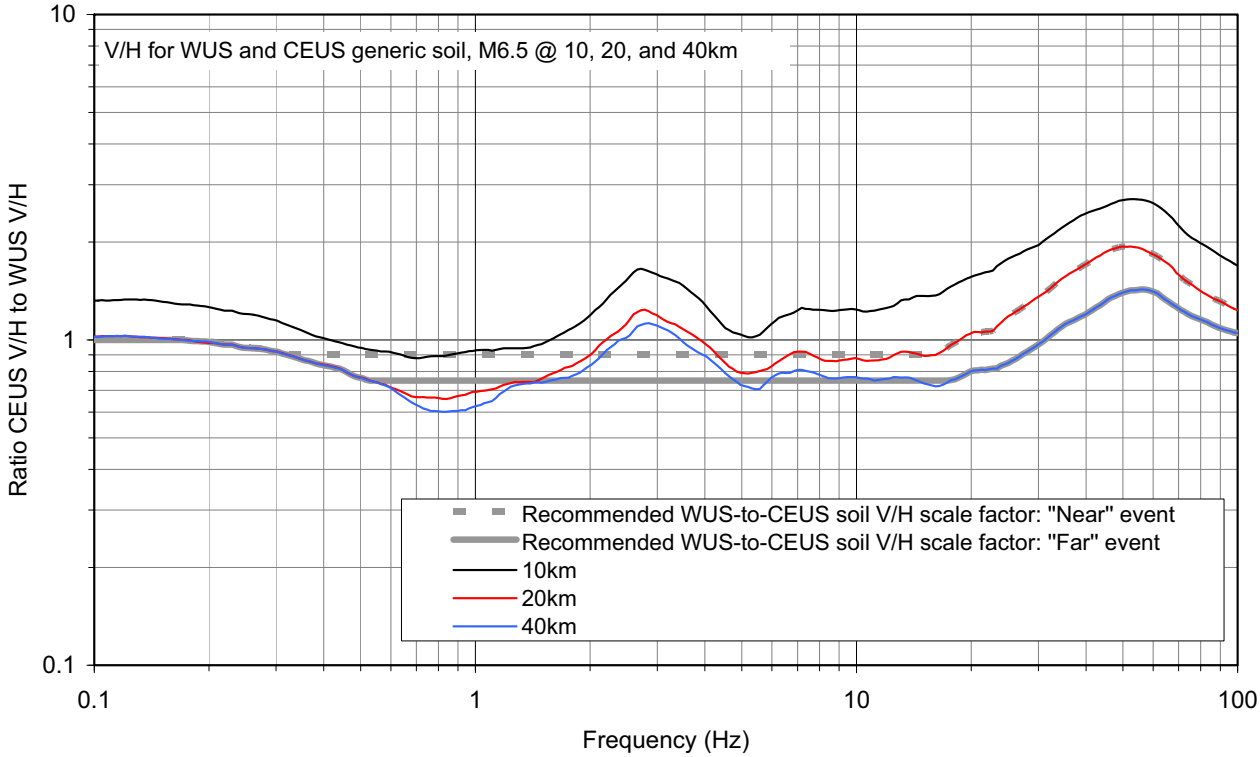

Note: The “near” and “far” ratios of V/H ratios recommended for this study are also shown.

Figure 2.5.2-40 Plots of [$V/H_{CEUS,Soil,Model}$ / $V/H_{WUS,Soil,Model}$] Term of Equation 2.5.2-6 for M6.5 and Distances of 10, 20, and 40 km, as Available in NUREG/CR-6728 (McGuire et al 2001)

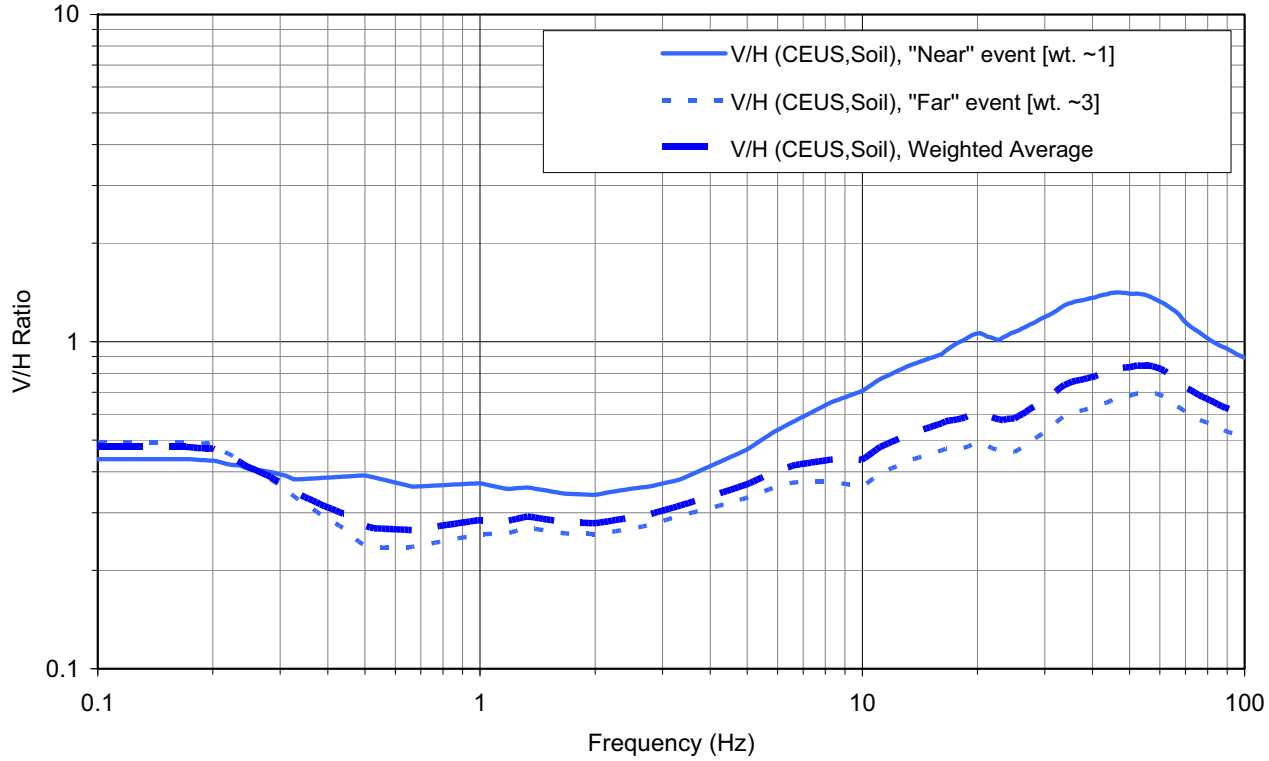

Note: Considering the relative contribution of the "near" and "far" events to the horizontal SSE design response spectrum, the approximately 1:3 weighted average is the recommended $V/H_{CEUS,Soil}$.

Figure 2.5.2-41 Plots of Recommended $V/H_{CEUS,Soil}$ from Equation 2.5.2-6 for "Near" and "Far" Events Using Results from NUREG/CR-6728 (McGuire et al 2001)

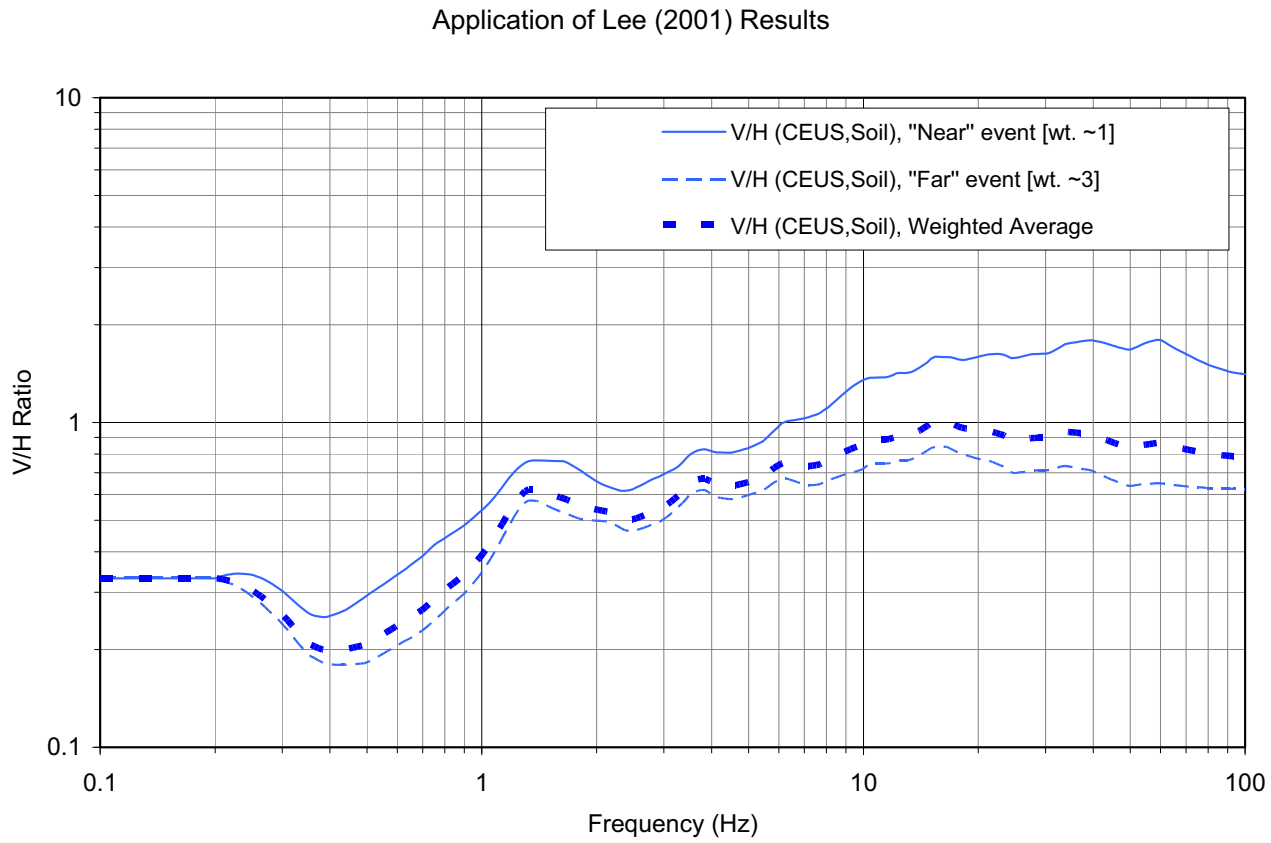

Note: Considering the relative contribution of the “near” and “far” events to the horizontal SSE design response spectrum, the approximately 1:3 weighted average is shown.

Figure 2.5.2-42 Plots of Recommended $V/H_{CEUS,Soil}$ from Equation 2.5.2-6 for “Near” and “Far” Events Using Results from Lee (2001)

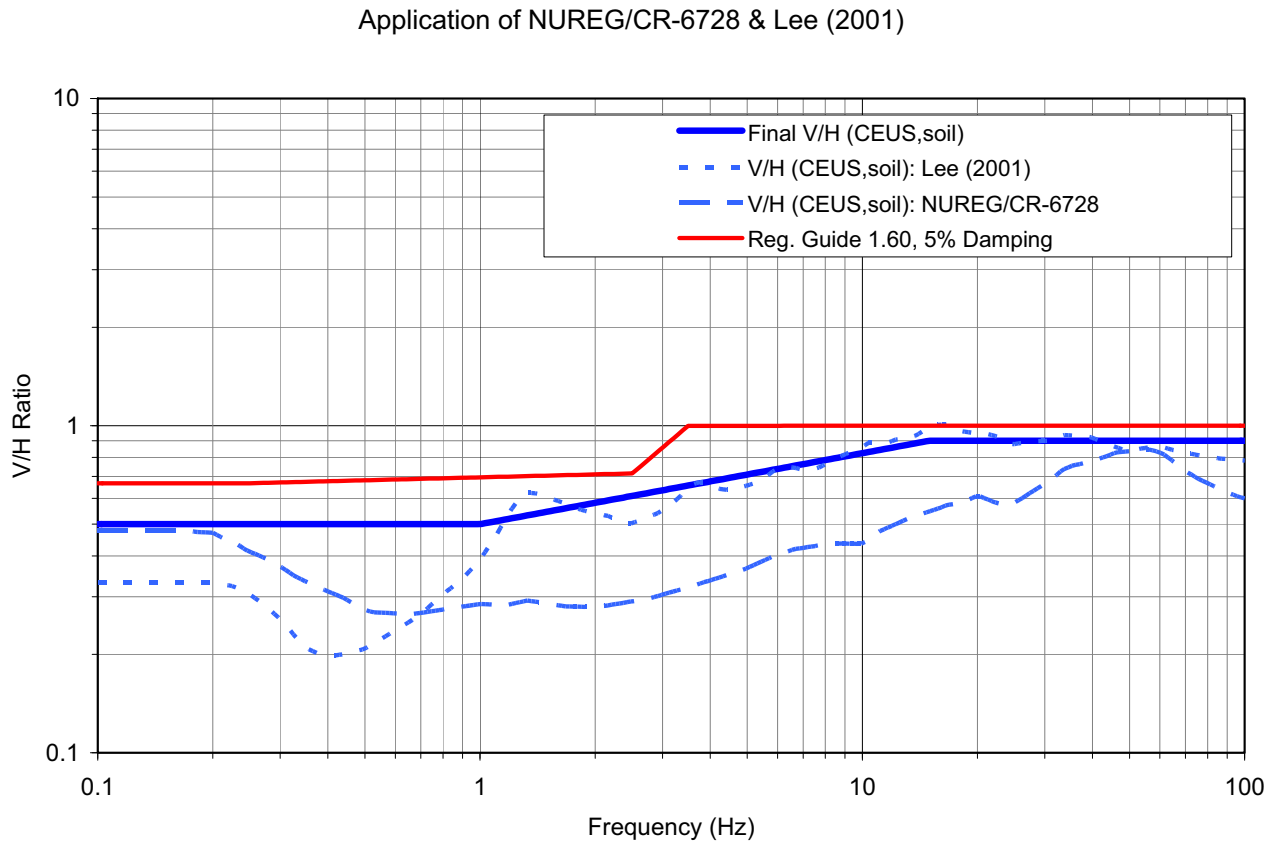

Note: Considering the site-specific aspects of the Lee (2001), it is preferred, guiding the recommended final $V/H_{CEUS,Soil}$ (blue solid). The V/H from RG 1.60 is shown (red) for comparison.

Figure 2.5.2-43 Plots of $V/H_{CEUS,Soil}$ (Blue Patterned) Derived from Results from NUREG/CR-6728 (McGuire et al 2001) and Lee (2001)

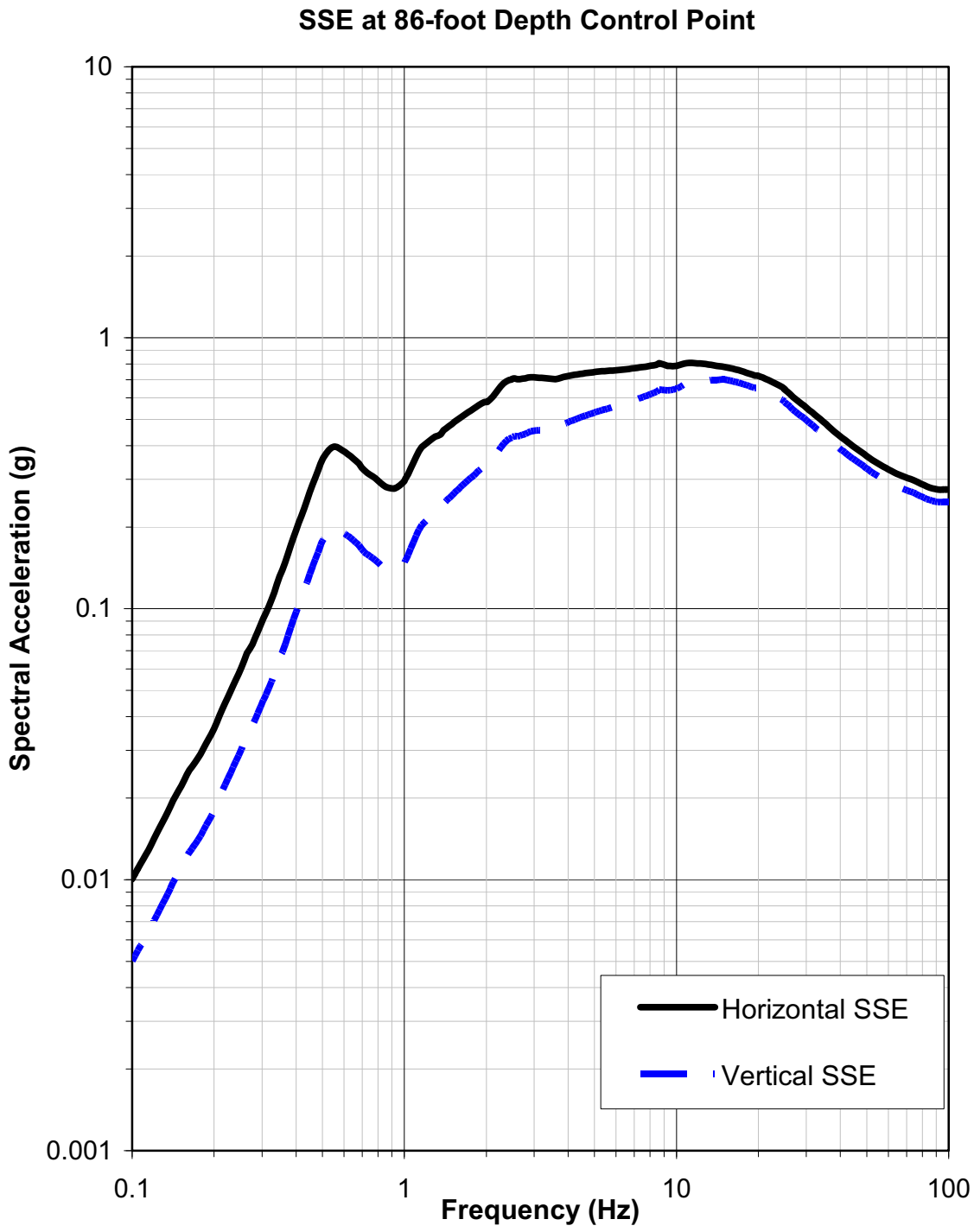

Figure 2.5.2-44 VEGP ESP Horizontal and Vertical SSE Spectra, Top of Blue Bluff Marl (5% Damping)

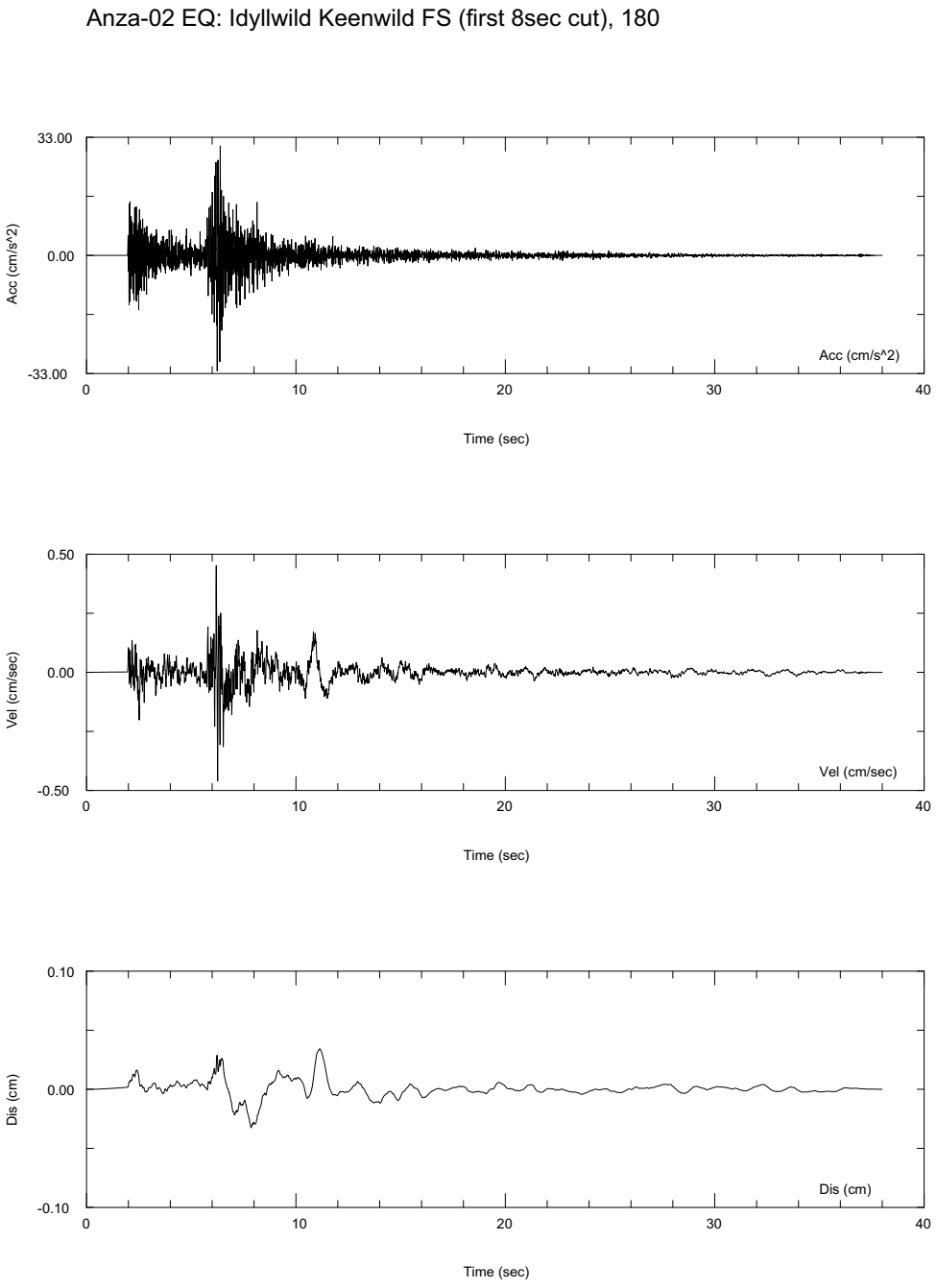

Figure 2.5.2-45a Initial Seed Input Time Acceleration, Velocity, and Displacement Time Histories (One of Thirty) for High Frequency Target Spectrum

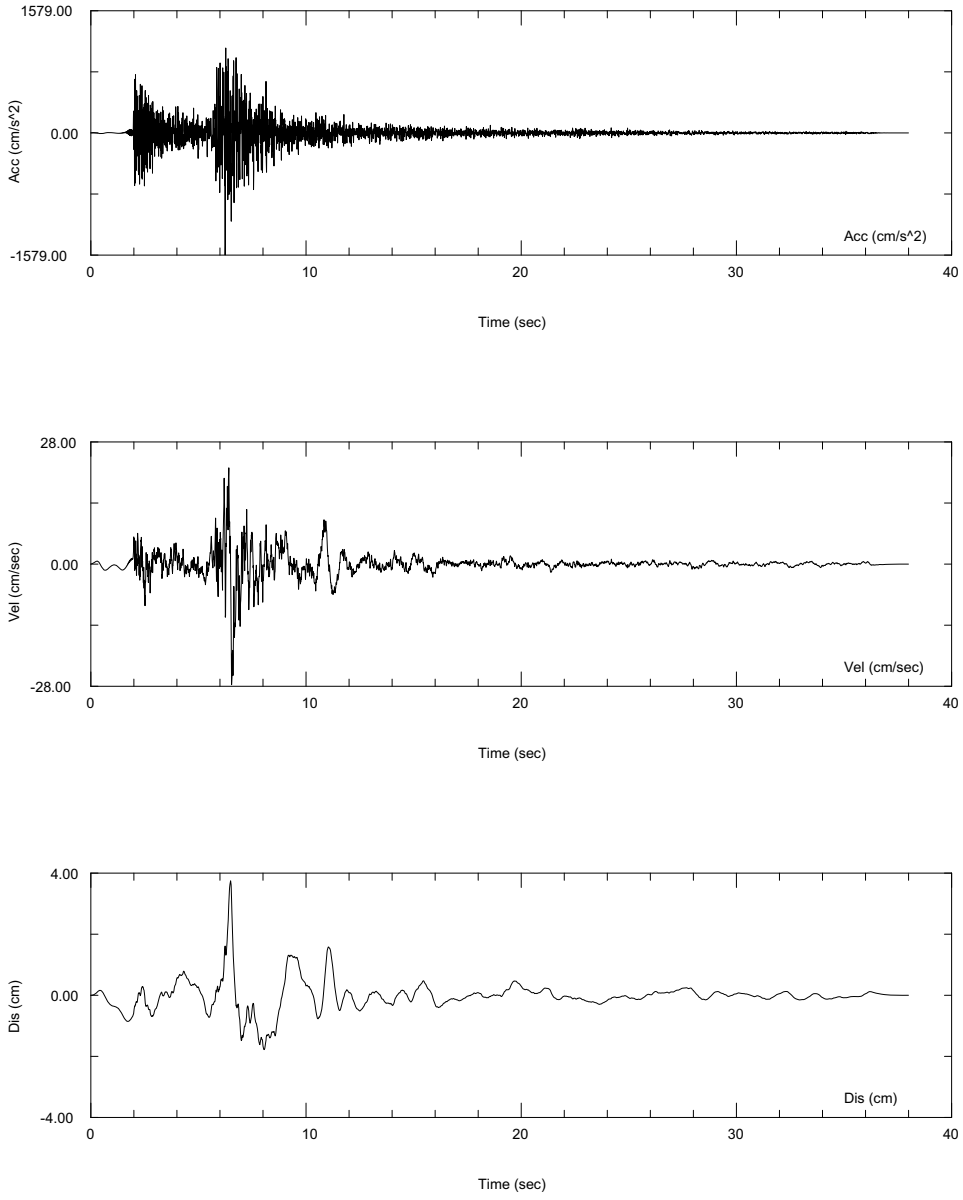

Figure 2.5.2-45b Final Modified Spectrum-Compatible Acceleration, Velocity, and Displacement Time Histories (One of Thirty) for 10^{-6} High Frequency Target Spectrum

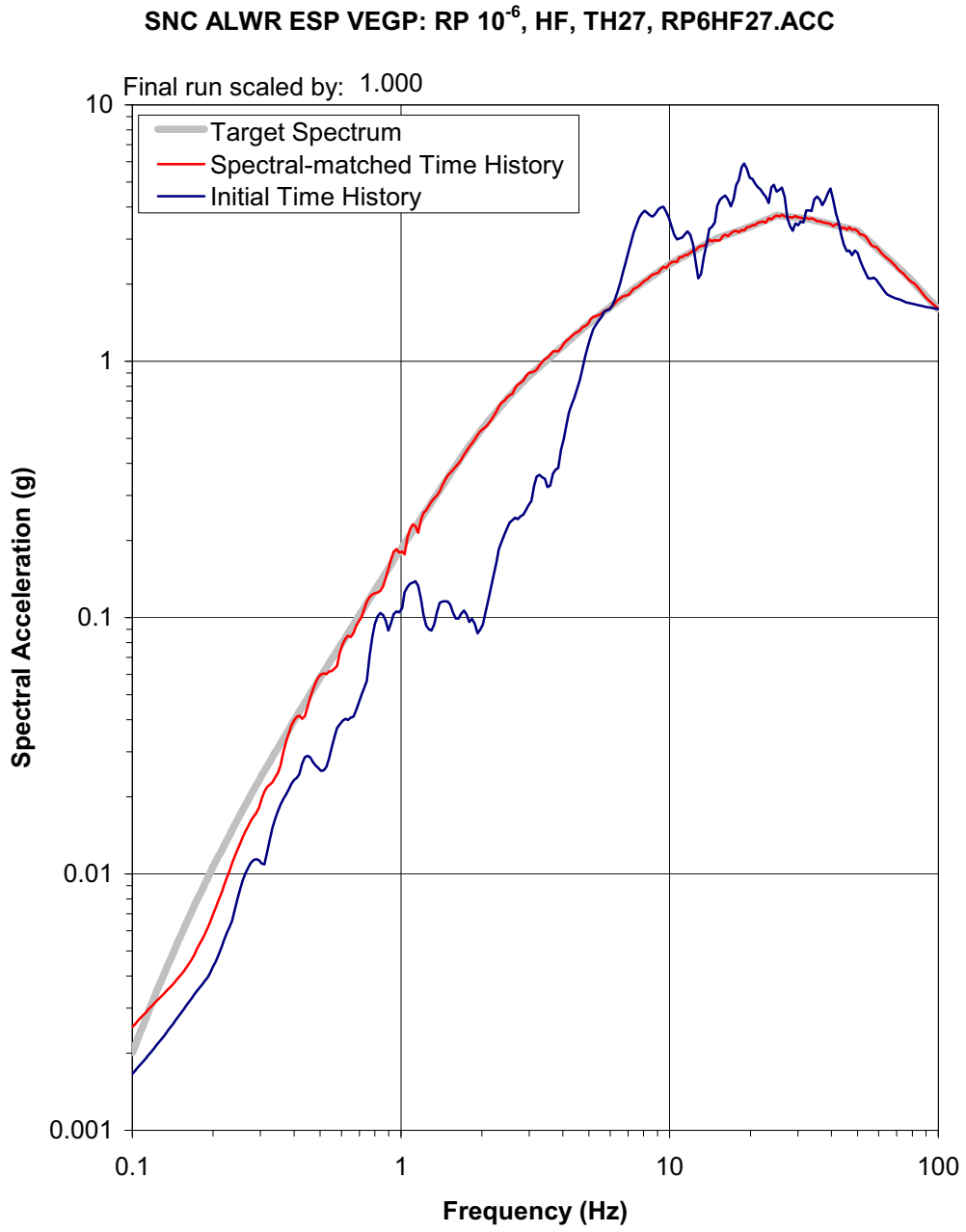

Figure 2.5.2-46 Comparison of 10^{-6} High Frequency Target Spectrum (Thick Grey Line), Response Spectrum from Initial Seed Input Acceleration Time History Scaled to Target PGA (Thin Blue Line), and Acceleration Response Spectrum for Final Modified Spectrum Compatible Time History (Thin Red Line)

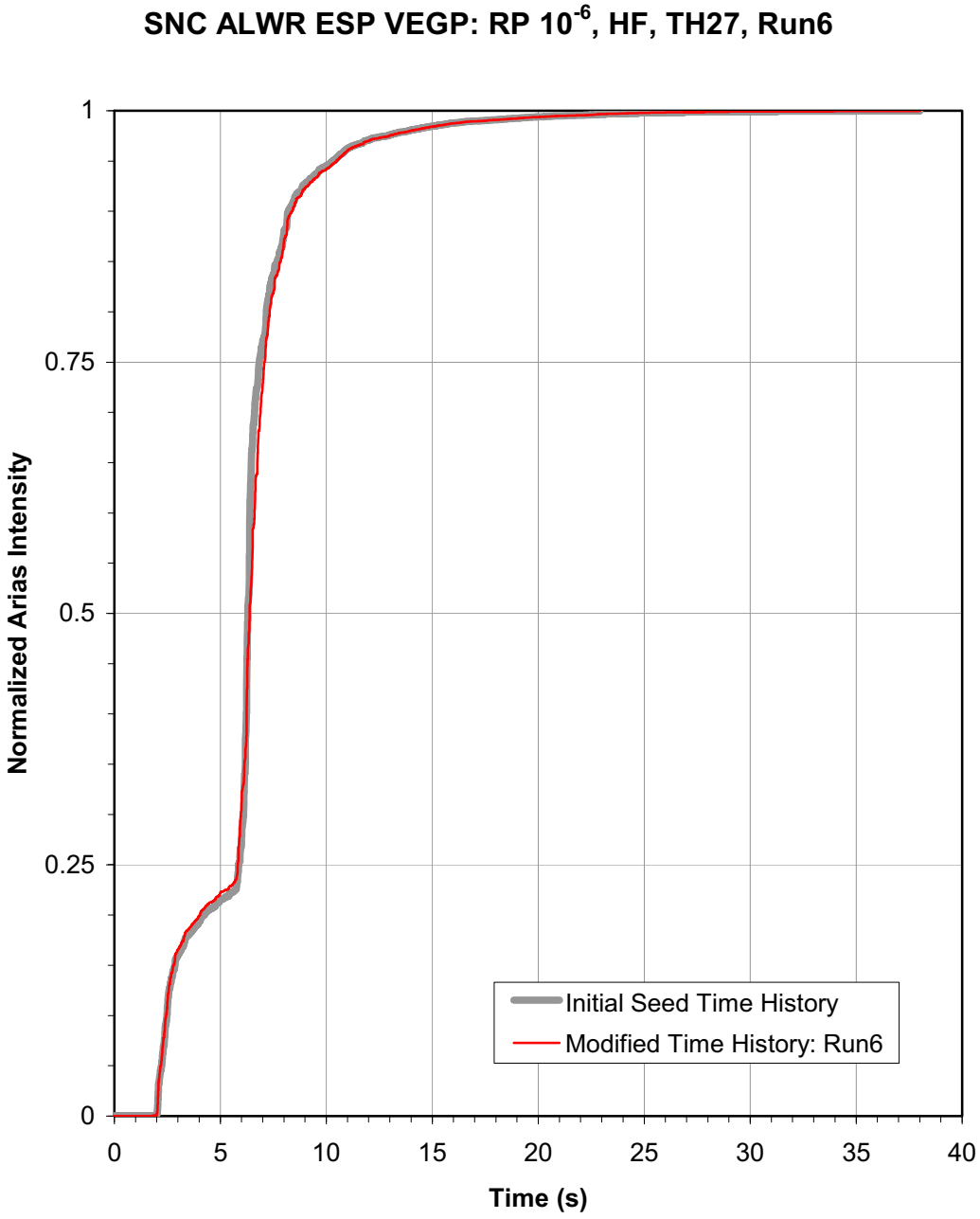

Figure 2.5.2-47 Comparison of Normalized Arias Intensity from Initial Seed Input Time History (Thick Grey Line) and Final Modified Spectrum Compatible (10^{-6} High Frequency Target Spectrum) Time History (Thin Red Line) for an Example Case

Section 2.5.2 References

(Abrahamson and Silva 1997) Abrahamson, N. N.,A. and W. J. Silva. "Empirical response spectral attenuation relations for shallow crustal earthquakes," Bull. Seism. Soc. Am.,Empirical Response Spectral Attenuation Relations for Shallow Crustal Earthquakes, Seismological Research Letters, v. 68, n. 1, 94-127, Jan/Feb 1997.

(Amick 1990) Amick, D., Paleoliquefaction Investigations Along the Atlantic Seaboard With Emphasis on the Prehistoric Earthquake Chronology of Coastal South Carolina, unpub. Ph.D. dissertation, University of South Carolina, selected pages, 1990.

(Amick et al. 1990a) Amick, D., Gelinas, R., Maurath, G., Cannon, R., Moore, D., Billington, E., and Kemppinen, H., Paleoliquefaction Features Along the Atlantic Seaboard, U.S. Nuclear Regulatory Commission Report, NUREG/CR-5613, 147p., 1990a.

(Amick et al. 1990b) Amick, D., Maurath, G., and Gelinas, R., Characteristics of Seismically Induced Liquefaction Sites and Features Located In the Vicinity of the 1886 Charleston, South Carolina Earthquake, Seismological Research Letters, v. 61, no. 2, p. 117-130, 1990b.

(ANSS 2005) The Advanced National Seismic System catalog is website: http://quake.geo.berkeley.edu/anss/catalog-search.html. Catsearch.16391.txt, 27 pages, downloaded on June 3, 2005

(ASCE 2005) American Society of Civil Engineers, "Seismic Design Criteria for Structures, Systems, and Components in Nuclear Facilities", ASCE/SEI 43-05, 2005.

(Atkinson and Boore 1995) Atkinson, G. M. and D. M. Boore, Ground-Motion Relations for Eastern North America. Bull. Seism. Soc. Am., v. 85, n. 1, 17-30 (1995).

(Bakun and Hopper 2004) Bakun, W. H. and Hopper, M. G., Magnitudes and Locations of the 1811-1812 New Madrid, Missouri, and the 1886 Charleston, South Carolina, Earthquakes, Bulletin of the Seismological Society of America, v. 94, no. 1, p. 64-75, 2004

(Bechtel 1984) Bechtel Power Corporation, Seismic Analysis Report, Vogtle Nuclear Generating Plant Units 1 and 2, October 1984.

(Bechtel 2000) Bechtel Corporation, *Theoretical and User's Manual for SHAKE 2000,* prepared by N Deng and F Ostadan, San Francisco, CA, 2000.

(Bechtel 2006d) Lindvall, S. C. and Hartleb, R. D., Update of Charleston Seismic Source and Integration with EPRI Source Models, Bechtel engineering study report 25144-006-V14-CY06-00006, revision 001, 2006.

(Behrendt and Yuan 1987) Behrendt, J. C. and Yuan, A., The Helena Banks Strike-slip (?) Fault Zone in the Charleston, South Carolina, Earthquake Area: Results From a Marine, High-

resolution, Multichannel, Seismic-reflection Survey, Geological Society of America Bulletin, v. 98, p. 591-601, 1987.

(Behrendt et al 1981) Behrendt, J. C., Hamilton, R. M., Ackermann, H. D., and Henry, V. J., Cenozoic Faulting in the Vicinity of the Charleston, South Carolina, 1886 Earthquake: Geology, v. 9, no. 3, p. 117-122, 1981.

(Behrendt et al 1983) Behrendt, J. C., Hamilton, R. M., Ackermann, H. D., Henry, V. J., and Bayer, K. C., Marine Multichannel Seismic-reflection Evidence for Cenozoic Faulting and Deep Crustal Structure Near Charleston, South Carolina: U. S. Geological Survey Professional Paper 1313-J, p. J1-J29, 1983.

(Behrendt et al 1988) Behrendt, J. C., Klitgord, K. D., and Hutchinson, D. R., Reactivated Boundary Fault Zones of Buried Early Mesozoic Basins as Possible Sources of Seismicity in the Charleston, S.C. Region: Abstracts with Programs - Geological Society of America Southeastern Section, v. 20, no. 4, p. 253, 1988.

(Bollinger 1977) Bollinger, G. A., Reinterpretation of the Intensity Data for the 1886 Charleston, South Carolina, Earthquake in Studies Related to the Charleston, South Carolina, Earthquake of 1886- A Preliminary Report (D. W. Rankin, ed.), U. S. Geological Survey Professional Paper 1028, p. 17-32, 1977.

(Bollinger 1992) Bollinger, G. A. Specification of Source Zones, Recurrence Rates, Focal Depths, and Maximum Magnitudes for Earthquakes Affecting the Savannah River Site in South Carolina, U.S. Geological Survey Bulletin 2017, 1992.

(Bollinger et al. 1985) Bollinger, G. A., Chapman, M. C., Sibol, M. S., and Costain, J. K., An analysis of earthquake focal depths in the southeastern U. S., Geophysical Research Letters, v. 12, no. 11, p. 785-788, 1985.

(Bollinger et al. 1991) Bollinger, G. A., Johnston, A. C., Talwani, P., Long, L. T., Shedlock, K. M., Sibol, M. S., and Chapman, M. C., Seismicity of the Southeastern United States; 1698-1986 in Neotectonics of North America, Decade Map Volume to Accompany the Neotectonic Maps (D. B. Slemmons, E. R. Engdahl, M. D. Zoback, D. B. Blackwell, eds.), p. 291-308, 1991.

(Bronk Ramsey 1995) Bronk Ramsey, C., Radiocarbon calibration and analysis of stratigraphy: the OxCal program, Radiocarbon, v. 37, no. 2, p. 425-430, 1995.

(Bronk Ramsey 2001) Bronk Ramsey, C., Development of the radiocarbon program OxCal: Radiocarbon, v. 43, no. 2A, p. 355-363, 2001.

(Chapman 2005b) Chapman, M., Personal Communication, 2005.

(Chapman and Talwani 2002) Chapman, M. C. and Talwani. P., Seismic Hazard Mapping for Bridge and Highway Design in South Carolina, South Carolina Department of Transportation Report, 2002.

(Chapman et al. 2002) Chapman, M. C., Munsey, J. W., Powell, C. A., Whisner, S. C., and Whisner J., The Eastern Tennessee Seismic Zone - Summary after 20 Years of Network Monitoring: Seismological Research Letters, v. 73, no. 2, p. 245, 2002.

(Colquhoun et al. 1983) Colquhoun, D. J., Woollen, I. D., Van Nieuwenhuise, D. S., Padgett, G. G., Oldham, R. W., Boylan, D. C., Bishop, J. W., and Howell, P. D. Surface and Subsurface Stratigraphy, Structure and Aquifers of the South Carolina Coastal Plain: SCDHEC Report ISBN 0-9613154-0-7, 78 p., 1983.

(Cook et al. 1979) Cook, F. A., Albaugh, D. S., Brown, L. D., Kaufman, S., Oliver, J. E., Hatcher, R. D. Jr., Thin-skinned Tectonics in the Crystalline Southern Appalachians: COCORP Seismic Reflection Profiling of the Blue Ridge and Piedmont. Geology, vol. 7, p. 563-567, 1979.

(Cook et al. 1981) Cook, F.A., L.D. Brown, S. Kaufman, J.E. Oliver, and T.A. Petersen, COCORP Seismic Profiling of the Appalachian Orogen Beneath the Coastal Plain of Georgia, Geological Society of America Bulletin, v. 92, no. 10, p. 738-748, 1981.

(Costantino, 1996) Costantino, C. J. (1996). Recommendations for Uncertainty Estimates in Shear Modulus Reduction and Hysteretic Damping Relationships. Published as an appendix in Silva, W. J., N. Abrahamson, G. Toro and C. Costantino (1997). "Description and validation of the stochastic ground motion model." Report Submitted to Brookhaven National Laboratory, Associated Universities, Inc. Upton, New York 11973, Contract No. 770573.

(Cornell 1968) Cornell, C. A., Engineering Seismic Risk Analysis, Bulletin of the Seismological Society of America, v. 58, no. 5, p. 1583-1606, 1968.

(Cornell and Winterstein 1988) Cornell, C. A. and Winterstein, S. R., Temporal and Magnitude Dependence in Earthquake Recurrence Models, Bulletin of the Seismological Society of America, v. 79, p. 1522-1537, 1988.

(Cramer 2001) Cramer, C. H., A Seismic Hazard Uncertainty Analysis for the New Madrid Seismic Zone, Engineering Geology, v. 62, p. 251-266, 2001.

(Ellsworth et al. 1999a) Ellsworth, W. L., Matthews, M. V., Nadeau, R. M., Nishenko, S. P., Reasenberg, P. A., and Simpson, R. W., A Physically-Based Earthquake Recurrence Model for Estimation of Long-Term Earthquake Probabilities, U.S. Geological Survey Open-File Report 99-522, 22p., 1999.

(EPRI NP-4726 1986) Electric Power Research Institute (EPRI), Volumes 5–10, Seismic Hazard Methodology for the Central and Eastern United States, Tectonic Interpretations, July 1986.

(EPRI NP-4726-A 1988) Seismic Hazard Methodology for the Central and Eastern United States, Volume 1, Part 2: Methodology (Revision 1). EPRI NP-4726-A, Rev. 1, dated November 1988.

(EPRI NP-6452-D 1989) Electric Power Research Institute (EPRI), EQHAZARD Primer, Prepared by Risk Engineering for Seismicity Owners Group and EPRI, June 1989.

(EPRI NP-6395-D 1989). Probabilistic seismic hazard evaluation at nuclear plant sites in the central and eastern United States, resolution of the Charleston Earthquake issue, EPRI Rept. 6395-D, Palo Alto, CA, April 1989.

(EPRI TR-102293 1993) Electric Power Research Institute. Guidelines for Determining Design Basis Ground Motions. Volume 5: Quantification of Seismic Source Effects. EPRI Report TR-102293, Project 3302, Final Report, November 1993.

(EPRI 1009684 2004) Electric Power Research Institute, CEUS Ground Motion Project Final Report, Elec. Power Res. Inst, Technical Report 1009684, dated December 2004.

(Fletcher et al. 1978) Fletcher, J. B., Sbar, M. L., and Sykes, L. R., Seismic Trends and Travel-time Residuals in Eastern North America and Their Tectonic Implications: Geological Society of America Bulletin, v. 89, p. 1656-1676, 1978.

(Frankel et al. 1996) Frankel, A., Barnhard, T., Perkins, D., Leyendecker, E. V., Dickman, N., Hanson, S., and Hopper, M., National seismic-hazard maps: documentation, U.S.G.S. Open-File Report 96-532, 1996.

(Frankel et al. 2002) Frankel, A. D., Petersen, M. D., Mueller, C. S., Haller, K. M., Wheeler, R. L., Leyendecker, E. V., Wesson, R. L., Harmsen, S. C., Cramer, C. H., Perkins, D. M., and Rukstales, K. S., Documentation for the 2002 Update of the National Seismic Hazard Maps, U.S. Geological Survey Open-File Report 02-420, 2002.

(Grant and Sieh 1994) Grant, L. B. and Sieh, K., Paleoseismic Evidence of Clustered Earthquakes on the San Andreas Fault in the Carrizo Plain, California, Journal of Geophysical Research, v. 99, n. B4, p. 6819-6841, 1994.

(Hamilton et al 1983) Hamilton, R. M., Behrendt, J. C., and Ackermann, H. D., Land multichannel seismic-reflection evidence for tectonic features near Charleston, South Carolina, Studies Related to the Charleston, South Carolina, Earthquake of 1886- Tectonics and Seismicity, U.S. Geologic Survey Professional Paper 1313-I, p. I1-I18, 1983.

(Johnston 1996) Johnston, A. C., Seismic Moment Assessment of Earthquake in Stable Continental Regions – III. New Madrid 1811-1812, Charleston 1886 and Lisbon 1755, Geophysical Journal International, v. 126, p.314-344, 1996.

(Lee 1996) Lee, R., "Investigations of Nonlinear Dynamic Properties at the Savannah River Site," *Report No. WSRC-TR-96-0062, Rev. 1*, Aiken, SC, 1996.

(Lee 2001) Lee, R.C., "Development of MFFF-Specific Vertical-to-Horizontal Seismic Spectral Ratios," Report No. WSRC-TR-2001-00342, Rev. 0, Westinghouse Savannah River Co., Aiken, SC, 2001.

(Lennon 1986) Lennon, G., Identification of a Northwest Trending Seismogenic Graben Near Charleston, South Carolina, U. S. Nuclear Regulatory Commission Report, NUREG/CR-4075, 43p., 1986.

(Madabhushi and Talwani 1993) Madabhushi, S. and Talwani, P., Fault Plane Solutions and Relocations of Recent Earthquakes in Middleton Place-Summerville Seismic Zone near Charleston, South Carolina, Bulletin of the Seismological Society of America, v. 83, no. 5, p. 1442-1466, 1993.**(Marple and Talwani 1990)** Marple, R. T., and Talwani, P., Field investigations of the Woodstock Lineament: Seismological Research Letters, v. 61, no. 3-4, p. 156, 1990.

(Marple and Talwani 1993) Marple, R. T. and Talwani, P., Evidence for possible tectonic upwarping along the South Carolina coastal plain from an examination of river morphology and elevation data: Geology, v. 21, p. 651-654, 1993.

(Marple and Talwani 2000) Marple, R. T. and Talwani, P., Evidence for a Buried Fault System in the Coastal Plain of the Carolinas and Virginia - Implications for Neotectonics in the Southeastern United Sates, Geological Society of America Bulletin, v. 112, no. 2., p. 200-220, 2000.

(Marple and Talwani 2004) Marple, R. T. and Talwani, P., Proposed Shenandoah Fault and East Coast-Stafford Fault System and Their Implications for Eastern U. S. Tectonics, Southeastern Geology, v. 43, no. 2, p. 57-80, 2004.

(Martin and Clough 1994) Martin, J. R. and Clough, G. W., Seismic Parameters from Liquefaction Evidence, Journal of Geotechnical Engineering, v. 120, no. 8, p. 1345-1361, 1994.

(Matthews et al. 2002) Matthews, M. V., Ellsworth, W. L., and Reasenberg, P. A., A Brownian model for recurrent earthquakes, Bulletin of the Seismological Society of America, v. 92, p. 2233-2250, 2002.

(McGuire et al. 2001) McGuire, R.K., W. J. Silva, and C. J. Costantino. Technical Basis for Revision of Regulatory Guidance on Design Ground Motions, Hazard- and Risk-Consistent Ground Motion Spectra Guidelines. prepared for Nuclear Regulatory Commission, NUREG/CR-6728, 2001.

(McGuire et al. 2002) McGuire, R. K., W. J. Silva, and C. J. Costantino, Technical Basis for Revision of Regulatory Guidance on Design Ground Motions: Development of Hazard- & Risk-Consistent Seismic Spectra for Two Sites, Revision 0, prepared for Nuclear Regulatory Commission, NUREG/CR-6769, 2002

(NIST/SEMATECH 2006) NIST/SEMATECH, e-Handbook of Statistical Methods, http://www.itl.nist.gov/div898/handbook/, accessed 11 January 2006.

(Obermeier 1996) Obermeier, S., Liquefaction-induced features: in Paleoseismology, J. McCalpin (ed.), Academic Press, San Diego, p. 331-396, 1996.

(Obermeier 2005) Obermeier, S., personal communication, September 2, 2005.

(Obermeier et al. 1989) Obermeier, S. F., Weems, R. E., Jacobson, R. B., and Gohn, G. S., Liquefaction evidence for Repeated Holocene Earthquakes in the Coastal Region of South Carolina, Annals of the New York Academy of Sciences, v. 558, p. 183-195, 1989.

(Rockwell et al. 2000) Rockwell, T. K., Lindvall, S., Herzberg, M., Murbach, D., Dawson, T., and Berger, G., Paleoseismology of the Johnson Valley, Kickapoo, and Homestead Valley faults: clustering of earthquakes in the Eastern California shear zone, Bulletin of the Seismological Society of America, v. 90, no. 5, p. 1200-1236, 2000.

(Savage 1991) Savage, J. C., Criticism of Some Forecasts of the National Earthquake Evaluation Council, Bulletin of the Seismological Society of America, v. 81, n. 3, p. 862-881, 1991.

(Savy et al. 2002) Savy, J. B., Foxall, W., Abrahamson, N., and Bernreuter, D., Guidance for Performing Probabilistic Seismic Hazard Analysis for a Nuclear Plant Site: Example Application to the Southeastern United States, U.S. Nuclear Regulatory Commission, NUREG/CR-6607, 2002.

(Seeber and Armbruster 1981) Seeber, L., and Armbruster, J. G., The 1886 Charleston, South Carolina earthquake and the Appalachian detachment: Journal of Geophysical Research, v. 86, no. B9, p. 7874-7894, 1981.

(SEUSSN 2005) The South Eastern United States Seismic Network catalog is available from the Virginia Tech Seismic Observatory FTP site:
http://www.geol.vt.edu/outreach/vtso/anonftp/catalog/susn2003cat.txt, (266 pages),
Susn2003cat.txt, bulletin.txt and catalog.txt, downloaded on June 3, 2005.

(Sieh et al. 1989) Sieh, K., Stuiver, M., and Brillinger, D., A More Precise Chronology of Earthquakes Produced by the San Andreas fault in Southern California, Journal of Geophysical Research, v. 94, n. B1, p. 603-623, 1989.

(Smith and Talwani 1985) Smith, W. A., and Talwani, P., Preliminary interpretation of a detailed gravity survey in the Bowman and Charleston, S.C. seismogenic zones: Abstracts with Programs - Geological Society of America southeastern section, v. 17, no. 2, p. 137, 1985.

(SSHAC 1997) SSHAC, Recommendations for Probabilistic Seismic Hazard Analysis: Guidance on Uncertainty and Use of Experts, Prepared by Senior Seismic Hazard Analysis Committee (SSHAC), NUREG/CR-6372, 1997.

(Sykes 1978) Sykes, L. R., Intraplate Seismicity, Reactivation of Preexisting Zones of Weakness, Alkaline Magmatism, and Other Tectonism Postdating Continental Fragmentation: Reviews of Geophysics, v. 16, p. 621-688, 1978.

(Talwani 1982) Talwani, P. An internally consistent pattern of seismicity near Charleston, South Carolina, Geology, Volume 10, 655–658, 1982.

(Talwani 1999) Talwani, P., Fault Geometry and Earthquakes in Continental Interiors, Tectonophysics, v. 305, p. 371-379, 1999.

(Talwani 2000) Talwani, P., Macroscopic Effects of the 1886 Charleston Earthquake, A Compendium of Field Trips of South Carolina Geology, South Carolina Geological Survey, p. 1-6, 2000.

(Talwani 2005) Talwani, P., Personal Communication, September 8, 2005.

(Talwani and Katuna 2004) Talwani, P. and Katunam M., Macroseismic effects of the 1886 Charleston earthquake: Carolina Geological Society field trip guidebook, p. 18, 2004.

(Talwani and Schaeffer 2001) Talwani, P. and Schaeffer, W. T., Recurrence Rates of Large Earthquakes in the South Carolina Coastal Plain Based on Paleoliquefaction Data, Journal of Geophysical Research, v. 106, no. B4, p. 6621-6642, 2001.

(Tarr and Rhea 1983) Tarr, A. C. and Rhea, S., Seismicity Near Charleston, South Carolina, March 1973 to December 1979 in Studies Related to the Charleston, South Carolina Earthquake of 1886: Tectonics and Seismicity, G. S. Gohn (ed.), U. S. Geological Survey Professional Paper 1313, R1-R17, 1983.

(Tarr et al. 1981) Tarr, A. C., Talwani, P., Rhea, S., Carver, D., and Amick, D., Results of recent South Carolina seismological studies: Bulletin of the Seismological Society of America, v. 71, no. 6, p. 1883-1902, 1981.

(Toro 1996) Toro, G. R. (1996). Probabilistic Models of Site Velocity Profiles for Generic and Site-Specific Ground-Motion Amplification Studies. Published as an appendix in Silva, W. J., N. Abrahamson, G. Toro and C. Costantino (1997). "Description and validation of the stochastic ground motion model." Report Submitted to Brookhaven National Laboratory, Associated Universities, Inc. Upton, New York 11973, Contract No. 770573.

(Toro 1997) Toro, G.R. (1997). Probabilistic Models of Site Velocity Profiles at the Savannah River Site, Aiken, South Carolina. Report by Risk Engineering, Inc. to Pacific Engineering and Analysis, April. Published as an appendix in Lee, R.C.; Maryak, M.E.; and McHood, M.D. 1997. SRS Seismic Response Analysis and Design Basis Guidelines. WSRC-TR-97-0085, Rev. 0. Aiken, South Carolina: Westinghouse Savannah River Company.

(Toro 2005) Toro, G.R. (2005). Site-Wide Probabilistic Model of Shear-Wave Velocity Profiles at the Savannah River Site, Aiken, South Carolina. Report by Risk Engineering, Inc. to Bechtel Savannah River Co., October.

(Tuttle 2001) Tuttle, M. P., The Use of Liquefaction Features in Paleoseismology: Lessons Learned in the New Madrid Seismic Zone, central United States, Journal of Seismology, v. 5, p. 361-380, 2001.

(Weems and Lewis 2002) Weems, R. E., and Lewis, W. C., Structural and tectonic setting of the Charleston, South Carolina, region; evidence from the Tertiary stratigraphic record: Geological Society of America Bulletin, v. 114, no. 1, p. 24-42, 2002.

(Weems et al 1997) Weems, R. E., Lemon, E. M., Jr., and Nelson, M. S., Geology of the Pringletown, Ridgeville, Summerville, and Summerville Northwest 7.5-minute quadrangles, Berkeley, Charleston, and Dorchester counties, South Carolina: Miscellaneous Investigations Series - U. S. Geological Survey, 1997.

(Wells and Coppersmith 1994) Wells D.L. and K.J. Coppersmith. New Empirical Relationships Among Magnitude, Rupture Length, Rupture Width, Rupture Area, and Surface Displacement," Bulletin Seismological. Society of America, 84, 4, 974-1002, August 1994.

(Wentworth and Mergener-Keefer 1983) Wentworth, C.M., and Mergener-Keefer, M., Regenerate Faults of the Southeastern United States, in Studies Related to the Charleston, South Carolina, Earthquake of 1886: Tectonics and seismicity, Gohn, G. S. (ed., US Geological Survey Professional Paper 1313, pp. S1-S20, 1983.

(Wheeler 2005) Wheeler, R. L., Known or Suggested Quaternary Tectonic Faulting, Central and Eastern United States- New and Updated Assessments for 2005: U. S. Geological Survey Open-File Report 2005-1336, 2005.

(WGCEP 1995) Working Group on California Earthquake Probabilities, Seismic Hazards in Southern California: Probable earthquakes, 1994 to 2024, Bulletin of the Seismological Society of America, v. 85, p. 379-439, 1995.

(WGCEP 2003) Working Group on California Earthquake Probabilities, Earthquake Probabilities in the San Francisco Bay region: 2002-2031, U. S. Geological Survey Open-File Report 03-2134, 2003.

(WSRC 1998) General SRS Strain Compatible Soil Properties for 1886 Charleston Earthquake (U), Calculation K-CLC-G-0060, McHood, M.D, October 29, 1998.

This page is intentionally blank.

2.5.3 Surface Faulting

NRC Regulatory Guide 1.165, *Identification and Characterization of Seismic Sources and Determination of Safe Shutdown Earthquake Ground* Motion (RG 1.165), defines a capable tectonic source as a tectonic structure that can generate both vibratory ground motion and tectonic surface deformation, such as faulting or folding at or near the earth's surface in the present seismotectonic regime. This section evaluates the potential for tectonic surface deformation and non-tectonic surface deformation at the site. Information contained in Section 2.5.3 was developed in accordance with RG 1.165 and is intended to satisfy 10 CFR 100.23, *Geologic and Seismic Siting Criteria*.

There are no capable tectonic sources within the 5-mi VEGP site area radius, and there is a negligible potential for tectonic fault rupture. There is only limited potential for non-tectonic surface deformation in shallow deposits within the 5-mi site area radius, and this potential can be mitigated by means of excavation. The following sections provide the data, observations, and references to support these conclusions.

2.5.3.1 Geological, Seismological, and Geophysical Investigations

The following investigations were performed to assess the potential for tectonic and non-tectonic deformation at and within a 5-mi radius of the VEGP site:

- Compilation and review of existing data and literature
- Interpretation of aerial photography
- Field reconnaissance
- Aerial reconnaissance
- Review of historical and recorded seismicity
- Collection and interpretation of seismic reflection data at the VEGP site
- Discussions with current researchers in the area
- Collection and interpretation of survey data collected from a Quaternary fluvial terrace located at the SRS overlying the surface projection of the Pen Branch fault.

An extensive body of information is available for the VEGP site. This information is contained in five main sources:

- Work performed for the existing VEGP Units 1 and 2.

- Published geologic mapping performed by the US Geological Survey (USGS), the South Carolina Department of Natural Resources, and other researchers.
- Numerous, detailed investigations of the nearby Savannah River Site (SRS), perhaps the most extensively studied portion of the US Atlantic Coastal Plain.
- Seismicity data compiled and analyzed in published journal articles, EPRI (1986a), and the updated EPRI catalog, performed as part of this study.
- Seismic reflection data collected near the site within the Savannah River channel **(Henry 1995)**.

This existing information was supplemented by aerial and field reconnaissance performed within and beyond the 25-mi site vicinity radius, and by interpretation of aerial photography within the 5-mi site area radius. Given the extensive geologic and geomorphic studies performed previously at the SRS, the interpretation of aerial photography performed for the ESP study focused on the area southeast of the SRS. These studies were performed to document, where possible, the presence or absence of geomorphic features indicative of potential Quaternary fault activity within the Coastal Plain sediments or underlying bedrock.

2.5.3.1.1 Previous VEGP Site Investigations

This section summarizes previous site investigations performed for existing VEGP Units 1 and 2. Previous investigations for VEGP Units 1 and 2 did not identify the existence of tectonic faulting **(Bechtel 1974a, 1974b, 1978e, 1981, 1989)**. Detailed geologic mapping and inspection of excavations during VEGP construction revealed no evidence of geologically recent or active faulting. However, minor, non-tectonic dissolution-induced collapse features (including minor folds and small joints and faults confined to the near-surface) were recognized and logged in detail on site **(Bechtel 1984b)**.

Bechtel (1974a) identified, discussed in Section 2.5.1.2.3, a northwest-dipping monoclinal flexure beneath the site in the Blue Bluff Marl. This feature, referred to as a dip reversal because the strata locally dip gently northwest against the regional southeast dip of the Coastal Plain sediments, was interpreted as a syndepositional, sedimentary feature **(Bechtel 1974b)**. Later investigations by Bechtel (1978, 1981) describe “stratigraphic irregularities” recognized in site excavations associated with the Blue Bluff Marl. Because these stratigraphic irregularities were observed to be underlain by flat-lying, laterally continuous strata, Bechtel (1978, 1981) concluded that these irregularities were produced by syn-depositional processes.

Alterman (1984) reported observing a number of “clastic dikes” at the VEGP site and in the site vicinity during an NRC visit. Alterman’s report does not, however, interpret the origin of these features. Bechtel (1984) identified the presence of a variety of small-scale deformation

structures in the walls of a garbage trench on the VEGP site within Tertiary Coastal Plain sediments. These structural features, including warped bedding, fractures, joints, minor offsets, and injected sand dikes, were interpreted as local phenomena related to dissolution of the underlying Utley Limestone and resultant plastic and brittle collapse of overlying Tertiary sediments. These features and their potential for non-tectonic surface deformation at the site are further discussed in Section 2.5.3.8.2.1 below. Bechtel (1984) also noted the presence of "clastic dikes" in the garbage trench and interpreted these features to be the result of near-surface pedogenic processes.

As described in Section 2.5.1.2.4.1, the Pen Branch fault was first discovered at the SRS in 1989, which initiated investigations at the VEGP site and a series of studies at the SRS. Investigations at the VEGP site concluded that the fault was not onsite or in close proximity to Units 1 and 2 **(Bechtel 1989)**. Studies of the Pen Branch fault at the SRS continued through the 1990s, but had still not definitively located the southwestward projection of the fault to the Georgia side of the Savannah River. As shown in Figures 2.5.1-21, 2.5.1-22, 2.5.1-23 and 2.5.1-34, projections of the fault into Georgia included locations northwest of the VEGP site **(Snipes et al. 1993a)** and directly southeast of the VEGP site **(Cumbest et al. 2000)**.

In light of the data gathered from studies of the Pen Branch fault at the SRS during the 1990s and recent investigations at the VEGP site, some conclusions of the previous studies regarding the location of the Pen Branch fault in site studies and the FSAR should be revised. Because the Pen Branch fault has been located adjacent to the VEGP site and beneath the monocline in the Blue Bluff Marl, it is now clear that the Pen Branch fault is associated with the monocline (or dip reversal) and that there is a Tertiary fault within 5 mi of the VEGP site. However, the new information only alters the past location of the Pen Branch fault. After considerable study, no new information gathered on the Pen Branch fault has changed the original conclusions of Snipes et al. (1989) that the youngest strata deformed by the fault are late Eocene and that the fault is not a capable tectonic source. In fact, recent studies, for this ESP study, have provided additional lines of evidence to support the non-capable status of the Pen Branch fault, a conclusion that has been supported in multiple NRC and DOE reviews (NUREG-1137, NUREG-1137-8, NUREG-1821).

2.5.3.1.2 Published Geologic Mapping

Geologic mapping of the site vicinity (25-mi radius) and site area (5-mi radius) in the past two decades has been largely focused on the SRS and surrounding regions of South Carolina (Figure 2.5.1-28). The USGS has published 1:100,000 scale and 1:48,000 scale geologic maps of the SRS area **(Prowell 1994a, 1996)**. In addition, the South Carolina Department of Natural Resources has published numerous 1:24,000 scale geologic maps within the site vicinity. Significantly fewer and less detailed geologic maps have been published for the Georgia portion of the VEGP site vicinity (Figure 2.5.1-28).

Additional studies focused on mapping and assessing specific geologic and/or tectonic features in the site vicinity. These include mapping and interpreting small-scale deformation structures **(McDowell and Houser 1983; Bartholomew et al. 2002)** and possible Quaternary tectonic features **(Crone and Wheeler 2000; Wheeler 2005)**.

McDowell and Houser (1983) mapped the distribution of small-scale deformation structures in the Upper Coastal Plain in the greater Columbia, South Carolina, to Augusta, Georgia, area. They identified small-scale folds, brittle faults, and convoluted bedding features exposed in roadcuts, excavations, and stream cuts. McDowell and Houser noted that some of these features appear to be non-tectonic in origin, whereas others are less clear and may be related to strong ground shaking.

Bartholomew et al. (2002) described exposures of “clastic dikes” in the VEGP site vicinity. One of these exposures is located in the upper Eocene Tobacco Road sand near Hancock landing (north of existing VEGP Units 1 and 2 within the VEGP site area). They interpret these clastic dikes as evidence for "strong paleoearthquakes, probably associated with late Eocene to late Miocene oblique-slip".

In addition, the USGS has published a compilation of all known Quaternary faults, liquefaction features, and possible tectonic features in the central and eastern United States **(Crone and Wheeler 2000)**, updated in **(Wheeler 2005)** (Figure 2.5.1-17). The only feature within the 5-mi VEGP site area radius identified by this compilation is the Pen Branch fault (discussed in detail in Section 2.5.1.2.4.1). Crone and Wheeler (2000) classified the Pen Branch fault as a Class C feature (Table 2.5.1-1) because of its demonstrated early Cenozoic activity but absence of evidence for post-Eocene slip.

2.5.3.1.3 Previous Savannah River Site Investigations

SRS studies include numerous geological, geophysical, seismologic, and hydrologic investigations. These studies identified a number of basement faults that are mapped at the SRS based on interpretation of seismic reflection data, borehole data, gravity and magnetic data, and/or groundwater anomalies. Several of these faults are located within the 5-mi radius of the VEGP site (Figures 2.5.1-21, 2.5.1-22, and 2.5.1-23).

The SRS is one of the most extensively studied portions of the Coastal Plain in terms of geology. Accordingly, an exhaustive description of all SRS geologic studies is not given here. Instead, the key studies that locate and characterize tectonic features of the SRS are summarized in this section. These studies include Chapman and DiStefano (1989), Snipes et al. (1993), Stieve et al. (1991), Stephenson and Stieve (1992), Geomatrix (1993), Domoracki (1994), Stieve and Stephenson (1995), and Cumbest et al. (1998, 2000). As described in Section 2.5.1.1.4.5, the majority of evidence for the presence of faults at the SRS is based on the interpretation of seismic reflection surveys; therefore, the depiction of buried fault locations

differs between researchers and has also evolved through time with the successive availability of additional data.

Chapman and DiStefano (1989) conducted a vibroseis seismic reflection survey to refine existing knowledge of the basement structure beneath the SRS. This survey identifies first-order features of the basement surface, including the northern boundary fault of the Mesozoic Dunbarton Basin, later named the Pen Branch fault.

Based on core logs and supplemented by seismic reflection data from Chapman and DiStefano (1989), Snipes et al. (1993) mapped the location of the Pen Branch fault across the SRS. Snipes et al. (1993) recognized up-to-the-southeast movement for the Pen Branch fault and suggested that the fault formed originally as a Mesozoic normal fault bordering the northwestern Dunbarton Basin that was later reactivated in the Tertiary as a reverse fault.

Stieve et al. (1991) presented the results of a drilling program designed to further characterize the displacement history of the Pen Branch fault on the SRS. This study concludes that the base of the late Miocene Upland Formation is not deformed across the projected trace of the fault and thus provides direct stratigraphic evidence for the absence of activity on the Pen Branch fault within the past 5 Ma (million years ago).

Stephenson and Stieve (1992) and Stieve and Stephenson (1995) combined seismic data, borehole data, and potential field data to construct a subsurface structure model for the SRS. Their subsurface fault map identifies six basement-involved faults, including the Pen Branch, Steel Creek, ATTA, Ellenton, Crackerneck, and Upper Three Runs faults (Figure 2.5.1-21). These faults are described in Section 2.5.1.1.4.5 and Section 2.5.3.2.

Geomatrix (1993) performed a Quaternary and neotectonic study to assess geologic and geomorphic evidence for active tectonic deformation at the SRS. No evidence for active tectonic deformation was observed. Longitudinal profiles on Savannah River fluvial terraces show no evidence for warping or faulting of terrace surfaces associated with the surface projections of the Pen Branch and Steel Creek faults within a resolution of 7 to 10 ft (2 to 3 m).

Domoracki (1994) used 170 mi of reprocessed seismic reflection lines to map the geometry of the Dunbarton Basin and to refine the subsurface locations of SRS basement-involved faults. The report identified the Dunbarton Basin as a half-graben bounded solely by the Pen Branch fault and suggested that the Pen Branch fault possibly soles into the Augusta fault at depth (see Section 2.5.1.1.4.3 for discussion of the Augusta fault).

Cumbest et al. (1998, 2000) integrated data from more than 60 boreholes and more than 100 mi of seismic reflection profiles to provide the most-recent mapping of subsurface structure and basement-involved faults at the SRS. Cumbest et al. (1998) found no evidence for capability on any faults at the SRS. These data were used in combination with geometrical fault models to constrain slip histories for the Pen Branch and Crackerneck faults **(Cumbest et al. 2000)**.

Cumbest et al. (2000) also compared the SRS faults with other Atlantic Coastal Plain faults and concluded that both sets of faults exhibit the same general characteristics and are closely associated. These characteristics include:

- Maximum offset less than 80 m (260 ft) at the base of the Coastal Plain sediments
- Regional-scale features that strike approximately northeast-southwest
- Predominantly reverse sense of slip
- Movement beginning in the Cretaceous Period and decreasing with time

Based on the strength of this association, and based on the fact that many of the other Coastal Plain faults are known to be non-capable, Cumbest et al. (2000) concluded by association that the SRS faults are also non-capable.

In situ stress measurements in basement rocks have been made in deep boreholes at the SRS. As part of a study of seismic hazards, magnitudes and orientations of in situ stresses were determined in five boreholes in 1998 and a 4,000-ft-deep borehole in 1992 **(Moos and Zoback 2001)**. Results from the 4,000-ft-deep well (NPR hole) and previous borehole measurements at the SRS are consistent with a northeast-southwest direction of maximum compressive stress in the Altantic Coastal Plain province **(Moos and Zoback 2001)**. While the orientation of maximum horizontal stress was observed to range from N75ºE to N33ºE in the NPR hole, the majority of other orientations are closer to approximately N60ºE. Thus, the maximum horizontal stress is oriented roughly parallel to the Pen Branch fault (about N55ºE), indicating that it is unlikely to accommodate reverse or strike-slip faulting earthquakes in the present stress regime **(Moos and Zoback 2001)**.

2.5.3.1.4 Previous Seismicity Data

The EPRI catalog of historical seismicity has demonstrated that no known earthquake greater than body wave magnitude (m_b) 3 has occurred within the VEGP site vicinity (25-mi radius) prior to 1984 (Figure 2.5.1-16). Considering micro-seismicity (m_b<3) recorded since 1976 by the SRS seismic recording network, there has been no recent earthquake activity within the site area (5-mi radius) (Figure 2.5.1-16). The nearest micro-earthquake to the VEGP site is about 7 mi (about 11 km) to the northeast and located on the SRS **(Stevenson and Talwani 2004)**.

The local SRS seismic network recorded three small earthquakes in 1985 (magnitude 2.6), 1988 (magnitude 2.0), and 1997 (magnitude 2.5), and a small earthquake sequence in 2001–2002 within the boundaries of the SRS **(Stevenson and Talwani 2004)**. These small SRS earthquakes, as well as a 1993 event located north of the SRS in Aiken, South Carolina, have been studied by researchers in an effort to evaluate possible correlations to tectonic features. As described in Section 2.5.3.3, this minor activity is not correlated with any known faults.

2.5.3.1.5 Previous Seismic Reflection Data

In addition to the numerous seismic reflection surveys conducted at the SRS, several other seismic reflection studies have been performed in the VEGP site area. These include two surveys conducted within the Savannah River **(Bechtel 1982; Henry 1995)** and one conducted in a land-based survey located about 1.5 mi west of VEGP Units 1 and 2 **(Summerour et al. 1998)**.

As part of its investigation of the postulated Millett fault, Bechtel (1982) collected seismic reflection data along the Savannah River. Nelson (1989) reprocessed and re-interpreted these data from Utley Point southeastward to about 1 mi northwest of Griffins Landing to evaluate whether the Pen Branch fault extends southwest across the Savannah River beneath the VEGP site (Figure 2.5.1-34). Nelson (1989) concluded that there is no evidence of faulting and concluded that if the Pen Branch fault does occur in the SRS area in South Carolina, its upward termination is below the limit of survey penetration at approximately 750 ft (beneath at least the upper part of the Late Cretaceous Tuscalloosa Formation).

As part of a groundwater contamination study in Burke County, Georgia, Henry (1995) collected and interpreted seismic reflection data from two lines located in the Savannah River between Hancock Landing and the VEGP boat ramp (Figure 2.5.1-34). Henry (1995) concluded that the Pen Branch fault appears as a high-angle, southeast-side-up reverse fault located approximately 1,000 ft downstream from Hancock Landing (Figure 2.5.1-34). Henry (1995) interpreted the Pen Branch fault as a growth fault extending upward through the Paleocene Black Mingo Formation and into Eocene strata that lie below the unconformity at the base of Savannah River alluvium.

A land-based seismic reflection survey was performed along an unimproved road about 0.5 mi west of River Road (about 1.5 mi west of VEGP Units 1 and 2) and included in a report by Summerour et al.(1998) (Figure 2.5.1-34). Similar to Henry (1995), this research was also part of a groundwater contamination study in Burke County, Georgia. The seismic line was roughly situated across the westward projection of the Pen Branch fault within the site area and southwest of the VEGP site. Numerous, minor faults belonging to the Pen Branch fault were interpreted to cut reflectors within the Coastal Plain section. The basement reflector, however, is not clearly faulted and, therefore, these data suggesting the location of the Pen Branch fault are questionable.

2.5.3.1.6 Current Seismic Reflection Studies

Seismic reflection and refraction data were collected on the VEGP site in January and February 2006 as part of this ESP study. The seismic array was designed to: (1) image the Pen Branch fault, with the assumption that it continues on strike to the southwest from the SRS into the VEGP site area, and (2) assess the depth and character of the basement rocks beneath the

Coastal Plain deposits. The survey included four seismic reflection and three seismic refraction lines (Figures 2.5.1-35 and 2.5.1-36, respectively). The results of this seismic reflection profiling clearly document that the Pen Branch fault is imaged in the basement beneath the VEGP site (see discussion in Section 2.5.1.2.4.2, and Figures 2.5.1-34 and 2.5.1-37). These data indicate that the Pen Branch fault strikes between N34ºE and N45ºE across the VEGP site, and dips 45º to the southeast.

2.5.3.1.7 Current Aerial and Field Reconnaissance

Field and aerial reconnaissance inspections reveal no evidence for surface rupture, surface warping, or the offset of geomorphic features indicative of active faulting. Likewise, interpretation of aerial and satellite photography and topographic maps reveals no evidence of geomorphic features indicative of potential for tectonic surface deformation (faulting or warping).

As part of the field reconnaissance performed for the ESP study, many of the features previously mapped within the site vicinity (25-mi radius) as evidence for possible tectonic activity have been observed [including those mapped by **(McDowell and Houser 1983)** and **(Bartholomew et al. 2002)**]. Based on field observations and similar characteristics to features studied in a large excavation at the VEGP site **(Bechtel 1984b)**, these features are assessed to be of non-tectonic origin. Even if the Bartholomew et al. (2002) "clastic dikes" are of tectonic origin, they interpret these features to be evidence for earthquakes that occurred during or prior to the late Miocene. "Clastic dikes" are discussed in detail in Section 2.5.3.8.2.2.

2.5.3.2 Geological Evidence, or Absence of Evidence, for Surface Deformation

As shown in Figure 2.5.1-21, four bedrock faults are mapped within 5 mi of the VEGP site **(Cumbest et al. 1998, 2000; Stieve and Stephenson 1995)**. These four faults are:

- Pen Branch fault
- Ellenton fault
- Steel Creek fault
- Upper Three Runs fault

These faults were first identified on the SRS based on the interpretation of seismic reflection, borehole, gravity and magnetic, and/or groundwater data **(Chapman and DiStefano 1989; Stieve et al. 1991; Stephenson and Stieve 1992; Snipes et al. 1993a; Domoracki 1994; Stieve and Stephenson 1995; and Cumbest et al. 1992, 1998, 2000)**. Each of these faults appears to terminate upward beneath the near surface. The youngest deposits deformed are Eocene in age. No deformation or geomorphic features indicative of potential Quaternary activity have been reported in the literature for these faults. Aerial and field reconnaissance and air photo interpretation performed for the current ESP study show that no geomorphic features

indicative of Quaternary activity exist along any of the mapped fault traces. These four faults are summarized in Table 2.5.3-1 and described below.

2.5.3.2.1 Pen Branch Fault

The more than 20-mi-long (more than 30-km-long) Pen Branch fault is the northwest bounding fault of the Mesozoic Dunbarton Basin, strikes northeast, traverses the central portion of the SRS, and trends southwestward into Georgia near the VEGP site **(Snipes et al. 1989, 1993a)**. Seismic reflection profiling performed as part of this ESP study has imaged the southeast-dipping Pen Branch fault beneath the VEGP site (see discussion in Section 2.5.1.2.4.2, Figure 2.5.1-40). The Pen Branch fault was reactivated in the Tertiary as an up-to-the-southeast reverse fault **(Snipes et al. 1993a)**, and possibly soles into the Augusta fault (described in Section 2.5.1.1.4.3) at depth **(Domoracki 1994; Stieve and Stephenson 1995)**.

The Pen Branch fault is not exposed or expressed at the surface **(Snipes et al. 1993a; Stieve and Stephenson 1995; Cumbest et al. 2000)**. Borehole and seismic reflection data collected from the SRS show no evidence for post-Eocene slip on the Pen Branch fault **(Cumbest et al. 2000)**. SRS studies have been specifically designed to assess the youngest deformed strata overlying the fault through shallow, high-resolution reflection profiles, drilling of boreholes, and geomorphic analyses and have consistently concluded that late Eocene is the youngest strata deformed as described in Section 2.5.1.2.4.1.

The Pen Branch fault is not expressed geomorphically, nor is microseismicity associated with this fault. Therefore, it is concluded that the Pen Branch fault is not a capable fault within the site area. Within a resolution of 7 to 10 ft (2 to 3 m), longitudinal profiles along Quaternary fluvial terraces overlying the surface projection of the Pen Branch fault show no evidence of warping or faulting of the 350 ka to 1 Ma Ellenton (Qte) fluvial terrace **(Geomatrix 1993)**.

Additional work performed for the ESP study has more accurately located the Pen Branch fault beneath a remnant of this terrace (Figure 2.5.1-43). The geomorphic evaluation of the Quaternary Ellenton terrace (Qte) surface overlying the Pen Branch fault is described in Section 2.5.1.2.4.3. The results of this study demonstrate a lack of tectonic deformation in the 350 ka to 1 Ma fluvial terrace surface within a resolution of about 3 ft. This observation is consistent with previous studies at both the VEGP site and the SRS that have concluded the Pen Branch fault is not a capable tectonic source.

2.5.3.2.2 Ellenton Fault

The Ellenton fault had been located in the southeastern portion of the SRS, about 4.6 mi from the VEGP site (Figure 2.5.1-21), but the Ellenton fault does not appear on the most recent SRS fault maps **(Cumbest et al. 1998, 2000)**. The approximately 4-mi-long Ellenton fault had been interpreted to strike north-northwest, with near vertical to steeply east dip and east-side-down

sense of slip **(Domoracki 1994; Stieve and Stephenson 1995)**. No clear relationship exists between the previously located Ellenton fault and regional structural features.

Because the data originally used to identify this fault are of poor quality according to Stieve and Stephenson (1995), the fault is not expressed geomorphically, and microseismicity is not associated with this fault; the current assessment is that this fault likely does not exist. Therefore, it is concluded that the Ellenton fault is not a capable tectonic source within the site area. Neither the Crone and Wheeler (2000) compilation of Quaternary faults and tectonic features in the central and eastern United States, nor the Wheeler (2005) compilation update, identifies the Ellenton fault as a potential Quaternary feature.

2.5.3.2.3 Steel Creek Fault

The Steel Creek fault is located in the northwest portion of the SRS, about 3 mi from the VEGP site **(Stieve and Stephenson 1995; Cumbest et al. 2000)** (Figures 2.5.1-21 and 2.5.1-23). This greater than 11-mi-long, northeast-trending, northwest-dipping, up-to-the-northwest reverse fault is located within the Dunbarton Basin and, along with the Pen Branch fault, forms a horst structure within the basin **(Stieve and Stephenson 1995)**. The Steel Creek fault extends upward into Cretaceous units, but the uppermost extent of faulting remains unresolved **(Stieve and Stephenson 1995)**.

Within a resolution of 7 to 10 ft (2 to 3 m), longitudinal profiles along Quaternary fluvial terraces overlying the surface projection of the Steel Creek fault show no evidence of warping or faulting of the fluvial terraces **(Geomatrix 1993)**. The Steel Creek fault is not expressed geomorphically, nor is microseismicity associated with this fault. Therefore, it is concluded that this fault is not a capable tectonic source within the site area. Neither the Crone and Wheeler (2000) compilation of Quaternary faults and tectonic features in the central and eastern United States, nor the Wheeler (2005) compilation update, identifies the Steel Creek fault as a potential Quaternary feature.

2.5.3.2.4 Upper Three Runs Fault

The Upper Three Runs fault is located in the northwest portion of the SRS, about 5 mi from the VEGP site **(Stieve and Stephenson 1995)** (Figure 2.5.1-21). The location of the Upper Three Runs fault is mapped based on potential field data and interpretation of seismic reflection profiles **(Stieve and Stephenson 1995)**. The Upper Three Runs fault has been interpreted as an older (initially Paleozoic) fault that soles into the Augusta fault at depth, possibly reactivated as a Mesozoic normal fault **(Cumbest and Price 1989b; Domoracki 1994; Stieve and Stephenson 1995)**. The Augusta fault is discussed in Section 2.5.1.1.4.3.

The greater than 20-mi-long, northeast-trending Upper Three Runs fault is restricted to basement rocks. Seismic reflection profiling shows that the Coastal Plain sediments are not offset or deformed by this fault **(Chapman and DiStefano 1989; Stieve and Stephenson**

1995). The Upper Three Runs fault is not expressed geomorphically, nor is microseismicity associated with this fault. Therefore, it is concluded that this fault is not a capable tectonic source within the site area. Neither the Crone and Wheeler (2000) compilation of Quaternary faults and tectonic features in the central and eastern United States, nor the Wheeler (2005) compilation update, identifies the Upper Three Runs fault as a potential Quaternary feature.

2.5.3.3 Correlation of Earthquakes With Capable Tectonic Sources

Seismicity within the VEGP site vicinity (25-mi radius) is shown in Figure 2.5.1-16. As shown on this figure, there is no spatial correlation of earthquake epicenters with known or postulated faults. No faults or geomorphic features within the site vicinity (25 mi radius) can be correlated with earthquakes. Based on review of existing literature, no reported historical earthquake epicenters have been associated with bedrock faults within a 25 mi radius of the VEGP site (Figure 2.5.1-16). None of these faults within 25 mi of the VEGP site are classified as capable tectonic sources.

In general, the South Carolina and Georgia portions of the Coastal Plain and Piedmont provinces exhibit a higher rate of seismicity than elsewhere in these provinces (Figure 2.5.1-18). This diffuse earthquake activity is not concentrated or aligned with any mapped faults, nor is it associated with any known tectonic structures. Figure 2.5.1-16 shows that no earthquakes of magnitude 3.0 or larger are known to have occurred within 25 mi of the site. However, several small events (m_b<3.0) have occurred within the site vicinity.

The SRS seismic recording network, which consists of nine instruments located within and adjacent to the SRS, has been recording microseismicity in the VEGP site vicinity since it was installed in 1976. This local network recorded three small earthquakes (in 1985 [magnitude 2.6], 1988 [magnitude 2.0], and 1997 [magnitude 2.5]) and a small earthquake sequence in 2001–2002 within the boundaries of the SRS **(Stevenson and Talwani 2004)**. These small SRS earthquakes, and also a 1993 event located north of the SRS in Aiken, have been studied in an effort to evaluate possible correlations with tectonic features (Figure 2.5.1-16).

The June 9, 1985, earthquake of local duration magnitude (M_D) 2.6 was located about 5 mi north of the northwest margin of the Dunbarton Basin (Figure 2.5.1-16). The depth of this event was initially determined to be approximately 0.6 mi (1 km) **(Talwani et al. 1985)**, and was later listed at a depth of 3.5 mi (5.8 km) **(Stevenson and Talwani 2004)**. This earthquake had a focal plane solution that suggests either a sinistral component of slip on a northeast-striking plane or a dextral component of slip on a northwest-striking plane **(Talwani et al. 1985)**. The close location of the event to the northwest margin of the Dunbarton Basin and northeast strike of the sinistral nodal plane led Talwani et al. (1985) to associate this event with the northeast-striking basin border fault (later named the Pen Branch fault). However, Crone and Wheeler (2000) point out that the sinistral sense of slip from the fault plane solution is inconsistent for the

Pen Branch fault given the northeast-southwest orientation of principal horizontal stress. Therefore, it is highly unlikely that this event is associated with the Pen Branch fault.

The August 5, 1988, earthquake of magnitude 2.0 was centered southeast of the Pen Branch fault within the Dunbarton Basin (Figure 2.5.1-16*)*. The hypocenter of this event was located at a depth of about 1.5 mi (2.5 km) **(Stevenson and Talwani 2004)** and no focal mechanism solution could be obtained **(Domoracki et al. 1999)**. Domoracki et al. (1999) suggested that this earthquake was associated with the Pen Branch fault. However, Stevenson and Talwani's (2004) more recent hypocenter location for this event suggests no spatial association with a known fault.

The August 8, 1993, Aiken, South Carolina, earthquake with a body wave magnitude estimated from Rayleigh surface waves (m_{blg}) of 3.2 was studied in detail by Stevenson and Talwani (1996), who determined that the event was located within a steep gravity gradient that they interpret to be the edge of a granitic pluton (Figure 2.5.1-16*)*. The hypocenter of this event was located at a depth of about 6 mi (about 10 km) **(Stevenson and Talwani 2004)**. The event is not spatially associated with a known fault.

The May 17, 1997, earthquake of magnitude 2.5 was located about 0.5 to 1 mi northwest of the Pen Branch fault (Figure 2.5.1-16). Given that this event had a depth of about 3 mi (5 km) **(Stevenson and Talwani 2004)**, it is located in excess of 3 mi from the southeast-dipping Pen Branch fault.

The most recent activity, termed the Upper Three Runs earthquake sequence, included an October 8, 2001, main event of m_{blg} 2.6 centered near Upper Three Runs Creek and a series of seven very small aftershocks occurring through March 6, 2002, in a small area of 6.0 to 6.5 square km **(Stevenson and Talwani 2004)** (Figure 2.5.1-16). All events within this earthquake sequence occurred within depths of approximately 1.8 to 3 mi (3 to 5 km), with a positional uncertainty of about 1600 ft (about 500 m) due to the proximity of the local SRS seismic stations. Single event and composite focal mechanisms indicate a predominantly reverse motion on a fault plane oriented N25ºW, 41ºSW. A 3-D plot of hypocenters defined a fault plane of similar orientation **(Stevenson and Talwani 2004)**.

Stevenson and Talwani (2004) examined gravity data and found a northeast-trending grain to the Bouguer gravity map. Upon further processing to derive a map of the first horizontal derivative of gravity, they defined a small local northwest-trending ridge of gravity that they interpreted as the causative structure. The shallowness and small areal extent of the Upper Three Runs earthquake sequence, combined with the apparent association of a very small basement feature running counter to the regional structural trend, suggest that this earthquake activity is extremely localized and is not attributable to any regional features **(Stevenson and Talwani 2004**).

2.5.3.4 Ages of Most Recent Deformations

As presented in Section 2.5.3.2, none of the four faults within 5 mi of the VEGP site exhibit evidence of Quaternary activity. The Pen Branch fault represents the northern bounding normal fault of the Mesozoic Dunbarton Basin, and this structure was reactivated as a Tertiary oblique-reverse fault. Borehole and seismic data provide no evidence for post-Eocene slip on the Pen Branch fault **(Cumbest et al. 2000)**. Geomatrix (1993) concluded that the Pen Branch fault does not deform Quaternary fluvial terraces of the Savannah River within a resolution of 7 to 10 ft (2 to 3 m). The geomorphic evaluation of this same 350 ka to 1 Ma fluvial terrace surface performed as part of this ESP study demonstrates a lack of tectonic deformation within a resolution of about 3 ft (about 1 m) (described in Section 2.5.1.2.4.3).

The Ellenton fault was previously interpreted as a north-northeast-striking fault **(Stieve and Stephenson 1995)**, but it does not appear in the most recent maps of subsurface SRS faults **(Cumbest et al. 1998, 2000)** and likely does not exist.

The Steel Creek fault extends upward into Cretaceous units, but the uppermost extent of faulting remains unresolved **(Stieve and Stephenson 1995)**. Geomatrix (1993) concluded that the Steel Creek fault does not deform Quaternary fluvial terraces of the Savannah River within a resolution of 7 to 10 ft (2 to 3 m).

The Upper Three Runs fault is restricted to basement rocks. Seismic reflection profiling revealed no evidence for this fault deforming overlying Coastal Plain sediments **(Chapman and DiStefano 1989; Stieve and Stephenson 1995)**.

2.5.3.5 Relationships of Tectonic Structures in the Site Area to Regional Tectonic Structures

The four faults identified within the site area (i.e., the Pen Branch, Ellenton, Steel Creek, and Upper Three Runs faults) are located on the SRS. Only one of these faults (the Pen Branch) is observed west of the Savannah River in Georgia. As described in Section 2.5.3.6, none of the four faults within the site area is considered a capable tectonic feature.

2.5.3.5.1 Pen Branch Fault

The Pen Branch fault likely is the northern boundary fault of the Mesozoic Dunbarton Basin. During the Mesozoic, the fault accommodated crustal extension and thinning with a southeast-side-down normal sense of slip **(Snipes et al. 1993a; Domoracki 1994; Stieve and Stephenson 1995)**. Snipes et al. (1993) suggested that the southeastern margin of the Dunbarton Basin may also be bounded by a fault (the Martin fault), although Domoracki et al. (1999) suggested that the Dunbarton Basin is instead a half-graben bounded only by the Pen Branch fault to the north.

The Pen Branch fault was reactivated as a reverse or reverse-oblique fault during Cretaceous and into Tertiary time, with an up-to-the-southeast sense of slip **(Stephenson and Chapman**

1988; Snipes et al. 1993a; Cumbest et al. 2000). Stephenson and Stieve (1992) and Stieve and Stephenson (1995) suggested that the Pen Branch fault may sole into the shallow dipping Augusta fault (described in Section 2.5.1.1.4.3) or a Paleozoic/Mesozoic regional decollement at depth (Figure 2.5.1-2).

2.5.3.5.2 Ellenton Fault

The Ellenton fault as mapped by Stieve and Stephenson (1995) is a north-northwest striking fault located within the Dunbarton Basin between the Upper Three Runs and Pen Branch faults. The Ellenton fault orientation is roughly normal to the regional structural grain and to the other SRS faults and bears no clear relationship to regional structures. The Ellenton fault does not appear on the most recent SRS fault maps **(Cumbest et al. 1998, 2000)** and likely does not exist.

2.5.3.5.3 Steel Creek Fault

This northeast-trending Steel Creek fault is roughly parallel to the regional structural grain and is located within the Dunbarton Basin. The Steel Creek fault is an up-to-the-northwest, secondary structure associated with the Pen Branch fault, with which it forms a horst structure within the basin **(Stieve and Stephenson 1995)**.

2.5.3.5.4 Upper Three Runs Fault

The northeast-trending Upper Three Runs fault is roughly parallel to the regional structural grain and is restricted to basement rocks; seismic reflection profiles show that the fault does not offset Coastal Plain sediments **(Chapman and DiStefano 1989; Stieve and Stephenson 1995)**. The Upper Three Runs fault has been interpreted as an older (initially Paleozoic) fault, possibly reactivated as a Mesozoic normal fault **(Cumbest and Price 1989b; Domoracki, 1994; Stieve and Stephenson 1995)**. The Upper Three Runs fault possibly soles into the Augusta fault (described in Section 2.5.1.1.4.3) or a Paleozoic/Mesozoic regional decollement at depth **(Stieve and Stephenson 1995)** (Figure 2.5.1-2).

2.5.3.6 Characterization of Capable Tectonic Sources

Based on studies evaluated in the preceding sections, SNC concluded that there are no capable tectonic sources within 5 mi of the VEGP site. The Pen Branch fault, the nearest fault to the VEGP site, has undergone extensive study and multiple reviews by the NRC. All of these studies, including investigations as part of this ESP study, support the non-capable status of the Pen Branch fault as outlined below:

- NUREG-1137-8 concludes that the Pen Branch fault is not a capable fault and does not represent a hazard to the VEGP site. Similarly, other NRC reviews of the Pen Branch fault

for facilities such as the Mixed Oxide Fuel (MOX) Fabrication Facility at SRS have also concluded that the Pen Branch fault is not a capable fault (NURERG-1821).

- The "association clause" of Appendix A 10 CFR 100.23 applies to this discussion as follows: Cumbest et al. (2000) noted that the Pen Branch fault shares characteristics with other Atlantic Coastal Plain faults that are considered non-capable. These characteristics include northeast-southwest strikes, small total offsets of Cenozoic strata in relation to fault age, slip histories that began in the Cretaceous, and offsets that decrease with decreasing age. Cumbest et al. (2000) argued that the abundance of shared characteristics between these faults implies that these faults are genetically related. Several of these faults have been shown to be non-capable. Therefore, Cumbest et al. (2000) concluded that the Pen Branch fault is likely non-capable as well.

- The Pen Branch fault is not exposed or expressed at the surface **(Snipes et al. 1993a; Stieve and Stephenson 1995; Cumbest et al. 2000)**. Reconnaissance work and aerial photograph interpretation performed for the ESP study confirm that there is no exposure of the fault or geomorphic expression of potential Quaternary activity.

- Snipes et al. (1993) investigated a 10- to 20-ft-thick (3- to 6-m-thick) Quaternary light tan soil horizon in railroad cuts overlying the projected trend of the Pen Branch fault at the SRS. They observed no detectable offset of this unit. According to Snipes et al. (1993), the youngest horizon known from borehole studies to be faulted is the top of the Dry Branch Formation of Late Eocene age.

- Regional principal stress orientations based on stress-induced wellbore breakouts and hydraulically induced fracturing show that the maximum horizontal stress is parallel to the regional orientation of the Pen Branch fault, which makes "strike-slip faulting unlikely" and "reverse faulting essentially impossible" **(Moos and Zoback 2001)**. The most-recent deformation observed for this fault in Tertiary sediments is reverse faulting.

- Geomatrix (1993) evaluated longitudinal profiles along Quaternary fluvial terraces of the Savannah River and concluded that no evidence of terrace surface warping or faulting exists within a resolution of 7 to 10 ft (2 to 3 m). Additionally, as part of the ESP study, local longitudinal terrace profiles across the now well-located Pen Branch fault support the earlier conclusion that no deformation is observed in the terrace remnant of the Ellenton terrace (estimated as 350 ka to 1 Ma) overlying the Pen Branch fault.

- As part of this ESP study, geomorphic analysis of the 350 ka to 1 Ma fluvial terrace overlying the surface projection of the Pen Branch fault at the SRS demonstrates the lack of tectonic deformation of this Quaternary geomorphic surface within a resolution of about 3 ft.

The resolution of this study compared with the previous studies makes it by far the most definitive evidence for the non-capability of the Pen Branch fault both at the Savannah River Site and the VEGP site. Results are described in more detail in Section 2.5.1.2.4.3.

2.5.3.7 Designation of Zones of Quaternary Deformation Requiring Detailed Fault Investigation

No zones of quaternary deformation require detailed investigation within the site area.

2.5.3.8 Potential for Tectonic or Non-Tectonic Deformation at the Site

The potential for tectonic deformation at the site is negligible. There is, however, the evidence for past, and the potential for future, non-tectonic deformation at the site in the form of dissolution-induced collapse features. These conclusions are discussed in the following sections.

2.5.3.8.1 Potential for Tectonic Deformation at the Site

The potential for tectonic deformation at the site is negligible. The presence of the Pen Branch fault adjacent to the VEGP Units 3 and 4 footprint and beneath the monocline in the Blue Bluff Marl (Figures 2.5.1-39 and 2.5.1-42) suggests that past deformation of the Eocene strata has occurred in the form of non-brittle folding. However, this type of deformation associated with the non-capable Pen Branch fault is no longer active and will not impact the ground surface in the future. Since the original site studies in the early 1970s, no new information has been reported to suggest the existence of any Quaternary surface faults or capable tectonic sources within the site area.

2.5.3.8.2 Potential for Non-Tectonic Deformation at the Site

Several non-tectonic features are present in the site area. These include dissolution-induced collapse structures and clastic dikes. As described below, permanent ground deformation at the site may be produced by dissolution within the Utley Limestone, whereas clastic dikes are not potential sources of permanent ground deformation. Dissolution-related permanent ground deformation would be mitigated at the site by the excavation and removal of the Utley Limestone during construction of the site.

Clastic dikes have been reported at the site and in the site vicinity **(Siple 1967; Alterman 1984; Bechtel 1984b; Bartholomew et al. 2002)**. The origin of these features has been subject to considerable debate, but those on-site features described as “clastic dikes” likely were formed by soil weathering processes, as described in Section 2.5.3.8.2.2. NUREG-1137 concludes that no evidence exists that these features represent a safety issue for the plant, whatever their origin.

2.5.3.8.2.1 Dissolution Collapse Features

The potential for non-tectonic deformation at the site resulting from near-surface dissolution-induced collapse has long been recognized as a possibility and has been the subject of several studies e.g., **(Bechtel 1981, 1984b)**. Bechtel (1984b) identified the presence of a variety of small-scale deformation structures in the walls of a garbage trench on the VEGP site within Tertiary Coastal Plain sediments (Figure 2.5.1-34). These structural features, including warped bedding, fractures, joints, minor offsets, and injected sand dikes, were interpreted as local phenomena related to dissolution of the underlying Utley Limestone and resultant plastic and brittle collapse of overlying Tertiary sediments **(Bechtel 1984b)** (Figures 2.5.3-1 and 2.5.3-2).

The dissolution origin for the warped bedding, fractures, small-scale faults, “clastic dikes,” and sand-injected dikes is interpreted largely from the observations and detailed documentation of these features in a large trench exposure that was over 900 ft long, 30 to 45 ft deep, and 25 to 40 ft across **(Bechtel 1984b)**. The high concentration of these features within the trench and the spatial and kinematic relationships between different types of deformation features provide some of the best information regarding their origin. Field mapping efforts performed as part of the VEGP ESP application also identified “clastic dikes” within the VEGP site and surrounding site area, and similarly concluded these features are of a non-tectonic origin based on field observations.

The three-dimensional nature of the warped bedding, combined with the spatial and kinematic relationships of the small-scale faults and fractures along the margins of the more strongly warped depressions, clearly demonstrates a dissolution or sediment collapse origin. The highly irregular, discontinuous nature of folding is consistent with a non-tectonic dissolution origin and inconsistent with a tectonic origin, since there are no laterally persistent fold axes. For example, the upper contact of Unit F, a 1-to-2-ft-thick, moderately consolidated, laminated, red and yellow, silty fine sand, is folded into a highly irregular surface **(Bechtel 1984b)** (Figure 2.5.3-3). If this minor fold deformation was associated with the underlying Pen Branch fault, fold axes should be laterally persistent and parallel to the fault. The discontinuous nature of domes and depressions in an “egg carton” or “dimpled” pattern reflects the more random, non-tectonic process of dissolution (Figure 2.5.3-3).

Most of the small-scale faults have normal displacement toward or into the depressions, and a few exhibit minor reverse slip near the crests of some arches **(Bechtel 1984b)**. These features are of limited dimensions and cannot be traced laterally across the width of the trench. The orientations of fractures and small faults are locally consistent with the limbs of the individual arches and depressions, but vary strongly from fold to fold. In some cases, such as shown in Figure 2.5.3-2, the small faults actually arc over the centers of some of the depressions. These field relationships all support an origin related to very localized settlement of the depressions resulting from dissolution and collapse of underlying strata.

The age of these dissolution features is poorly constrained; however, they are younger than the Eocene and Miocene host sediment and older than the overlying late Pleistocene or eolian sand of the Pinehurst Formation **(Bechtel 1984b)**. No late Pleistocene or Holocene dissolution features have been identified at the site.

Anecdotal accounts provide additional evidence for the potential for dissolution-induced collapse at the site. The presence of a cave located near Mathes Pond, currently under water, and accounts of "soft zones" encountered in boreholes above the Blue Bluff Marl suggest the possibility of dissolution at the VEGP site.

Dissolution-induced collapse structures are not tectonic features, nor do they indicate regionally significant seismicity **(Bechtel 1984b)**. NUREG-1137 concludes that no evidence exists that these features represent a safety issue for the plant. Dissolution collapse, however, represents a potential minor, non-tectonic surface deformation hazard in areas underlain by the Utley Limestone at the site. This hazard could be mitigated during construction through excavation and removal of the Utley Limestone to establish the foundation grade of the plant.

Not all depressions in the VEGP site area are the result of dissolution collapse. Carolina bays are non-tectonic, surficial geomorphic depressions that may resemble surface expression of dissolution collapse features. Carolina bays are commonly found throughout the VEGP site area and discussed in greater detail in Section 2.5.1.1.1. Unlike Carolina bays, surface depressions resulting from dissolution collapse are irregularly shaped and randomly oriented.

Pre-construction topographic maps of the VEGP site show several closed depressions at the site. Site reconnaissance performed for the ESP study shows that these depressions no longer exist and that they were likely destroyed by site excavations and activities. No present-day surface depressions were identified at the VEGP site as part of the ESP study.

2.5.3.8.2.2 Clastic Dikes

Clastic dikes are relatively planar, clay-filled features that typically flare out upward and are on the order of centimeters-to-decimeters wide and decimeters-to-meters long. Clastic dikes are widespread in the Coastal Plain of Georgia and South Carolina in the upper Miocene Barnwell and Hawthorne Formations. Despite the widespread occurrence of clastic dikes, however, their origin or origins are poorly understood. They have been variously attributed to seismic shaking or tectonic activity, to solution of underlying carbonate horizons and sediment collapse, and to weathering and soil-forming hypotheses [e.g., **(Siple 1967; Bechtel 1984b; Bartholomew et al. 2002)**].

Clastic dikes on the VEGP site, in the site area, and on the SRS were described in detail by Alterman (1984), who noted feature dimensions, composition, grain size, and color, but did not propose a favored formation mechanism.

In describing clastic dikes exposed in the walls of a garbage trench more than 900 ft long located on the VEGP site, Bechtel (1984) differentiated two distinct classes of dikes: (1) "sand dikes" that resulted from plastic or liquid injection of loosely consolidated fine sand into overlying, fractured, relatively consolidated sediment, and (2) "clastic dikes" that resulted primarily from weathering and soil-forming processes preferentially enhanced along pre-existing fractures that formed during dissolution collapse. According to Bechtel (1984), the present geographic distribution of clastic dikes is controlled by the depth of weathering and paleosol development in the Coastal Plain sediments and by subsequent erosion of the land surface. Bechtel (1984) concluded that the dikes are primarily a weathering phenomenon that formed at least 10 ka to 100 ka. As part of the field reconnaissance performed for the ESP study, abundant "clastic dikes" have been observed in the site area that have characteristics consistent with a pedogenic or weathering origin, but no features were observed that can reasonably be interpreted to have formed as a result of injected sand. The field reconnaissance of "clastic dikes" exhibited the following primary characteristics, which were summarized by the Bechtel (1984) study of these features within a large trench exposure on the VEGP site:

1. The dikes are widely distributed through the region in deeply weathered clayey and silty sands of the Eocene Hawthorne and Barnwell Formations.
2. The dikes occur in nearly all exposures of the weathered profile but are rare in exposures of stratigraphically lower, less weathered sediment.
3. The dikes contain a central zone of bleached host rock bounded by a cemented zone of iron oxide. Some dikes contain a clay core.
4. Grain size analyses on samples indicate that the dike interval contains the same grain distribution as the host sediment with slightly more silt and clay (excluding clay core).
5. The dikes and associated mottling decrease downward in density and size. In most cases, the dikes taper downward and pinch out over a 5-to-15-ft distance.

NUREG-1137 concluded that no evidence exists that the clastic dikes represent a safety issue for the VEGP site. The SER suggests that the clastic dikes on the VEGP site may be non-tectonic, soft-sediment deformation features that formed 20 to 25 Ma.

In contrast to non-tectonic "clastic dikes," Bartholomew et al. (2002) interpreted sand dike features found in the upper Eocene Tobacco Road Sand near Hancock Landing, Georgia, less than five mi north of the VEGP site, as evidence for strong paleoearthquakes probably associated with late Eocene to late Miocene earthquake activity possibly associated with the Pen Branch and/or Crackerneck faults. Bartholomew et al. (2002) describe sand dikes that cut across poorly bedded clay-rich strata and are filled with massive, medium to coarse sand.

However, the sand dikes identified by Bartholomew et al. (2002) are syndepositional due to the presence of marine animal burrows that cross cut the dikes. The formation of these dikes

occurred during the late Eocene while the sediments were in a subaqueous marine environment **(Bartholomew et al. 2002)**. Whether these dikes of Bartholomew et al. (2002) formed as a result of seismic shaking or some other process related to soft sediment deformation (e.g., compaction and de-watering), these features are significantly older than Quaternary and, therefore, do not reflect geologically recent seismic activity.

Table 2.5.3-1 Summary of Bedrock Faults Mapped Within the 5-Mile VEGP Site Radius

Fault Name	Proximity to VEGP Site (mi)	Length (mi/km)	Orientation	Sense of Slip	Relationship to Dunbarton Basin	Evidence for Non-Capability
Pen Branch	On site	>20/>30	NE	SE up, reverse	NW border (normal) fault, reactivated as reverse	a, b, c, d
Ellenton	~4	~4/~6.5	NNW	E down, unknown	Unknown; located NW of basin	b, c, e
Steel Creek	~2	>11/>18	NNE	NW up, reverse	Secondary structure forming horst with Pen Branch	b, c, d
Upper Three Runs	~5	>20/>30	NE-NNE	Unknown	Unknown; located NW of basin	b, c, f

Note: Fault locations based on Cumbest et al. (1998), Stieve and Stephenson (1995), and work performed as part of this ESP study

[a]Seismic reflection and borehole data show lack of post-Eocene slip (NUREG-1137-8; **Cumbest et al. 2000**)

[b]Lack of geomorphic expression

[c]Lack of seismicity associated with fault

[d]Quaternary fluvial terraces of Savannah River overlying projection of fault appear undeformed **(Geomatrix 1993)**

[e]Fault does not appear in most recent SRS fault maps **(Cumbest et al. 1998, 2000)**

[f]No disruption to base of Coastal Plain section (pre-Cretaceous age) **(Stieve and Stephenson 1995)**

Source: Bechtel 1984b

Figure 2.5.3-1 Contorted Bedding in Garbage Trench at VEGP Site

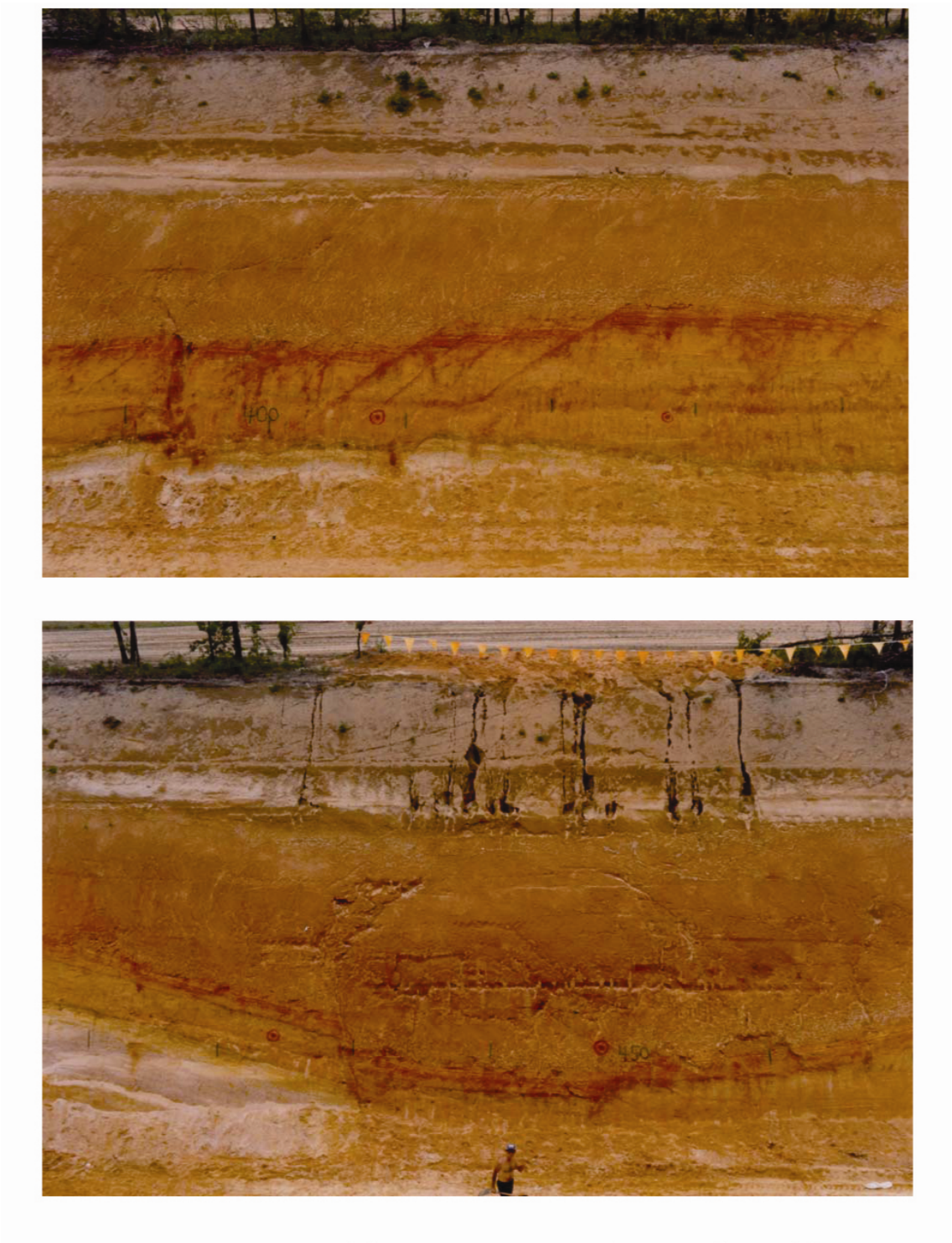

Source: Bechtel 1984b

Figure 2.5.3-2 West Wall of Garbage Trench Showing Small Offsets (1–24 inches) (Upper) and Arcuate Fractures and Clastic Dikes Over Center of Depression (Lower)

This page is intentionally blank.

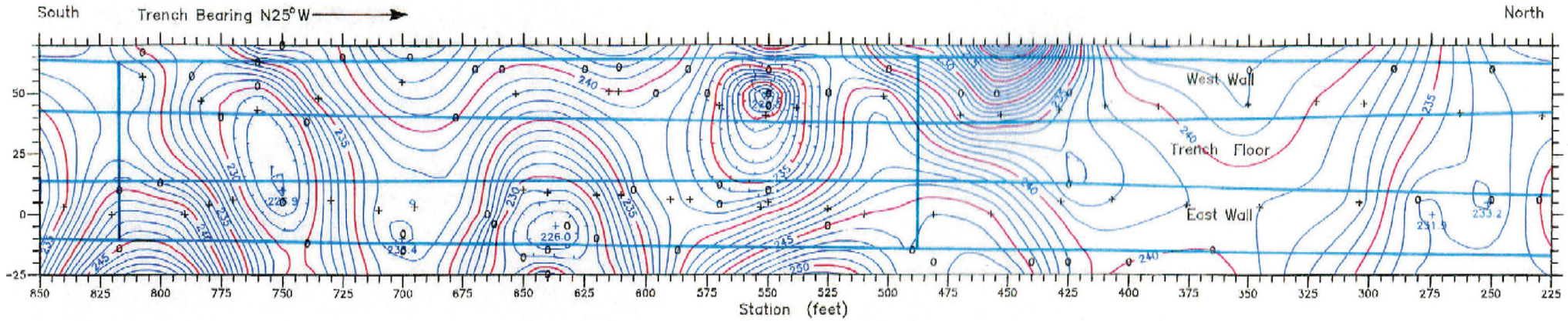

Modified from Figure 5 of Bechtel (1984b)

Figure 2.5.3-3. Surface Geometry of Unit F Illustrating Localized Nature of Deformation

This page is intentionally blank.

Section 2.5.3 References

(Alterman 1984) Alterman, I., Summary of visit to examine clastic dikes near Vogtle, June 21–22, 1984, US Nuclear Regulatory Commission docket nos. 50-424 and 50- 425, 26 pp., 1984.

(Bartholomew et al. 2002) Bartholomew, M.J., Brodie, B.M., Willoughby, R.H., Lewis, S.E., and Syms, F.H., Mid-Tertiary paleoseismites: syndepositional features and section restoration used to indicate paleoseismicity, Atlantic coastal plain, South Carolina and Georgia, Geological Society of America Special Paper 359, pp. 63–74, 2002.

(Bechtel 1974a) Crane, D., Report of marl investigation – Alvin W. Vogtle nuclear plant, Bechtel Power Corporation – Geotechnical Services,11 pp. + attachments, 1974.

(Bechtel 1974b) Bechtel Power Corporation, Report on foundation investigations for Alvin W. Vogtle nuclear power plant, v. 1 and 2, prepared for Southern Services, Inc., and Georgia Power Company, file no. 25144-006-T14-CY06-00006, 1974.

(Bechtel 1978e) Bechtel Incorporated, Report on stratigraphic irregularities exposed in the auxiliary building excavation – Alvin W. Vogtle nuclear power plant, prepared for Southern Services, Inc., and Georgia Power Company, 12 pp., 1978.

(Bechtel 1981) Bechtel Power Corporation, Report on joints in marl near cooling tower 2A, 10 pp., 1981.

(Bechtel 1982) Bechtel Power Corporation, Studies of postulated Millett fault – Vogtle electric generating power plant, prepared for Georgia Power Company, 1982.

(Bechtel 1984b) Bechtel Power Corporation – Geology Group, Geologic evaluation of trench exposure – Vogtle electric generating plant, 43 pp., 1984.

(Bechtel 1989) Bechtel, Field review of geologic conditions near the Vogtle site relative to possible extension of the postulated “Pen Branch fault” into Georgia, report prepared for Georgia Power Company, September 1989.

(Chapman and DiStefano 1989) Chapman, W.L. and DiStefano, M.P., Savannah River plant seismic survey, 1987–1988, Conoco Inc. Research Report 1809-005-006-1-89, 121 pp., 1989.

(Crone and Wheeler 2000) Crone, A.J. and Wheeler, R.L., Data for Quaternary faults, liquefaction features, and possible tectonic features in the Central and Eastern United States, east of the Rocky Mountain front, US Geological Survey Open-File Report 00-260, 2000.

(Cumbest et al. 1992) Cumbest, R.J., Price, V. and Anderson, E.E., Gravity and magnetic modeling of the Dunbarton Basin, South Carolina: Southeastern Geology, v. 33, no. 1, p. 37-51, 1992.

(Cumbest and Price 1989b) Cumbest, R.J. and Price, V., Continued extension of the Dunbarton basin: an explanation for faulting in the coastal plain of South Carolina, Westinghouse Savannah River Company Report WSRC-RP-89-1263, 1989.

(Cumbest et al. 1998) Cumbest, R.J., Stephenson, D.E., Wyatt, D.E., and Maryak, M., Basement surface faulting and topography for Savannah River site and vicinity, Westinghouse Savannah River Company Technical Report 98-00346, 45 pp., 1998.

(Cumbest et al. 2000) Cumbest, R.J., Wyatt, D.E., Stephenson, D.E., and Maryak, M., Comparison of Cenozoic faulting at the Savannah River site to fault characteristics of the Atlantic Coast fault province: implications for fault capability, Westinghouse Savannah River Company Technical Report 2000-00310, 51 pp., 2000.

(Domoracki 1994) Domoracki, W.J., A geophysical investigation of geologic structure and regional tectonic setting at the Savannah River site, South Carolina, excerpts from a doctoral dissertation in preparation at Virginia Polytechnic Institute, technical report prepared for Westinghouse Savannah River Company, WSRC-TR-94-0317, 173 pp., 1994.

(Domoracki et al. 1999) Domoracki, W.J., Stephenson, D.E., Coruh, C., and Costain, J., Seismotectonic structures along the Savannah River Corridor, South Carolina, U.S.A.: Journal of Geodynamics, v. 27, p. 97-118, 1999.

(EPRI 1986a) Electric Power Research Institute (EPRI), Volumes 5–10, Seismic hazard methodology for the Central and Eastern United States, Tectonic Interpretations, July 1986.

(Geomatrix 1993) Geomatrix Consultants, Inc., Preliminary Quaternary and neotectonic studies, Savannah River site, South Carolina, prepared for Lawrence Livermore National Laboratory and Westinghouse Savannah River Company, 1993.

(Henry 1995) Henry, V.J., Summary of results of a seismic survey of the Savannah River adjacent to the Savannah River plant site, Burke County, Georgia, Georgia Geologic survey project report 24, 22 pp., 1995.

(McDowell and Houser 1983) McDowell, R.C. and Houser, B.B., Map showing distribution of small-scale deformation structures in part of the upper coastal plain of South Carolina and adjacent Georgia, US Geological Survey, misc. field studies map MF-1538, 1:250,000 scale, 1983.

(Moos and Zoback 2001) Moos, D. and Zoback, M.D., In situ stress measurements in the NPR Hole, Volume I – results and interpretations: Final Report submitted to Westinghouse Savannah River Company, WSRC-TR-2001-00499, DOE Contract No. DE-AC09-96SR18500, 41 p., 2001.

(Nelson 1989) Nelson, J.S., A review of seismic reflection data – postulated Pen Branch fault area, Savannah River project, report prepared for Bechtel Civil and Minerals, 8 pp. + attachments, 1989.

(Prowell 1994a) Prowell, D.C., Preliminary geologic map of the Barnwell 30' x 60' quadrangle, South Carolina and Georgia, US Geological Survey Open-File Report 94-673, 1:100,000 scale, 1994.

(Prowell 1996) Prowell, D.C., Geologic map of the Savannah River site, Aiken, Allendale, and Barnwell Counties, South Carolina, US Geological Survey, misc. field studies map MF-2300, 1996.

(Siple 1967) Siple, G.E., Geology and groundwater on the Savannah River plant and vicinity, US Geological Survey Professional Paper 1841, pp. 9–13, 1967.

(Snipes et al. 1989) Snipes, D.S., Fallaw, W.C., and Price Jr., V., The Pen Branch fault; documentation of late Cretaceous-Tertiary faulting in the coastal plain of South Carolina, unpub. Draft manuscript, 31 pp. + attachments, 1989.

(Snipes et al. 1993a) Snipes, D.S., Fallaw, W.C., Price Jr., V., and Cumbest, R.J., The Pen Branch fault; documentation of late Cretaceous-Tertiary faulting in the coastal plain of South Carolina, Southeastern Geology, v. 33, no. 4, pp. 195–218, 1993.

(Stephenson and Chapman 1988) Stephenson,D.S. and Chapman, W.L., Structure associated with the buried Dunbarton basin, South Carolina from recent seismic data: Geological Society of America – Abstracts with Programs, v. 20, p. 318, 1988.

(Stephenson and Stieve 1992) Stephenson, D.E. and Stieve, A., Structural model of the basement in the central Savannah River area, South Carolina and Georgia, Westinghouse Savannah River Company Technical Report 92-120, 1992.

(Stevenson and Talwani 1996) Stevenson, D.A., and Talwani, P., Aiken earthquake of August, 1993, Seismological Research Letters, v. 67, pp. 43-50, 1996.

(Stevenson and Talwani 2004) Stevenson, D. and Talwani, P., 2001–2002 Upper Three Runs sequence of earthquakes at the Savannah River site, South Carolina, Seismological Research Letters, v. 75, pp. 107–116, 2004.

(Stieve and Stephenson 1995) Stieve, A. and Stephenson, D.E., Geophysical evidence for post late Cretaceous reactivation of basement structures in the central Savannah River area, Southeastern Geology, v. 35, no. 1, pp. 1–20, 1995.

(Stieve et al. 1991) Stieve, A., Stephenson, D.E., and Aadland, R.K., Pen Branch fault program: consolidated report on the seismic reflection surveys and the shallow drilling (U), Westinghouse Savannah River Company Technical Report WSRC-TR-91-87, 48 pp., 1991.

(Summerour et al. 1998) Summerour, J. H., Shapiro, E. A., and Huddlestun, P. F., An investigation of Tritium in the Gordon and other aquifers in Burke County, Georgia – Phase II: Georgia Department of Natural Resources, Georgia Geologic Survey information circular 102, 12 p., 1998.

(Talwani et al. 1985) Talwani, P., Rawlins, J., and Stephenson, D.E., The Savannah River plant, South Carolina earthquake of June 09, 1985 and its tectonic setting, Earthquake Notes, v. 56, pp. 101–106, 1985.

(Wheeler 2005) Wheeler, R.L., Known or suggested Quaternary tectonic faulting, central and eastern United States- new and updated assessments for 2005, US Geological Survey Open-File Report 2005-1336, 37 pp., 2005.

2.5.4 Stability of Subsurface Materials and Foundations

This section presents information on the stability of subsurface materials and foundations at the VEGP site that may affect the proposed new unit's seismic Category 1 facilities. This geological, geophysical, geotechnical, and seismological information is developed and used as a basis to evaluate the stability of subsurface materials and foundations at the site.

Information presented in this section was developed from onsite geotechnical and geophysical investigations, a review of analysis and reports prepared for the existing VEGP units, and a review of geotechnical literature. Site specific reports prepared by Bechtel Power Corporation were included in this review; these reports addressed foundation investigation **(Bechtel 1974b)**, backfill material investigations **(Bechtel 1978a, 1978b and 1979)**, dynamic properties of the backfill **(Bechtel 1978c)**, and the test fill program **(Bechtel 1978d)**.

The ESP geotechnical field and laboratory investigation performed for the application was intended to enhance the understanding of the VEGP site and complement the existing geotechnical data developed for VEGP Units 1 and 2. The ESP geotechnical investigation data report was finalized in February 2006 and is included as Appendix 2.5A. The ESP seismic reflection/refraction data report was finalized in February 2006 and is included as Appendix 2.5B. Additional structure-specific exploration and testing will be performed at the COL phase.

2.5.4.1 Geologic Features

Section 2.5.1.1 describes the regional geology, including regional physiography and geomorphology, regional geologic history, regional stratigraphy, and the regional tectonic setting. Section 2.5.1.2 addresses site-specific geology and structural geology, including site physiography and geomorphology, site geologic history, site stratigraphy, site structural geology, and a site geologic hazard evaluation.

2.5.4.2 Properties of Subsurface Materials

2.5.4.2.1 Introduction

This section describes the static and dynamic engineering properties of the VEGP site subsurface materials. An overview of the subsurface profile and materials is given in Section 2.5.4.2.2. The field investigations, described in Section 2.5.4.3, are summarized in Section 2.5.4.2.3. The soils encountered during the ESP subsurface investigation constitute alluvial and Coastal Plain deposits and can be placed in three groups for stability of subsurface materials and foundation purposes (i.e., for geotechnical purposes). These soils include, from top to

bottom, sands with silt and clay (Group 1), clay marl (Group 2), and coarse-to-fine sand with interbedded thin seams of silt and/or clay (Group 3). The Upper Sand Stratum (Group 1 soils) will be completely removed and replaced with compacted structural fill prior to the construction of VEGP Units 3 and 4. The static and dynamic engineering properties of the three principal soil groups and the compacted backfill were determined by field investigation and laboratory testing. The laboratory tests and their results are summarized in Section 2.5.4.2.4. The engineering properties of the subsurface materials are presented in Section 2.5.4.2.5.

2.5.4.2.2 Description of Subsurface Materials

The site soils and bedrock are divided into five strata (Upper Sand Stratum, Marl Bearing Stratum, Lower Sand Stratum, Dunbarton Triassic Basin bedrock, and Paleozoic Crystalline bedrock), which correspond to the three soil groups mentioned in Section 2.5.4.2.1 plus the two bedrock units:

I Upper Sand Stratum (Barnwell Group) – predominantly sands, silty sands, and clayey sands with occasional clay seams. A shelly limestone (Utley Limestone) layer was encountered at the base of the Upper Sand Stratum or the top of the Blue Bluff Marl. The limestone contains solution channels, cracks, and discontinuities and was the cause of severe fluid loss observed during drilling for the ESP subsurface investigation.

II Marl Bearing Stratum (Blue Bluff Marl or Lisbon Formation) – slightly sandy, cemented, calcareous clay.

III Lower Sand Stratum (comprises several formations from the Still Branch just beneath the Blue Bluff Marl to Cape Fear just above the Dunbarton Triassic Basin rock) – fine-to-coarse sand with interbedded silty clay and clayey silt.

IV Dunbarton Triassic Basin Rock – red sandstone, breccia, and mudstone, weathered through the upper 120 ft.

V Paleozoic Crystalline Rock - a competent rock with high shear wave velocities that underlies the non-capable Pen Branch Fault, which underlies the site.

These strata have been previously used as a means for classifying the soils and rock with regard to engineering properties, and is also used in this ESP SSAR.

The following is a brief description of the subsurface materials, giving the soil and rock constituents, and their range of thickness encountered at the site. The information has been taken from the 14 borings and 10 cone penetrometer tests (CPTs) performed during the ESP subsurface investigation. The locations of the ESP borings and CPTs are shown on

Figure 2.5.4-1. Reference is made, as appropriate, to borings performed for VEGP Units 1 and 2. For reference, the VEGP site elevations in the areas explored range from about El. 219 to 256 ft msl, with a median of about El. 222 ft msl. It is noted that most of the VEGP ESP site is flat at about El. 220 ft msl with surrounding areas at higher elevations of about 250 ft msl. A finished plant grade of El. 220 ft msl is used for the new unit ESP analysis. The engineering properties are provided in Section 2.5.4.2.5. Figures 2.5.4-3, 2.5.4-4, and 2.5.4-5 provide illustrations of the subsurface conditions across the VEGP site. A profile legend is provided as Figure 2.5.4-2.

2.5.4.2.2.1 Upper Sand Stratum (Barnwell Group)

The ESP subsurface investigation (Appendix 2.5A) determined that the Upper Sand Stratum ranged in thickness from 78 to 157 ft beneath the ground surface at the completed boring locations. The wide range of thickness was due to two factors. First, three borings (B-1004, B-1005, and B-1006) were drilled from elevations about 30 ft higher than the remaining borings. Second, the top of the Blue Bluff Marl dips down toward the west and northwest portions of the VEGP site. The average thickness of the Upper Sand Stratum was 102 ft, and the median thickness was 94 ft at the ESP boring locations.

Field Standard Penetration Test (SPT) N-values obtained according to ASTM D 1586 **(ASTM D 1586 1999)** within the Upper Sand Stratum during the ESP subsurface investigation ranged from weight of rod (WOR) to 50 blows for 0-in. penetration (50/0”). The very high blow count values are indicative of zones containing the shelly limestone. The average field SPT N-value was 25 blows per foot (bpf), and the median N-value was 21 bpf. These field values are un-corrected for hammer efficiency of the respective drill rig hammers used. Measurements of hammer energy were performed in borings B-1006 and B-1013. The measured energy transfer efficiency ranged from 65 to 87 percent, with an average value of 76 percent and a median value of 75 percent.

Selected samples recovered within the Upper Sand Stratum were submitted for laboratory testing, including percent fines, moisture content, and Atterberg limits. The percent fines ranged from 3 to 60 percent, with an average value of 21 percent and a median value of 19 percent. The Plastic Limit ranged from 19 to 30, with an average value of 25 and a median value of 26. The Liquid Limit ranged from 43 to 97, with an average value of 62 and a median value of 53. The Plasticity Index ranged from 21 to 67, with an average value of 37 and a median value of 29. The natural moisture content of samples tested for Atterberg limits ranged from 20 to 93 percent, with an average value of 63 percent and a median value of 70 percent.

Site geotechnical investigations for the existing units determined that the Upper Sand Stratum (Barnwell Group) is approximately 90 ft thick. A shelly limestone (Utley Limestone) is

encountered at the base of this stratum and/or the top of the Blue Bluff Marl. The Upper Sand Stratum was determined to be susceptible to liquefaction during a seismic event equivalent to the safe shutdown earthquake (SSE) developed for VEGP Units 1 and 2. In addition, the underlying limestone layer was determined to contain significant channeling, cracking, and other discontinuities. Therefore, it was considered necessary to remove both the Upper Sand Stratum and limestone layers before constructing VEGP Units 1 and 2. The standard penetration test data from previous studies indicate that the relative density of the Upper Sand Stratum is highly variable with a range from very loose to dense. Clay lenses encountered within the stratum ranged in consistency from soft to medium stiff.

Existing Units 1 and 2 unconsolidated undrained (UU) triaxial test results of samples within the Upper Sand Stratum indicate that the Mohr strength envelope of total stresses ranges from c=2,100 pounds per square foot (psf), Φ=6° to c=440 psf, Φ=32°, depending on the clay and sand content within the sample. Likewise, previous consolidated undrained (CU) triaxial test results for samples within the Upper Sand Stratum indicate that the Mohr strength envelope ranges from c=1,650 psf, Φ=17° to c=4,000 psf, Φ=25° for total stress and Φ=33° to Φ=34.5° for effective stresses. Because of the large number of UU and CU triaxial tests previously performed on Upper Sand Stratum samples, and the fact that this stratum would be completely removed before constructing the ESP units, no new strength tests were performed during the ESP subsurface investigation.

The design properties of the Upper Sand Stratum are provided in Table 2.5.4-1 and were developed from laboratory and field test results, and published engineering correlations.

2.5.4.2.2.2 Blue Bluff Marl (Lisbon Formation)

The ESP subsurface investigation (Appendix 2.5A) determined that the Blue Bluff Marl was found to range in thickness from 63 to 95 ft at three locations where the stratum was fully penetrated, with an average thickness of 76 ft and a median thickness of 69 ft. The typical thickness of the Blue Bluff Marl is illustrated on the subsurface profiles on Figures 2.5.4-3, 2.5.4-4, and 2.5.4-5. The profiles on Figures 2.5.4-3 and 2.5.4-4 also illustrate the downward dip of the top of the Blue Bluff Marl toward the west side of the VEGP site.

Field SPT N-values obtained within the Blue Bluff Marl during the ESP subsurface investigation ranged from 26 bpf to 50 blows for 1-in. penetration (50/1”). The average field SPT N-value was 83 bpf, and the median N-value was 100 bpf. SPT blow counts corresponding to less than 12 in. of sampler penetration were linearly extrapolated to the 12 in. standard penetration. SPT blow counts that were linearly extrapolated to more than 100 bpf were truncated at 100 bpf when calculating SPT averages. The field values are uncorrected for hammer efficiency of the respective drill rig hammers used. It is noted that the 26 bpf value was measured near the

bottom of the stratum in boring B-1002, and most measured values were above 50 bpf. Also, the SPT N-values did not suggest the presence of a likely weathered portion at the top of the stratum.

Selected samples recovered within the Blue Bluff Marl during the ESP subsurface investigation were submitted for laboratory testing, including percent fines, moisture content, and Atterberg limits. The percent fines ranged from 24 to 64 percent, with an average value of 37 percent and a median value of 35 percent. The plastic limit ranged from non-plastic (NP) to 51 percent, with an average value of 29 percent and a median value of 27 percent. The liquid limit ranged from NP to 99 percent, with an average value of 51 percent and a median value of 43 percent. The plasticity index ranged from NP to 58 percent, with an average value of 22 percent and a median value of 16 percent. The natural moisture content of samples tested for Atterberg limits ranged from 14 to 67 percent, with an average value of 35 percent and a median value of 29 percent. In addition, 15 one-point UU tests were performed on Blue Bluff Marl samples. The laboratory measured undrained shear strength ranged from 150 to 4,300 psf. The low end of measured values (150 psf) is lower than previously reported (260 psf) for VEGP Units 1 and 2, and the high end of measured values (4,300 psf) is significantly lower than previously reported (500,000 psf) for VEGP Units 1 and 2. The SPT N-values measured during the ESP and values previously measured in the laboratory for VEGP Units 1 and 2 support the use of a 10,000-psf design value. The reason for the sharp disagreement between the ESP laboratory values and previously reported undrained shear strength for the Blue Bluff Marl is severe sample disturbance due to sampling technique (pitcher sampler) and preparation of testing specimen. The SPT N-values measured during the ESP and values previously measured in the laboratory for VEGP Units 1 and 2 support the use of a 10,000-psf design value. Additional confirmatory tests will be performed during the COL phase.

Site investigations for the existing units determined that the marl stratum (Blue Bluff Marl or Lisbon Formation) consists of hard, slightly sandy, cemented, calcareous clay and ranges in thickness from approximately 60 ft to 100 ft. The comparative consistency of the Blue Bluff Marl ranges from hard to very hard. The materials are moderately brittle and resemble a calcareous claystone or siltstone. Previous seismic exploration within this stratum indicates a velocity interface approximately 15 ft beneath the top of the stratum. The upper 15 ft, a likely weathered portion, of the stratum recorded a compressive wave velocity of approximately 5,000 ft per second (fps), while the underlying material recorded a compressive wave velocity of approximately 7,000 fps. The static engineering properties of the Blue Bluff Marl stratum are summarized in Table 2.5.4-1.

Previous laboratory results indicate the Blue Bluff Marl to be highly preconsolidated. Plasticity index values ranged from 2 to 70 with an average value of 25. Based on work by Skempton **(1957)**, using the average PI value yields an s_u/p ratio of approximately 0.2, where s_u is

undrained shear strength and p is the effective preconsolidation pressure at sample depth. An undrained shear strength of 16,000 psf was determined using the average value of shear strength test results which failed at less than 50,000 psf. Therefore, using the 16,000 psf value for undrained shear strength and a s_u/p ratio of 0.2, the preconsolidation pressure of the Blue Bluff Marl stratum was estimated to be 80,000 psf. Settlements due to loadings from new structures would be small due to this high preconsolidation pressure.

The undrained shear strength of the Blue Bluff Marl was verified during the excavation for VEGP Units 1 and 2. Core samples of the Blue Bluff Marl were obtained and tested. The design value of c = 10,000 psf, Φ = 0° was found to be appropriately conservative. The average undrained shear strength of the core samples was 20,000 psf, and the lowest value obtained was 11,700 psf.

The heave of the Blue Bluff Marl stratum was monitored during the excavation for VEGP Units 1 and 2. Measurements were taken at nine locations at regular intervals. After excavation completion, an average heave of 1.25 in. was observed. Based on the heave measurements, the undrained Young's modulus, E, of the Blue Bluff Marl stratum was calculated to be 10,000 kips/ft^2, similar to values of E estimated from Menard pressuremeter and seismic velocity measurements during previous field investigations.

The static design properties of the Blue Bluff Marl stratum are provided in Table 2.5.4-1 and were developed from laboratory and field test results, available data from VEGP Units 1 and 2, as well as published engineering correlations.

A summary of the design dynamic shear modulus at strain levels of 10^{-4} percent, or lower, for the Blue Bluff Marl stratum is given in Table 2.5.4-2. Dynamic shear modulus values were computed from the in situ shear wave velocity measurements shown in Table 2.5.4-6.

2.5.4.2.2.3 Lower Sand Stratum

The ESP subsurface investigation (Appendix 2.5A) determined that the Lower Sand Stratum encompassed a number of geologic formations, including, listed in top to bottom order, the Still Branch, Congaree, Snapp, Black Mingo, Steel Creek, Gaillard/Black Creek, Pio Nono/Unnamed, and Cape Fear formations. The Lower Sand Stratum was fully penetrated at boring B-1003 and found to have a thickness of 900 ft at this location. Boring B-1003 also disclosed that the Lower Sand Stratum rests upon Dunbarton Triassic Basin rock. Typical depths are illustrated on the subsurface profile in Figure 2.5.4-4.

Field SPT N-values obtained to depths of about 300 ft within the Lower Sand Stratum during the ESP subsurface investigation ranged from 9 bpf to 50 blows for 4-in. penetration (50/4"). The average field SPT N-value was 59 bpf, and the median N-value was 47 bpf. These field values

are uncorrected for hammer efficiency of the respective drill rig hammers used and comprise values measured mostly in the Still Branch Formation directly beneath the Blue Bluff Marl.

ESP subsurface investigation selected samples recovered within the Lower Sand Stratum were submitted for laboratory testing, including percent fines, moisture content, and Atterberg limits. The percent fines ranged from 3 to 79 percent, with an average value of 18 percent and a median value of 14 percent. The plastic limit ranged from NP to 38 percent, with average and median values of 30 percent. The liquid limit ranged from NP to 53 percent, with average and median values of 47 percent. The plasticity index ranged from NP to 19 percent, with average and median values of 17 percent. The natural moisture content for samples tested for Atterberg limits ranged from 21 to 41 percent, with an average value of 30 percent and a median value of 28 percent. Samples with the higher percent fines and plasticity were from the silty clay and clayey silt layers.

Site geotechnical investigations for the existing units determined that the Lower Sand Stratum consists of sands with interbedded silty clay or clayey silt. The thickness of this stratum was estimated to be 900 to 1,000 ft. SPT N-values obtained to depths of about 300 to 400 ft below grade during previous field investigations within the Lower Sand Stratum ranged from 70 to 100 bpf, indicative of a very dense material.

The static design properties of the Lower Sand Stratum are provided in Table 2.5.4-1 and were developed from laboratory and field test results, available data from VEGP Units 1 and 2, as well as published engineering correlations.

A summary of the design dynamic shear modulus at strain levels of 10^{-4} percent, or lower, for the Lower Sand Stratum is given in Table 2.5.4-2. Dynamic shear modulus values were computed from the in situ shear wave velocity measurements shown in Table 2.5.4-6.

2.5.4.2.2.4 Dunbarton Triassic Basin Rock

The Dunbarton Triassic Basin Rock was cored at borehole B-1003 only, and consisted of red sandstone, breccia, and mudstone, weathered through the upper 120 ft. Further details are provided in Section 2.5.1. Because the rock was too deep to be of any interest to foundation design, no laboratory tests were performed on the rock cores. Shear wave velocity was measured in the upper 274 ft of the rock profile, and these results were used to develop the shear wave velocity profile for site amplification that are presented in Section 2.5.4.7.1.

2.5.4.2.2.5 Paleozoic Crystalline Rock

As indicated in Figure 2.5.4-4, the VEGP site sits on over 1,000 feet of Coastal Plain sediments underlain by Triassic Basin sedimentary rock. Borehole B-1003 encountered the bottom of the

Coastal Plain sediments and the start of a weathered section of the Triassic Basin at a depth of 1,049 feet. Under the part of Savannah River Site [SRS] adjacent to the VEGP site, the southeast dipping Pen Branch fault separates the Triassic Basin rock from Paleozoic crystalline rock to the northwest (**Lee et al. 1997**). A seismic reflection survey in and around the VEGP site (shown in Appendix 2.5B and discussed in section 2.5.1.2.4.2), has been interpreted to show the southwest continuation of the Pen Branch fault beneath the site and to indicate that the depth to the bottom of the Coastal Plain sediments is about 1,000 feet (Figure 2.5.1-40). This and interpretation of flexures within the older Coastal Plain sediments suggest that the Pen Branch fault lies below the area of the new containment units. Therefore, the information available implies that at some depth below the VEGP site the Paleozoic crystalline rock underlies the Triassic Basin rock.

2.5.4.2.2.6 Subsurface Profiles

Figures 2.5.4-3, 2.5.4-4, and 2.5.4-5 illustrate typical subsurface profiles across the power block area proposed for the proposed VEGP Units 3 and 4. A profile legend is provided as Figure 2.5.4-2. The locations of the borings used to develop profiles are shown in Figure 2.5.4-1. These profiles are discussed in Section 2.5.4.5 with respect to excavation for the new units and in Section 2.5.4.10.1 for bearing capacity considerations.

2.5.4.2.3 Field Investigations

The exploration programs performed previously for VEGP Units 1 and 2 are referenced, as warranted, and the ESP subsurface investigation is described in Section 2.5.4.3. The borings from previous explorations are not included here. The borings and cone penetrometer tests from the ESP subsurface investigation program are summarized in Tables 2.5.4-7. Previous geophysical surveys and new geophysical surveys for the ESP study are described in Section 2.5.4.4. Boring logs and CPT logs from the recent field exploration are included in Appendix 2.5A.

2.5.4.2.4 Laboratory Testing

2.5.4.2.4.1 Testing Overview

Numerous laboratory tests of soil samples were performed previously for VEGP Units 1 and 2, and new tests have been performed as part of the ESP subsurface investigation. Previous test results are contained within Bechtel Power Corporation's Report on Foundation Investigations **(Bechtel 1974b)**. The types and numbers of tests completed during the ESP subsurface investigation are shown in Table 2.5.4-3, and the test results are contained within the MACTEC report for the ESP subsurface investigation (Appendix 2.5A). A summary of all laboratory test

results performed as part of the ESP subsurface investigation is provided in Table 2.5.4-4. The following sections focus on the tests performed for the ESP subsurface investigation.

2.5.4.2.4.2 Laboratory Tests for the ESP Subsurface Investigation

Laboratory testing for the ESP investigation was performed in accordance with the guidance presented in Regulatory Guide 1.138, *Laboratory Investigations of Soils for Engineering Analysis and Design of Nuclear Power Plants*, US Nuclear Regulatory Commission, 2003 (RG 1.138). The laboratory work was performed under an approved quality program with work procedures developed specifically for the ESP application. Soil samples were shipped under Chain-of-Custody protection from the on-site storage area (described in Section 2.5.4.3.2) to the testing laboratory. Laboratory testing was performed at the MACTEC laboratories in Atlanta, Georgia.

The types and numbers of laboratory tests performed on the soil samples from the ESP exploration program are included on Table 2.5.4-3. The ESP tests focused primarily on verifying the basic properties of the Upper Sand Stratum, Blue Bluff Marl, and the upper formations in the Lower Sand Stratum.

The details and results of the laboratory testing are included in Appendix 2.5A. This appendix includes references to the industry standard used for each specific laboratory test. The results of the tests on soil samples are shown on Table 2.5.4-4.

2.5.4.2.5 Engineering Properties

The engineering properties for the Upper Sand Stratum, Blue Bluff Marl, and Lower Sand Stratum, derived from the previous studies and from the ESP subsurface investigation and laboratory testing program, are provided in Table 2.5.4-1. The engineering properties obtained from the ESP subsurface investigation and laboratory testing program (Appendix 2.5A) were similar to those obtained from the previous field and laboratory testing programs.

Rock densities were derived from Tables 5-2 and 5-3 of WSRC **(1998)** for crystalline and Triassic rock, respectively. Rock densities increased with depth from 2.75 gm/cc to 3.42 gm/cc in the crystalline rock, and from 2.53 gm/cc to 3.42 gm/cc in the Triassic rock.

The following sections briefly describe the sources and/or methods used to develop the selected properties shown in Table 2.5.4-1.

2.5.4.2.5.1 Rock Properties

The Recovery and Rock Quality Designations (RQD) are based on the results provided from the deep boring, B-1003. Rock coring was not performed during the previous investigations for

VEGP Units 1 and 2. Geophysical testing at the deep boring, B-1003, extended for about 290 ft into the bedrock encountered at depth of 1,049 ft below the ground surface. The shear and compressional wave velocities are based on the suspension P-S velocity seismic test performed in borehole B-1003 as part of the ESP subsurface investigation (Appendix 2.5A). Laboratory strength testing of rock cores was not performed because the rock is deemed to be too deep to provide any additional useful engineering information.

2.5.4.2.5.2 Soil Properties

Sieve analyses of 30 Upper Sand Stratum samples (including 1 fill sample), 19 Blue Bluff Marl samples, and 12 Lower Sand Stratum samples were performed as part of the ESP laboratory testing program (Appendix 2.5A).

The natural moisture content and Atterberg Limits of 4 Upper Sand Stratum, 19 Blue Bluff Marl, and 4 Lower Sand Stratum samples were determined as part of the ESP laboratory testing program. Design values shown on Table 2.5.4-1 were taken as the average of these test results for the respective soil strata.

The undrained shear strength of the Blue Bluff Marl bearing stratum is estimated from SPT N-values and from previous test results of high quality Blue Bluff Marl samples obtained during the excavation for VEGP Units 1 and 2.

The effective angle of internal friction of the Upper Sand Stratum was determined to be 34 degrees **(Bowles 1982)** from correlation with the average SPT N-value (based on N = 25 bpf). The N-value of 25 bpf represents the measured value of 20 bpf corrected to account for the higher automatic hammer efficiency measured in the field. This correction was made following the guidelines in ASTM D 6066 (1996).

The effective angle of internal friction of the Lower Sand Stratum was determined to be 41 degrees **(Bowles 1982)** from correlation with the average SPT N-value (based on N = 62 bpf). The N-value of 62 bpf represents the measured value of 50 bpf corrected to account for the higher automatic hammer efficiency measured in the field. This correction was made following the guidelines in ASTM D 6066 (1996).

Unit weights were measured in selected samples of the Blue Bluff Marl and Lower Sand Stratum. Unit weight of 15 Blue Bluff Marl samples ranged from 103.6 pounds per cubic foot (pcf) to 140.2 pcf, with an average of 120 pcf. Unit weights of three Lower Sand Stratum samples were 119.4 pcf, 121.7 pcf, and 128.3 pcf, with an average of 123 pcf. The in situ moist unit weights of the Upper Sand Stratum, Blue Bluff Marl, and Lower Sand Stratum for VEGP Units 1 and 2 were 118 pcf, 119 pcf, and 117 pcf, respectively. However, there were only a few measurements made for the ESP investigation in the Lower Sand Stratum. Measurements

made at the adjacent SRS site in the deeper sands indicate an average total unit weight of about 127 pcf **(WSRC 1998).**

The design SPT N-value for the Upper Sand Stratum is taken as 25 bpf. This value is based on the results reported in Table 2.5.4-5 and includes correction for hammer efficiency. The results in Table 2.5.4-5 show an average uncorrected field SPT N-value of 25 bpf and median value of 21 bpf. The design corrected N-value of 25 bpf corresponds to a field N-value of 20 bpf, which is lower than the average and median values. SPT N-values for VEGP Units 1 and 2 ranged from 2 to 60 bpf with an average of 30 bpf. The design value is within the range and near the average of the previous investigation values.

The design SPT N-value for the Blue Bluff Marl is taken as 100 bpf. This value is based on the results reported in Table 2.5.4-5 and includes correction for hammer efficiency. The results in Table 2.5.4-5 show an average uncorrected field SPT N-value of 83 bpf and median value of 100 bpf. The design corrected N-value of 100 bpf corresponds to a field N-value of 80 bpf, which is lower than the average and median values. SPT N-values for VEGP Units 1 and 2 ranged from 10 to over 100 bpf with an average of over 100 bpf. The design value is within the range and near the average of the previous investigation values.

The design SPT N-value for the Lower Sand Stratum is taken as 62 bpf. This value is based on the results reported in Table 2.5.4-5 and includes correction for hammer efficiency. The results in Table 2.5.4-5 show an average uncorrected field SPT N-value of 59 bpf and median value of 47 bpf. The design corrected N-value of 62 bpf corresponds to a field N-value of 50 bpf, which is lower than the average value and slightly higher than the median value. SPT N-values for VEGP Units 1 and 2 ranged from 70 to 100+ bpf with an average of 100+ bpf. The design value is somewhat less than the previous investigation range of values. This may partially be due to limited sampling within the upper formations of the Lower Sand Stratum compared to ample sampling during the previous investigations. During the ESP subsurface investigation, only 16 SPTs were performed within the Lower Sand stratum.

Shear wave velocities were measured by suspension P-S velocity tests and seismic CPTs during the ESP subsurface investigation (Appendix 2.5A). The suspension P-S velocity tests were performed in boreholes B-1002, B-1002A, B-1003, B-1005, and C-1005A. Three seismic CPTs were performed in accordance with ASTM D 5778 (2000) at C-1003, C-1005, and C-1009A. Seismic CPT tests did not extend into the very hard underlying Blue Bluff Marl stratum. Further discussion of suspension P-S velocity and seismic CPT testing is provided in Section 2.5.4.4.2.

A complete shear wave velocity profile was developed from the ground surface to about 300 ft into the Dunbarton Triassic Basin rock for a total depth of about 1,340 ft using both suspension

P-S velocity and seismic CPT testing. Shear wave velocities within the Upper Sand Stratum ranged from about 570 fps to 3,310 fps. Shear wave velocities ranged from 1,060 fps to 4,260 fps within the Blue Bluff Marl stratum, 930 fps to 4,670 fps within the underlying Lower Sand Stratum, and 2,320 fps to 9,350 fps within the Dunbarton Triassic Basin. Shear wave velocity measurements were made to depths of up to 290 ft during previous investigations for VEGP Units 1 and 2. In addition, shear wave velocity data were reviewed from seven deep borings performed at the neighboring Savannah River Site. Typical shear wave velocity values were determined for the Upper Sand Stratum, Blue Bluff Marl, Lower Sand Stratum, and the Dunbarton Triassic Basin rock data based upon review of all the available data and are provided in Table 2.5.4-6. Shear wave velocity values within the Lower Sand Stratum were determined for each of the geologic formations contained within. A more detailed discussion of shear wave velocity values and establishment of the shear wave velocity profile for site amplification are presented in Section 2.5.4.7.1. The profile of shear wave velocity versus depth for the subsurface soils is given in Section 2.5.4.7.

The high strain (i.e., in the range of 0.25 to 0.5 percent) elastic modulus values, tabulated in Table 2.5.4-1, for the Upper Sand Stratum and Lower Sand Stratum have been derived using the relationship with the SPT N-value given in **Davie and Lewis (1988)**. The high strain elastic modulus for the Blue Bluff Marl stratum has been derived using the relationship with undrained shear strength given in **Davie and Lewis (1988)**. The shear modulus values have been obtained from the elastic modulus values using the relationship between elastic modulus, shear modulus, and Poisson's ratio **(Bowles 1982)**.

The low strain (i.e., 10^{-4} percent) shear modulus, tabulated in Table 2.5.4-2, for the Upper Sand Stratum has been derived from the average shear wave velocity of 930 fps. The low strain shear modulus of the Blue Bluff Marl stratum has been derived from the average shear wave velocity of 2,354 fps. The low strain shear modulus of the Lower Sand Stratum has been derived from the average shear wave velocity of 2,282 fps. The elastic modulus values have been obtained from the shear modulus values using the relationship between elastic modulus, shear modulus, and Poisson's ratio **(Bowles 1982)**. The low strain shear modulus for the compacted backfill has been derived assuming an average shear wave velocity of 1,000 fps.

The values of unit coefficient of subgrade reaction are based on values for medium dense sand (Upper Sand Stratum), very-stiff-to-hard clay (Blue Bluff Marl), and dense-to-very-dense sand (Lower Sand Stratum) provided by Terzaghi (1955).

The earth pressure coefficients are Rankine values, assuming level backfill and a zero friction angle between the soil and the wall.

2.5.4.2.5.3 Chemical Properties

Chemical tests were not included in the ESP laboratory testing program. Chemical tests would be required of backfill materials placed in proximity of planned concrete foundations and buried metal pipes, and would be included in the COL investigation phase.

2.5.4.3 Exploration

Section 2.5.4.3.1 summarizes previous subsurface investigation programs performed at the VEGP site, while Section 2.5.4.3.2 describes the ESP subsurface investigation program.

2.5.4.3.1 Previous Subsurface Investigation Programs

Field investigations for VEGP Units 1 and 2 were initiated in January 1971. Field investigations consisted of borings, geophysical methods, and groundwater studies. Additional investigation was completed during excavation for VEGP Units 1 and 2 to verify and obtain further details concerning subsurface conditions in the power block area. A total of 474 borings and 60,000 ft of drilling were completed during these investigations. An additional 111 borings were completed after the initial investigations mentioned above for the following purposes: 41 borings were drilled to define soil conditions and lateral extent of the Blue Bluff Marl in the river facilities, 38 borings were drilled in the power block to collect samples of the Blue Bluff Marl and perform confirmatory testing, and 32 borings were drilled to collect subsurface data for the natural draft cooling tower foundation design. During the previous investigations, electric logging, natural gamma, density, neutron, caliper, and 3-D velocity logs (Birdwell) were performed at selected borings. Water pressure tests and Menard pressuremeter tests were completed to determine properties of the Blue Bluff Marl bearing stratum. Fossil, mineral, or soluble carbonate tests were performed on recovered samples as warranted.

Geophysical methods were applied to supplement the test borings. The geophysical methods are described in Section 2.5.4.4. For the previous investigations, a total of 28,400 ft of shallow refraction lines, 5,000 ft of deep refraction lines, and cross-hole velocities of subsurface were performed extending from the ground surface to a depth of 290 ft.

Several of the previously drilled borings for VEGP Units 1 and 2 fall within the proposed VEGP Units 3 and 4 site. Results of previous investigations are referenced and are used here as needed to supplement subsurface data obtained during the ESP subsurface investigation.

2.5.4.3.2 ESP Subsurface Investigation Program

The ESP subsurface investigation was performed during September through December 2005 over a substantial portion of the site enveloping the area that would contain the new reactors as

well as the switchyard and the cooling towers for the proposed VEGP Units 3 and 4. This investigation consisted of exploration points that were located primarily to confirm the results obtained from the previous extensive investigations.

Additional structure-specific exploration would be performed at the COL phase. The ESP exploration point locations are shown in Figure 2.5.4-1. The exploration points from the ESP investigation are combined with selected boring locations from the previous investigations in Figure 2.5.4-1.

The scope of work and the special methods used by the subsurface investigation contractor (MACTEC) and its subcontractors to collect data are listed below:

- Thirteen exploratory borings were drilled by MACTEC. Two of these borings (B-1002A and C-1005A) were drilled without sampling to allow suspension P-S velocity testing to be performed above zones of drilling fluid loss encountered in the Upper Sand Stratum above the Blue Bluff Marl.
- The efficiency of the automatic hammers employed by the two rotary drill rigs was determined by SPT energy measurements. These services were provided by GRL Engineers, Inc., of Cleveland, Ohio, working as a subcontractor to MACTEC.
- One continuous soil and rock coring borehole was completed at B-1003 by MACTEC.
- Ten CPTs were performed, including three down-hole seismic CPTs. These services were provided by Applied Research Associates (ARA) of South Royalton, Vermont, working as a subcontractor to MACTEC.
- In-situ hydraulic conductivity testing was performed by MACTEC (Section 8 of ASTM D 4044 2002) in 15 groundwater observation wells. Southern Company Services installed these wells and the report is in Appendix 2.4A.
- Geophysical down-hole suspension P-S velocity logging was performed in five completed boreholes (B-1002, B-1002A, B-1003, B-1004, and C-1005A). These services were provided by GEOVision Geophysical Services (GEOVision) of Corona, California, working as a subcontractor to MACTEC. GEOVision also performed caliper, natural gamma, resistivity, and spontaneous potential measurements in boreholes B-1002, B-1003, and B-1004, and a borehole deviation survey at B-1003.
- A topographic survey of all exploration points was performed by MACTEC.
- Laboratory testing of selected borehole samples was performed by MACTEC in its Atlanta, Georgia, laboratories.

The exploration program was performed following the guidelines in Regulatory Guide 1.132, *Site Investigations for Foundations of Nuclear Power Plants*, US Nuclear Regulatory Commission, 2003 (RG 1.132). The fieldwork was performed under an audited and approved quality program and work procedures developed specifically for the ESP application. The subsurface investigation and sample/core collection were directed by the MACTEC site manager, who was on site at all times during the field operations. A Bechtel geotechnical engineer or geologist, along with an SNC representative, was also on site during these operations. MACTEC's QA/QC expert made periodic visits to the site and was on site to audit MACTEC's subcontractors. The draft boring and well logs were prepared in the field by MACTEC geologists.

An on-site storage facility for soil samples and rock cores was established before the fieldwork began. Each sample and core was logged into an inventory system. Samples removed from the facility were noted in the sample inventory logbook. A Chain-of-Custody form was also completed for all samples removed from the facility.

Complete details and results of the exploration program appear in Appendix 2.5A. The borings, CPTs, field permeability testing, and geophysical surveys are summarized below. The laboratory tests are summarized and the results discussed in Section 2.5.4.2. The geophysical tests are summarized and the results discussed in Section 2.5.4.4.

Additionally, a seismic reflection and refraction survey was performed at the site in early 2006 to collect data to help delineate the rock profile associated with the non-capable Pen Branch fault. The results of the seismic reflection and refraction survey are presented in Appendix 2.5B and interpreted results are discussed in Section 2.5.1.2.4.2.

2.5.4.3.2.1 Borings and Samples/Cores

Thirteen borings (excluding B-1003) were drilled to depths ranging from 90 ft (C-1005A) to 304 ft (B-1004). The borings were advanced in the soil using mud-rotary drilling techniques and polymer and/or bentonite drilling fluids. Table 2.5.4-7 provides a summary of the ESP boring and CPT locations and depths, and identifies geophysical testing performed in the boreholes.

The soil was sampled using an SPT sampler at continuous intervals to a 15-ft depth and at 5- or 10-ft intervals below 15 ft. The SPT was performed with automatic hammers and was conducted in accordance with ASTM D 1586 (1999). The recovered soil samples were visually described and classified by the onsite geologist in accordance with ASTM D 2488 (2000). A selected portion of the soil sample was placed in a glass sample jar with a moisture-proof lid. The sample jars were labeled, placed in boxes, and transported to the on-site storage area. Additionally, undisturbed samples of the Blue Bluff Marl (Lisbon Formation) were obtained using rotary pitcher samplers. Disturbed materials were removed from the upper and the lower ends

of the tube, and both ends were trimmed square to establish an effective seal. Pocket penetrometer tests were taken on the trimmed lower end of the samples. Both ends of the sample were then sealed with hot microcrystalline wax and protected with plastic caps. Tubes were labeled and transported to the on-site storage area. Table 2.5.4-8 provides a summary all undisturbed samples of the Blue Bluff Marl collected during the ESP subsurface investigation.

The energy transfer efficiency of the automatic SPT hammers used by the drill rigs was obtained using a PAK model pile driving analyzer for both drill rigs. Testing was performed at borings B-1006 and B-1013 from depth ranges of 5 to 20 ft, 30 to 50 ft, and 75 to 100 ft. Resultant energy transfer efficiency measurements ranged from 65 to 87 percent. The average energy transfer efficiency was 75 percent. Table 2.5.4-9 provides the SPT hammer energy transfer efficiency results.

The continuous core boring, B-1003, was performed with a Christensen 94 mm wire line system. A Speedstar Quickdrill 275 drill rig was used. Casing was installed through the soil column to prevent cave-ins and to allow coring of rock at depths below 1,049 ft. Rock coring was performed using a HW-size, double-tube core barrel in accordance with ASTM D 2113 (1999). The recovered soil and rock core samples were placed in wooden core boxes, lined with plastic sheeting. The onsite geologist visually described the core, noting the presence of joints and fractures, and distinguishing natural breaks from mechanical breaks. The geologist also computed the percentage recovery and the RQD. The average core recovery was 77 percent for the entire borehole depth (Appendix 2.5A). Filled core boxes were transported to the on-site sample storage facility, where a photograph of each core was taken.

The boring logs and the photographs of the rock cores appear in Appendix 2.5A. The soil materials encountered in the ESP borings are similar to those found in the previous borings conducted at the VEGP site.

2.5.4.3.2.2 Cone Penetrometer Tests

The CPTs were advanced in accordance with ASTM D 5778 (2000) using a 30-ton self-contained truck rig. Each CPT was advanced to refusal at depths ranging from 6 to 116.7 ft. Shallow refusal was encountered at locations C-1001 and C-1009, and offset CPT tests were performed at locations C-1001A and C-1009A. All remaining CPT locations met refusal at or near the top of the Blue Bluff Marl bearing stratum. Down-hole seismic testing was performed at 5 ft intervals in CPTs C-1003, C-1005, and C-1009A (see Section 2.5.4.4) to measure the shear wave velocity in the Upper Sand Stratum. Pore pressure dissipation tests were performed at 68 ft and 79 ft depths in C-1003; 66 ft depth in C-1004; 56 ft, 73 ft, and 82 ft depths in C-1005; and 60 ft, 77 ft, 90 ft, and 99 ft depths in C-1009A.

The CPT logs, shear wave velocity results, and pore pressure versus time plots are contained in Appendix 2.5A. CPT locations and depths are summarized in Table 2.5.4-7.

2.5.4.3.2.3 In Situ Hydraulic Conductivity Testing

Fifteen observation wells were installed at the ESP project limits during May and June 2005, and a replacement observation well was installed in October 2005. Observation well details are provided in Appendix 2.4A and discussed in Section 2.4.12.

Each well was developed by pumping. The well was considered developed when the pH and conductivity stabilized and the pumped water was reasonably free of suspended sediment. Permeability tests were then performed in each well in accordance with Section 8 of ASTM D 4044 (2002) using a procedure that is commonly termed the slug test method. Slug testing involves establishing a static water level, lowering a solid cylinder (slug) into the well to cause an increase in water level in the well, and monitoring the time rate for the well water to return to the pre-test static level. The slug is then rapidly removed to lower the water level in the well, and the time rate for the water to recover to the pre-test static level is again measured. Electronic transducers and data loggers were used to measure the water levels and times during the test.

Appendix 2.5A contains the well permeability test results and Appendix 2.4A contains the boring logs for the observation wells and the well installation records.

2.5.4.4 Geophysical Surveys

Section 2.5.4.4.1 summarizes previous geophysical investigations performed at the VEGP site, and Section 2.5.4.4.2 summarizes the VEGP site geophysical program for this ESP application.

2.5.4.4.1 Previous Geophysical Survey Programs

Field investigations that included geophysical methods for VEGP Units 1 and 2 were initiated in January 1971. Geophysical seismic refraction and cross-hole surveys were conducted at the site to evaluate the occurrence and characteristics of subsurface materials. The seismic refraction survey was used to determine depths to seismic discontinuities, based on measured compressive wave velocities. Shallow and deep refraction profiles were obtained throughout the site area, totaling 28,400 and 5,000 linear ft, respectively. The cross-hole seismic survey was conducted in the VEGP Units 1 and 2 power block area to determine in situ velocity data for both compressional and shear waves to a depth of 290 ft (82 ft below sea level) in bore holes 136, 146G, 148, 149, 151, and 154. In this procedure, three-component geophones were

lowered into four of the bore holes to equal elevation levels. Energy was generated in a fifth bore hole, at the same elevation level, to determine cross-hole velocities.

The seismic (compressional wave) velocities measured in the subsurface soils from depths of 0 to 290 ft ranged from 1,400 fps to 6,800 fps. The shear wave velocities measured in the subsurface soils from depths of 0 to 290 ft ranged from 600 to 1,800 fps. The Upper Sand Stratum, extending from a depth of 0 to 90 ft, has a compressional wave velocity range of 1,400 to 6,650 fps and a shear wave velocity range from 600 to 1,650 fps. The Blue Bluff Marl stratum (and underlying Lower Sand Stratum), extending from a depth of 90 to 290 ft, has a compressional wave velocity of 6,800 fps and shear wave velocities ranging from 1,600 to 1,800 fps (Note that this range is lower than that measured at the VEGP ESP site). Young's Modulus and Shear Modulus were determined from these results. For the Upper Sand Stratum, Young's Modulus ranged from 0.2×10^5 to 2.0×10^5 pounds per square inch (psi), and Shear Modulus ranged from 0.8×10^4 to 6.8×10^4 psi. For the Blue Bluff Marl (and underlying Lower Sand Stratum), Young's Modulus was 2.3×10^5 psi, and Shear Modulus was 8.0×10^4 psi.

2.5.4.4.2 ESP Geophysical Surveys

Three down-hole seismic CPT tests and five suspension P-S velocity tests were performed during the VEGP site investigation, as described in Section 2.5.4.3.2. In addition a seismic reflection and refraction survey was performed to image the subsurface and characterize the basement lithology and velocities beneath the VEGP site. This survey provided an image of the basement rock across the VEGP ESP site. The results of this survey are presented in Appendix 2.5B and the interpreted results are discussed in Section 2.5.1.2.4.2. The incorporation of these results into the development of the rock shear wave velocity profile is described in Section 2.5.4.7.1.2.

2.5.4.4.2.1 Suspension P-S Velocity Tests in Boreholes

Suspension P-S velocity testing was conducted in borings B-1002, B-1002A, B-1003, B-1004, and C-1005A. Details of the equipment used to create the seismic compressional and shear waves and to measure the seismic wave velocities are described in detail by Ohya (1986) and are also provided in Appendix 2.5A. Appendix 2.5A also contains a detailed description of the results and the method used to compute the results. Because no ASTM standard is currently available for the suspension P-S velocity testing, a brief description is provided here. The suspension P-S velocity logging system uses a 23-ft (7-m) probe containing a source near the bottom, and two geophone receivers spaced 3.3 ft (1 m) apart, suspended by a cable. The probe is lowered into the borehole to a specified depth, where the source generates a pressure wave in the borehole fluid (drilling mud). The pressure wave is converted to seismic waves (P-wave and S-wave) at the borehole wall. Along the wall, at each receiver location, the P- and

S-waves are converted back to pressure waves in the fluid and received by the geophones, which send the data to the recorder on the surface. This procedure is typically repeated at every 1.65 ft (0.5 m) or 3.3 ft (1 m) as the probe is moved up the borehole. The elapsed time between arrivals of the waves at the geophone receivers is used to determine the average velocity of a 3.3-ft (1-m) high column of soil around the borehole. Source to receiver analysis is also performed for quality assurance. The results are summarized below.

The shear wave velocity was defined to the maximum explored depth of 1,338 ft (Appendix 2.5A). For the Upper Sand Stratum, shear wave velocities ranged from 590 to 3,300 fps, with an average value of 1,089 fps. For the Blue Bluff Marl, shear wave velocities ranged from 1,060 to 4,260 fps, with an average value of 2,354 fps. For the Lower Sand Stratum, shear wave velocities ranged from 930 fps to 4,670 fps, with an average value of 2,282 fps. Typical values for the shear wave velocities of each geologic formation contained within the Lower Sand Stratum are as follows: 1,700 fps for the Still Branch, 1,950 fps for the Congaree, 2,050 fps for the Snapp, 2,350 fps for the Black Mingo, 2,650 fps for the Steel Creek, 2,850 fps for the Gaillard/Black Creek, 2,870 fps for the Pio Nono, and 2,710 fps for the Cape Fear. The shear wave velocity in the portion of the Dunbarton Triassic Basin rock measured ranged from 2,320 to 9,350 fps. There was an upper weathered rock zone about 120 ft thick, where shear wave velocities increased linearly with depth at a very high rate. This high rate of linear increase with depth abated once shear wave velocities achieved values of about 5,300 fps, and shear wave velocities increased linearly with depth at a smaller rate. It is noted that sound rock with an average shear wave velocity of 9,200 fps was not encountered. However, enough data are available to linearly extrapolate to the sound rock horizon from the measurements.

The compressional wave was also defined to the maximum explored depth of 1,338 ft (Appendix 2.5A). For the Upper Sand Stratum, the compressional wave velocity ranged from 1,300 to 7,960 fps, with an average value of 2,572 fps. For the Blue Bluff Marl, compressional wave velocities ranged from 4,640 to 9,830 fps, with an average value of 6,793 fps. For the Lower Sand Stratum, compressional wave velocities ranged from 4,990 to 9,030 fps, with an average value of 6,610 fps. The compressional wave velocity in the Dunbarton Triassic Basin rock ranged from 7,300 to 18,360 fps.

Poisson's ratio was determined from the shear wave and compressional wave velocities (Appendix 2.5A). Poisson's ratio ranged from 0.09 to 0.49 within the Upper Sand Stratum, 0.33 to 0.48 within the Blue Bluff Marl, 0.32 to 0.49 within the Lower Sand Stratum, and 0.10 to 0.46 within the Dunbarton Triassic Basin.

2.5.4.4.2.2 Down-Hole Seismic Tests with Cone Penetrometer

The tests were performed at 5-ft intervals in C-1003, C-1005, and C-1009A. A seismic source, located on the surface, primarily generates shear waves and two geophones mounted horizontally inside near the bottom of the cone string record incoming seismic data. Measurements were only obtained at depths within the Upper Sand Stratum because all CPTs reached refusal at the top of the Blue Bluff Marl.

The shear wave speed and time of peak versus depth plots are included in Appendix 2.5A. The shear wave velocities ranged from 572 to 1,317 fps, with an average value of 930 fps. These values were lower than those measured using the suspension P-S velocity technique and may reflect site variability.

2.5.4.4.2.3 Discussion and Interpretation of Results

Shear and compressional wave velocity measurements made during the ESP subsurface investigation were used as the basis for developing the recommended design values for each stratum that are provided in Section 2.5.4.2. Results from seismic CPTs and suspension velocity logging were used to develop recommended values for the Barnwell Group. Because the seismic CPTs could not penetrate into the Blue Bluff Marl, the recommended values for the Blue Bluff Marl and the Lower Sand Stratum are based on suspension velocity logging results only. No shear or compressional wave velocity measurements were made for the compacted fill during the ESP subsurface investigation. Recommended values for the compacted fill will be based on data for existing VEGP Units 1 and 2 **(Bechtel 1984)**, as discussed in Section 2.5.4.7.1.

The profile of shear wave velocity versus depth for the subsurface strata is provided in Section 2.5.4.7.

2.5.4.5 Excavation and Backfill

This section covers the following topics:

- The extent (horizontally and vertically) of anticipated safety-related excavations, fills, and slopes.
- Excavation methods and stability.
- Backfill sources and quality control.
- Construction dewatering impacts.

2.5.4.5.1 Extent of Excavations, Fills, and Slopes

Within the VEGP Units 3 and 4 footprint (Figure 2.5.4-1) that will contain all safety-related structures, existing ground elevations are about El. 220 ft msl. The subsurface profiles in Figures 2.5.4-3, 2.5.4-4, and 2.5.4-5 provide an impression of the grade elevation range across the VEGP ESP site. Plant grade for the proposed VEGP Units 3 and 4 will be at El. 220 ft msl. The base of the containment and auxiliary building foundations for the new units will be about El. 180 ft msl. This level corresponds to a depth of approximately 40 ft below final grade (below El. 220 ft msl), or approximately 50 to 60 ft above the top of the Blue Bluff Marl bearing stratum based on the borings completed during the ESP subsurface investigation. Other foundations in the power block area will be placed at nominal depths near final grade.

Construction of the new units will require a substantial amount of excavation. The excavation will be necessary to completely remove the Upper Sand Stratum. Excavation total depth to the Blue Bluff Marl bearing stratum will range from approximately 80 to 90 ft below existing grade, based on the borings completed during the ESP subsurface investigation. Deeper localized excavations will be required to remove shelly, porous material that may be encountered near the top surface of the Blue Bluff Marl. The excavation plan will be developed during the COL phase of the project.

Filling will be performed from the top of the Blue Bluff Marl to the bottom of the Containment and Auxiliary Buildings at a depth of about 40 ft below final grade. Filling will continue up around these structures to final grade. The fills will primarily consist of granular materials, selected from portions of the excavated Upper Sand Stratum and from other available onsite borrow sources. Fill material properties and source locations will be considered further during the COL phase of the project.

Temporary slopes will be graded as the excavation through the Upper Sand Stratum progresses. Other temporary or permanent slopes planned for the project will be considered for stability as warranted.

2.5.4.5.2 Excavation Methods and Stability

Excavation in the Upper Sand Stratum will be achieved with conventional excavating equipment. Excavation must adhere to OSHA regulations **(OSHA 2000)**. The excavation will be open-cut, with slopes no steeper than 2-horizontal to 1-vertical. Since the sandy soils can be highly erosive, even temporary slopes cut into the Upper Sand Stratum will be sealed and protected. Where insufficient space for open-cut slopes exists, vertical cuts will be supported with sheet pile or soldier pile and lagging walls. Dewatering will be required once the

excavation progresses to depths beneath the groundwater table (approximately El. 165 ft), based on the groundwater monitoring results contained in Section 2.4.12.

Possible soft zones that may be encountered in the upper portion of the Blue Bluff Marl will be removed using conventional excavating equipment. These excavations will be sloped to facilitate placement of compacted structural fill, and the excavation areas will be thoroughly cleaned of loose materials before fill is placed.

2.5.4.5.3 Backfill Sources and Quality Control

Although a large amount of sandy soil will be excavated for VEGP Units 3 and 4, this material will not entirely be used as structural fill. Portions of the Upper Sand Stratum contain significant fines content (greater than 25 percent), as shown in soil laboratory results in Appendix 2.5A and summarized in Table 2.5.4-4.

Following the guidelines used during construction of VEGP Units 1 and 2, structural fill will be a sandy or silty sand material with no more than 25 percent of the particle sizes smaller than the No. 200 sieve. Borrow locations from the previous construction will be re-evaluated as a potential source of material. Also, potential new borrow areas within the project vicinity will be evaluated as warranted. Estimates of total borrow volume required and evaluation of borrow sources will be determined during the COL phase of the project. This structural fill will be compacted following the same criteria used for VEGP Units 1 and 2 (i.e., to a minimum of 93 percent and an average of 97 percent, and with no more than 10 percent of field compaction tests at between 93 and 95 percent of the maximum dry density, as determined by ASTM D 1557 [2002]). The fill will be compacted to within 3 percent of its optimum moisture content. Fill placement procedures will be developed through a Test Fill Program, similar to that implemented for VEGP Units 1 and 2.

An on-site soils testing laboratory will be established to control the quality of the fill materials and the degree of compaction, and to ensure that the fill conforms to the requirements of the earthwork specification. The soil testing firm will be independent of the earthwork contractor and will have an approved quality program. Sufficient laboratory compaction (modified Proctor) and grain size distribution tests will be performed to ensure that variations in the fill material are taken into account. Field density tests will be performed, with a minimum test per lift of one per 10,000 square ft of fill placed.

2.5.4.5.4 Control of Groundwater During Excavation

Construction dewatering is discussed in Section 2.5.4.6.2. Since the Upper Sand Stratum soils can be highly erosive, sumps and ditches constructed for dewatering will be lined. The tops of

excavations will be sloped back to prevent runoff down the excavated slopes during heavy rainfall.

2.5.4.6 Groundwater Conditions

2.5.4.6.1 Groundwater Measurements and Elevations

Groundwater conditions at the site are discussed in detail in Section 2.4.12, and only a summary is presented here. Groundwater is present in unconfined conditions in the Upper Sand Stratum and in confined conditions in the Lower Sand Stratum at the VEGP site. The Blue Bluff Marl is considered to be an aquiclude that separates the unconfined aquifer in the Upper Sand Stratum from the confined aquifer in the Lower Sand Stratum. The groundwater generally occurs at a depth of about 60 ft below the existing ground surface.

Fifteen observation wells were installed at the site during June and July 2005, before the start of the ESP subsurface investigation program. Ten of these wells were installed in the unconfined aquifer, and five were installed in the confined aquifer. Additionally, 22 existing wells were used as part of the groundwater monitoring program for the ESP study. Thirteen of these wells were installed in the unconfined aquifer, and nine were installed in the confined aquifer. The wells installed in the unconfined aquifer exhibit groundwater levels ranging from about El. 133 to El. 165 ft, while the wells installed in the confined aquifer exhibit groundwater levels ranging from about El. 82 to El. 128 ft. The logs and details of well installation and testing are contained in Appendix 2.4A and Appendix 2.5A. Hydraulic conductivity (slug) tests were performed in the wells installed during the ESP field investigation, as described in Section 2.5.4.3.2.3. Hydraulic conductivity (k) values for the unconfined aquifer in the Upper Sand Stratum, based on the slug test results, range from 4.4×10^{-5} to 9.3×10^{-4} cm/second, with a geometric mean of 1.75×10^{-4} cm/second. The hydraulic conductivity of the confined aquifer in the Lower Sand Stratum, based on the slug test results, ranges from 1.3×10^{-4} to 7.5×10^{-4} cm/second, with a geometric mean of 2.9×10^{-4} cm/second. A detailed description of groundwater conditions is provided in Section 2.4.12.

Groundwater levels at the site will require temporary dewatering of excavations extending below the water table during construction of new Units 3 and 4. Dewatering will be performed in a manner that will minimize drawdown effects on the surrounding environment and VEGP Units 1 and 2. Drawdown effects are expected to be limited to the VEGP site and to be negligible for VEGP Units 1 and 2. The relatively low permeability of the Upper Sand Stratum and underlying Blue Bluff Marl means that sumps and pumps should be sufficient for successful construction dewatering, as discussed in Section 2.5.4.6.2.

The design groundwater level for VEGP Units 3 and 4 will be taken at El. 165 ft msl based on the results of groundwater monitoring performed during a period of 10 years prior to the ESP subsurface investigation, and during the ESP subsurface investigation, as discussed in Section 2.4.12. This level corresponds to the design groundwater level for the existing VEGP Units 1 and 2. The static stability of the proposed structures based on this design groundwater level is discussed in Section 2.5.4.10.

2.5.4.6.2 Construction Dewatering

Dewatering for all major excavations could be achieved by gravity-type systems. Due to the relatively impermeable nature of the Upper Sand Stratum, sump-pumping of ditches will be adequate to dewater the soil. These ditches will be advanced below the progressing excavation grade.

During construction of VEGP Units 1 and 2, the excavation materials were dewatered by a series of ditches oriented in an east-west direction. They were connected by a north-south ditch, which drained to a sump in the southwest corner of the excavation. The sump was equipped with four pumps each with a capacity of 500 gal./min to remove inflows from groundwater. Additional capacity was provided for the removal of inflows of storm water in the excavation.

Similar dewatering procedures will be implemented during the excavation for VEGP Units 3 and 4.

2.5.4.7 Response of Soil and Rock to Dynamic Loading

All new safety-related structures will be founded on the planned structural backfill, which will completely replace the existing Upper Sand Stratum soils. The seismic acceleration at the sound bedrock level will be amplified or attenuated up through the soil and rock column. To estimate this amplification or attenuation, the following data are required.

- Shear wave velocity profile of the soils and rock
- Variation with strain of the shear modulus and damping values of the soils
- Site-specific seismic acceleration-time history

In addition, an appropriate computer program is required to perform the analysis.

2.5.4.7.1 Shear Wave Velocity Profile

2.5.4.7.1.1 Soil Shear Wave Velocity Profile

Various measurements have been made at the VEGP ESP site to obtain estimates of the shear wave velocity in the soil.

All safety-related structures will be founded on the structural backfill that will be placed on top of the Blue Bluff Marl after complete removal of the Upper Sand Stratum. Shear wave velocity was not determined for the compacted backfill during the ESP subsurface investigation. Data for existing Units 1 and 2 is used **(Bechtel 1984)**, and the backfill shear wave velocity values are summarized in Table 2.5.4-10. Additional evaluation of shear wave velocity of structural backfill will be performed for the COL application to confirm the values shown in Table 2.5.4-10.

Figure 2.5.4-6 shows the shear wave velocity values measured in the subsurface soil and rock strata for the ESP subsurface exploration program using suspension P-S velocity and CPT down-hole seismic testing. The shear wave velocity profile shown in Figure 2.5.4-7 is the profile interpreted from the results shown in Figure 2.5.4-6 for strata below the Upper Sand Stratum, plus the shear wave velocity values for the backfill shown on Table 2.5.4-10. The shear wave velocity values corresponding to the profile shown on Figure 2.5.4-7 for the different soil strata encountered by the borings are provided in Table 2.5.4-11.

The shear wave velocity profile shown in Figure 2.5.4-7 is used in the seismic amplification/attenuation analysis. The soil profile used consists of: Compacted backfill from 0 to 86 ft, Blue Bluff Marl from 86 to 149 ft, Upper Sand Stratum from 149 to 1,049 ft, Dunbarton Triassic Basin and Paleozoic Crystalline Rock below 1,049 ft.

2.5.4.7.1.2 Rock Shear Wave Velocity Profile

As discussed in Section 2.5.4.2.2, the VEGP ESP site sits on over 1,000 feet of Coastal Plain sediments underlain by Triassic Basin sedimentary rock, which in turn is underlain by Paleozoic crystalline rock (see Figure 2.5.1-40). For the purpose of subsequent site response analysis, for which input rock time histories must be inserted at a depth where the material shear-wave velocity is approximately 9,200 ft/s, it is necessary to know the shear-wave velocity profile and materials properties for the site down to the depth at which this velocity is encountered. Because the site overlies both Triassic Basin and Paleozoic crystalline rocks, it is necessary to consider effect of shear-wave velocities and material properties of both rock types and their geometries.

As indicated in Figure 2.5.4-6, the shear-wave velocities measured at the top of the Triassic Basin, even through the weathered portion, do not reach the velocity of 9,200 ft/s. Inspection of

available deep borehole shear-wave velocity at SRS **(SRS 2005)** along with the B-1003 data [Figure 2.5.4-8], however, suggests the following character of rock shear-wave in the Triassic Basin:

- A weathered zone of ~200 feet thickness occurs at the top of the Triassic Basin, characterized by a steep shear-wave velocity gradient, where the shear-wave velocity rapidly increases with depth to a point where a relatively high shear-wave velocity, but less than 9,200 ft/s is reached;
- Below the weathered zone the shear-wave velocity increases with a gentler gradient within the unweathered rock;
- Considering the SRS data as a guide for shear-wave velocity within deep portions of the Triassic Basin, there are a range of gentle gradients and a range of shear-wave velocities for the top of the unweathered Triassic Basin that could be considered as a continuation of the site-specific profile presented by B-1003.

Figure 2.5.1-41 indicates that the non-capable Pen Branch fault separates the Triassic Basin from the Paleozoic crystalline rocks. The structural geometry of these rock units and the fault, relative to the locations of boreholes B-1002 and B-1003 (approximate locations of the proposed nuclear units) and considering the velocity profiles shown in Figure 2.5.4-8, a shear-wave velocity profile through the Triassic Basin would not likely reach 9,200 ft/s before encountering the Paleozoic crystalline rock. Several observations and studies at SRS [e.g., (**Geovision 1999**, **Lee et al 1997**, **Domaracki 1994**)] indicate that the shear-wave velocity of the Paleozoic crystalline rock is at least 9,200 ft/s.

Therefore, to represent the variability of the depth at which the Paleozoic crystalline rock is encountered, with a shear-wave velocity of at least 9,200 ft/s, and the uncertainty of the shear-wave velocity gradient and velocity at the top of the unweathered Triassic Basin, six rock shear-wave velocity profiles were considered to comprise the base case used in the seismic amplification/attenuation analysis. Figure 2.5.4-7 shows a plot of these six rock shear-wave velocity profiles and Table 2.5.4-11, Part B presents their tabulation.

Figures 2.5.1-40 and Figure 2.5.4-8 suggest additional geometries for the shear-wave velocity profiles of the Triassic Basin and the Paleozoic crystalline rock that could impact site response. As interpreted in Figure 2.5.1-41, further to the northwest of the footprint of the project site the coastal Plain sediments would be underlain immediately by the Paleozoic crystalline rock. Conversely, further to the southeast of the footprint of the project, the Paleozoic crystalline rock is at such a depth that the shear-wave velocity gradient in the Triassic Basin would result in 9,200 ft/s being reached in the shear-wave velocity profile while still within the Triassic Basin. Close inspection of the DRB-9 shear-wave velocity profile in Figure 2.5.4-8 suggests a low-

velocity zone at the bottom of the Triassic Basin at the encountering of the Pen Branch fault. Sensitivity analyses were performed that indicated that alternate shear-wave velocity models suggested by these observations result in insignificant variations in the site response, relative to the six profiles that were explicitly considered, as discussed above.

2.5.4.7.2 Variation of Shear Modulus and Damping with Shear Strain

2.5.4.7.2.1 Shear Modulus

The variation of soil shear modulus values of sands, gravels, and clays with shear strain is well-documented by researchers such as Seed and Idriss (1970); Seed et al. (1984); and Sun et al. (1988). This research, along with additional work, has been summarized by EPRI **(EPRI TR-102293 1993)**.

Shear modulus is derived from the respective unit weight and shear wave velocity of the soil strata with the following equation:

$G_{max} = \rho \cdot (V_s)^2 = \gamma \cdot (V_s)^2/g$ Equation (20-27) on page 758 of Bowles (1982)

Shear wave velocity data are shown on Table 2.5.4-11. Unit weight data are shown on Table 2.5.4-1. Values for shear modulus are tabulated during analysis with the SHAKE 2000 program **(Bechtel 2000)**, and the low strain values are also shown on Tables 2.5.4-2 for the existing soils and rock, and on Table 2.5.4-10 for the compacted backfill.

From EPRI **(EPRI TR-102293 1993)**, the dynamic shear modulus reduction is derived in terms of depth for granular soils (Upper and Lower Sand Strata) and in terms of Plasticity Index (PI) for cohesive soils (Blue Bluff Marl).

The EPRI curves for sands **(EPRI TR-102293 1993, Figure 7.A-18)** were used to derive the shear modulus reduction factors for the granular soil strata (compacted backfill and Lower Sand Stratum). The EPRI curves for clays **(EPRI TR-102293 1993, Figure 7.A-16)** were used to derive the shear modulus reduction factors for the Lisbon Formation using PI = 25 percent. The shear modulus reduction factors are provided in Table 2.5.4-12 and Figure 2.5.4-9. These shear modulus degradation relationships were used in the SHAKE analysis. The shear modulus reduction factors developed for the neighboring Savannah River Site and contained in Lee (1996) were also used. The SRS-based shear modulus degradation relationships are provided in Table 2.5.4-13 and Figure 2.5.4-10.

Site-specific dynamic shear modulus reduction curves for the compacted backfill, Lisbon Formation, and Lower Sand Stratum will be developed for the COL.

2.5.4.7.2.2 Damping

The publications cited above address the variation of soil damping with cyclic shear strain as well as the variation of shear modulus with shear strain.

From EPRI **(EPRI TR-102293 1993)**, the damping ratio is derived in terms of depth for granular soils (Upper and Lower Sand Strata) and in terms of PI for cohesive soils (Blue Bluff Marl).

The EPRI curves for sands **(EPRI TR-102293 1993, Figure 7.A-19)** were used to derive the damping ratios for the granular soil strata (compacted backfill and Lower Sand Stratum). The EPRI curves for clays **(EPRI TR-102293 1993, Figure 7.A-17)** were used to derive the damping ratios for the Lisbon Formation using PI = 25 percent. The damping ratios are provided in Table 2.5.4-12 and Figure 2.5.4-11. These damping degradation relationships were used in the SHAKE analysis. The damping ratio values developed for the neighboring Savannah River Site and contained in Lee (1996) were also used. The SRS-based damping degradation relationships are provided in Table 2.5.4-13 and Figure 2.5.4-12.

After randomization, the damping curves were cut off at 15 percent damping ratio per NUREG-0800, Section 3.7.2 (1996).

Site-specific damping ratios for the compacted backfill, Lisbon Formation, and Lower Sand Stratum will be developed for the COL.

2.5.4.7.3 Soil/Rock Column Amplification/Attenuation Analysis

The SHAKE2000 **(Bechtel 2000)** computer program was used to compute the site dynamic responses for the soil/rock profiles described in Section 2.5.4.7.1. The computation was performed in the frequency domain using the complex response method. Section 2.5.2.5 describes in detail the soil/rock column amplification/attenuation analysis.

SHAKE2000 uses an equivalent linear procedure to account for the non-linearity of the soil by employing an iterative procedure to obtain values for shear modulus and damping that are compatible with the equivalent uniform strain induced in each sublayer. At the outset of the analysis, a set of properties (based on the values of shear modulus and damping presented in Section 2.5.4.7.1, and total unit weight) was assigned to each sublayer of the soil profile. The analysis was conducted using these properties, and the shear strain induced in each sublayer was calculated. The shear modulus and damping ratio for each sublayer was then modified based on the shear modulus and damping ratio versus strain relationships presented in Section 2.5.4.7.2. The analysis was repeated until strain-compatible modulus and damping values were achieved.

2.5.4.8 Liquefaction Potential

Soil liquefaction is a process by which loose, saturated, granular deposits lose a significant portion of their shear strength due to pore pressure buildup resulting from cyclic loading, such as that caused by an earthquake. Soil liquefaction can occur, leading to foundation bearing failures and excessive settlements, when all of the following criteria are met:

1. Design ground acceleration is high.

2. Soil is saturated (i.e., close to or below the water table).

3. Site soils are sands or silty sands in a loose or medium dense condition.

The naturally occurring Upper Sand Stratum soils at the VEGP site meet these three criteria. These soils consist of sands with varying fines content. An approximate 30-ft depth of the Upper Sand Stratum occurs beneath the groundwater table at a depth of 60 ft beneath the ground surface. The average corrected SPT N-value within the Upper Sand Stratum was 25 bpf, indicating a medium dense condition. The underlying Blue Bluff Marl soils are significantly cohesive, and the Lower Sand Stratum is sufficiently dense and deep; therefore, liquefaction is not a concern within these strata. The only material discussed here regarding liquefaction is the Upper Sand Stratum.

During construction of VEGP Units 1 and 2, the entire portion of the Upper Sand Stratum was removed and replaced with engineered fills due to susceptibility to liquefaction. A similar excavation will be executed for VEGP Units 3 and 4.

In Section 2.5.4.8.1, Regulatory Guide 1.198, *Procedures and Criteria for Assessing Seismic Soil Liquefaction at Nuclear Power Plant Sites*, US Nuclear Regulatory Commission, November 2003 (RG 1.198) is used as a guide.

2.5.4.8.1 Acceptable Factor of Safety Against Liquefaction

RG 1.198 states that factors of safety (FS) $\leq$ 1.1 against liquefaction are considered low, FS $\approx$ 1.1 to 1.4 are considered moderate, and FS $\geq$ 1.4 are considered high. The Committee of Earthquake Engineering of the National Research Council **(NRC/NAP 1985)** states:

> *There is no general agreement on the appropriate margin (factor) of safety, primarily because the degree of conservatism thought desirable at this point depends upon the extent of the conservatism already introduced in assigning the design earthquake. If the design earthquake ground motion is regarded as reasonable, a safety factor of 1.33 to 1.35...is suggested as adequate. However, when the design ground motion is excessively conservative, engineers are content with a safety factor only slightly in excess of unity.*

2.5.4.8.2 Previous Liquefaction Analyses

The liquefaction potential of the Upper Sand Stratum was previously evaluated using the standard penetration test blow counts obtained during the investigations for VEGP Units 1 and 2 and the simplified procedure of Seed and Idriss. This evaluation indicated that the Upper Sand Stratum below the groundwater table was susceptible to liquefaction when subjected to the maximum SSE acceleration of 0.2g developed for VEGP Units 1 and 2. Based on this evaluation, the Upper Sand Stratum was removed to an approximate elevation of 130 to 135 ft in the VEGP Units 1 and 2 power block area. Select sand and silty sand compacted to 97 percent of the maximum density determined by ASTM D 1557 was placed from the top of the Blue Bluff Marl stratum to the design elevation of the various power block structures with the exception of an area north of the turbine building. The liquefaction potential of compacted backfill in the power block area was evaluated, and the analysis indicated a factor of safety against liquefaction on the order of 1.9 to 2.0. The analysis was done utilizing cyclic strength data (PSAR data) obtained from tests on specimens of compacted backfill.

During the investigations for borrow sources for VEGP Units 1 and 2, additional dynamic data (borrow source data) were obtained to supplement the cyclic strength data for the compacted fill. Cyclic triaxial tests were performed on compacted specimens of sands obtained from stockpiles and borrow areas. The cyclic stress ratios versus the number of cycles to 2.5 percent total strain (initial liquefaction) showed that the stress ratios for the cleaner sands were substantially lower than for silty sands. In the liquefaction analysis performed using the PSAR data, stress ratios for the cleaner sands were used to obtain the safety factor against liquefaction. Therefore, the cyclic stress ratios for the cleaner sands obtained during investigations for borrow material were compared with values obtained during the PSAR investigations. A comparison of the two test data (PSAR data versus borrow source data) indicates that the PSAR data represent a lower bound of test values. If the liquefaction analysis were performed using the upper bound values (borrow source data), a factor of safety higher than 1.9 to 2.0 would have been obtained for the design SSE conditions.

From the discussion presented above for the VEGP Units 1 and 2, it is concluded that there exists an adequate factor of safety against liquefaction for backfill compacted to 97 percent of the maximum density obtained by ASTM D 1557.

2.5.4.8.3 Liquefaction Analyses Performed for the ESP Application

Based on previous investigations and excavation completed for the existing VEGP Units 1 and 2 and their proximity to proposed VEGP Units 3 and 4, the Upper Sand Stratum will be completely removed and replaced with select compacted non-liquefiable fills back to the plant grade within the footprint of the planned power block.

Because select compacted non-liquefiable fills will be used to replace the Upper Sand Stratum in the power block area of proposed VEGP Units 3 and 4, no liquefaction study was performed for this ESP investigation. Confirmatory liquefaction analysis will proceed once backfill materials are determined during the COL phase of the project.

2.5.4.8.4 Liquefaction Conclusions

Based on the foregoing sections on the analysis of liquefaction potential, the following conclusions are made:

- Only the Upper Sand Stratum below the groundwater table falls into the gradation and relative density categories where liquefaction would be considered possible.
- The Upper Sand Stratum was completely removed and replaced with compacted structural fill before construction of the existing VEGP Units 1 and 2. The same approach will be used before construction of the proposed VEGP Units 3 and 4.
- The compacted structural fill, consisting of sands and silty sands, at VEGP Units 1 and 2 provides an adequate factor of safety against liquefaction (minimum 1.9 to 2.0). Similar soils and compaction effort will be used for construction of VEGP Units 3 and 4.

Confirmatory analysis to determine a factor of safety of the compacted structural fill against liquefaction will be performed during the COL phase of the project.

2.5.4.9 Earthquake Design Basis

The Safe Shutdown Earthquake (SSE) is derived and discussed in detail in Sections 2.5.2.6 and 2.5.2.7.

The Operating Basis Earthquake (OBE) is discussed in Section 2.5.2.8.

2.5.4.10 Static Stability

All safety-related structures will be founded on the structural backfill that will be placed on top of the Blue Bluff Marl after complete removal of the Upper Sand Stratum. The base of the Containment and Auxiliary Building foundations for VEGP Units 3 and 4 will be about El. 180 ft msl. This level corresponds to a depth of 40 ft below final grade (below El. 220 ft msl), or 50 to 60 ft above the top of the Blue Bluff Marl bearing stratum based on the borings completed during the ESP subsurface investigation. Other foundations in the power block area will be placed at depths of about 4 ft below final grade. The following sections on bearing capacity and settlement focus on these two scenarios.

2.5.4.10.1 Bearing Capacity

The allowable bearing capacity values for foundations placed at a depth of 4 ft below finish grade in Figure 2.5.4-13.

The allowable bearing capacity values are based on Terzaghi's bearing capacity equations modified by Vesic (1975), using the effective angle of friction provided for compacted fills beneath VEGP Units 1 and 2, that is shown on Table 2.5.4-1. The effects of the Blue Bluff Marl on the allowable bearing pressures shown in Figure 2.5.4-13 were evaluated using procedures outlined by Vesic (1975).

The allowable bearing capacity of the containment building foundation was calculated using the same assumptions summarized in the previous paragraph. For calculation purposes, the containment building mat was modeled as a circle with a diameter of about 142 ft placed at a depth of 39.5 ft below finish grade. The calculated allowable bearing pressure is 30.7 ksf under static loading conditions, and 46 ksf under dynamic loading conditions.

Section 2.5.4.10.2 contains the results of settlement analyses performed for typical foundations.

2.5.4.10.2 Settlement Analysis

For the large mat foundations that support the major power plant structures, general considerations based on previous site experience **(Bechtel 1986)** indicate that the total settlement can exceed the suggested limit of 2 in. encountered in the geotechnical literature (Peck et al. 1974). Settlement monitoring of VEGP Units 1 and 2 **(Bechtel 1986)** disclosed foundation settlements ranging from 2.7 to 3.2 in. for the containment buildings, versus calculated/design values of 4.0 to 4.3 in. Similar results were obtained for the control building (measured settlements ranging from 1.1 to 1.9 inches versus calculated/design values of 3.2 to 3.4 in.), auxiliary building (measured settlements ranging from 2.9 to 3.3 in. versus calculated/design values of 4.4 to 4.6 in.), and the NSCW towers (measured settlements ranging from 2.5 to 3.6 in. versus calculated/design values of 4.5 to 4.8 in.).

The measured differential settlements between mats of Units 1 and 2 **(Bechtel 1986)**, which can affect pipe connections, was generally within the suggested limit of ¾ in. encountered in the geotechnical literature **(Peck et al. 1974)**. The measured differential settlements within structures of Units 1 and 2 were smaller than the design limit of 1/670.

It is noted that settlements reported in Bechtel (1986) were essentially elastic, i.e., they took place during construction. This reflects the elastic nature of the compacted backfill, the heavily overconsolidated Blue Bluff Marl, and the underlying Lower Sand Stratum.

For footings that support smaller plant components, the total settlement can be limited to 1 inch, while the differential settlement between footings can be limited to ½ in. **(Peck et al. 1974)**.

The general approach used for Units 1 and 2 consisted of estimating total and differential settlements for powerblock structures and using them as design values. A detailed settlement monitoring program was established, and monitored settlements were compared with the design values. Reanalysis and/or corrective measures were employed if monitored settlements exceeded design values. An additional strategy consisted of installing pipes as late in the construction schedule as practicable and installing pipe supports only when construction of the structure the pipe was connected to was essentially complete. A similar approach will be developed for Units 3 and 4, and design values will be established for the COL.

2.5.4.10.2.1 Settlement of Compacted Fills

Any settlement of the compacted fill is essentially elastic and will occur during the construction period. Typical foundations have been analyzed for settlement assuming a profile consisting of 79 ft of compacted fills underlain by the Blue Bluff Marl and then the Lower Sand Stratum. The stiffness values used are the high-strain elastic modulus values given in Table 2.5.4-1 for the compacted fill, Blue Bluff Marl and Lower Sand Stratum. The foundations that were analyzed were square and rectangular with foundation length equal to twice the foundation width. An average bearing pressure of 5 ksf was used in the settlement analyses. The computed total settlements of these foundations are shown on Figure 2.5.4-14.

The settlement of the containment building foundation was calculated using the same assumptions summarized in the previous paragraph. For calculation purposes, the containment building mat was modeled as a circle with a diameter of about 142 ft placed at a depth of 39.5 ft below finish grade. The calculated settlement under an average bearing pressure of 5 ksf was 1.6 in.

2.5.4.10.2.2 Settlement of Blue Bluff Marl

Settlement at the VEGP site is only a consideration for structures that would be founded directly on the compacted fills. The underlying materials consist of hard clay Blue Bluff Marl consolidated under approximately 90 ft of overburden, and dense Lower Sand Stratum. Minimal settlement of these strata would be anticipated under planned structure loads.

2.5.4.11 Design Criteria

The design criteria are covered in various sections of the SSAR. The criteria summarized below are considered geotechnical criteria. Other geotechnically related criteria that pertain to structural design (such as wall rotation, sliding, or overturning) are not included.

Section 2.5.4.8 specifies that the acceptable factor of safety against liquefaction of site soils should be ≥ 1.35.

Bearing capacity and settlement criteria are presented in Section 2.5.4.10. Figure 2.5.4-13 provides allowable bearing capacity values for typical foundations placed at a depth of 4 ft below finish grade. The allowable bearing capacity values shown on Figure 2.5.4-13 do not take into consideration foundation settlements. Total and differential settlement criteria will be developed for the COL and will follow the approach used for VEGP Units 1 and 2 that is described in Section 2.5.4.10.2.

Section 2.5.5.2 specifies that the minimum acceptable long-term static factor of safety against slope stability failure is 1.5. Section 2.5.5.3 specifies that the minimum acceptable long-term seismic factor of safety against slope stability failure is 1.1.

2.5.4.12 Techniques to Improve Subsurface Conditions

For the ESP investigation, ground improvement techniques were not considered beyond the removal and replacement of the Upper Sand Stratum. Additional ground improvement methods will be considered as warranted for specific locations of the project during the COL phase. For areas outside the power block excavation, surficial ground can be improved through densification with heavy vibratory rollers. Other ground improvement methods and the use of piles will be considered as warranted.

Table 2.5.4-1 Static Engineering Properties of Subsurface Materials

Parameter[1]	Stratum			
	Upper Sand	Compacted Structural Fill	Blue Bluff Marl	Lower Sand
Depth range below El. 220 ft, feet	79 to 124	79 to 124	63 to 95	900
Average thickness, feet	92	92	76	900
USCS symbol	SP/SM/SC/ML	SP/SM/SC	CL/ML	SP/SM/ML
Natural moisture content (ω), %	N/A	N/A	35	N/A
Unit weight (pcf)	115	123 (moist) 133 (saturated)	115	115
Atterberg limits				
Liquid limit (LL), %	N/A[2]	N/A	51	N/A
Plastic limit (PL), %	N/A	N/A	26	N/A
Plasticity index (PI), %	N/A	N/A	25	N/A
Measured SPT N-value, bpf	20	N/A	80	50
Adjusted SPT N_{60}-value, bpf	25	N/A	100	62
Strength properties				
Undrained shear strength (c_u), ksf	-	0	10	0
Internal friction angle (Ø'), degrees	34	34	0	34
Elastic modulus (high strain) (E_s), ksf	900	1,500	10,000	10,800[3] 13,500[4]
Shear modulus (high strain) (G_s), ksf	350	600	3,500	4,200[3] 5,200[4]
Shear modulus (low strain) (G_{max}), ksf	3088	3820	20,475	20,538
Coefficient of Subgrade Reaction (k_1), tcf	N/A	300	N/A	N/A
Earth Pressure Coefficients				
Active (K_a)	N/A	0.3	N/A	N/A
Passive (K_p)	N/A	3.5	N/A	N/A
At Rest (K_0)	N/A	0.5	N/A	N/A
Coefficient of Sliding	N/A	0.45	N/A	N/A
Poison's Ratio	0.09-0.49		0.33-0.48	0.32-0.49

Notes.
[1]The values tabulated above are for use as a design guideline only. Reference should be made to specific boring and CPT logs and laboratory test results for appropriate modifications at specific design locations.
[2]N/A indicates that the properties were not measured or are not applicable.
[3]This value applies between depth of 0 to 100 ft below the bottom of the Blue Bluff Marl.
[4]This value applies between depth of 100 to 300 ft below the bottom of the Blue Bluff Marl.
Engineering properties for the Dunbarton Triassic Basin are not included because the rock is too deep to be of interest for foundation design.
Dynamic properties, including those for the Dunbarton Triassic Basin, can be derived from the shear wave velocity profile shown on Table 2.5.4-10.

Table 2.5.4-2 Design Dynamic Shear Modulus

Geologic Formation	Depth (ft)	Elevation (ft)	G_{max} (ksf)
Upper Sand Stratum (Barnwell Group)	0 to 16	223 to 207	7,000
	16 to 41	207 to 182	2,286
	41 to 58	182 to 165	2,580
	58 to 86	165 to 137	2,893
Blue Bluff Marl (Lisbon Formation)	86 to 92	137 to 131	6,978
	92 to 97	131 to 126	10,321
	97 to 102	126 to 121	15,750
	102 to 105	121 to 118	10,321
	105 to 111	118 to 112	17,286
	111 to 123	112 to 100	19,723
	123 to 149	100 to 74	25,080
Lower Sand Stratum (Still Branch)	149 to 156	74 to 67	14,286
	156 to 216	67 to 7	9,723
(Congaree)	216 to 331	7 to -108	13,580
(Snapp)	331 to 438	-108 to -215	15,009
(Black Mingo)	438 to 477	-215 to -254	19,723
(Steel Creek)	477 to 587	-254 to -364	25,080
(Gaillard/Black Creek)	587 to 798	-364 to -575	29,009
(Pio Nono)	798 to 858	-575 to -635	29,418
(Cape Fear)	858 to 1,049	-635 to -826	26,229
Dunbarton Triassic Basin	1,049		

Note: G_{max} was calculated using γ from Table 2.5.4-1, and the shear wave velocity values from Table 2.5.4-6.

Table 2.5.4-3 Types and Numbers of Laboratory Tests Completed for the ESP Application

Type of Test	Number of Tests Performed
Grain size	61
Unit Weight	31
Natural Moisture Content	75
Atterberg Limits	27
UU Triaxial (1-point)	15

This page is intentionally blank.

Table 2.5.4-4 Summary of Laboratory Tests Performed on Selected Soils Samples from ESP Borings

SAMPLE DETAILS						SOIL TESTING							
Boring No.	Top Depth (ft)	Length (ft)	Type	Formation	SPT N-value (bpf)	% Fines	γ (pcf)	ω_N (%)	PL (%)	LL (%)	PI (%)	USCS Classification	UU s_u (ksf)
B-1002	7.5	1.5	SS	Fill	20	9.4		6.2					
	18.5	1.5	SS	Barnwell	19	37.1		24.4					
	28.5	1.5	SS	Barnwell	8	24.9		31.8					
	33.5	1.5	SS	Barnwell	6	31.6		58.8					
	38.5	1.5	SS	Barnwell	7			92.8	27	48	21		
	53.5	1.5	SS	Barnwell	8	10.5		42.9					
	63.5	1.5	SS	Barnwell	13	7.2		29.3					
	73.5	1.5	SS	Barnwell	12	10		24.5					
	83.5	1.5	SS	Barnwell	9	6.1		27.6					
	92.0	2.5	UD-Upper	Lisbon	N/A	28.9	103.6	52.1	37	72	35	GM	1.15
			UD-Middle				102.4						3.35
	103.5	2.5	UD	Lisbon	N/A	35.9	114.3	56.6	22	34	12	CL	
							114.5	26.5					2.4
	113.5	2.5	UD	Lisbon	N/A	33.8	132.8	25.5	19	29	10	SC	
							132.9	16.3					2.15
	123.5	2.5	UD	Lisbon	N/A	24.5	140.2	13.5	17	22	5	GC-GM	
	133.5	2.0	UD	Lisbon	N/A	24.3	118.0	28.6	25	32	7	SM	
							118.1	29.8					2.4
	153.5	1.5	SS	Lisbon	27	39.4		23.3	21	34	13	ML	
	188.5	1.5	SS	Still Branch	9	6.6		40.7	NP	NP	NP	SM	
	238.5	1.5	SS	Congaree	77	12.3		18.5					
B-1003	15	5	C	Barnwell	N/A	20.9		13.4					
	35	5	C	Barnwell	N/A	29.8		42.1					
	55	5	C	Barnwell	N/A	13.4		17.5					
	75	5	C	Barnwell	N/A	8.2		32.3					

This page is intentionally blank.

Table 2.5.4-4 (cont.) Summary of Laboratory Tests Performed on Selected Soils Samples from ESP Borings

SAMPLE DETAILS						SOIL TESTING							
Boring No.	Top Depth (ft)	Length (ft)	Type	Formation	SPT N-value (bpf)	% Fines	γ (pcf)	ω_N (%)	PL (%)	LL (%)	PI (%)	USCS Classification	UU s_u (ksf)
B-1003	88	5	C	Lisbon	N/A	33.4		67.4	42	93	51	SM	
	93	2.5	UD-1	Lisbon	N/A	40.6	115.7	30.6	32	54	22	SM	
							115.8	29.5					4.3
	104.7	2	C	Lisbon	N/A	31.7	111.5	40.6	51	83	32	SM	
	121.7	5	C	Lisbon	N/A	42.5	122.5	28.0	NP	NP	NP	SM	
	141.7	5	C	Lisbon	N/A	34.2	126.1	25.9	28	46	18	SM	
B-1003	165.7	5	C	Still Branch	N/A	5.4	121.7	23.6	NP	NP	NP	SP-SM	
	185.7	5	C	Still Branch	N/A	16.4		32.3					
	205.7	5	C	Still Branch	N/A	21.4		39.3					
	240.7	5	C	Congaree	N/A	10.9		23.2					
	280.7	5.0	C	Congaree	N/A	14.2		23.2					
	315.7	5.0	C	Congaree	N/A	3.3		32.7	38	53	15	GW	
							119.4	31.0					
	350.7	5.0	C	Snapp	N/A	78.5	128.3	21.3	22	41	19	ML	
	400.7	5.0	C	Snapp	N/A	15.8		18.9					
	450.7	5.0	C	Black Mingo	N/A	15.9		28.6					
	496.7	5.0	C	Steel Creek	N/A	13.2		26.4					
B-1004	9.0	1.5	SS	Barnwell	13	24.4		13.8					
	12.0	1.5	SS	Barnwell	12	23.1		14.5					
	23.5	1.5	SS	Barnwell	8	14.9		18.5					
	43.5	1.5	SS	Barnwell	4	60.0		46.2	24	58	34	ML	
	53.5	1.5	SS	Barnwell	7	41.0		62.9					
	68.5	1.5	SS	Barnwell	6	19.9		24.1					
	83.5	1.5	SS	Barnwell	6	11.5		28.8					
	123.5	1.5	SS	Barnwell	5	19.2		19.7	19	43	24	GM	

This page is intentionally blank.

Table 2.5.4-4 (cont.) Summary of Laboratory Tests Performed on Selected Soils Samples from ESP Borings

SAMPLE DETAILS						SOIL TESTING							
Boring No.	Top Depth (ft)	Length (ft)	Type	Formation	SPT N-value (bpf)	% Fines	γ (pcf)	ω_N (%)	PL (%)	LL (%)	PI (%)	USCS Classification	UU s_u (ksf)
B-1004	144.0	1.5	UD-Upper	Lisbon	N/A	46.3	105.1	44.6	38	59	21	SM	
							105.2	52.0					0.15
			UD-Middle				114.2	29.8					0.8
	153.5	1.5	UD	Lisbon	N/A	41.7		30.1	27	43	16	SM	
							117.4	25.2					
							119.3	28.7					3.75
	163.5	2.5	UD-Upper	Lisbon	N/A	32.2		25.1	22	31	9	GM	
							117.4	30.2					1.05
			UD-Middle				125.6	24.5					1.2
	177.0	2.5	UD-Upper	Lisbon	N/A	41.7	124.7	20.8	22	31	9	SM	
							124.6	22.4					0.8
			UD-Middle				131.8	39.2					1.9
B-1004	188.5	2.0	UD	Lisbon	N/A	23.8	120.4	29.0	27	34	7	SM	
							120.6	28.4					4.0
	198.5	2.0	UD	Lisbon	N/A	34.5	128.1	26.2	21	31	10	SM	
							128.2	21.7					3.0
B-1006	7.5	1.5	SS	Barnwell	3	7.3		3.8					
	33.5	1.5	SS	Barnwell	13	26.1		19.7					
	58.5	1.5	SS	Barnwell	W HAMM	58.3		92.8	30	97	67	CH	
	68.5	1.5	SS	Barnwell	W HAMM	3.1		25.4					
	88.5	1.5	SS	Barnwell	W HAMM	15.7		51.9					
	108.5	1.5	SS	Barnwell	42	21.5		22.0					
	123.5	1.5	SS	Lisbon	50/2"	64.1		53.7	43	99	56	MH	

This page is intentionally blank.

Table 2.5.4-4 (cont.) Summary of Laboratory Tests Performed on Selected Soils Samples from ESP Borings

SAMPLE DETAILS						SOIL TESTING							
Boring No.	Top Depth (ft)	Length (ft)	Type	Formation	SPT N-value (bpf)	% Fines	γ (pcf)	ω_N (%)	PL (%)	LL (%)	PI (%)	USCS Classification	UU s_u (ksf)
B-1010	7.5	1.5	SS	Barnwell	27	7.8		5.7					
	33.5	1.5	SS	Barnwell	23	17.0		18.9					
	58.5	1.5	SS	Barnwell	19	13.3		27.3					
	73.5	1.5	SS	Barnwell	6	23.9		30.8					
	98.5	1.5	SS	Lisbon	77	44.9		49.9	36	94	58	CH	

Legend: NP = non-plastic

ω_N = natural moisture content

γ = unit weight

% Finer = % finer than the #200 sieve

PL = plastic limit

LL = liquid limit

PI = plasticity index

UU s_u = undrained strength from UU triaxial test

SS = split spoon or split barrel sample

UD = undisturbed sample

UD-Upper = test specimen taken from top of UD sample

UD-Middle = test specimen taken from middle of UD sample

C = soil core

W HAMM = weight of hammer (sampler penetrated at least 18" under the weight of the hammer, no blows applied by the hammer)

This page is intentionally blank.

Table 2.5.4-5 Summary of SPT N-Values Measured at the ESP Borings

Boring Number	Measured SPT N-value (blows/ft) for Different Formations		
	Upper Sand Stratum (Barnwell Group)	Blue Bluff Marl (Lisbon Formation)	Lower Sand Stratum
B-1001	47, 32, 22, 22, 22, 23, 21, 23, 23, 37, 13, 10, 7, 5, 6, 12, 13, 30, 11, 37, 36, 47, WOR, 50/5"	50/5", 50/4", 51, 50/4", 50/6", 50/4", 50/5"	Not measured
B-1002	30, 67, 28, 33, 19, 10, 8, 6, 7, 12, 22, 8, 11, 13, 18, 12, 10, 9	77/11", 68/7", 54, 72, 50/2", 78/8", 65, 40, 27	46, 26, 50/4", 40, 9, 43, 32, 41, 50, 77
B-1004	21, 24, 25, 16, 16, 13, 19, 12, 14, 10, 8, 17, 13, 14, 4, 5, 7, 7, 18, 6, 5, 9, 5, 5, 17, 11, 16, 20, 18, 34, 5, 9, 50/5"	77, 50/4", 50/0", 50/3", 50/3", 77, 79, 50/5", 50/4", 70/10", 81, 78, 58	79/10", 35, 50/5", 95, 47, 104
B-1005	27, 29, 26, 15, 11, 11, 10, 17, 13, 19, 17, 19, 11, 7, WOH, 37, 17, 34, 28, 25, 50/1", 56, 37, 69, 46, 54, 57, 33, 31, 37, 95, 30, 32, 50/4", 80/9", 39	50/5", 50/4"	Not measured
B-1006	19, 20, 15, 9, 2, 3, 4, 8, 10, 11, 30, 24, 17, 13, 10, 2, 8, 7, WOH, 9, WOH, WOH, 13, 7, WOH, 14, 19, 28, 42, 50	50/5", 50/2"	Not measured
B-1007	30, 32, 10, 10, 8, 14, 23, 20, 27, 26, 31, 25, 23, 15, 15, 24, 21, 26, 36, 37, 27, 36, 18, 13	50/2", 50/3", 45, 50/2", 50/5", 50/4", 74	Not measured
B-1008	19, 30, 53, 67, 34, 31, 19, 24, 30, 36, 30, 20, 17, 17, 25, 18, 22, 33, 39, 22, 25, 50/5", 50/4", 50/5"	46, 65, 53, 71/9", 50/3", 50/3", 50/4"	Not measured
B-1009	19, 37, 42, 44, 20, 21, 27, 21, 20, 30, 29, 35, 19, 31, 37, 42, 23, 13, 27, 32, 20, 8, 10, 40, 24	51, 50/5"	Not measured
B-1010	13, 18, 29, 24, 20, 27, 9, 13, 18, 29, 72, 23, 27, 23, 30, 26, 15, 34, 19, 6, 28, 6, 20, 10, 15, 21	67, 50/4"	Not measured
B-1011	8, 7, 11, 10, 14, 15, 15, 20, 13, 44, 42, 12, 25, 48, 28, 41, 37, 49, 60, 40, 50/0", 50/4"	69, 74, 50/3", 50/1", 36	Not measured
B-1013	9, 14, 26, 26, 12, 26, 26, 33, 9, 22, 16, 41, 16, 34, 22, 25, 21, 28, 12, 26, 15, 8, 18, 36, 13, 26	50/2", 76	Not measured
Range:	WOR-50/0"	27-50/1"	9-50/4"
Average:	25	83	59
Median	21	100	47

NOTES:
[a]SPT blow counts will be adjusted to reflect the measured hammer efficiencies.
[b]WOR means that the sampler penetrated 18" or more under weight of the rods, and WOH means that the sampler penetrated 18" or more under weight of the rods and hammer. These values were taken as zero when calculating the average.
[c]SPT blow counts linearly extrapolated to more than 100 bpf were truncated at 100 bpf when calculating the average.
[d]SPT N-values shown for the Barnwell Group exclude measurements in the fill layers encountered at borings B-1001, B-1002, B-1004, and B-1005.

This page is intentionally blank.

Table 2.5.4-6 Typical Shear Wave Velocity Values for Existing Strata

Geologic Formation	Depth (ft)	Elevation (ft)	V_s (fps)
Upper Sand Stratum (Barnwell Group)	0 to 16	223 to 207	1,400
	16 to 41	207 to 182	800
	41 to 58	182 to 165	850
	58 to 86	165 to 137	900
Blue Bluff Marl (Lisbon Formation)	86 to 92	137 to 131	1,400
	92 to 97	131 to 126	1,700
	97 to 102	126 to 121	2,100
	102 to 105	121 to 118	1,700
	105 to 111	118 to 112	2,200
	111 to 123	112 to 100	2,350
	123 to 149	100 to 74	2,650
Lower Sand Stratum (Still Branch)	149 to 156	74 to 67	2,000
	156 to 216	67 to 7	1,650
(Congaree)	216 to 331	7 to -108	1,950
(Snapp)	331 to 438	-108 to -215	2,050
(Black Mingo)	438 to 477	-215 to -254	2,350
(Steel Creek)	477 to 587	-254 to -364	2,650
(Gaillard/Black Creek)	587 to 798	-364 to -575	2,850
(Pio Nono)	798 to 858	-575 to -635	2,870
(Cape Fear)	858 to 1,049	-635 to -826	2,710
Dunbarton Triassic Basin	1,049	-826	2,710
	1,093	-870	5,300
	1,323	-1,100	7,800

Table 2.5.4-7 Summary of ESP Borings and CPTs

Boring Number	Plant Coordinates		State Coordinates		Elevation (ft msl)	Depth (ft)
	Northing (ft)	Easting (ft)	Northing (ft)	Easting (ft)		
B-1001	7,662	6,220	1,142,662	620,220	221.64	123.9
B-1002[a, b]	7,999	6,985	1,142,999	620,985	221.98	260
B-1002A[a, d]	7,986	6,986	1,142,986	620,986	222.27	105
B-1003[a, b, c]	7,974	7,890	1,142,974	621,890	223.21	1338
B-1004[a, b]	7,985	6,131	1,142,985	620,131	249.78	304
B-1005	8,992	6,155	1,143,992	620,155	253.14	164.3
B-1006	8,810	7,343	1,143,810	621,343	255.95	124.2
B-1007	7,662	7,120	1,142,662	621,120	221.02	125
B-1008	7,671	7,996	1,142,671	621,996	219.51	124.3
B-1009	6,001	6,361	1,141,001	620,361	220.39	98.9
B-1010	6,000	7,280	1,141,000	621,280	218.60	104.3
B-1011	8,741	8,378	1,143,741	622,378	219.38	100
B-1013	5,976	8,272	1,140,976	622,272	218.62	105
C-1005A[a, d]	7,990	8,179	1,142,990	622,179	223.66	90
CPT Number	**Plant Coordinates**		**State Coordinates**		**Elevation (ft msl)**	**Depth (ft)**
	Northing (ft)	**Easting (ft)**	**Northing (ft)**	**Easting (ft)**		
C-1001A	8,028	6,356	1,143,028	620,356	248.57	116.7
C-1002	7,668	6,575	1,142,668	620,575	222.13	78.5
C-1003[e, f]	7,669	7,478	1,142,669	621,478	219.80	80
C-1004[f]	7,646	8,362	1,142,646	622,362	220.82	77
C-1005[e, f]	7,995	8,175	1,142,995	622,175	223.81	82
C-1006	8,001	7,262	1,143,001	621,262	222.80	74
C-1007	8,271	8,055	1,143,271	622,055	222.81	81.7
C-1008	8,268	6,931	1,143,268	620,931	221.30	76
C-1009A[e, f]	5,980	6,798	1,140,980	620,798	218.93	99
C-1010	6,008	7,754	1,141,008	621,754	219.06	96

[a] Location of suspension P-S velocity logging.

[b] Location of caliper, natural gamma, resistivity, and spontaneous potential measurements.

[c] Location of borehole deviation survey.

[d] Boreholes drilled without sampling to allow the performance of suspension P-S velocity logging above the zone of drilling fluid loss.

[e] Location of seismic CPT.

[f] Location of pore pressure dissipation tests.

Note: State Plane Coordinates are from NAD27 Georgia East state grid system. Plant coordinates are converted from the following formula:
Plant North + 1,135,000 = State North
Plant East + 614,000 = State East

Table 2.5.4-8 Summary of Undisturbed Samples of the Blue Bluff Marl

Boring Number	Sample Number	Depth at Top of Sample (ft)	Length of Sample (in.)
B-1002	UD-1	92.0	30
B-1002	UD-2	103.5	30
B-1002	UD-3	113.5	30
B-1002	UD-4	123.5	30
B-1002	UD-5	133.4	30
B-1003	UD-1	92.0	30
B-1004	UD-1	144.0	18
B-1004	UD-2	148.5	18
B-1004	UD-3	163.5	30
B-1004	UD-4	177.0	30
B-1004	UD-5	188.5	30
B-1004	UD-6	198.5	30

Table 2.5.4-9 Summary of SPT Hammer Energy Transfer Efficiency

Borehole and Sample Number	Energy Transfer Efficiency (%)
B1013-SS5	65
B1013-SS8	70
B1013-SS10	68
B1013-SS13	71
B1013-SS14	72
B1013-SS15	73
B1008-SS26	79
B1008-SS27	75
B1008-SS28	75
B1006-SS7	71
B1006-SS8	74
B1006-SS10	77
B1006-SS15	85
B1006-SS16	86
B1006-SS17	87
B1006-SS26	83
B1006-SS27	80
B1006-SS28	82
Range:	65-87
Average:	76
Median:	75

Table 2.5.4-10 Estimated Shear Wave Velocity and Dynamic Shear Modulus Values for the Compacted Backfill

Depth (ft)	V_s [(1)] (fps)	G_{max} [(2)] (ksf)
0 to 6	573	1,255
6 to 10	732	2,049
10 to 14	811	2,510
14 to 18	871	2,898
18 to 23	927	3,280
23 to 29	983	3,694
29 to 36	1040	4,130
36 to 43	1092	4,553
43 to 50	1137	4,940
50 to 56	1175	5,274
56 to 63	1209	5,588
63 to 71	1232	5,796
71 to 79	1253	6,001
79 to 86	1273	6,186

(1) From Figure 6-1 of **Bechtel (1984)**.
(2) G_{max} were calculated using γ from Table 2.5.4-1.

Table 2.5.4-11 Shear Wave Velocity Values for Site Amplification Analysis Part A: Soil Shear-Wave Velocities

Geologic Formation	Depth (feet)	V_s (fps)
Compacted Backfill	0 to 6	573
	6 to 10	732
	10 to 14	811
	14 to 18	871
	18 to 23	927
	23 to 29	983
	29 to 36	1,040
	36 to 43	1,092
	43 to 50	1,137
	50 to 56	1,175
	56 to 63	1,209
	63 to 71	1,232
	71 to 79	1,253
	79 to 86	1,273
Blue Bluff Marl (Lisbon Formation)	86 to 92	1,400
	92 to 97	1,700
	97 to 102	2,100
	102 to 105	1,700
	105 to 111	2,200
	111 to 123	2,350
	123 to 149	2,650
Lower Sand Stratum (Still Branch)	149 to 156	2,000
	156 to 216	1,650
(Congaree)	216 to 331	1,950
(Snapp)	331 to 438	2,050
(Black Mingo)	438 to 477	2,350
(Steel Creek)	477 to 587	2,650
(Gaillard/Black Creek)	587 to 798	2,850
(Pio Nono)	798 to 858	2,870
(Cape Fear)	858 to 1,049	2,710
Dunbarton Triassic Basin & Paleozoic Crystalline Rock	> 1,049	see Table 2.5.4-11, Part B

Table 2.5.4-11 Shear Wave Velocity Values for Site Amplification Analysis Part B: Rock Shear-Wave Velocities - Six Alternate Profiles

	Vs (ft/s)	
Depth (ft)	**Gradient #1**	**Gradient #2**
1,049 to 1,100	4,400	4,400
1,100 to 1,150	5,650	5,650
1,150 to 1,225	6,650	6,650
1,225 to 1,337.5	7,600	7,600
1,337.5 to 1,402.5	8,000	8,700
1,402.5 to 1,405	8,005	8,703
1,405 to 1,525	8,059	8,739
> 1,525	9,200	9,200

Rock Vs profile corresponding to the location midway between B-1002 and B-1003.

	Vs (ft/s)	
Depth (ft)	**Gradient #1**	**Gradient #2**
1,049 to 1,100	4,400	4,400
1,100 to 1,150	5,650	5,650
1,150 to 1,225	6,650	6,650
1,225 to 1,337.5	7,600	7,600
1,337.5 to 1,450	8,000	8,700
1,450 to 1,550	8,090	8,760
1,550 to 1,650	8,180	8,820
1,650 to 1,750	8,270	8,880
1,750 to 1,830	8,360	8,940
1,830 1,900	8,414	8,976
> 1,900	9,200	9,200

Rock Vs profile corresponding to the location of B-1003.

	Vs (ft/s)	
Depth (ft)	**Gradient #1**	**Gradient #2**
1,049 to 1,100	4,400	4,400
1,100 to 1,150	5,650	5,650
1,150 to 1,225	6,650	6,650
1,225 to 1,337.5	7,600	7,600
1,337.5 to 1,450	8,000	8,700
1,450 to 1,550	8,090	8,760
1,550 to 1,650	8,180	8,820
1,650 to 1,750	8,270	8,880
1,750 to 1,850	8,360	8,940
1,850 to 1,950	8,450	9,000
1,950 to 2,050	8,540	9,060
2,050 to 2,127.5	8,630	9,120
2,127.5 to 2,155	8,679.5	9,153
2,155 to 2,275	8,733.5	9,189
> 2,275	9,200	9,200

Table 2.5.4-12 Summary of Modulus Reduction and Damping Ratio Values – EPRI-Based

Shear Strain (%)	0-20 ft (Compacted Backfill)		20-50 ft (Compacted Backfill)		50-86 ft (Compacted Backfill)		86-149 ft (Blue Bluff Marl)		149-215.7 ft (Lower Sand Stratum-Still Branch Formation)		Between 215.7 and 500 ft (Lower Sand Stratum below Still Branch)		Soil between 500 ft and top of rock (about 1,000 ft) (Deep Sands)	
	G/G_{max}	Damping Ratio	G/G_{max}	Damping Ratio	G/G_{max}	Damping Ratio	G/G_{max}	Damping Ratio	G/G_{max}	Damping Ratio	G/G_{max}	Damping Ratio	G/G_{max}	Damping Ratio
0.0001	1	1.4	1	1.2	1	1	1	1.4	1	0.8	1	0.7	1	0.6
0.00032	1	1.5	1	1.2	1	1	1	1.4	1	0.9	1	0.8	1	0.6
0.001	0.98	1.8	0.99	1.4	1	1.2	0.99	1.5	1	1	1	0.8	1	0.6
0.00316	0.914	2.8	0.946	2.1	0.97	1.64	0.96	2	0.98	1.33	0.988	1.12	0.99	0.81
0.01	0.75	5	0.82	3.6	0.87	2.8	0.84	2.9	0.9	2.2	0.93	1.8	0.95	1.2
0.03162	0.509	9.3	0.608	7	0.68	5.49	0.63	6	0.74	4.36	0.791	3.53	0.852	2.5
0.1	0.27	15.3	0.36	12.4	0.43	10.2	0.36	11.4	0.5	8.6	0.57	7.1	0.65	5.3
0.3162	0.116	21.9	0.165	19.1	0.22	16.5	0.16	17	0.27	14.61	0.321	12.78	0.41	10.27
1	0.04	27	0.06	24.9	0.09	22.9	0.06	19.4	0.12	21.2	0.15	19.3	0.2	16.7

Table 2.5.4-13 Summary of Modulus Reduction and Damping Ratio Values – SRS-Based

Cyclic Shear Strain (%)	Blue Bluff Marl		Shallow Sand (<300 ft)		Deep Sand (>300 ft)	
	G/G_{max}	Damping Ratio	G/G_{max}	Damping Ratio	G/G_{max}	Damping Ratio
0.0001	1	0.8	1	0.6	1	0.5
0.0002	1	0.8	1	0.6	1	0.5
0.0003	1	0.8	1	0.7	1	0.5
0.0005	1	0.8	1	0.7	1	0.5
0.001	0.99	0.9	0.99	0.8	0.995	0.6
0.002	0.98	1.1	0.98	1	0.99	0.7
0.003	0.965	1.2	0.96	1.1	0.985	0.8
0.005	0.94	1.5	0.93	1.4	0.96	0.9
0.01	0.89	2.1	0.87	2.2	0.92	1.4
0.02	0.8	3.3	0.77	3.5	0.85	2.2
0.03	0.72	4.3	0.69	4.7	0.78	3
0.05	0.61	6.1	0.57	6.7	0.69	4.5
0.1	0.43	9.6	0.4	10.4	0.53	7.3
0.2	0.28	13.1	0.25	14.8	0.36	11.2
0.3	0.205		0.18		0.27	13.8
0.5	0.13	19	0.12	21	0.18	
0.7	0.1		0.09		0.14	
1	0.08		0.07	27	0.1	23

This page is intentionally blank.

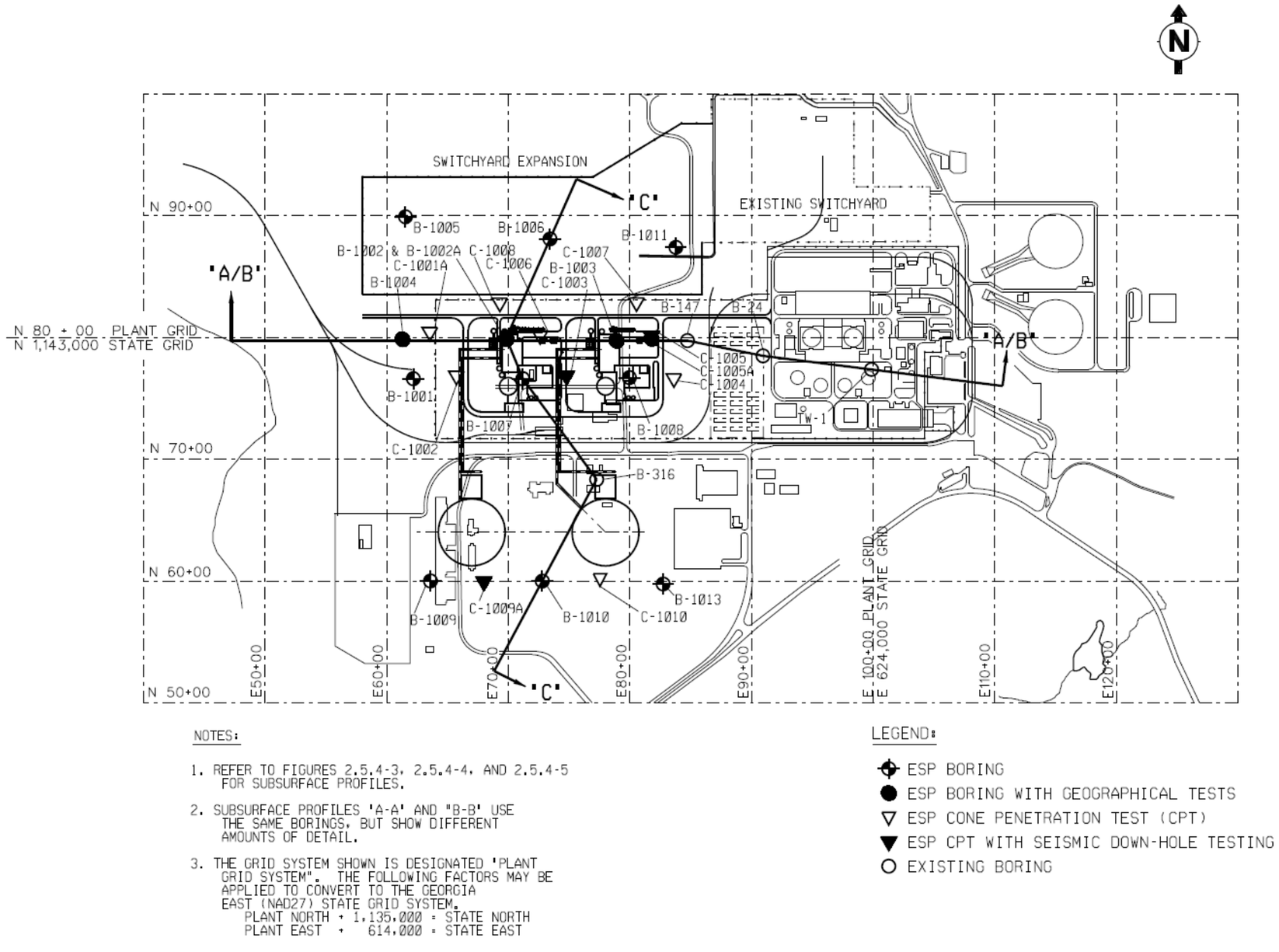

NOTES:

1. REFER TO FIGURES 2.5.4-3, 2.5.4-4, AND 2.5.4-5 FOR SUBSURFACE PROFILES.
2. SUBSURFACE PROFILES 'A-A' AND "B-B' USE THE SAME BORINGS, BUT SHOW DIFFERENT AMOUNTS OF DETAIL.
3. THE GRID SYSTEM SHOWN IS DESIGNATED 'PLANT GRID SYSTEM". THE FOLLOWING FACTORS MAY BE APPLIED TO CONVERT TO THE GEORGIA EAST (NAD27) STATE GRID SYSTEM.
   PLANT NORTH + 1,135,000 = STATE NORTH
   PLANT EAST + 614,000 = STATE EAST

LEGEND:

- ESP BORING
- ESP BORING WITH GEOGRAPHICAL TESTS
- ESP CONE PENETRATION TEST (CPT)
- ESP CPT WITH SEISMIC DOWN-HOLE TESTING
- EXISTING BORING

Figure 2.5.4-1 ESP Study Boring Location Plan

This page is intentionally blank.

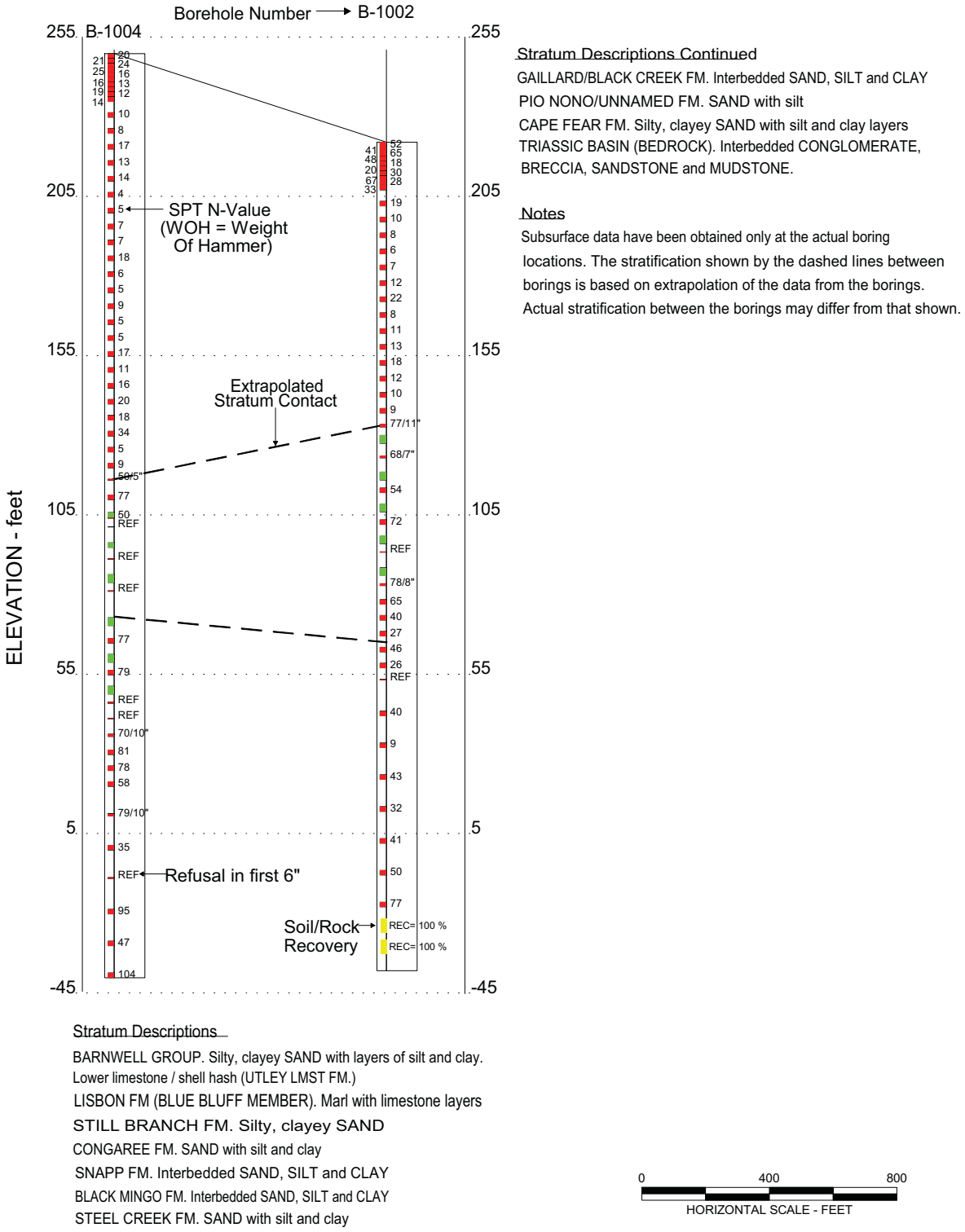

Figure 2.5.4-2 Subsurface Profile Legend

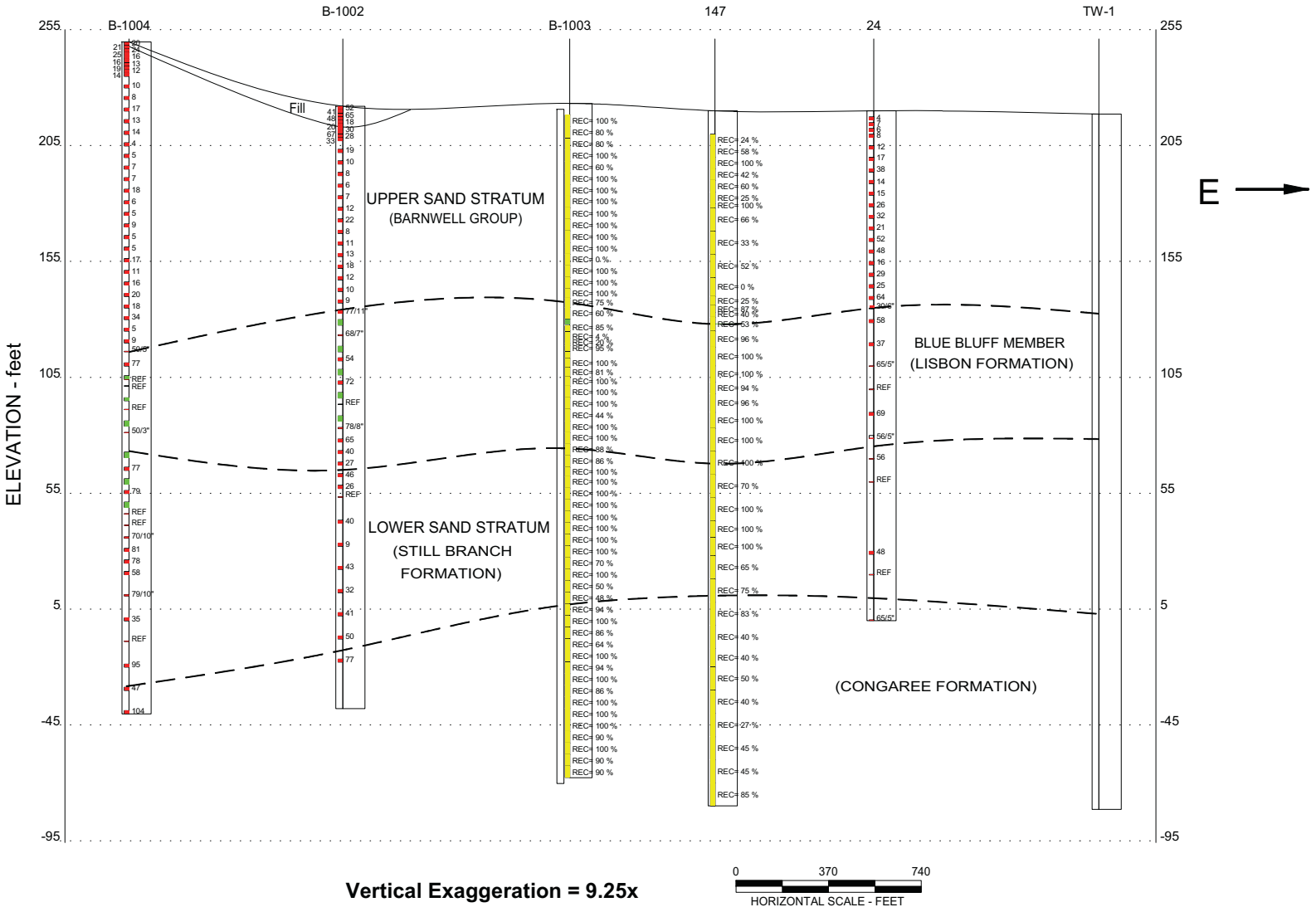

Figure 2.5.4-3 Subsurface Profile A–A'

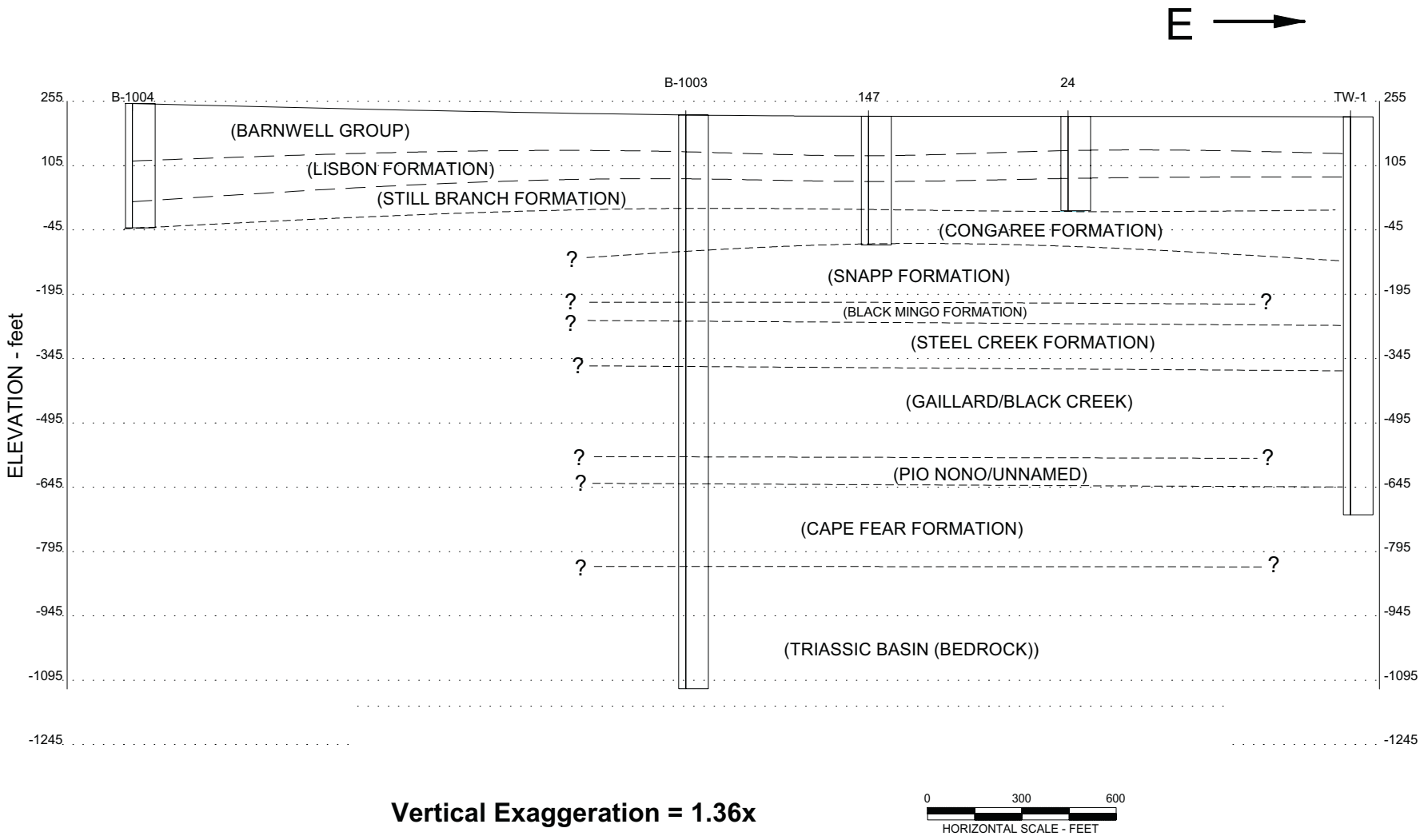

Figure 2.5.4-4 Subsurface Profile B–B'

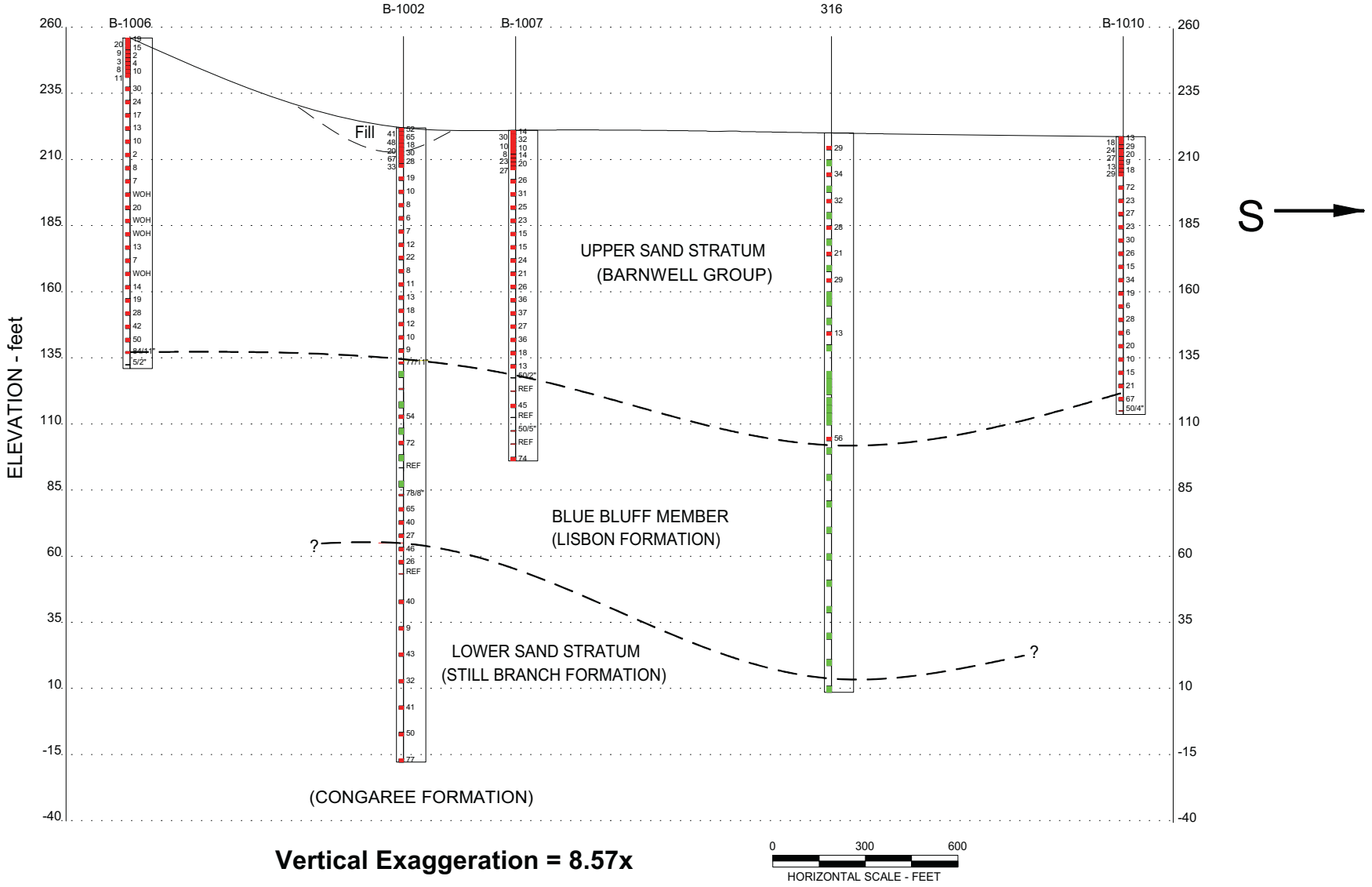

Figure 2.5.4-5 Subsurface Profile C–C'

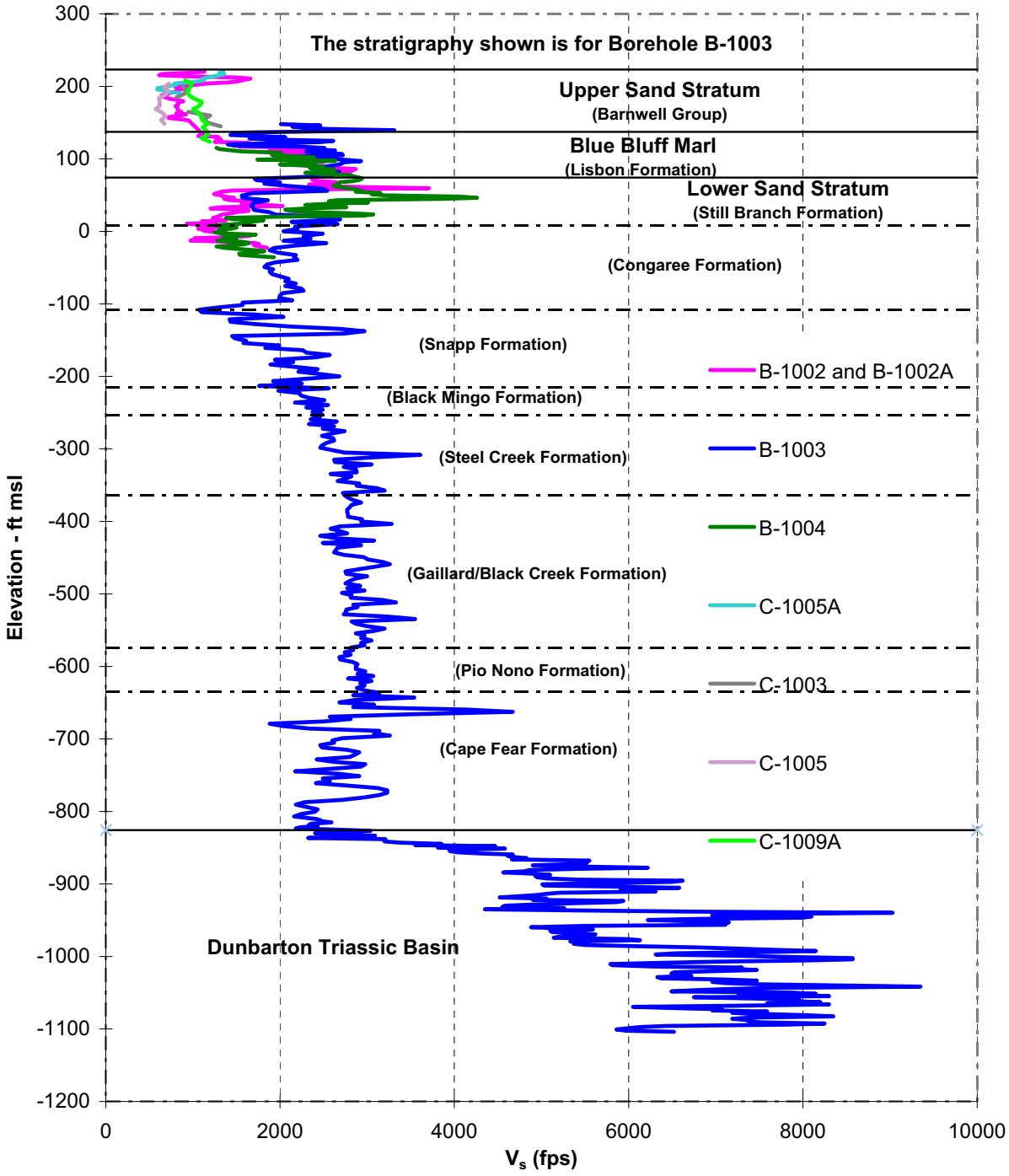

Figure 2.5.4-6 Shear Wave Velocity Measurements

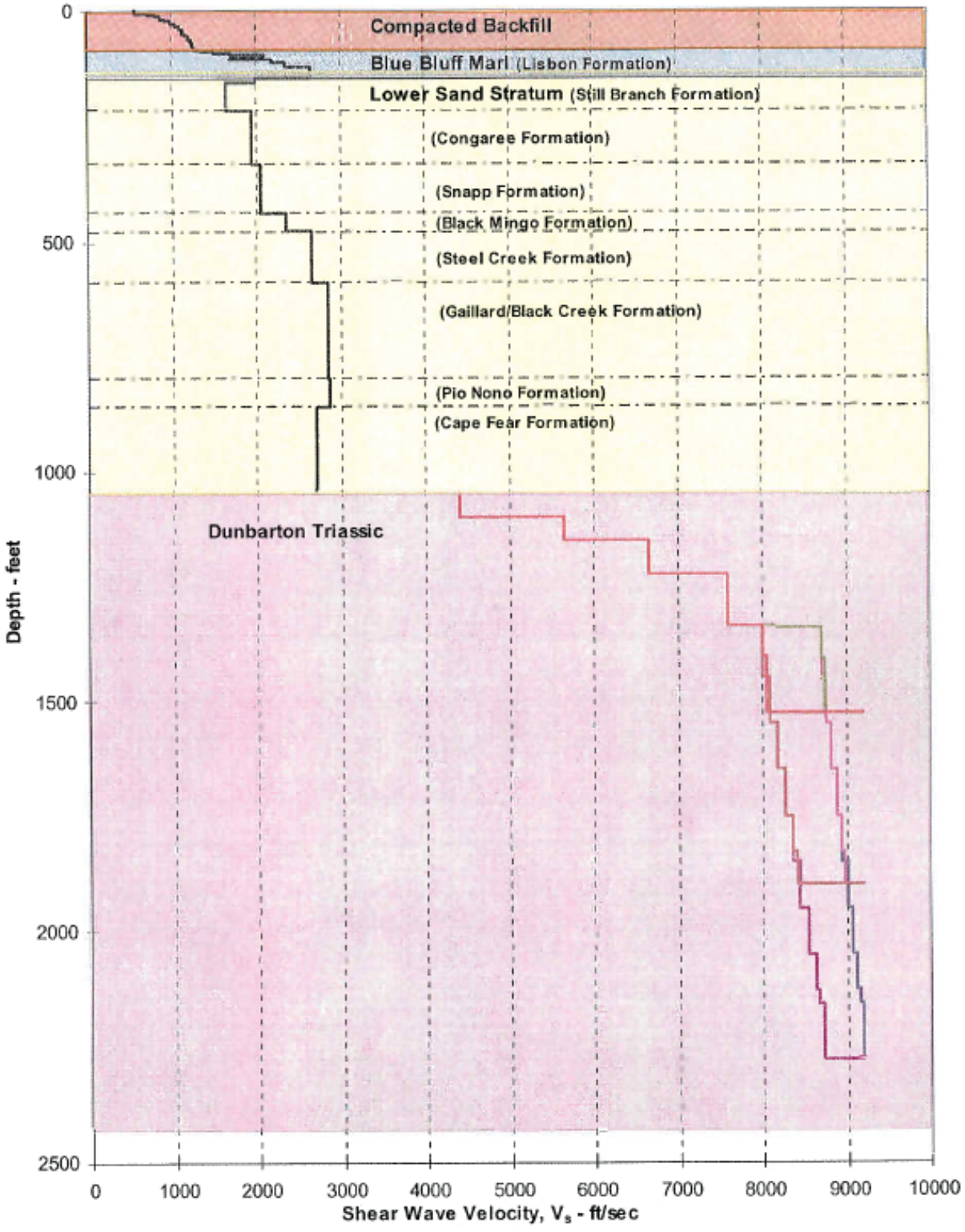

Figure 2.5.4-7 Shear Wave Velocity for SHAKE Analysis

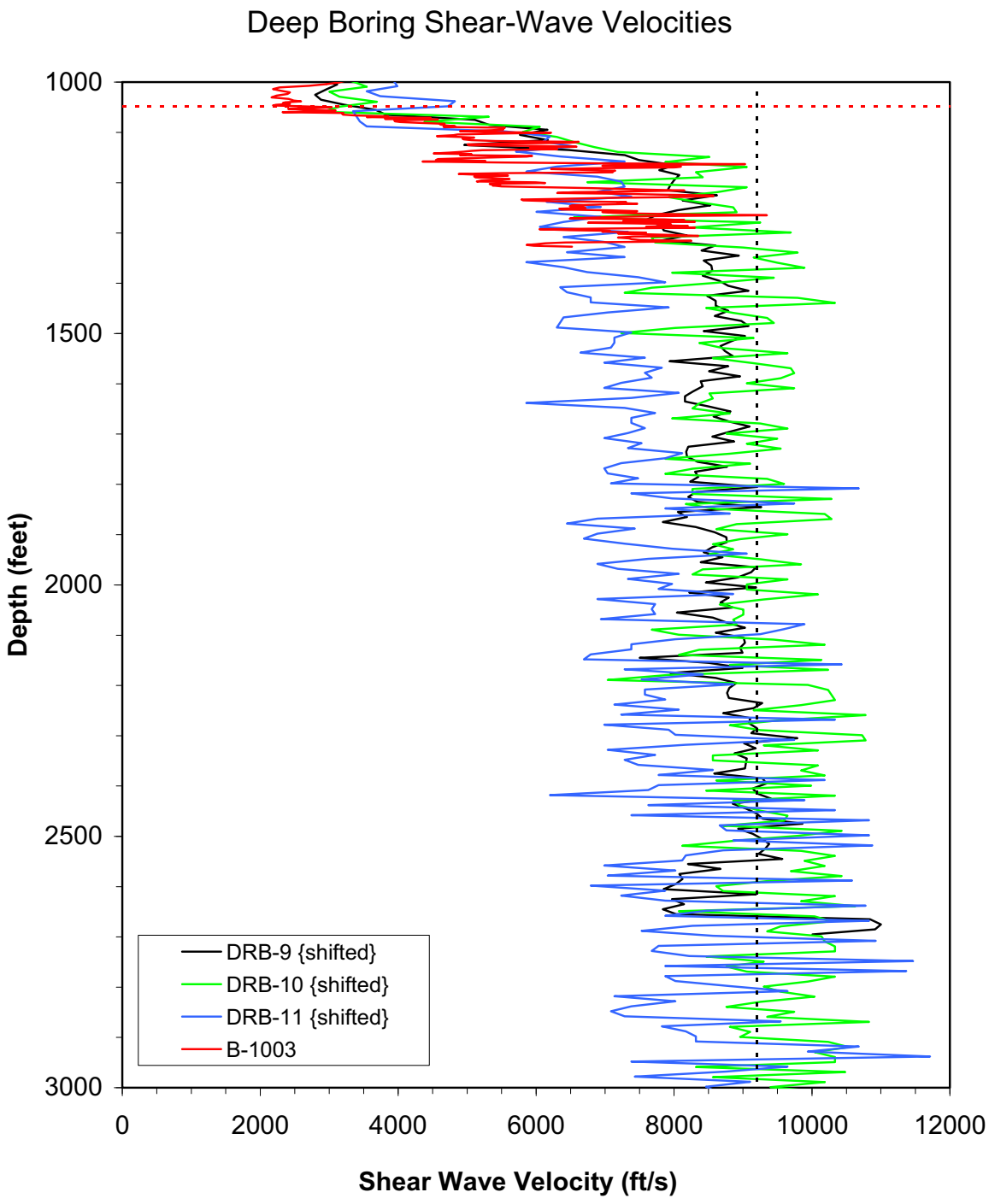

Figure 2.5.4-8 Rock shear-wave velocities for three SRS sites [DRB] (SRS 2005) and B-1003 [Figure 2.5.4-6]. The DRB data has been shifted in depth so that the depth to top of rock is consistent with B-1003.

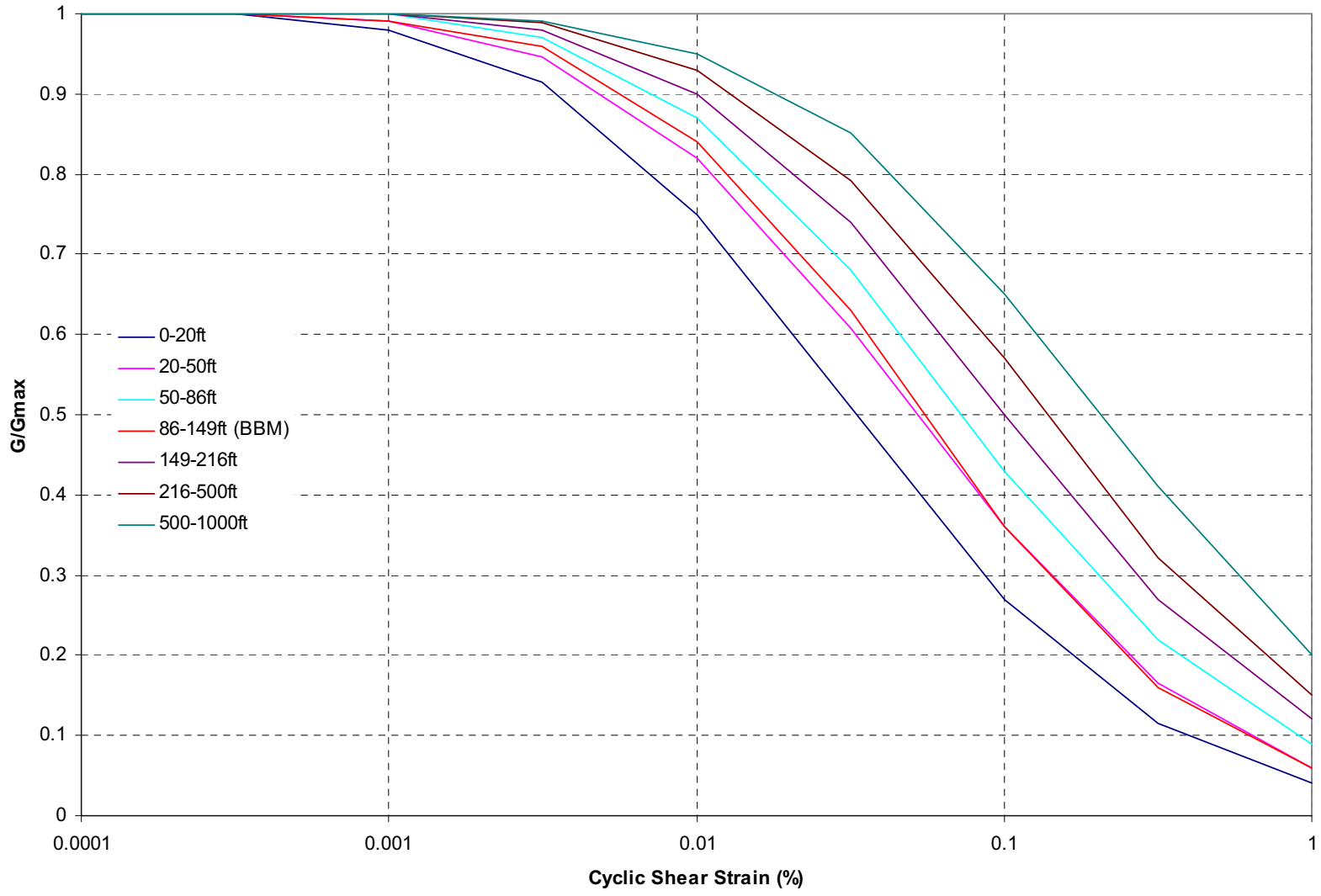

Figure 2.5.4-9 Shear Modulus Reduction Curves for SHAKE Analysis – EPRI Curves

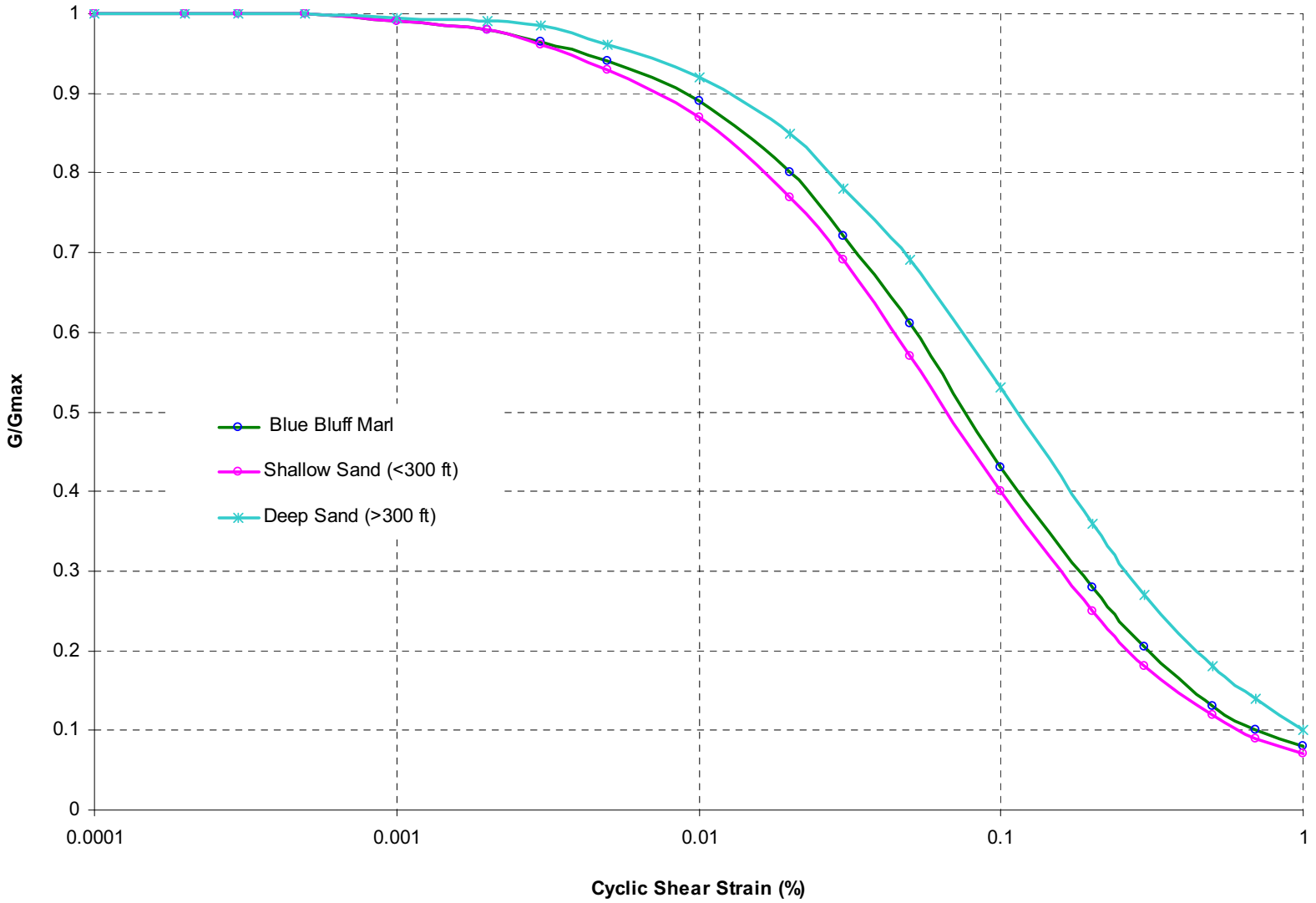

Figure 2.5.4-10 Shear Modulus Reduction Curves for SHAKE Analysis – SRS Curves

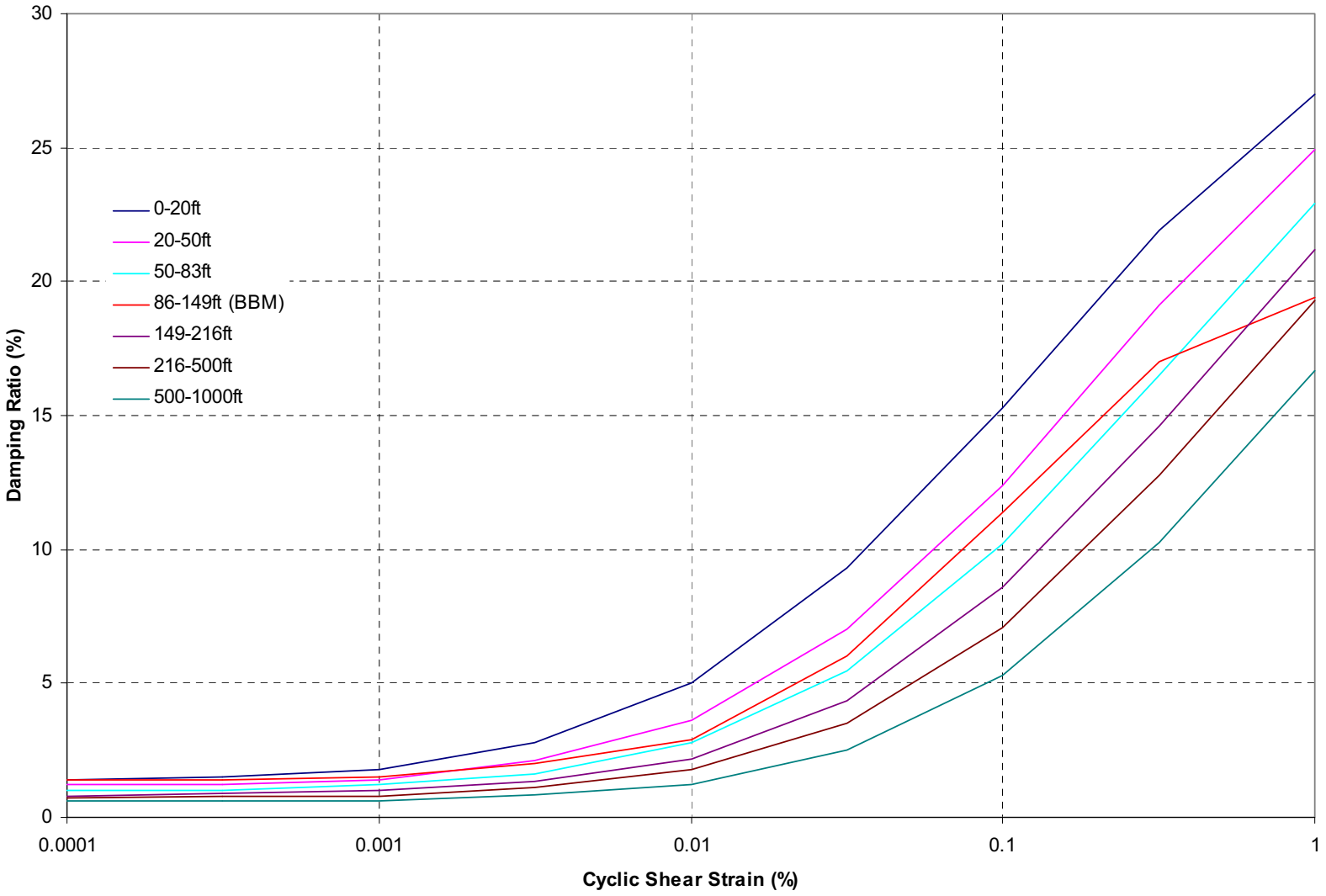

Figure 2.5.4-11 Damping Ratio Curves for SHAKE Analysis – EPRI Curves

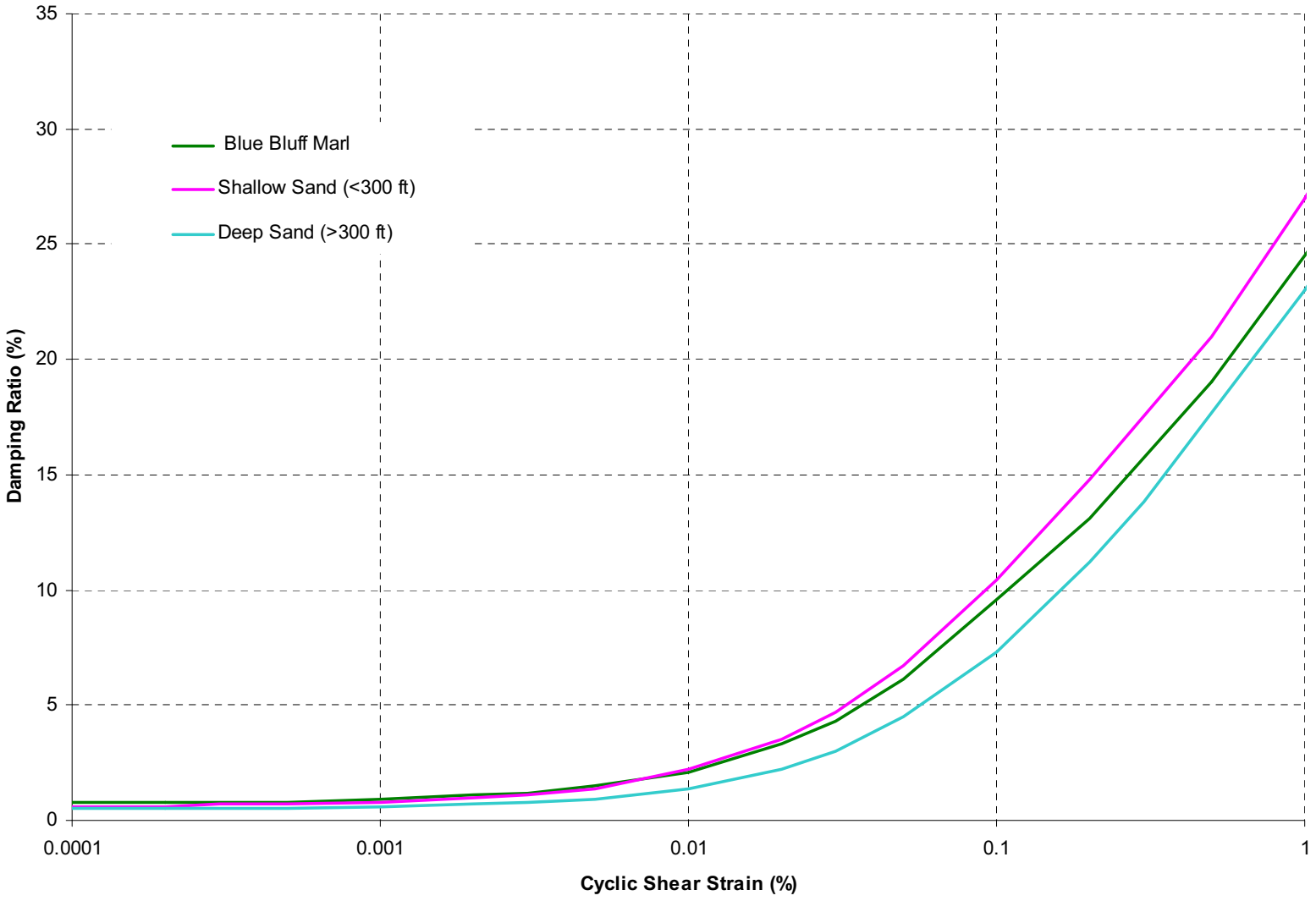

Figure 2.5.4-12 Damping Ratio Curves for SHAKE Analysis – SRS Curves

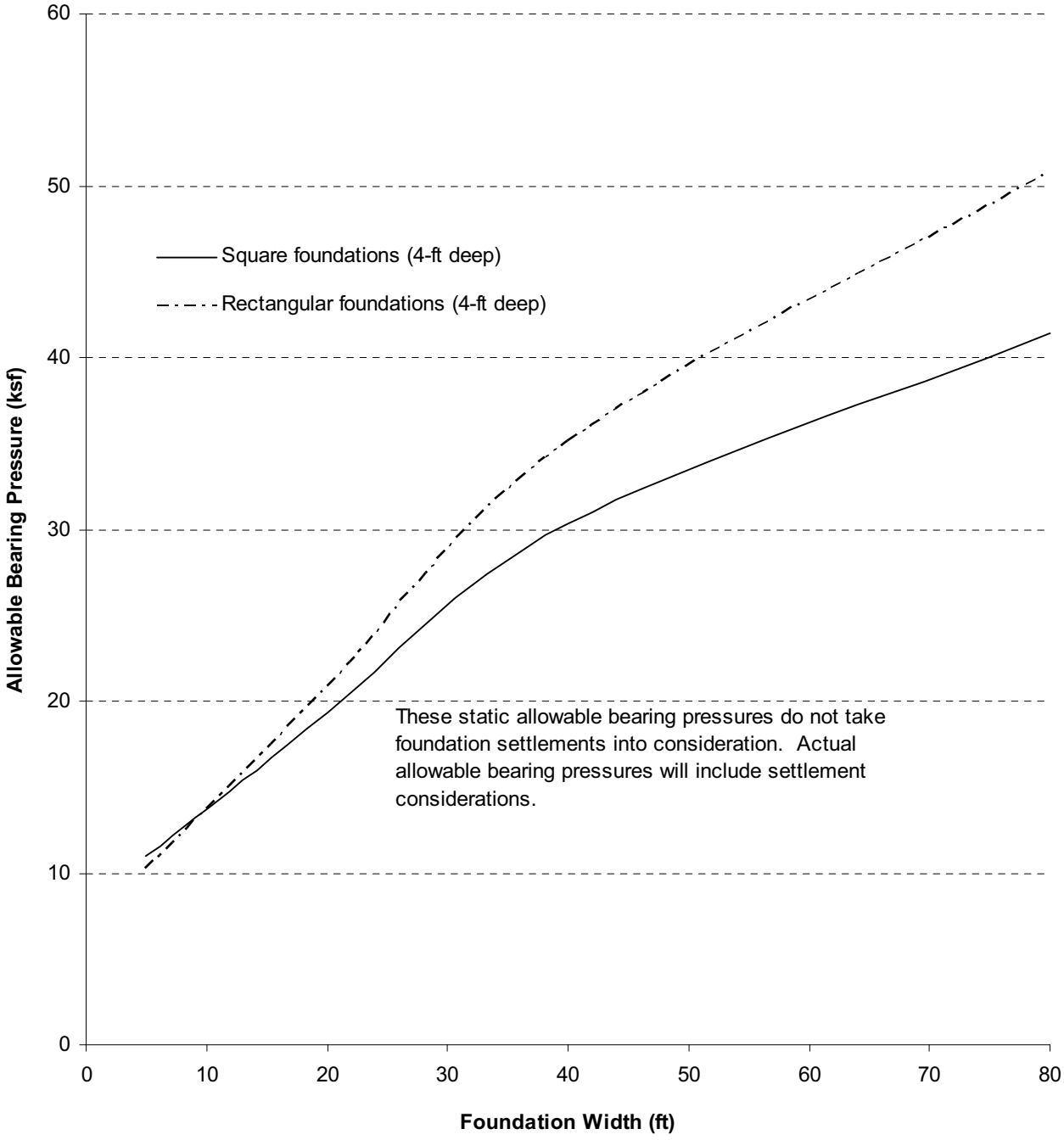

Figure 2.5.4-13 Allowable Bearing Capacity of Typical Foundation

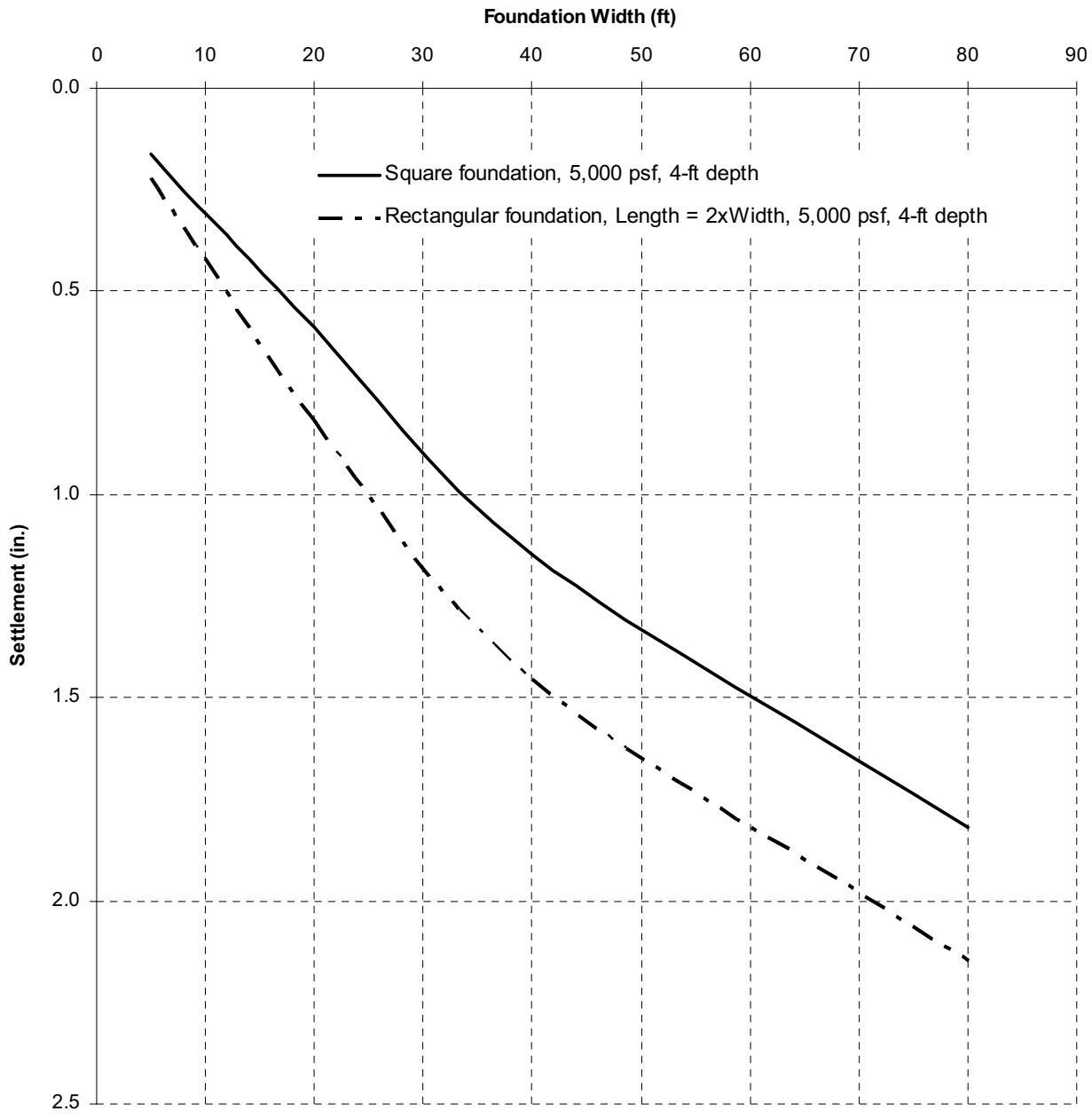

Figure 2.5.4-14 Settlement of Typical Foundations

Section 2.5.4 References

(ASTM D 1557 2002) ASTM International, *Standard Test Methods for Laboratory Compaction Characteristics of Soil Using Modified Effort (56,000 ft-lbf/ft^3 (2,700 kN-m/m^3))*, ASTM D 1557, Conshohocken, PA, 2002.

(ASTM D 1586 1999) ASTM International, *Standard Test Method for Penetration Test and Split-Barrel Sampling of Soils*, ASTM D 1586 Conshohocken, PA, 1999.

(ASTM D 2113 1999) ASTM International, *Standard Practice for Rock Core Drilling and Sampling of Rock for Site Investigation*, ASTM D 2113, Conshohocken, PA, 1999.

(ASTM D 2488 2000) ASTM International, *Standard Practice for Description and Identification of Soils (Visual-Manual Procedure)*, ASTM D 2488, Conshohocken, PA, 2000.

(ASTM D 4044 2002) ASTM International, *Standard Test Method (Field Procedure) for Instantaneous Change in Head (Slug) Tests for Determining Hydraulic Properties of Aquifiers*, ASTM D 4044, Conshohocken, PA, 2002.

(ASTM D 5778 2000) ASTM International, *Standard Test Method for Performing Electronic Friction Cone and Piezocone Penetration Testing of Soils*, ASTM D 5778, Conshohocken, PA, 2000.

(ASTM D 6066 1996) ASTM International, *Standard Practice for Determining the Normalized Penetration Resistance of Sands for Evaluation of Liquefaction Potential*, ASTM D 6066, Conshohocken, PA, 1996.

(Bechtel 1974b) Bechtel Power Corporation, Report on Foundation Investigations, Alvin W. Vogtle Nuclear Project, July 1974.

(Bechtel 1978a) Bechtel Power Corporation, Report on Backfill Material Investigations, Alvin W. Vogtle Nuclear Project, January 1978.

(Bechtel 1978b) Bechtel Power Corporation, Report on Backfill Material Investigations, Alvin W. Vogtle Nuclear Project, Addendum No. 1, October 1978.

(Bechtel 1978c) Bechtel Power Corporation, Report on Dynamic Properties for Compacted Backfill, Alvin W. Vogtle Nuclear Project, February 1978.

(Bechtel 1978d) Bechtel Power Corporation, Test Fill Program, Phase II, Alvin W. Vogtle Nuclear Project, October 1978.

(Bechtel 1979) Bechtel Power Corporation, Report on Backfill Material Investigations, Alvin W. Vogtle Nuclear Project, Addendum No. 2, November 1979.

(Bechtel 1984) Bechtel Power Corporation, Seismic Analysis Report, Vogtle Nuclear Generating Plant Units 1 and 2, October 1984.

(Bechtel 1986) Bechtel Power Corporation, VEGP Report on Settlement, Vogtle Nuclear Generating Plant Units 1 and 2, August 1986.

(Bechtel 2000) Bechtel Corporation, *Theoretical and User's Manual for SHAKE 2000,* prepared by N Deng and F Ostadan, San Francisco, CA, 2000.

(Bowles 1982) Bowles, J.E., *Foundation Analysis and Design,* Third Edition, McGraw-Hill Book Company, New York, 1982.

(Davie and Lewis 1988) Davie, J.R. and Lewis, M.R., "Settlement of Two Tall Chimney Foundations," *Proceedings, Second International Conference on Case Histories in Geotechnical Engineering*, St. Louis, MO, June 1988.

(Domoracki 1994) Domoracki, W.J. (1994). A Geophysical Investigation of Geologic Structure and Regional Tectonic Setting at the Savannah River Site, South Carolina., Virginia Polytechnic Institute and State University, excerpts of doctoral dissertation prepared for Westinghouse Savannah River Company.

(EPRI TR-102293 1993) Electric Power Research Institute (EPRI), *"Guidelines for Determining Design Basis Ground Motions," EPRI Report No. TR-102293, Volumes 1-5*, Palo Alto, CA, 1993.

(Geovision 1999) Geovision, Inc. (1999). Suspension velocity measurements at the Savannah River Site, GCB-8. Report 9211-01, prepared for Exploration Resources, dated March 26, 1999.

(Lee 1996) Lee, R., "Investigations of Nonlinear Dynamic Properties at the Savannah River Site," *Report No. WSRC-TR-96-0062, Rev. 1*, Aiken, SC, 1996.

(Lee et al. 1997) Lee, R.C., M.E. Maryak, and M.D. McHood. "SRS Seismic Response Analysis and Design Basis Guidelines," *Report No. WSRC-TR-97-0085, Rev. 0*, Westinghouse Savannah River Co., Savannah River Site, Aiken, SC, 1997.

(NRC/NAP 1985) National Research Council, *Liquefaction of Soils During Earthquakes,* Committee on Earthquake Engineering, National Academy Press, Washington, D.C. 1985.

(Ohya 1986) Ohya, S., "In Situ P and S Wave Velocity Measurement," *Proceedings of In Situ '86*, ASCE, New York, NY, 1986.

(OSHA 2000) Occupational Safety and Health Administration (OSHA), 29 CFR Part 1926, *Safety and Health Regulations for Construction*, 2000.

(Peck et al. 1974) Peck, R.B., Hanson, W.E., and Thornburn, T.H., *Foundation Engineering,* Second Edition, John Wiley and Sons, Inc., New York, 1974.

(Seed and Idriss 1970) Seed, H.B., and Idriss, I.M., *Soil Moduli and Damping Factors for Dynamic Response Analyses,* Report No. UCB/EERC-70/10, University of California, Berkeley, December 1970.

(Seed et al. 1984) Seed, H.B., Wong, R.T., Idriss, I.M., and Tokimatsu, K., *Moduli and Damping Factors for Dynamic Analyses of Cohesionless Soils,* Report No. UCB/EERC-84/14, University of California, Berkeley, September 1984.

(Skempton 1957) Skempton, A. W., "Discussion of the Planning and Design of the New Hong Kong Airport," Proceedings of the Institution of Civil Engineers, Vol. 7, pp. 305-307, 1957.

(SRS 2005) Birdwell elastic properties logs for SRS boreholes DRB-9, DRB-10, and DRB-11. per. comm.. Frank Syms, Savannah River Site, August 26, 2005.

(Sun et al. 1988) Sun, J.I., Golesorkhi, R., and Seed, H.B., *Dynamic Moduli and Damping Ratios for Cohesive Soils,* Report No. UCB/EERC-88/15, University of California, Berkeley, August 1988.

(Terzaghi 1955) Terzaghi, K., "Evaluation of Coefficients of Subgrade Reaction," *Geotechnique*, Volume 5, 1955.

(Vesic 1975) Vesic, A.S., *Bearing Capacity of Shallow Foundations*, in Foundation Engineering Handbook, H.F. Winterkorn and H-Y Fang, Editors, Van Nostrand Reinhold Company, New York, 1975.

(WSRC 1998) General SRS Strain Compatible Soil Properties for 1886 Charleston Earthquake (U), Calculation K-CLC-G-0060, McHood, M.D, October 29, 1998.

2.5.5 Stability of Slopes

2.5.5.1 Review of Existing Slopes

The location of VEGP Units 3 and 4 will be atop a bluff on the southwest bank of the Savannah River. The new units will be located to the west of the existing Units 1 and 2 as described in Section 1.2. The ground is flat to gently rolling and at approximately the same grade elevation of the existing units (220 ft msl). There are no existing slopes or embankments near the proposed location of Units 3 and 4; therefore, no dynamic slope stability analysis was performed for VEGP Units 3 and 4.

2.5.5.2 New Slopes

There is no planned permanent slope that would adversely affect, either directly or indirectly, any of the safety-related structures that would be built for the new AP1000 Units 3 and 4. Site grading for construction of the new units would result in non-safety-related permanent cut and fill slopes. Permanent cut slopes would have heights of the order of 50 feet or less, and would be located to the north and west of the new switchyard area, several hundred feet away from planned or existing safety-related structures. Permanent fill slopes would have heights of the order of 20 ft or less, and would be located to the south and west of the new cooling tower area, several hundred feet away from planned or existing safety-related structures.

Construction excavation cut slopes would be required in the new AP1000 power block area where soils above the Blue Bluff Marl would be removed and replaced with compacted structural fill. The construction excavation cut slopes would be temporary during the construction period only. Also, these excavation slopes would be sufficiently far away from the existing VEGP Unit 1 and 2 safety-related structures, and therefore, would not adversely affect, directly or indirectly, any of the existing safety-related structures.

The proposed permanent non-safety-related slopes will be analyzed for dynamic and static conditions during the design stage. The minimum acceptable factors of safety against stability failure of permanent slopes are 1.5 for long-term static conditions and 1.1 for long-term seismic conditions. The construction excavation cut slopes will be analyzed for static conditions during the design stage. The minimum acceptable factor of safety against stability failure of excavation slopes is 1.3, based on what was used for Units 1 and 2. These analyses will be performed to ensure that these slopes will not pose a hazard to the public. Such analyses are not part of the ESP SSAR.

This page intentionally blank.

2.5.6 Embankments and Dams

2.5.6.1 Review of Existing Embankments and Dams

There are no earth, rock or earth and rock fill embankments required for plant flood protection or for impounding cooling water required for the operation of the plant.

Figure 1-4 shows the locations of three existing non-safety-related impoundments at the VEGP site. They are:

- Mallard Pond located to the north of the proposed switchyard
- Debris Basin Dam #1 located to the southeast of the proposed AP1000 cooling towers
- Debris Basin Dam #2 located to the southwest of the proposed AP1000 cooling towers

These impoundments are not used for plant flood protection or for impounding cooling water required for the operation of the plant. However, brief descriptions of these impoundments are provided here.

The proposed finished grade elevation for the new AP1000 units is approximately 220 ft msl. The pool level in Mallard Pond is below El. 125 ft msl. In the event of a dam breach at Mallard Pond, the water would drain to the north and away from the proposed new units. The pool levels in Debris Basin Dams #1 and #2 are below El. 150 ft msl, and in the event of a dam breach, the water would drain to the south and away from the proposed new units.

2.5.6.2 New Embankments and Dams

No new embankments or dams would be constructed at the site for flood protection or for impounding cooling water required to operate the new AP1000 units. The proposed finished grade elevation for the new AP1000 units is approximately 220 ft msl. This site finished grade elevation is much higher than the probable maximum flood (PMF) elevation discussed in Section 2.4.3 and the dam break level discussed in Section 2.4.4. Therefore, no new embankments or dams would be required to be constructed at the site for flood protection. Also, the new AP1000 units use cooling towers, and makeup water would be pumped from the Savannah River. Therefore, no new embankments or dams would be required to be constructed at the site for impounding cooling water required to operate the new AP1000 units.

In summary, no embankments and dams are required to be addressed in this section.

This page intentionally blank.